# Contact Metamorphosed Granitoids: Their Metamorphic Zonation, Correlation With Associated Hornfelsic Isograds And Implications Upon Emplacement Mechanisms In The New England Batholith

BSc. Honours Thesis

Alan P. Clare

1988

**The author wishes to dedicate this thesis to the late Mr. R. Beaugeais, who made all probe slides, (often at short notice) and helped greatly in the thinsection work. He is especially remembered for his warmth, good nature and own particular brand of humour**

## ACKNOWLEDGEMENTS

The author wishes to thank his supervisor, Dr. R. H. Flood, for much helpful advice and patience in reading many drafts. and to express appreciation to Assoc. Prof. R.H. Vernon for the use of photographic equipment and for advice and Miss C. Braithwaite and Dr. N. Munksgaard for help in XRD, XRF and electron microprobe work. Also thanks to Dr. D.W. Durney, Mr P.Ingram, and Dr S.E. Shaw for ideas and computing facilities. Thanks must also go to the Palaeontology Department for use of their laboratory . Grateful acknowledgements go to D. Gilbert and Wescom for 3-D computer work and to the Geophysics Department for additional computer modelling facilities. Special thanks goes to the Quihampton family on the propoerty of " Arlemont " for accomodation, excellent hospitality and above all good friendship. The author would also wish to thank his family for their patient support, and a final and very special thanks goes to Sarah for her unfailing encouragement throughout the year.

# CONTACT METAMORPHOSED GRANITOIDS : THEIR METAMORPIC ZONATION, CORRELATION WITH ASSOCIATED HORNFELSIC ISOGRADS AND IMPLICATIONS UPON EMPLACEMENT MECHANISMS IN THE NEW ENGLAND BATHOLITH.


PAGE

ABSTRACT 1

INTRODUCTION 2

A. CONTACT METAMORPHISM OF AN UNDEFORMED S-TYPE ADAMELLITE IN THE AUREOLE OF THE I-TYPE BENDEMEER ADAMELLITE, N.S.W.

A . 1 . INTRODUCTION 6

A . 2 . REGIONAL GEOLOGY 7

A . 3 . HORNFELS 18

A . 4 . CONTACT METAMORPHISM OF THE BANALASTA ADAMELLITE 57

A . 5 . SUMMARY 95

B. CONTACT METAMORPHISM OF A WEAKLY DEFORMED I-TYPE GRANODIORITE IN THE AUREOLE OF THE I-TYPE GWYDIR RIVER ADAMELLITE, N.S.W.

B . 1 . INTRODUCTION 98

B . 2 . REGIONAL GEOLOGY 99

B . 3 . HORNFELS 114

B . 4 . CONTACT METAMORPHISM OF THE YARROWYCK GRANODIORITE 143

B . 5 . SUMMARY 166

C. SUMMARY OF FINDINGS AND THEIR IMPLICATIONS UPON INTRUSIVE MECHANISMS IN THE SOUTHERN NEW ENGLAND BATHOLITH

C . 1 . REVIEW OF FINDINGS 169

C . 2 . EMPLACEMENT MECHANISMS AND A MODEL FOR THE TWO STUDY AREAS 171

C . 3 . CONCLUSION 174

## D. REFERENCES AND APPENDICES

D. 1 . REFERENCES 177

D. 2 . APPENDIX 1 186

D . 3 . APPENDIX 2 191

D . 4 . MAPS 204

# ABSTRACT

Petrological and structural studies of the contact metamorphic effects of one granite upon another and the surrounding hornfels have been performed within the aureoles of two granitoids (the Bendemeer Adamellite, 41 km NE of Tamworth and the Gwydir River Adamellite, 30 km W of Armidale) in the Southern New England Batholith. The Bendemeer Adamellite is known to intrude (Chappell,1978) the Banalasta Adamellite, an S-type, microcline bearing pluton and the Gwydir River Adamellite likewise intrudes (Ransley,1970) the Yarrowyck Granodiorite, an I-type, orthoclase bearing pluton containing weak deformation associated with spaced micro-shear zones. Correlation of contact metamorphism in both the aureoles examined reveals essentially identical metamorphic zonations.

A mineralogical and microstructural examination of the metagranites away from the later intrusives reveals a regional unaffected zone ( 4 km in the Banalasta Adamellite and 1.5km in the Yarrowyck Granodiorite), a low grade strained zone (1.5-4 km, Banalasta Adamellite and 350-1200 m, Yarrowyck Granodiorite), characterised by high K-feldspar triclinicities and deformational microstructures and a high grade annealled zone (less than 1.5 km, Banalasta Adamellite and less than 350m Yarrowyck Granodiorite), characterised by low K-feldspar triclinicities and recovery and recrystallisation microstructures. The hornfelsic rocks in both areas record metamorphic changes within the intruding pluton's thermal envelope up to the hornblende-hornfels facies ( the pelites recording grades up to the cordierite - K-feldpsar facies and metabasalts recording prograde changes from blue-green, fibrous actinolitic hornblende to brown, granoblastic tschermakitic hornblende ), enabling a finer subdivision of the high grade zone.

This study has revealed two distinct, emplacement - induced domains within the aureoles; an outer strained envelope recording minor ductile deformation; and an inner envelope of continuous thermal annealling during emplacement.

The discordant nature of the intruding pluton's contacts, low contact temperatures (650 degrees celcius) and maximum shortening less than 17.9 %, preclude emplacement mechanisms by either doming (Castro, 1987); melt zoning (Ahern, 1981) or ballooning diapirism (Bateman, 1985) respectively. The meridonal trend of the plutonic suites of the New England Batholith (sub-paralleling the major regional faults and a once convergent plate margin), the metamorphic zonation outlined and its implications upon emplacement induced deformation and thermal annealling and only minor shortening, favour a regional emplacement mechanism of dyke propagation at depth and a proposed high-level mechanism of stoping and associated late stage diapiric processes for the two I-type plutons studied.

# INTRODUCTION

Although there has been a resurgence in interest in petrological and structural studies of both granitoid plutons and their contact aureoles as indicators of their emplacement mechanisms (Marsh,1982; Castro,1987; Pitcher,1978; Dixon,1975 and Bateman,1985), the documentation of contact metamorphic effects of one granitoid upon another and the application of the findings as indicators of emplacement mechanism has not been the focus of much detailed study. The relative age relationships as inferred from the order of emplacement using truncation relationships and foliation data (Chappell & White,1974 and Chappell, 1978) have been documented but there are few accounts of any contact metamorphic changes in the older pluton, even though the older granite is essentially 'country rock' and as such mineralogical and microstructural changes might be expected. The paucity of such studies is somewhat surprising as a granitic pluton is essentially a homogeneous rock in which even subtle changes might be recognisable and that the younger pluton essentially treats all country rocks (whether hornfelses or older granites) in the same way.

This thesis presents a petrological and structural study of both contact metamorphosed plutons and hornfelses in the contact aureole of two granitoid plutons in the New England Batholith, New South Wales. The aim is to record the contact metamorphic effects (both mineralogical and microstructural) observable in the intruded pluton (or metagranite) and correlate them with the effects delineated in the metasedimentary and metabasaltic hornfelses. Utilising the results of both the hornfels and metagranite metamorphic zonation, criteria may be erected to evaluate granitoid emplacement mechanisms in the New England Batholith.

Two field areas have been examined; one the Bendemeer - Hanning area 41 km north east of Tamworth and the other the Yarrowyck - Balala area, 30 km west of Armidale (figure 1).

The metagranite in the Bendemeer area is the Banalasta Adamellite which is the most southerly (Chappell,1978: see figure 2) of the S-type Carboniferous cordierite bearing granitoids of the Bundarra Plutonic Suite (Shaw & Flood,1981) and the oldest pluton in the Bendemeer area (Chappell, 1978). The hornfelses are metabasalts and siliceous metasediments and form part of the Silurian to early Carboniferous (Ishiga,1988) Woolomin Beds (Roberts & Engel,1987). These low grade regional metamorphic rocks have been intruded by the southern Bundarra Suite plutons. Both the Banalasta Adamellite and the hornfelses have then been intruded by the Late Permian Looanga and Bendemeer Adamellites. The Bendemeer area has formed the basis for most of the findings in this thesis and as such is examined in greater detail.

FIGURE 1 : GENERAL SETTING OF THE TWO FIELD AREAS STUDIED, ( BASED ON CHAPPELL,1978; SHAW AND FLOOD, 1981 AND HENSEL, 1985 ).

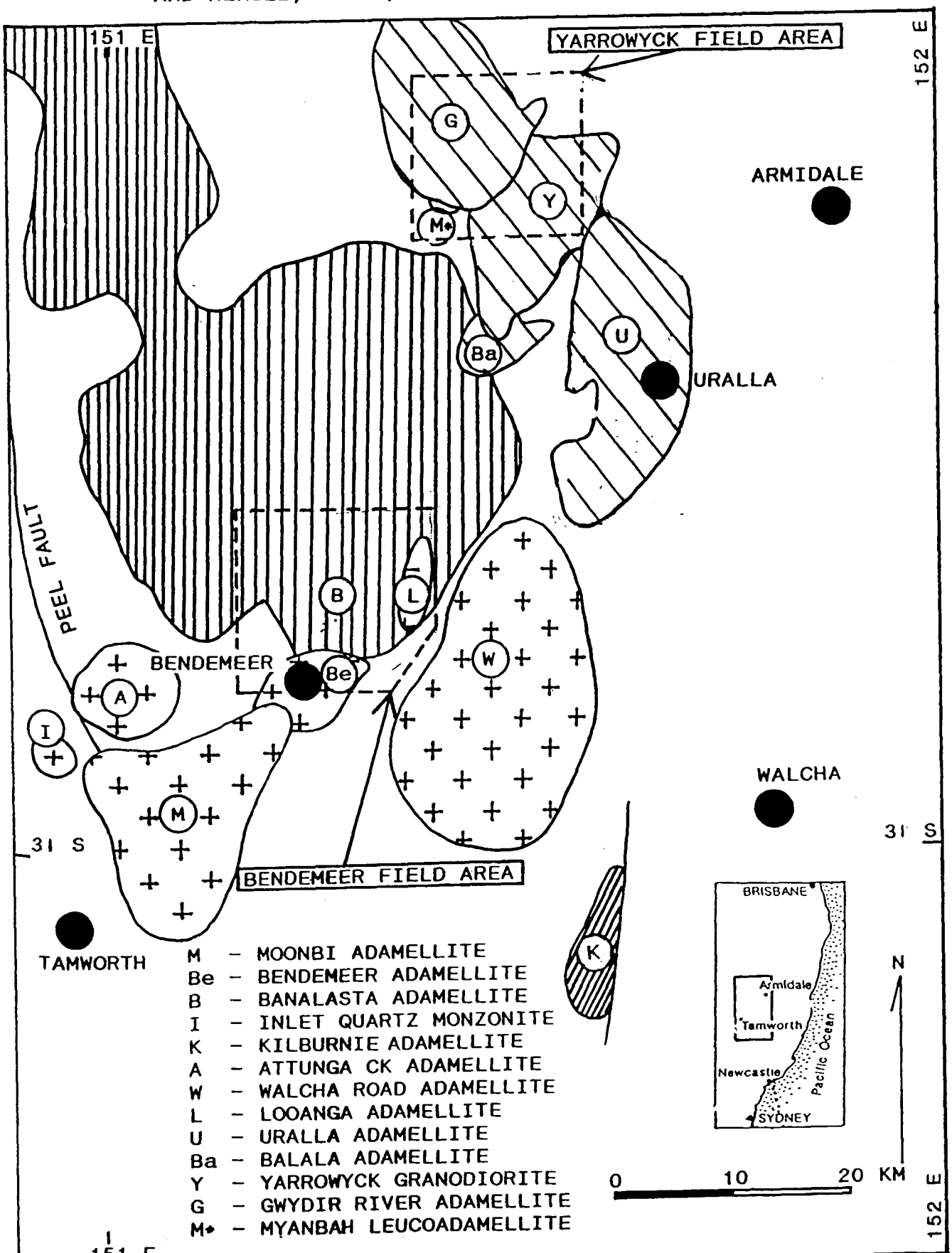

FIGURE 2a : GEOLOGICAL SKETCH MAP OF THE BENDEMEER FIELD AREA ( GEOLOGICAL BOUNDARIES ARE BASED UPON CHAPPELL, 1978 AND THE AUTHORS OWN FIELD WORK )

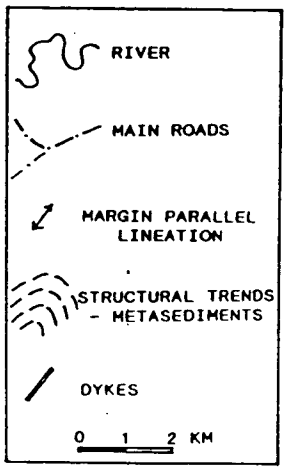


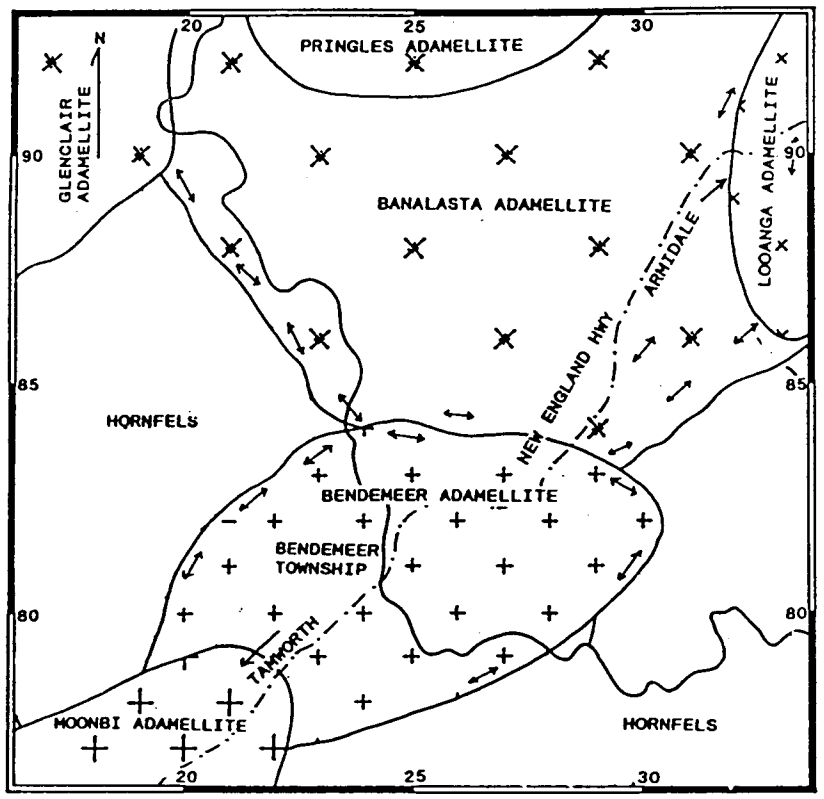


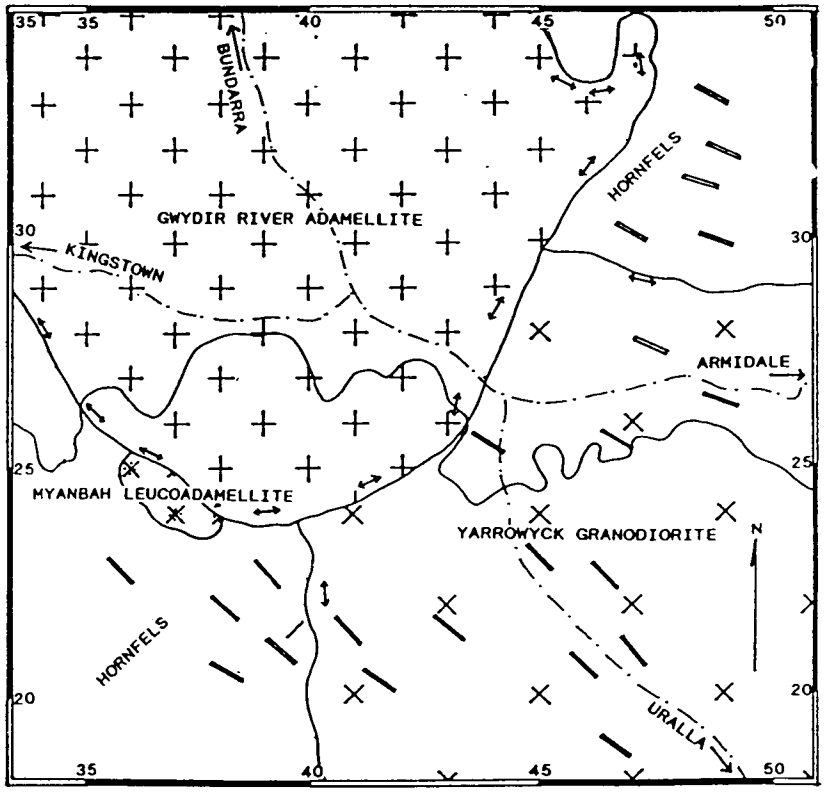


FIGURE 2b : GEOLOGICAL SKETCH MAP OF YARROWYCK FIELD AREA ( GEOLOGICAL BOUNDARIES ARE BASED ON THE AUTHORS OWN FIELD MAPPING AS PREVIOUS WORK BY RANSLEY, 1970 AND BROWN, 1987 PROVED NOT TO BE RELIABLE ).

The metagranite in the Yarrowyck area is the Yarrowyck Granodiorite, an I-type pluton from the Uralla Plutonic Suite, that shows minor localised shearing. It is of Mid-Permian age (O'Neil et al, 1977) and intrudes the low grade metamorphosed Sandon Beds (Roberts & Engels,1987) and the Kurrajong park Volcanics (Brown,1987). Both the metagranite and the hornfelses are intruded by the Gwydir River Adamellite, a younger granitoid of Mid to Late Permian age (also part of the Uralla Plutonic suite; Shaw & Flood, 1981) (figure 3). The Yarrowyck Granodiorite has been studied also as it differs from the Banalasta Adamellite in two important ways. Firstly it is an I-type hornblende-biotite granodiorite and, secondly, it was believed to be predominantly orthoclase bearing away from the intruding pluton rather than microcline. Thus it enables a comparison of two quite different metagranites within the contact aureoles of later intrusives. The Yarrowyck area is therefore an extension of the findings for the Bendemeer area and as such simply outlines the critical findings for the purpose of comparison.

This study of the contact metamorphism of one granite by another and the correlation of the 'isograds' in the metagranite with the more conventional isograds in the metapelites and metabasalts is not only a documentation of an unusual metamorphic progression (which will be useful where two plutons are adjacent but do not have an obvious truncation) but the structural and metamorphic effects are believed to be important information to permit more critical evaluation of the various intrusive mechanisms that have been proposed.

# A . CONTACT METAMORPHISM OF AN UNDEFORMED S-TYPE ADAMELLITE IN THE AUREOLE OF THE I-TYPE BENDEMEER ADAMELLITE N.S.W.

## A. CHAPTER I : INTRODUCTION

This study examines the contact metamorphism observed in the aureole of the Permian I-type Bendemeer Adamellite (Chappell, 1978) where it intrudes the Carboniferous S-type cordierite-bearing Banalasta Adamellite (Chappell, 1978) and surrounding low grade regionally metamorphosed Devonian to Carboniferous Woolomin Beds (Leitch, 1974) (figure 2, map 1).

The Bendemeer area (41 km NNE of Tamworth) was chosen on the basis of previously observed age relationships of adjacent truncating plutons (Chappell, 1978), expected mappable hornfelsic isograds (Binns, 1966 and Teale, 1974) and a known K-feldspar disordering in the Banalasta Adamellite within the aureole of the nearby Walcha Road Adamellite (Flood, 1971).

The examination is performed in two parts: an analysis of the mappable contact metamorphic isograds in both the metasediments and the metabasalts, and an examination of the less conventional isograds mappable in the S-type Banalasta Adamellite, with special emphasis on K-feldspar structural state and compositional changes with grade.

The results are correlated and summarised to establish the complete contact metamorphic zonation for the Bendemeer area and forms the foundation for a critical review of granite emplacement mechanisms in Part C.

# A . CHAPTER 2 : GENERAL OUTLINE OF GEOLOGY

## A . 2 . 1 : META-SEDIMENTARY ROCKS

The metamorphic rocks in the Bendemeer region are of Silurian to Early Carboniferous age (Ishiga,1988) and form part of the Woolomin formation (Roberts and Engels,1987). They are comprised predominantly of thinly bedded cherts, jaspers, argillites, metasiltstones, metabasalts and low abundances of Manganiferous deposits (Howarth,1973; Brown,1986), arenaceous rocks forming a very low proportion of the metasedimentary rocks (Howarth, 1973 and Harrington and Korsch, 1987). Leitch (1975) argued that these rocks formed part of an outer arc-abyssal sedimentary accumulation off a convergent Andean style plate margin that was active in the Devonian and Early Carboniferous (Ishiga,1988).

Deformation of these rocks has produced N-S trending tight to close, cylindrical to sinusoidal folds (Corbett,1976) due to a principle E-W compression associated with further plate convergence and a southward movement of the New England Orogen by the Early Visean (Roberts and Engels,1987). In the Bendemeer area a number of kilometre scale anticlines and synclines are mappable in the field (chapter 3.1, figure 3.1.1), with numerous parasitic folds on varying scales that are observable both from vergence relationships and in single outcrop (plate 2.1.1). The structure of these rocks is similar to that documeted by Corbett (1976) further to the north -west.

Associated with this deformation was the onset of regional metamorphism and uplift (Roberts and Engels,1987) resulting in these Woolomin beds being metamorphosed up to the Prehnite-Pumpellyite facies (Leitch, 1974; Teale, 1974; and Keuhn, 1985) in the mid - late Carboniferous (Harrington and Korsch, 1987). The later intrusion of both the Carboniferous S-type Bundara Suite plutons and the Upper Permian I-type Moonbi suite plutons have resulted in localised contact metamorphism up to the Hornblende-Hornfels facies.

## A . 2 . 2 : LATE CARBONIFEROUS BUNDARRA SUITE S-TYPE ADAMELLITES

This suite has been described by Shaw & Flood (1981) and dated by them at 286 +- 13 Ma. The suite is an elongate meridonal belt of leucocratic S-type granitoids on the western margin of the New England Batholith (figure 2.1.1). The plutons examined in this study are the four southern most of the suite and include the Banalasta Adamellite which is the oldest in the southern part of the suite (Chappell, 1978). The suite shows limited compositional variation and is coarse grained and typically megacrystic in K-feldspar in the southern plutons (O'Neil et al,1977; Chappell,1978). Modal analyses have been carried out by Chappell (1978) and are summarised for the four southern plutons in table 2.2.1. The adamellites of the Bundarra Plutonic Suite consist of subequal amounts of quartz, plagioclase and K-feldspar and minor biotite ( Chappell,1978) and is characterised by minor cordierite + -garnet + -tourmaline (Flood & Shaw,1977)(the tourmaline often occuring at the plutons margins and

PLATE 2.1.1 : OUTCROP SCALE FOLD FROM THE META - SEDIMENTS IN THE IN THE WESTERN AUREOLE OF THE BENDEMEER ADAMELLITE.

PLATE 2.2.3 : TYPICAL OUTCROP STYLE OF THE SOUTHERN BUNDARRA SUITE PLUTONS ( THIS PARTICULAR OUTCROP IS OF THE BANALASTA ADAMELLITE ).

FIGURE 2.1.1 : DISTRIBUTION OF PLUTONIC SUITES IN THE NEW ENGLAND BATHOLITH (SHAW & FLOOD, 1981)

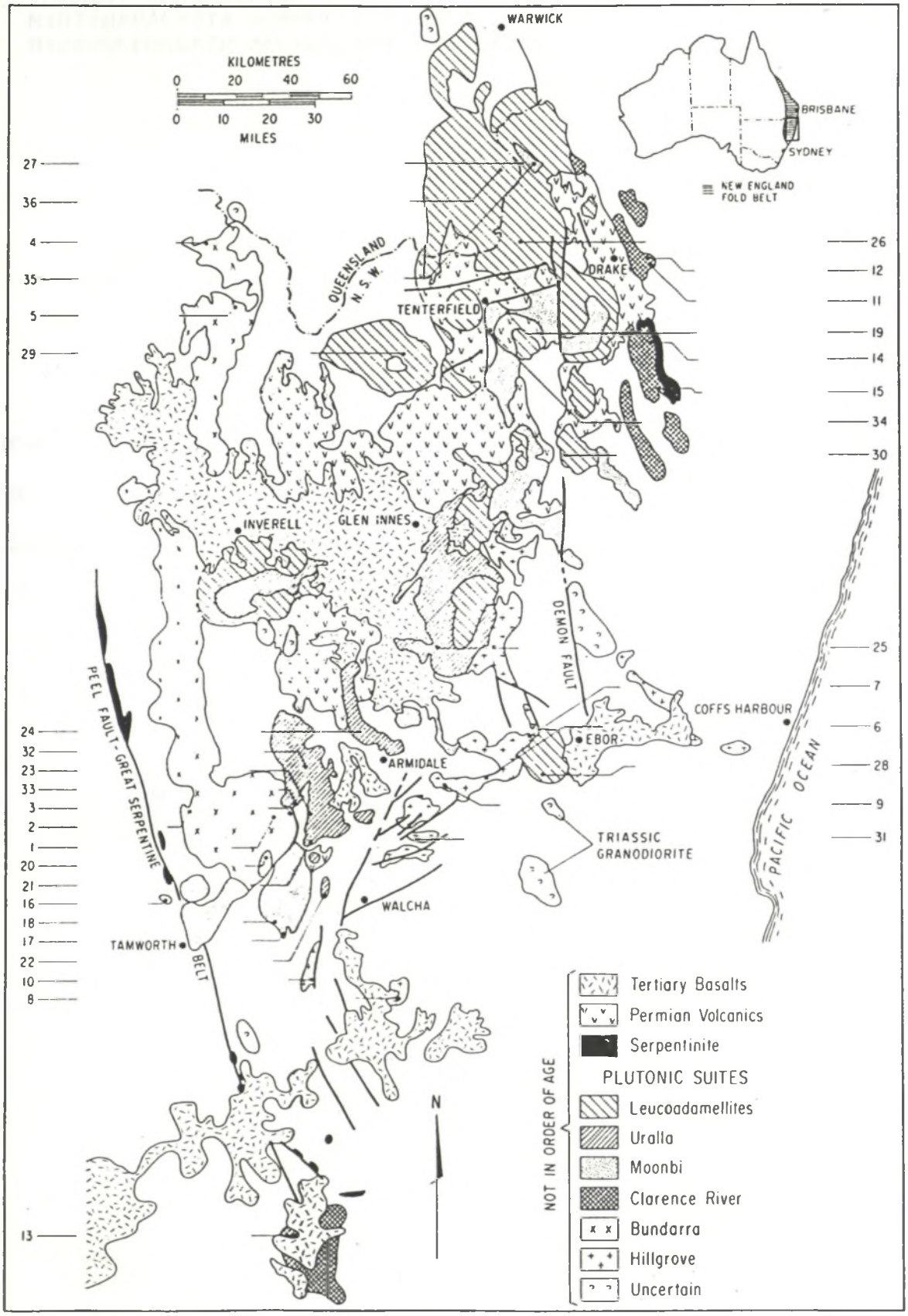

TABLE 2.2.1 : MODAL ABUNDANCES FOR PLUTONS FROM THE BENDEMEER AREA FROM CHAPPELL (1978), CHAPPELLS SAMPLE NUMBERS HAVE BEEN MAINTAINED: (M74=BENDEMEER ADAMELLITE, M101=LOOANGA ADAMELLITE M107=BANALASTA ADAMELLITE, M120=PRINGLES ADAMELLITE, M122=GLENCLAIR ADAMELLITE AND M125=TILMUNDA GRANITE

| | M O D A L A B U N D A N C E S | | | | | |
|---|---|---|---|---|---|---|
| SAMPLE | M74 | M101 | M107 | M120 | M122 | M125 |
| QUARTZ | 35.7 | 30.5 | 30.0 | 32.8 | 34.1 | 33.1 |
| PLAGIOCLASE | 33.0 | 31.9 | 22.2 | 30.3 | 33.8 | 42.2 |
| K-FELDSPAR | 27.6 | 31.4 | 34.1 | 29.1 | 24.0 | 20.9 |
| BIOTITIE | 3.6 | 5.8 | 12.5 | 7.4 | 5.7 | 3.7 |
| HORNBLENDE | 0.1 | 0.1 | - | - | - | - |
| MUSCOVITE | - | - | 0.6 | 0.3 | 2.2 | - |
| OPAQUES | - | 0.1 | 0.5 | - | 0.1 | 0.1 |
| SPHENE | - | 0.2 | - | - | - | - |
| APATITE | - | - | 0.1 | 0.1 | 0.1 | - |
| ALLANITE | - | - | - | - | - | - |

FIGURE 2.2.1 : STRIKE OF THE CONTACT PARALLEL FOLIATION DIRECTION FOR SAMPLE MU45836, THE STRIKE OF THE ADJACENT INTRUSIVE CONTACT IS SHOWN.

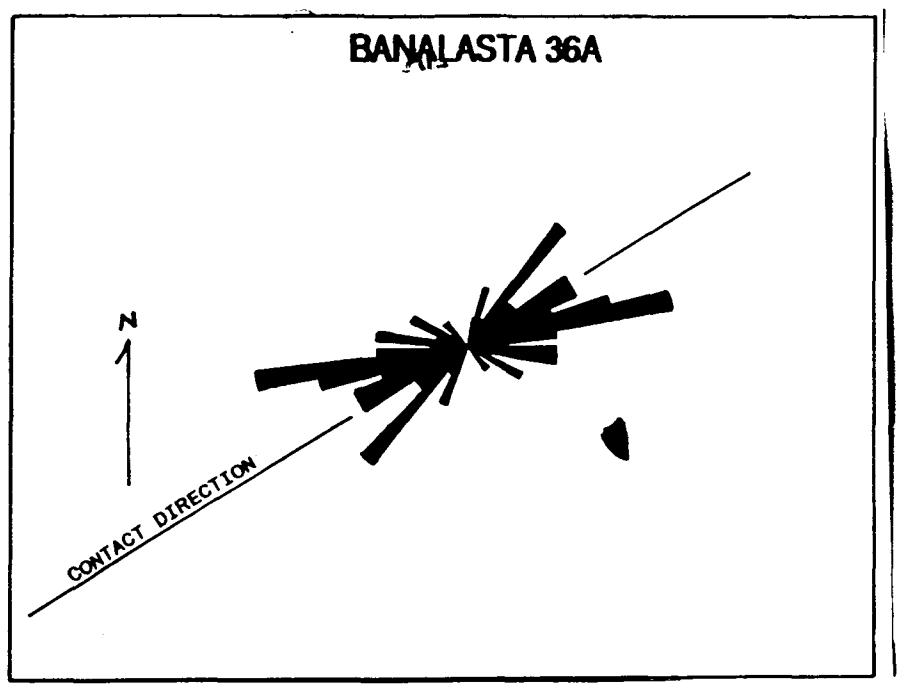


FIGURE 2.2.2 : STRINKE OF THE CONTACT PARALLEL FOLIATION IN THE BANALASTA ADAMELLITE SAMPLE, MU45889. ADJACENT CONTACT STRIKE AS SHOWN.

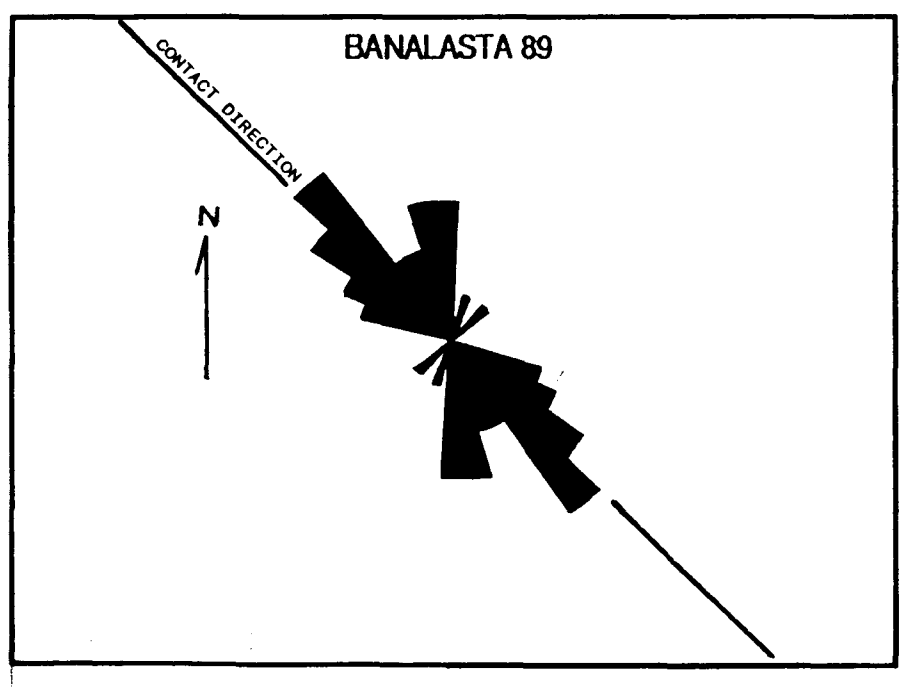

PLATE 2.2.4 : CLOSEUP OF THE BANALASTA ADAMELLITE SHOWING LARGE K-FELDSPAR MEGACRYSTS ( THE LARGEST IN THIS PHOTO BEING 65MM ).

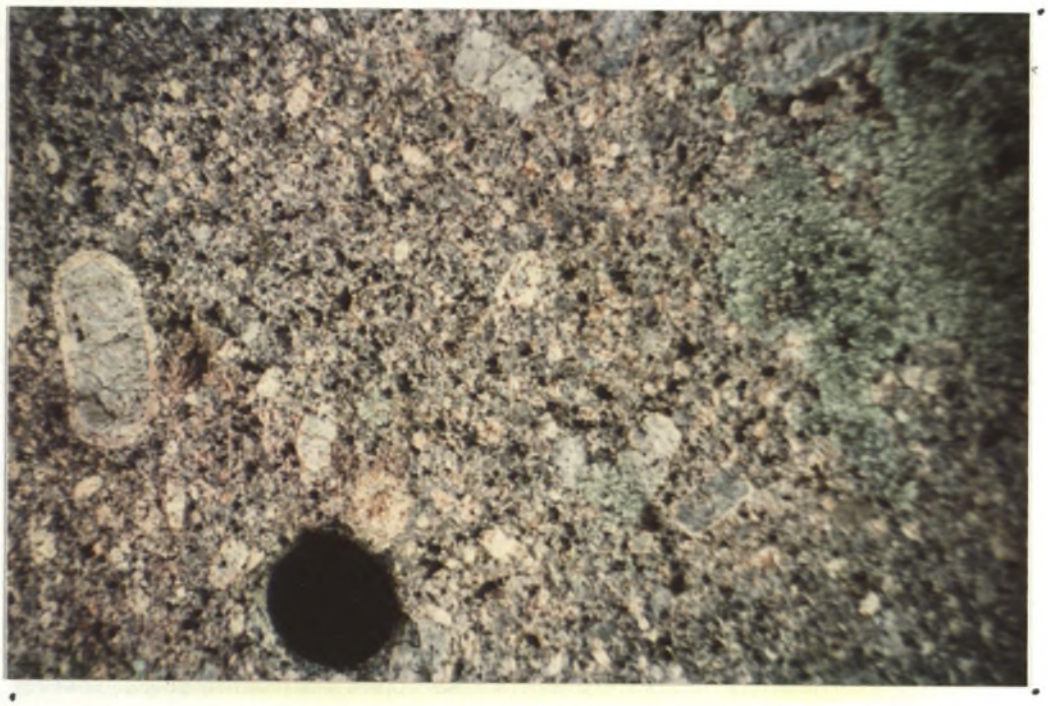

PLATE 2.3.1 : CLOSEUP OF THE MEGACRYSTIC BENDEMEER ADAMELLITE, MEGACRYSTS UP TO 20MM AND THE MICROGRANITOID ENCLAVE IS 80MM IN LENGTH.

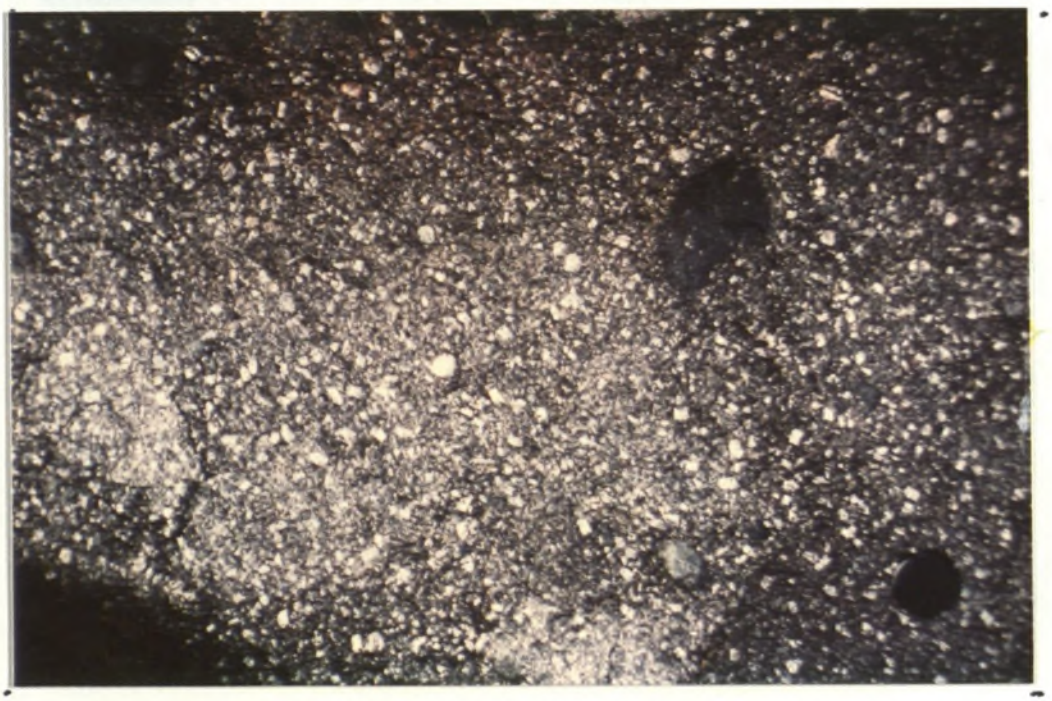

PLATE 2.3.2 TYPICAL LOW RELIEF " WHALE BACK " OUTCROP STYLE TO THE PERMIAN I-TYPE PLUTONS ( THIS PHOTO SHOWS THE LOOANGA ADAMELLITE NEAR THE PROPERTY OF " TALBINGO " ).

PLATE 2.2.2 : FIBROUS, 'PENCIL' AGGREGATE OF TOURMALINE ON THE MARGIN OF THE BANALASTA ADAMELLITE

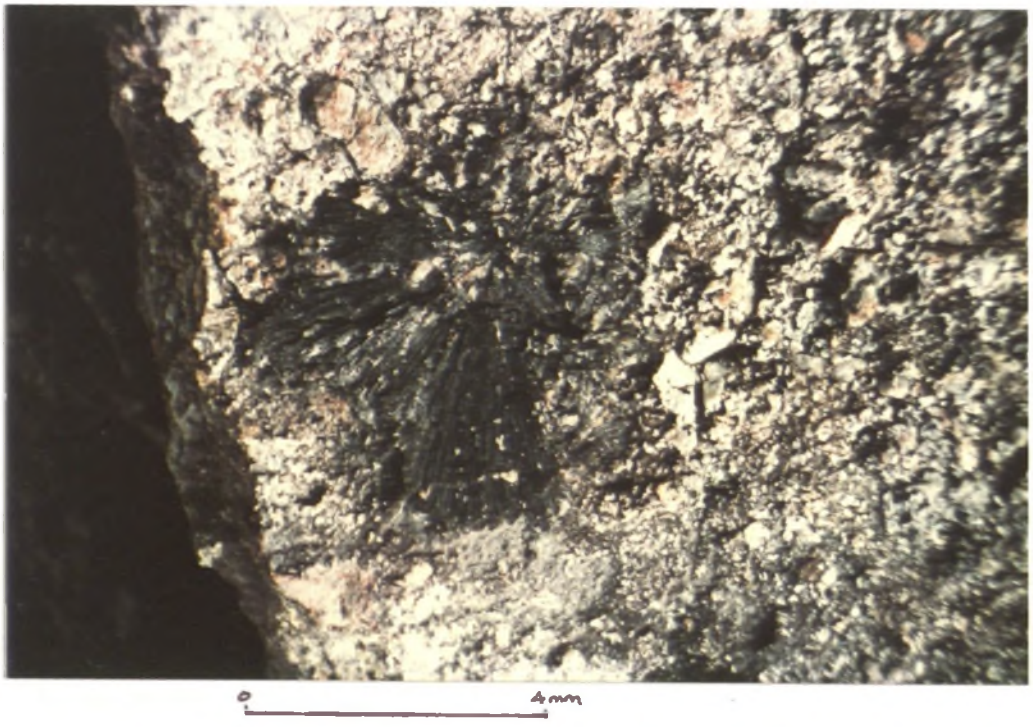

associated with late stage magmatic fluids, plate 2.2.2). Isotopic and chemical studies by Flood & Shaw (1977) and O'Neil et al (1977) show the suite to be characterised by $\delta O^{18}$ values greater than 10 but Sr87/Sr86 isotope ratios of only 0.706. These values are consistant with an origin involving partial melting of young volcanically derived meta-sedimentary rocks from a subducted trench - sedimentary wedge complex (Flood & Shaw, 1975, 1977 and Shaw & Flood, 1981, 1982 ) as a source material.

The outcrop styles of these southern Bundarra suite plutons are essentially very similar and show generally low to moderalte relief and predominantly outcrop as tors (plate 2.2.3) and less frequently as whale back style outcrops

The Banalasta Adamellite has been described by Chappell (1978) as a k-feldspar megacrystic (plate 2.2.4) pluton. Microcline is the dominant K-feldspar except near the contacts with the Permian Bendemeer, Looanga and Walcha Road plutons, where it is thermally disordered to orthoclase. Biotite occurs in this pluton predominantly as aggregates.

The pluton was observed to contain a margin parallel foliation (based on dip and strike measurements of K-feldspar megacrysts), these were determined by visual inspection in the field (map1) and at two localities (figures 2.2.1 and 2), determined by measuring the trend of long axes of 50 K-feldspar megacrysts and computer plotting rose diagrams of this data with an interval spacing of 5 degrees (adjacent pluton contact directions are also shown as a reference line).

The other 3 adjoining southern Bundarra Suite plutons differ from the Banalasta Adamellite in only very minor ways: (i) The Pringles Adamellite has a lower abundance of megacrysts and is finer grained; (ii) The Glenclair Adamellite is more silica rich and has more disseminated biotite than either the Banalasta or Pringles Plutons and (iii) The Tilmunda Granite is by definition more K-feldspar rich and is everywhere more felsic and more evngrained.

Apart from these differences the southern Bundarra suite plutons are essentially the same in nature and as such can be treated as one unit for the purpose of analysing the later contact metamorphism of these rocks in the aureole of the Permain Bendemeer Adamellite.

## A . 2 . 3 : LATE PERMIAN I-TYPE MOONBI SUITE ADAMELLITES

The Bendemeer (with a proposed age of 250 Ma, Shaw & Flood, 1981 and a bulk rock age of 265 Ma, Hensel et al, 1985) and Looanga (250 Ma, Shaw & Flood, 1981 and Hensel et al, 1985) Adamellites in the study area form part of the Moonbi I-type plutonic suite (Flood & Shaw, 1977). The suite is generally K-rich, has a Sr87/Sr86 initial isotopic ratio of 0.7045, a $\delta O^{18}$ value and a positive S value (+ 2). Shaw and Flood (1981) in a review of the New England Batholith suggest that the suite is commonly massive with minor K-feldspar megacryst flow foliation allignment and further suggest that the magma source was a large ion lithophile element-rich shoshonite. The suite comprises a

FIGURE 2.3.1 : STRIKE OF THE FOLIATION DIRECTION FOR SAMPLE MU46063 IN THE BENDEMEER ADAMELLITE, ADJACENT CONTACT DIRECTION AS SHOWN

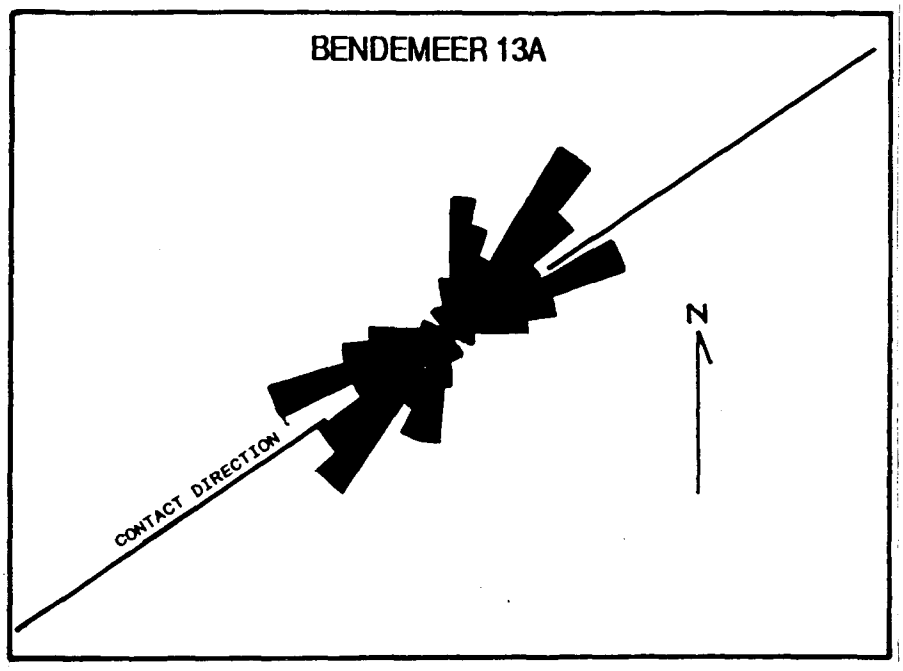


FIGURE 2.3.2 : STRIKE OF THE FOLIATION DIRECTION FOR SAMPLE MU46064 IN THE BENDEMEER ADAMELLITE, ADJACENT CONTACT DIRECTION AS SHOWN

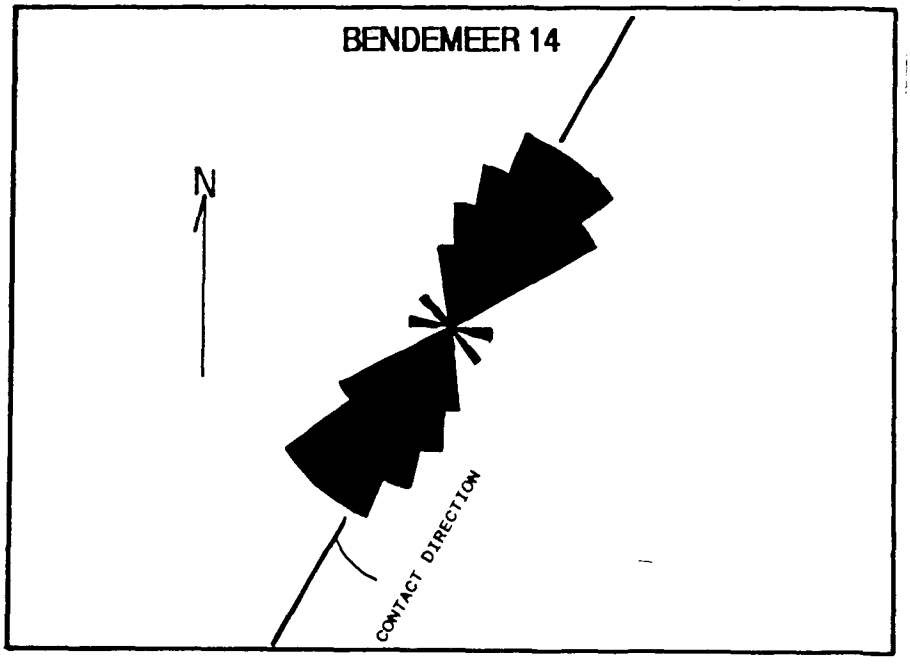

FIGURE 2.3.3 : STRIKE OF THE FOLIATION DIRECTION FOR SAMPLE MU46074 IN THE LOOANGA ADAMELLITE, ADJACENT CONTACT DIRECTION AS SHOWN

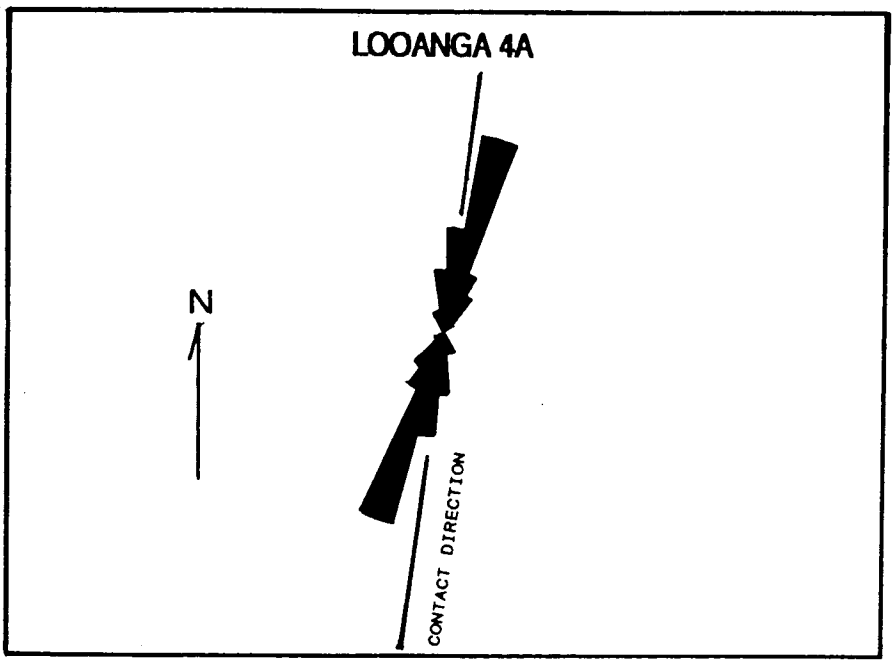

number of plutonic bodies, two of which (the Bendemeer and Looanga Adamellites) intrude the older S-type Banalasta Adamellite on its southern and south-eastern margins.

## 2 . 3 . 1 : BENDEMEER ADAMELLITE

This pluton is a biotite-hornblende adamellite of medium to coarse grainsize (0.5-2.5cm) throughout the pluton. It contains abundant potassium feldspar megacrysts (plate 2.3.1) that exhibit a strong contact - parallel lineation of the long axes near the contact(see figures 2.3.1 and 2). This fabric decreases in strength in from the contacts and at distances greater than 1 km this lineation is largely undiscernable. The contact parallel preferred orientation was measured as a foliation in one locality on the pluton's northern contact and reveals the the pluton dips steeply inwards.

Modal data (Chappell, 1978) is show in table 2.2.1. Close to the north-western contact there are numerous mafic micro - granitoid enclaves occuring both evenly distributed in the adamellite and in clusters (clusters being up to 30 cm diameter with individual microgranitoid enclaves being up to 8 cm in length).

## 2 . 3 . 2 : LOOANGA ADAMELLITE

The Looanga pluton is an I-type adamellite, is more leucocratic than the Bendemeer Adamellite and is emplaced within the Banalasta Adamellite except in the south-east where it has intruded the Woolomin Beds. It, like the Bendemeer Adamellite is a medium to coarse-grained biotite-hornblende adamellite, but differs from the Bendemeer Adamellite in that the K-feldspars are more obviuosly pink and there are fewer microgranitoid enclaves. A contact parallel lineation was observed within the meridonal elongate pluton and is still present in the pluton's core, where it has been measured as having a strong NNE-SSW orientation (figure 2.3.3). The pluton is modally similar to the Bendemeer Adamellite (table 2.2.1) and is unzoned, although showing a northern contact area that is more felsic than elsewhere and is possibly genetically related to the Bendemeer Adamellite (Chappell,1978). Its outcrop style is also similar to the Bendemeer Adamellite's and is characterised by broad low relief whale back outcrops (plate 2.3.2).

# A . CHAPTER 3 : HORNFELS

## A . 3 . 1 : STRUCTURE

Previous studies of the structural geology to the south east and west of the Bendemeer area have been performed by Lewington (1973) and Corbett (1976). Corbett proposed two main fold phases. The first generation of folds (F1) produced large scale close to isoclinal folds with an axial plane cleavage. F2 folds were described as steeply southward plunging synformal and antiformal structures. Both folding events (and the associated prehnite - pumpellyite facies regional metamorphism) have been dated as Late Carboniferous (Early Stephanian) by Roberts and Engel (1980, 1987). Later uplift in the Middle to Late Stephanian being induced by the Bundarra Plutonic Suite intrusive episode (Harrington and Korsch, 1985).

The hornfelsic rocks in the Bendemeer area are part of the Woolomin and Sandon Beds which have been described as members of an accretionary subduction complex comprising rocks of Silurian to Early Corboniferous age (Namurian) (Ishiga, 1988). These hornfelses consist of cherts, meta-basalts and siliceous meta-pelites and have been mapped to the east and west of the Bendemeer pluton.

Both F1 and F2 fold phases are observable in the Bendemeer area. F1 folds are NW - SE trending close to isoclinal folds and contain a weak discontinous axial plane cleavage. F2 folds were not observed in outcrop, but deflection of the F1 fold axes is traceable from regional trends and associated moderate to steep southerly plunges suggests a N - S compressional direction.

## A . 3 . 1a : THE WESTERN AUREOLE ( figure 3.1 and map 1 ) :

The hornfelses in this area are bordered on three sides by the Bendemeer, Banalasta and Glenclair Adamellite's, as shown in figure 3.1 and map 1. This area has two large, close, sinusoidal to chevron style folds. A stereoplot of bedding data (given in figure 3.1) reveals a moderate degree of scatter, but indicates a sub - vertical axial plane trending 124 degrees for the F1 fold phase, with moderate plunges. These differ from the steep plunges observed by Corbett (1976) and may be explained by the fact that the Bendemeer area is not affected by the Peel fault complex, which Corbett suggested was partly responsible for the steep plunges in the Woodsreef area. An alternative is that Lewington (1973) found both south and north steeply plunging folds and so what may be observed in the Bendemeer area is the southern limb of an F2 fold close to an antiformal fold nose (hence shallower plunges).

Parasitic folds have been observed in this area and vary in size from less than 2m (plates 3.1 and 3.2) to up to 10m. The parasitic folds observed, all plunge south and are close to tight and sinusoidal in style. Plate 3.1 shows slip planes have occured within these folds where the competent chert layers have moved on limb parallel glide planes.

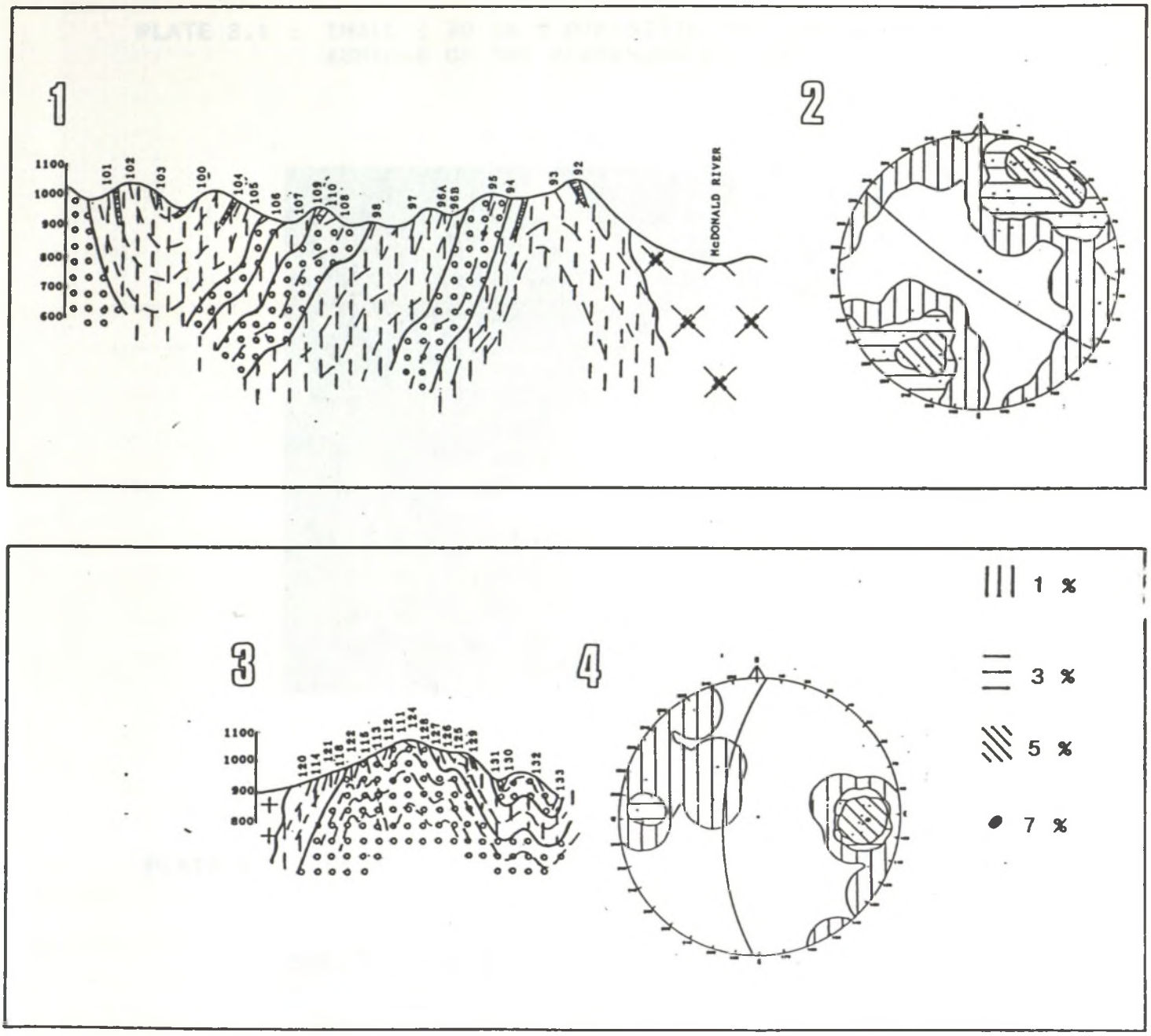


( VERTICAL SCALE SHOWN IN METRES ABOVE SEA LEVEL )

KEY : ( all numbers represent Bendemeer hornfels samples i.e. BHFnnn )

BENDEMEER ADAMELLITE

BANALASTA ADAMELLITE

SILICEOUS-PELITES

CHERTS

META-BASALTS

1 2 3 4 KM

HORIZONTAL SCALE

FIGURE 3·1
STRUCTURAL DATA FOR THE BENDEMEER AUREOLE;
A) WESTERN AUREOLE, SECTION AND STEREOPLOT
B) EASTERN AUREOLE, SECTION AND STEREOPLOT.
( THE DIPS ON THE GRANITOID INTRUSIONS ARE BASED UPON MEGACRYST FOLIATION MEASUREMENTS )

PLATE 3.1 : SMALL ( 30 cm ) PARASITIC FOLD FROM THE WESTERN AUREOLE OF THE BENDEMEER PLUTON.

PLATE 3.2 : METRE SCALE PARASITIC FOLD ( 1.5 m ) IN THE WESTERN AUREOLE OF THE BENDEMEER PLUTON.

These were also observed in the Limbri district by lewington (1973). Associated with this slippage, slickensides wrere observed in the long limbs of the larger parasitic folds and suggest movement towards the fold noses.

## A . 3 . 1b : THE EASTERN AUREOLE (FIGURE 3.1 AND MAP 1)

The hornfels in this area formed adjacent to the Bendemeer and Banalasta adamellités to the west and the Looanga and Banalasta adamellites to the north and west. Bedding measurements ( figure 3.1 and map 1) reveal an anticline to the west and syncline to the east, both of which plunge at moderate angles (up to 40 degrees) to the south south west. The stereoplot in figure 3.1 also reveals that the anticline's axial plane is steeply inclined, dipping approximately 68 degrees to the west on a trend of 183 degrees. No outcrop scale parasitic folds were observed in the field but vergence relationships identified a number parasitic folds of 10's metres in size. The fold style is similar to the western area, being open to close, predominantly sinusoidal small scale folds (their form being controlled by the competency of the cherts and siliceous mudstones). Similar slickensides to those found in the western aureole were observed and show the same movement direction up to fold noses on the long limbs of mapped parasitic folds.

In both the western and eastern areas, folds appear to maintain their style right up to the sharp intrusive contacts. This, coupled with parasitic folds within 10m of the Bendmeer Adamellite's contact, maintaining of primary bedding structures and no significant emplacement induced deformation in the eastern aureole where it lenses between the Bendemeer and Walcha Road Adamellites, are consistant with an intrusive mechanism whereby the later intrusives have imposed little deformation.

# A . 3 . 2 : META-BASALTS :

## 3 . 2 . 1 : INTRODUCTION

A large number of studies have focussed on the metamorphism of basaltic rocks (either in contact or regional terrains) including those of Binns (1965, 1966), Leake (1965, 1968), Shido & Miyashiro (1959), Sobolev (1970), Liou et al (1974, 1983). This analysis of the changes in microstructure, mineralogy and composition of the concordant meta-basalts associated with deep water metasediments in the aureole of the Bendemeer Adamellite (figure 3.2.1) is largely based on the findings of Binns (1966) for similar metabasalts in the aureole of the Moonbi Adamellite 20km to the south.

Binns (1966) found that with increasing contact metamorphic grade, calciferous amphiboles changed from a pale blue - green variety with a ragged - fibrous actinolitic habit, through a deep blue - green to green variety with ragged habit to a brown - green to tan granoblastic hornblende. He also found that with increasing grade, titanium and alkali contents noticeably increased.

The initial examination of the metabasalts in the Bendemeer area was based on the assumption that the highest grade in each sample was due to the thermal effects of the Bendemeer Adamellite. Initial observations of field samples confirmed such an assumption as in no sample is the grade induced by the Banalasta Adamellite ever as high as that caused by the Bendemeer Adamellite. Thus it would seem fair to conclude that analyses of the Bendemeer metabasaltic samples should reveal an amphibole metamorphic zonation similar to Binns' for his Moonbi study area.

Nevertheless, examination of the metabasaltic amphiboles in the Bendemeer area does not reveal the expected Binns - style zonation and hence the Bendemeer area will be re-evaluated in the light of this examination and those results obtained from chapter 4.1 for the Banalasta Adamellite.

## 3 . 2 . 2 : WHOLE ROCK ANALYSIS

The results of a whole rock examination obtained by electron microprobe analysis of melt samples (as outlined by Gulson (1967) and Reed (1969), see appendix 1 for methods) and the calculated CIPW norms are given in table 3.2.1 and plotted in figures 3.2.2 and 3. On the normative mineral diagram (Irvine and Barager, 1971) these metabasalts plot within the alkali olivine basalt compositional field with the outlier MU45964 being due to a heavily veined sample. The associated concordant deepwater sediments, the metabasalts' fibrous variolitic style plagioclase and the fact that they plot in the same field as the submarine basaltic glasses analysed by Bryan and Moore (1977), suggest that they were either deep submarine sills or extrusive pillow basalts. Limited exposure of the contacts of these units does not permit confirmation of their mode of origin.

FIGURE 3.2.1 : LOCATION OF METABASALTIC SAMPLES ADJACENT TO THE BENDEMEER ADAMELLITE

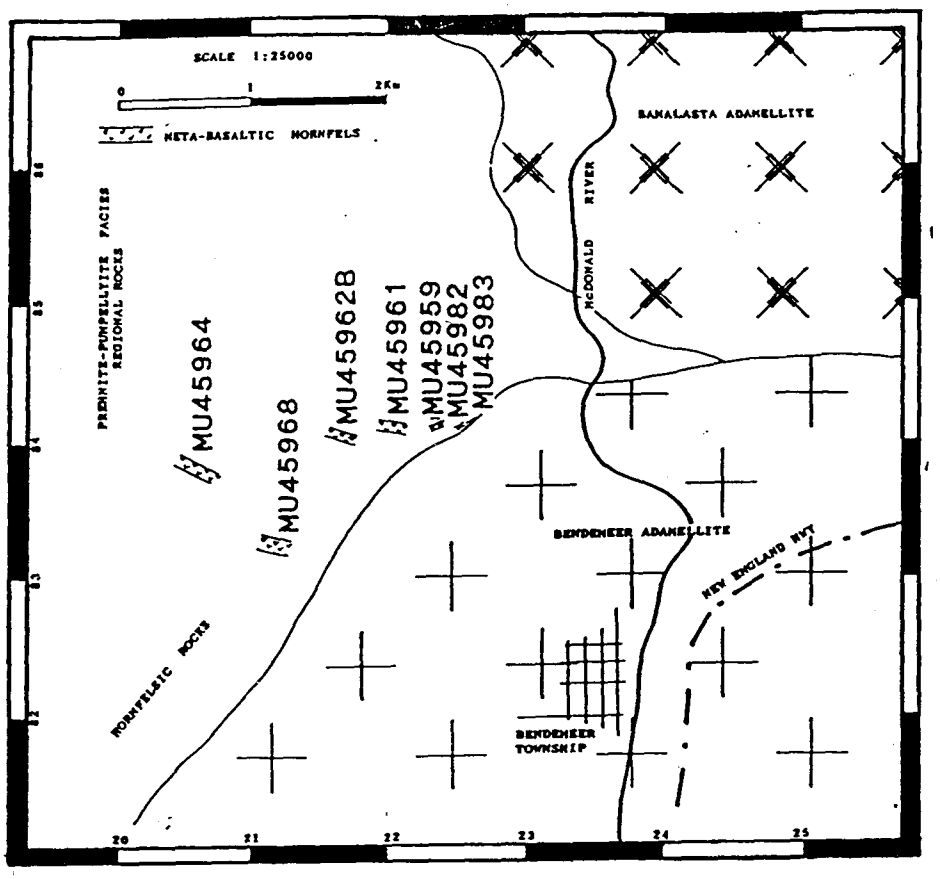


FIGURE 3.2.2 : NORMATIVE MINERAL PLOT FOR THE METABASALTIC SAMPLES IN THE BENDEMEER AREA

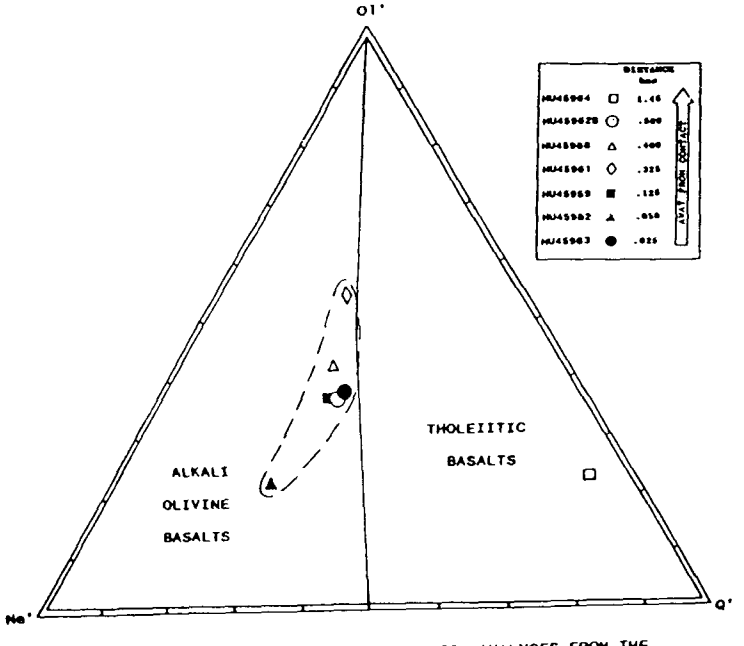


FIGURE : AFM DIAGRAM OF THE BULK ROCK ANALYSES FROM THE BENDEMEER META-BASALTIC SAMPLES.

FIGURE 3.2.3 : A F C DIAGRAM OF THE BULK ROCK ANALYSES FROM THE BENDEMEER METABASALTIC SAMPLES

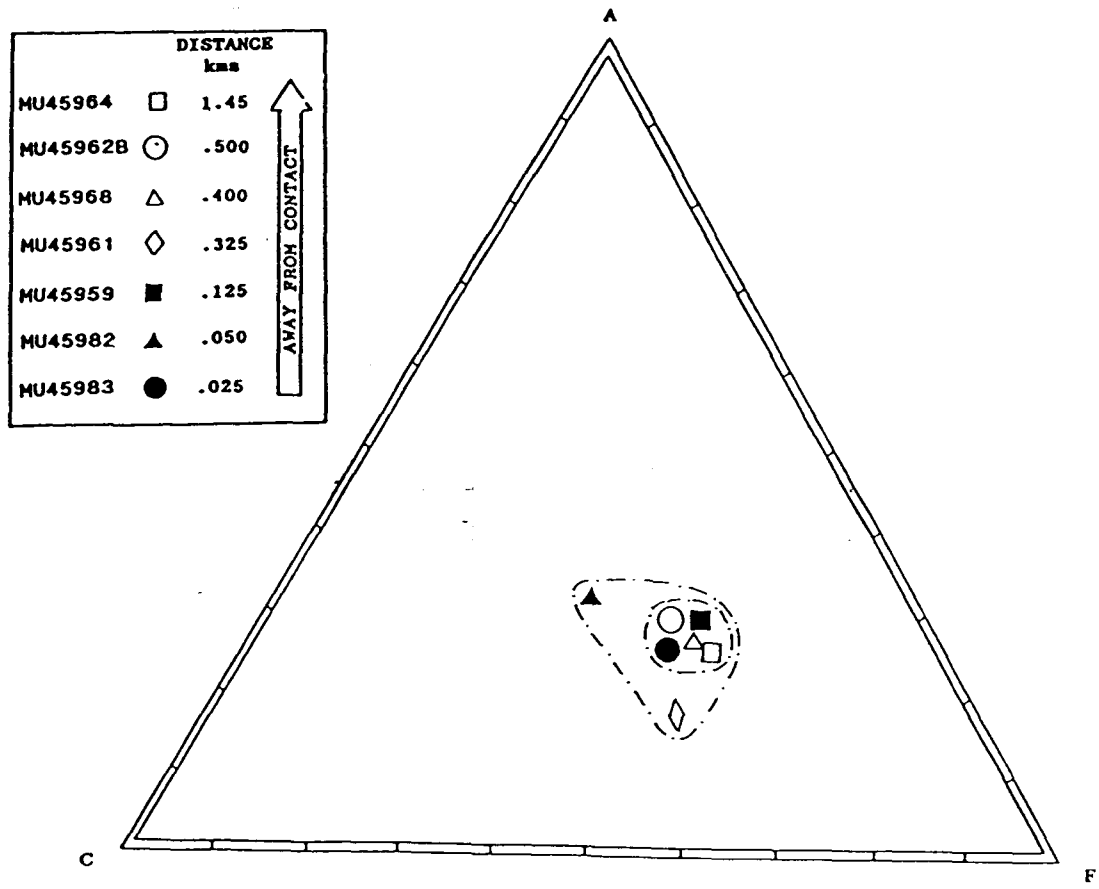

TABLE 3.2.1 : WHOLE ROCK ANALYSES AND CIPW NORMS FOR THE 7 METABASALTIC SAMPLES IN THE AUREOLE OF THE BENDEMEER ADAMELLITE

| SAMPLE | MU45964 | MU45962 | MU45968 | MU45961 | MU45959 | MU45982 | MU45983 |
|---|---|---|---|---|---|---|---|
| SiO2 | 66.71 | 51.71 | 50.38 | 49.52 | 50.11 | 48.19 | 50.05 |
| TiO2 | 0.97 | 0.95 | 1.02 | 1.29 | 1.18 | 1.26 | 0.95 |
| Al2O3 | 7.74 | 15.22 | 14.48 | 14.55 | 14.45 | 16.77 | 14.17 |
| Fe2O3 | 1.54 | 1.59 | 1.59 | 1.77 | 1.75 | 1.26 | 1.62 |
| FeO | 8.53 | 7.80 | 8.80 | 9.81 | 9.73 | 6.97 | 9.00 |
| MnO | 0.77 | 0.24 | 0.20 | 0.22 | 0.20 | 0.18 | 0.00 |
| MgO | 5.03 | 8.00 | 8.92 | 8.32 | 7.56 | 5.57 | 8.82 |
| CaO | 7.05 | 10.64 | 10.55 | 12.99 | 10.18 | 14.00 | 12.36 |
| Na2O | 0.73 | 3.23 | 2.96 | 1.52 | 3.67 | 3.19 | 2.63 |
| K2O | 0.24 | 0.64 | 0.28 | 0.13 | 0.21 | 0.64 | .0.29 |
| TOTAL | 99.37 | 100.02 | 99.18 | 100.12 | 100.04 | 98.03 | 99.89 |
| Q | 36.39 | 0.00 | 0.00 | 0.11 | 0.00 | 0.00 | 0.00 |
| Or | 1.42 | 3.78 | 1.65 | 0.77 | 1.24 | 3.78 | 1.71 |
| Ab | 6.18 | 27.32 | 25.04 | 12.86 | 30.82 | 16.26 | 22.25 |
| Ne | 0.00 | 0.00 | 0.00 | 0.00 | 0.12 | 5.81 | 0.00 |
| An | 17.13 | 25.13 | 25.39 | 32.49 | 25.06 | 29.54 | 26.00 |
| Di | 14.82 | 22.49 | 21.93 | 26.14 | 20.88 | 32.66 | 28.77 |
| Hy | 19.37 | 7.38 | 9.86 | 22.74 | 0.00 | 0.00 | 4.84 |
| Ol | 0.00 | 9.81 | 11.06 | 0.00 | 17.14 | 5.76 | 12.17 |
| Mt | 2.23 | 2.31 | 2.31 | 2.57 | 2.54 | 1.83 | 1.35 |
| Il | 1.84 | 1.80 | 1.94 | 2.45 | 2.24 | 2.39 | 1.80 |
| TOTAL | 99.38 | 100.02 | 99.18 | 100.12 | 100.04 | 98.03 | 99.89 |

The AFC diagram confirms that these rocks plot with essentially basaltic bulkrock compositions, with two of the samples (MU45961 and MU45982) acting as outliers in an otherwise narrow compositional field. Leake (1968) proposed that under ideal conditions, hornblende and plagioclase in metabasaltic rocks are excellent indicators of metamorphic grade, but that their use as grade indicators can be limited by the dependance upon a precise knowlege of bulk rock chemistry. As the metabasalts in the Bendemeer Adamellite's aureole plot with a moderate degree of chemical uniformity regardless of metamorphic grade it would seem that there might only be minor metasomatism associated with the pluton emplacement (MU45983 showing weak alteration associated with veining). Therefore the changes in the chemistry of the hornblendes and plagioclases may potentially be used as effective grade indicators.

## 3 . 2 . 3 : MINERALOGY AND MICROSTRUCTURES

The basic hornfelses sampled from the Bendemeer Adamellite's aureole all consist of plagioclase and amphibole with minor opaque oxides, sphene, epidote and vein minerals of epidote, calcite, quartz and chlorite ( garnet and diopside at higher grades ).

### 3 . 2 . 3a : Plagioclase

The plagioclases occur as elongate laths (plate 3.2.4) with high length to width ratios (up to 20:1) and their distribution throughout the rock is similar to a primary variolitic fabric suggesting a once glassy rock.

The plagioclase grain shapes show little variation with grade, laths occuring at all grades. However with increasing grade fine grained granoblastic plagioclase increases in abundance, similar to that observed by Binns (1966) in the aureole of the Moonbi Adamellite 20 km to the south. Deformation twins are evident in plagioclases from 1km to 300m from the contact whereas subgrain developement is evident, albeit in low abundance, within 50m of the contact (MU45982 and MU45983).

The metabasaltic plagioclases do not reveal significant systematic compositional variation with grade and this can be seen in the quite variable compositons of plagioclases in table 3.2.2. This finding is the same as those of Binns (1966) for the metabasaltic plagioclases in the Moonbi Adamellite's aureole.

### 3 . 2 . 3b : Amphiboles

#### 3 . 2 . 3b ( I ) : INTRODUCTION

Variations in amphibole colour, habit and composition at different matamorphic grades is by no means a new concept. Early workers such as Winchell (1941) and Shido and Miyashiro (1959) recognised the importance of coupled substitutions and colour-compositional relationships in amphiboles in metabasalts. The most detailed analyses that linked composition and colour in a regional metamorphic setting are those of Binns (1965) in the Broken

TABLE 3.2.2 : PLAGIOCLASE PROBE ANALYSES FOR THE BENDEMEER AUREOLE METABASALTS

| | MU45962B | MU45968 | MU45961 | MU45961 | MU45959 |
|---|---|---|---|---|---|
| | % | % | % | % | % |
| SiO2 | 61.29 | 56.71 | 52.36 | 51.49 | 59.39 |
| Al2O3 | 25.50 | 26.36 | 30.87 | 30.51 | 25.37 |
| CaO | 6.86 | 9.17 | 14.81 | 13.54 | 7.02 |
| Na2O | 7.25 | 6.40 | 1.90 | 3.73 | 7.74 |
| K2O | 0.08 | 0.06 | 0.17 | 0.03 | 0.03 |
| TOTAL | 100.69 | 98.70 | 100.11 | 99.30 | 99.55 |

| | MU45959 | MU45959 | MU45982 | MU45982 | MU45983 |
|---|---|---|---|---|---|
| | % | % | % | % | % |
| SiO2 | 60.95 | 59.14 | 55.89 | 57.71 | 63.05 |
| Al2O3 | 24.88 | 24.99 | 27.50 | 27.57 | 22.36 |
| CaO | 6.35 | 6.84 | 9.78 | 9.86 | 4.57 |
| Na2O | 8.34 | 7.86 | 6.27 | 6.23 | 8.74 |
| K2O | 0.07 | 0.05 | 0.07 | 0.22 | 0.04 |
| TOTAL | 100.59 | 98.87 | 99.51 | 101.49 | 98.75 |

Hill district and Leake (1965, 1968) in Ireland. These variations with grade were confirmed experimentally by Liou et al (1974, 1983) in work on regional metamorphic rocks in Vancouver Island and the Juan De Fuca Ridge.

Although, few studies have been made of these colour and habit variations in contact metamorphic aureoles, Binns (1966) proposed that amphibole colour and habit could be used as grade indicators and found that total alkali, titanium and aluminium contents increased and the Mg-number decreased with increase in contact metamorphic grade.

## 3 . 2 . 3b ( ii ) : COLOUR-TEXTURAL VARIATION

1. Textural variations: A textural variation occurring with grade was first documented by Binns (1965) in the greenschists, amphibolites and granulites at Broken Hill and in the hornfelses from the New England Orogen (1966). He noted a variation from low grade fibrous/ragged actinolite to fibrous, less-ragged, semi- granoblastic hornblende, to the highest grade predominantly granoblastic hornblende. Additional studies (Liou et al, 1974 & 1983; Leake,1965 & 1968) suggest that these fibrous, ragged and granoblastic habits are primarily a function of temperature increase.

The microstructures observed in the metabasaltic amphiboles from the Bendemeer aureole show a less simple variation with grade. Even though it is possible to observe fibrous amphiboles at the lowest grades (plate 3.2.1), ragged amphibole at intermediate grade (plate 3.2.2) and granoblastic amphibole at the highest grade (plate 3.2.3) (where increasing grade is a function of distance from the later intrusive contact), the most common habit occuring at all grades is ragged.

If it is assumed that the textural variations with grade documented by Binns (1966) and confirmed by others (cited above) should apply to the Bendemeer area, then a feasible solution to the anomalous behaviour of habit is that the occurance of prograde habits in the Bendemeer aureole have been overprinted by an intermediate grade ragged habit. No post - Carboniferous regional metamorphism has ever been recorded in these rocks and this would suggest that the ragged habit is peculiar to the western aureole of the Bendemeer Adamellite and may well represent an overprinting of grade by a blind pluton (see section 4.1). This will be discussed in more detail later.

2. Colour: Colour variation as a function of metamorphic grade has been documented by Wiseman (1934). Shido and Miyashiro (1959), Binns (1965, 1966) and Leake (1965). Leake suggested that this colour variation was largely temperature dependent in regional metamorphic facies. Binns (1966) confirmed this temperature dependence in a contact metamorphic terrain and further suggested that colour was a function of titanium contents.

The colour variation observed in the Bendemeer aureole amphiboles is by no means characterised by abrupt changes but shows a gradual colour variation with distance from the contact. At distances greater than 1.5 km the

PLATE 3.2.1 : RAGGED AND MINOR FIBROUS (TOP LEFT) BLUE GREEN ACTINOLITIC HORNBLENDES (MU45962)

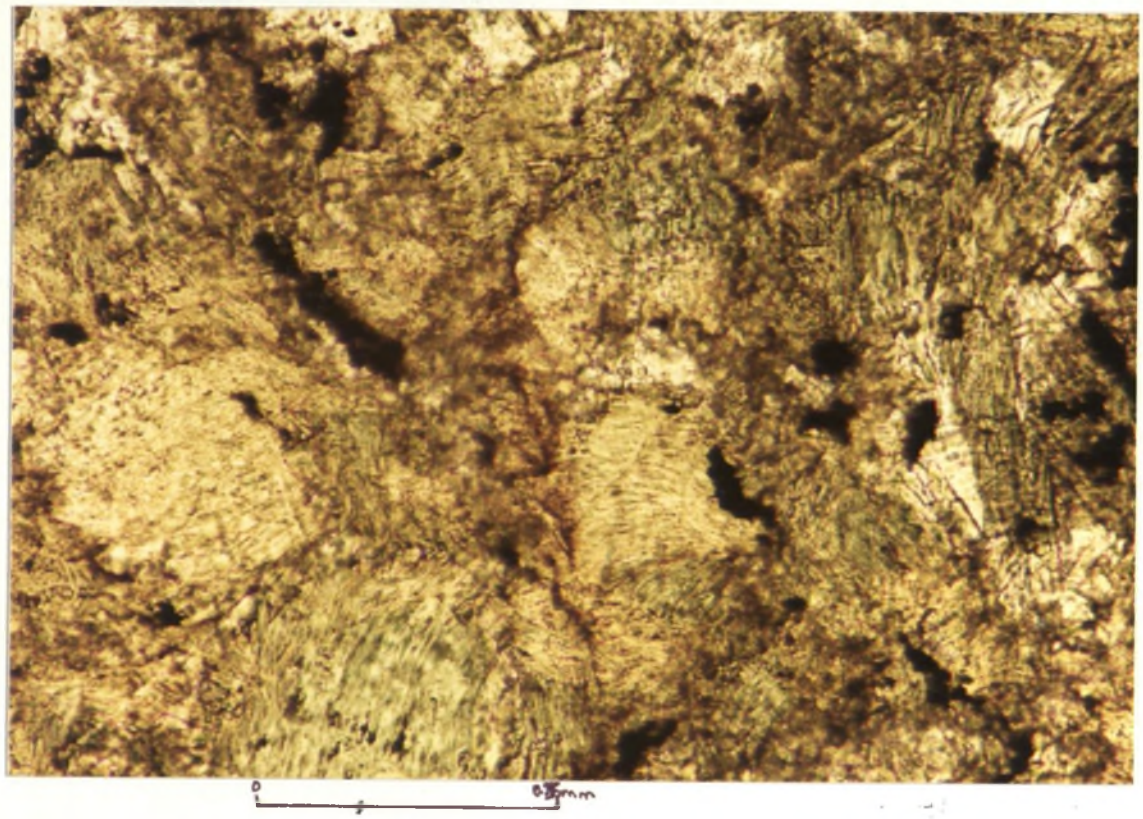

PLATE 3.2.2 : RAGGED PALE BLUE GREEN - YELLOW GREEN TO GREEN MAGNESIO - HORNBLENDE (MU45961)

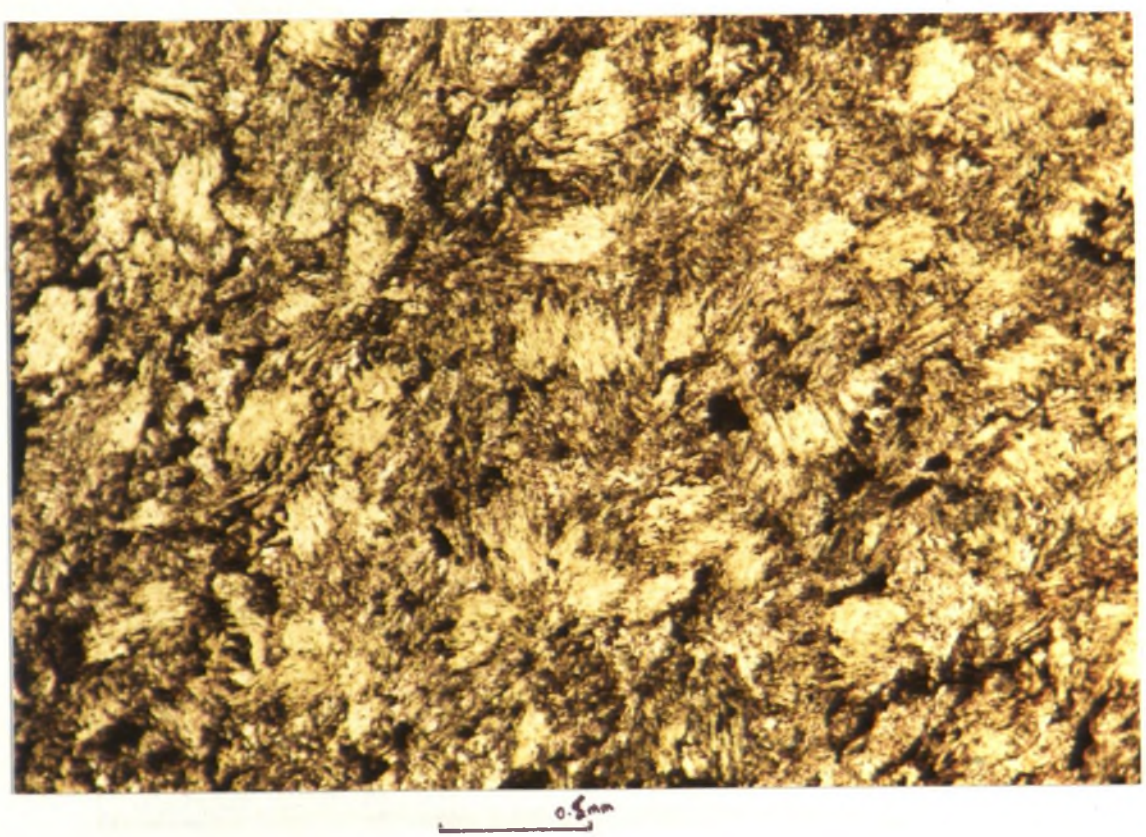

PLATE 3.2.3 : GRANOBLASTIC OLIVE GREEN TO BROWN TSCHERMAKITIC HORNBLENDE (MU45982)

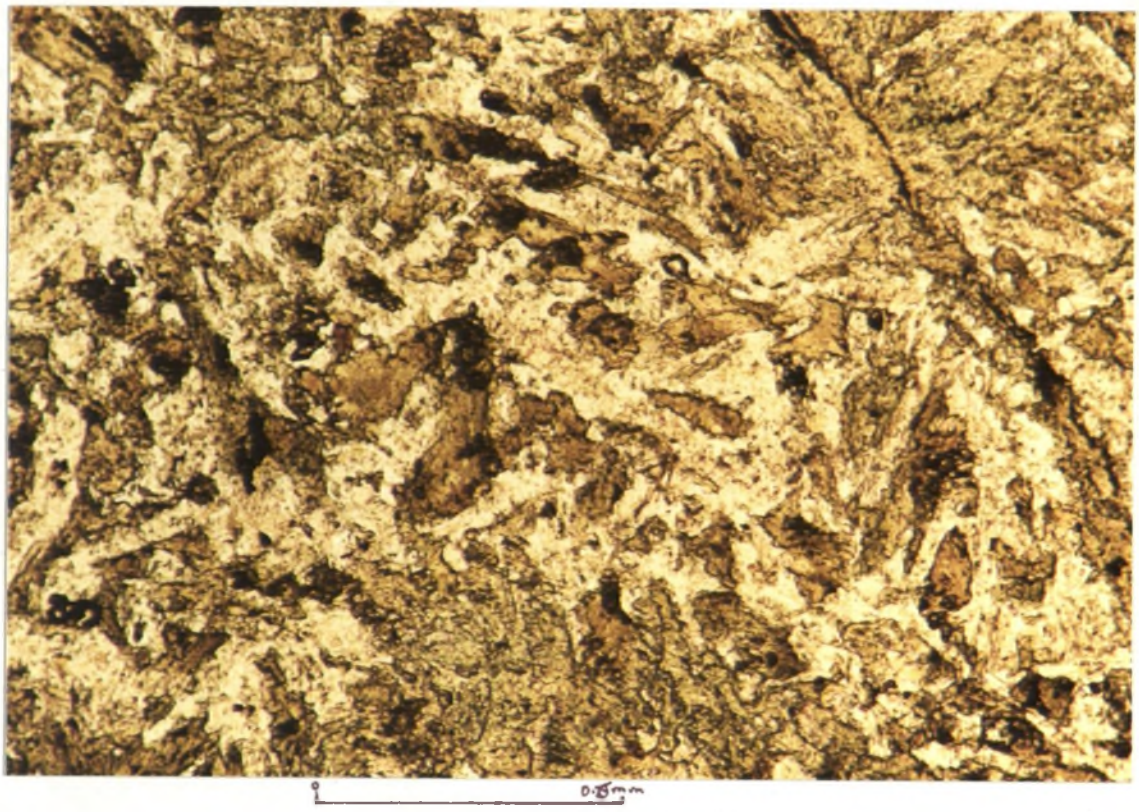

PLATE 3.2.4 : A. (LHS) PREDOMINANTLY GREEN TO BROWN GREEN COLOUR WEAKLY GRANOBLASTIC MICROSTRUCTURE (MU45982)
B. (RHS) STRONG TAN - BROWN AMPHIBOLE COLOUR AND PARTIAL GRANOBLASTIC CHARACTER (MU45983)

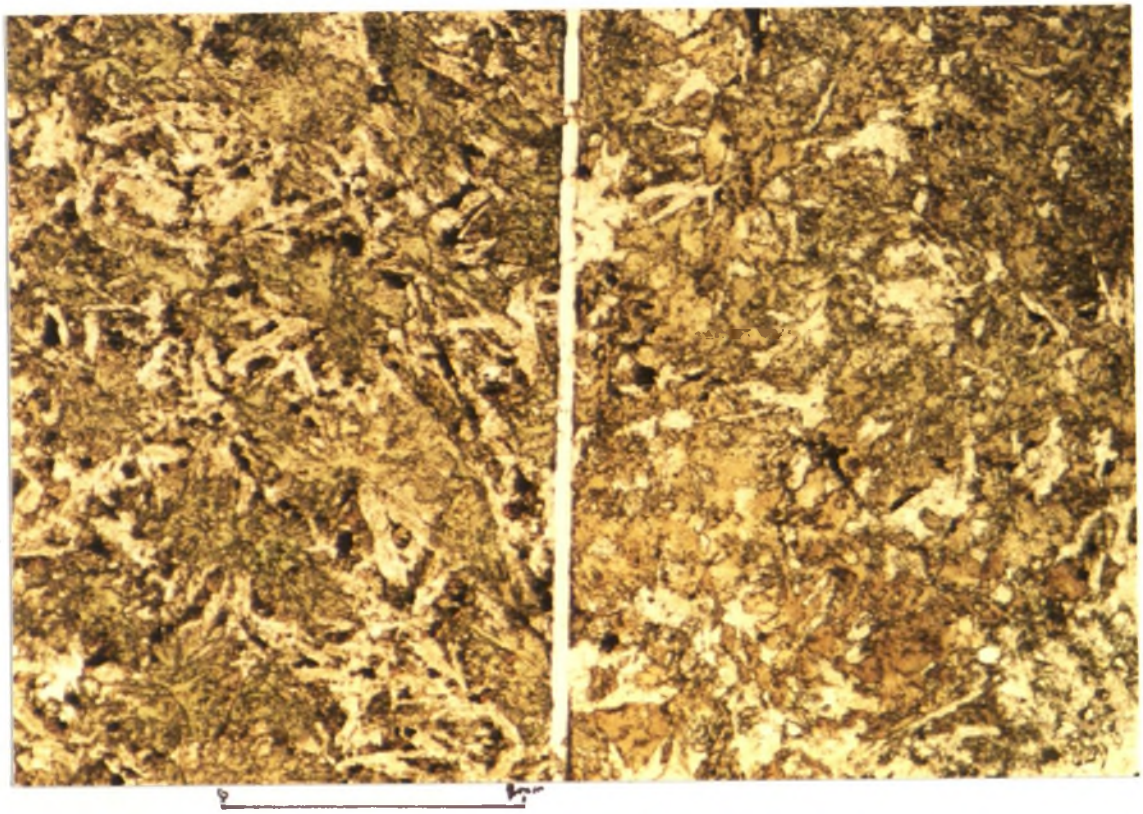

PLATE 3.2.5 : PREDOMINANTLY GREEN +- BLUE-GREEN TINGE FOR INTERMEDIATE ZONE AMPHIBOLE (MU45968)

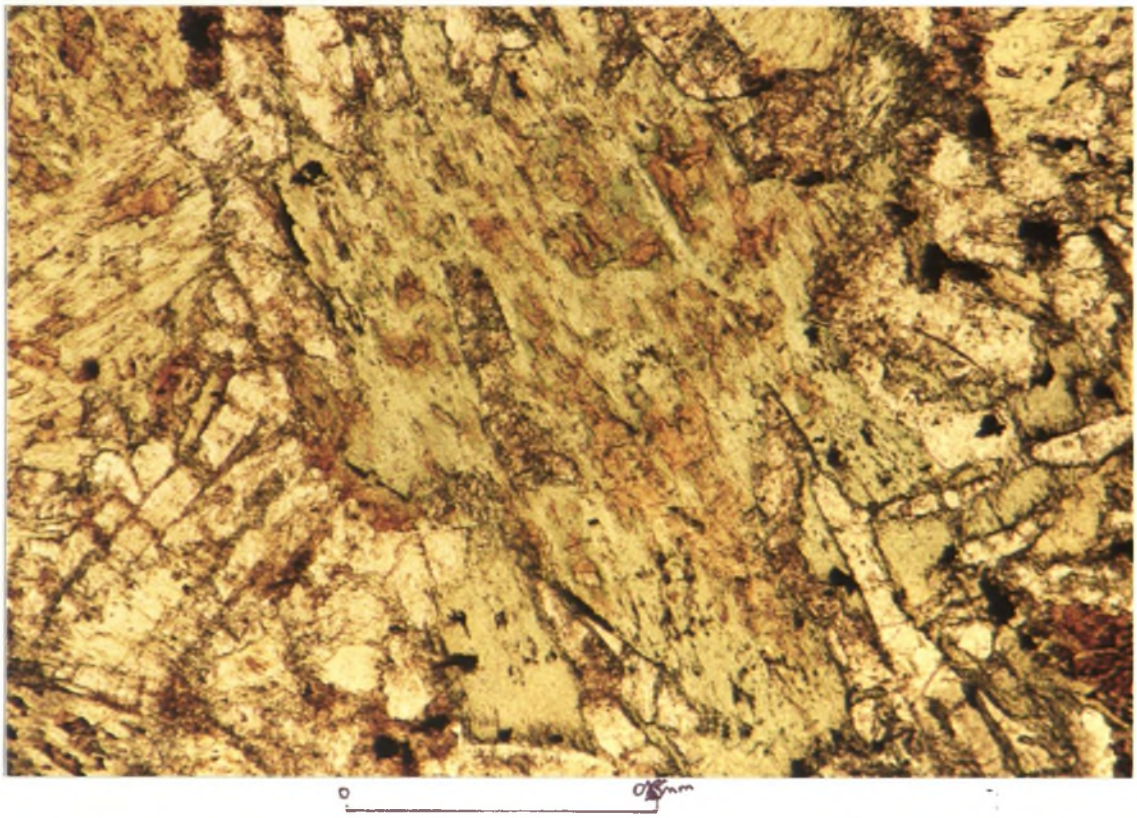

amphiboles are chiefly blue-green in colour (plate 3.2.1); between 200 m and 1.5 km the predominant colour is green (plates 3.2.5 and 4a) and at distances less than 200 m (and especially 2 m) the brown hornblendes appear (plate 3.2.4b). This brown hornblende in samples MU45982 and MU45983 is associated with the occurrence of simple twinned neoblasts of orthoclase, suggesting a correlation with the K-feldspar-cordierite hornfels facies(Winkler, 1967).

Although a colour zonation is evident, all samples (except MU45983) show a high proportion of green hornblende (table 3.2.3). Therefore the simple grade - colour relationship determined by Binns (1966) does not seem directly applicable to the meta-basaltic amphiboles in the Bendemeer area. If, however the observation of green hornblende is omitted from the samples, Binns' grade - colour relationship can at least be broadly applied. This would suggest that again an overprinting event might best explain this apparent anomalous behaviour of the amphiboles in this area.

## 3 . 2 . 3b ( III ) : COMPOSITION

In the light of these colour and habit variations, 111 analyses of the amphiboles from the seven metabasaltic samples were determined from the electron microprobe. An average for each sample is given in table 3.2.4 (all analyses are given in appendix 2) and all analyses are plotted in figures 3.2.4 to 7.

These compositional plots show general linear increases in titanium and alkali contents and associated decreases in silica and Mg - number with increasing grade. However, these can only be regarded as broad trends and more importantly all samples contain a range of amphibole compositions. If this internal compositional range was due to retrograde sliding reactions associated with the coolling of the Bendemeer Adamellite then one might expect that the compositional range in any one sample might decrease with decreasing grade. This is true for the high and intermediate grades but reverses with still lower grades.

As has been outlined in chapter 4.1 there is triclinicity evidence suggesting that a blind pluton exists to the north west of these metabasaltic samples (figure 4.1.4). The size and depth of this pluton cannot be determined accurately but the triclinicity contours suggest a small elongate pluton and hence maybe quite shallow to produce such an effect upon K-feldspar disordering.

If the proposed blind pluton is shown diagramatically in relation to the metabasaltic samples, then it is possible that all the various grade samples in the Bendemeer aureole have been overprinted by an intermediate grade effect induced by the blind pluton. If this is correct then it would account for the dominance of ragged, green to blue-green magnesio-hornblende in most samples and for the variation in compositional range. The lowest grade is overprinted by an intermediate grade (producing large ranges), the intermediate grade is overprinted by the same grade

TABLE 3.2.3 : AMPHIBOLE COLOUR VARIATION WITH DISTANCE TO THE BENDEMEER PLUTON'S CONTACT. PLEOCHROIC COLOURS FOR THE ALPHA, BETA AND GAMMA DIRECTIONS ARE GIVEN FOR EACH SAMPLE AND THE DISTANCES FROM THE INTRUSIVE CONTACT

| SAMPLE | MU45964 | MU45962B | MU45968 | MU45961 | MU45959 | MU45982 | MU45983 |
|---|---|---|---|---|---|---|---|
| A | PALE YELLOW GREEN | PALE YELLOW | PALE YELLOW GREEN | PALE YELLOW GREEN | PALE YELLOW GREEN | PALE YELLOW GREEN | STRAW YELLOW GREEN |
| B | PALE GREEN | PALE YELLOW GREEN | PALE YELLOW GREEN -PALE OLIVE | PALE OLIVE -PALE GREEN | OLIVE GREEN | BROWN TAN -BROWN GREEN | BROWN TAN |
| C | PALE BLUE GREEN COLOUR-LESS | PALE BLUE GREEN | PALE BLUE GREEN | STRONG BLUE GREEN | GREEN-BLUE GREEN | BROWN GREEN -GREEN | BROWN GREEN TAN GREEN |
| KM FROM CONTACT | 1.45 | 0.5 | 0.4 | 0.325 | 0.125 | 0.05 | 0.025 |

TABLE 3.2.4 : AVERAGE ANALYSES FOR THE METABASALTIC AMPHIBOLES FROM THE BENDEMEER AUREOLE

| SAMPLE | MU45964 | MU45962 | MU45968 | MU45961 | MU45959 | MU45982 | MU45983 |
|---|---|---|---|---|---|---|---|
| SiO2 | 51.99 | 49.02 | 47.51 | 51.24 | 48.59 | 42.29 | 46.73 |
| TiO2 | 0.17 | 0.36 | 0.64 | 0.25 | 0.58 | 1.43 | 0.95 |
| Al2O3 | 5.78 | 8.09 | 9.81 | 6.50 | 7.77 | 12.98 | 7.25 |
| FeO | 19.05 | 14.85 | 14.71 | 15.06 | 17.20 | 15.53 | 15.65 |
| MnO | 1.32 | 0.48 | 0.23 | 0.25 | 0.23 | 0.28 | 0.18 |
| MgO | 10.78 | 12.75 | 12.27 | 12.27 | 12.45 | 9.27 | 12.74 |
| CaO | 11.80 | 12.56 | 12.19 | 12.10 | 12.16 | 12.14 | 12.12 |
| Na2O | 0.36 | 0.85 | 1.84 | 0.58 | 1.45 | 2.23 | 1.41 |
| K2O | 0.09 | 0.29 | 0.21 | 0.14 | 0.15 | 1.18 | 0.29 |
| TOTAL | 101.33 | 99.23 | 99.41 | 98.39 | 100.58 | 97.31 | 96.32 |

FIGURE 3.2.4 : PLOT OF SILICA IN THE UNIT CELL AGAINST Mg - NUMBER FOR THE METABASALTIC AMPHIBOLES, BASED ON THE CLASSIFICATION BY Leake, 1968

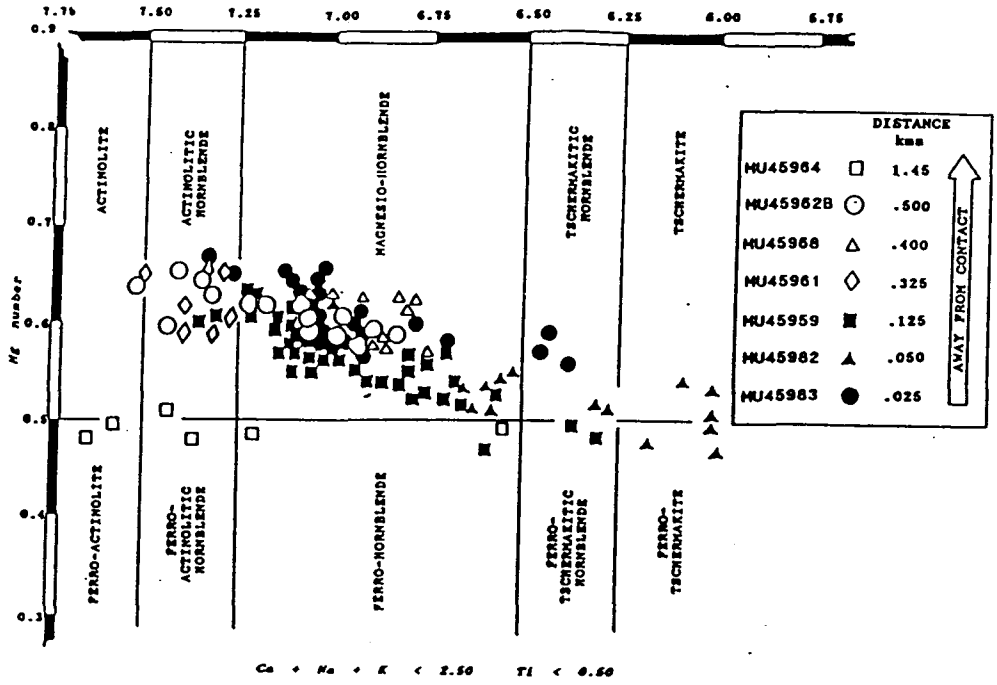


FIGURE 3.2.5 : PLOT OF NET ALKALI CONTENT AGAINST ALUMINIUM - NET ALKALI (after Sobolev, 1970)

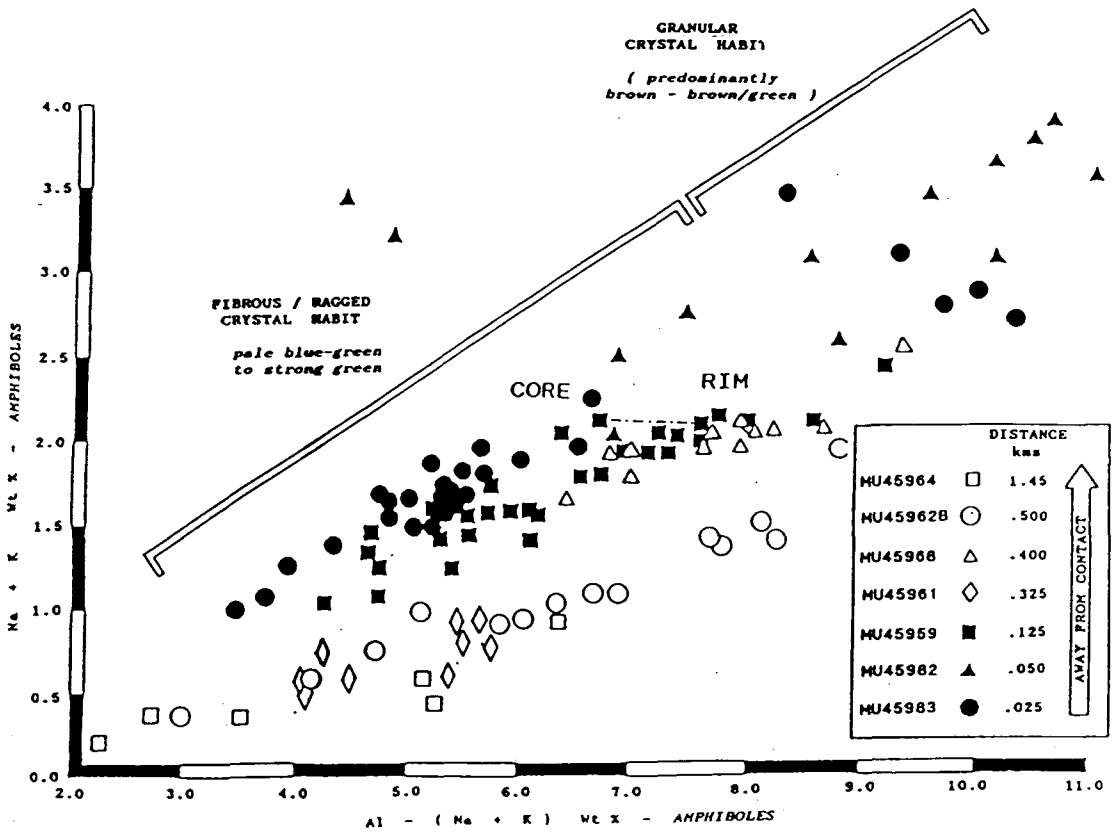

FIGURE 3.2.6 : PLOT OF ALKALI AGAINST TITANIUM WT % FOR THE BENDEMEER AREA METABASALTIC AMPHIBOLES (Leake, 1968)

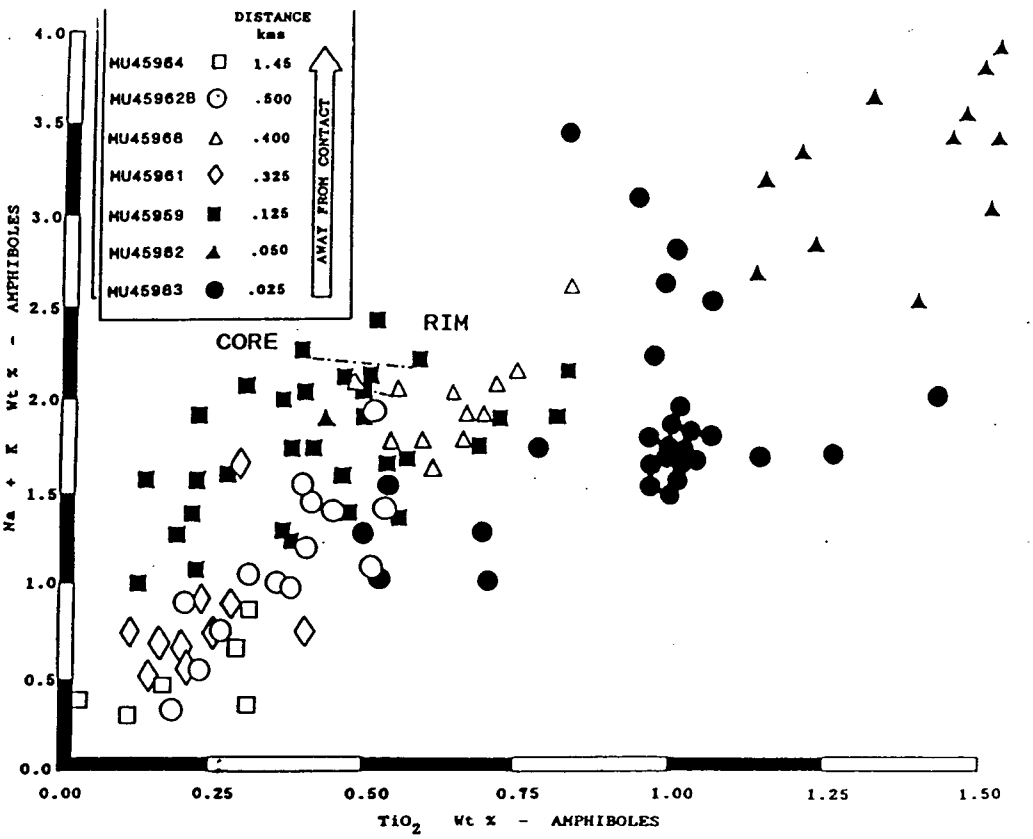


FIGURE 3.2.7 : PLOT OF THE METABASALTIC AMPHIBOLE'S SODIC/CALCIC AGAINST ALUMINIUM/SILICA EXCHANGES (Leake,1965 & Sobolev, 1970)

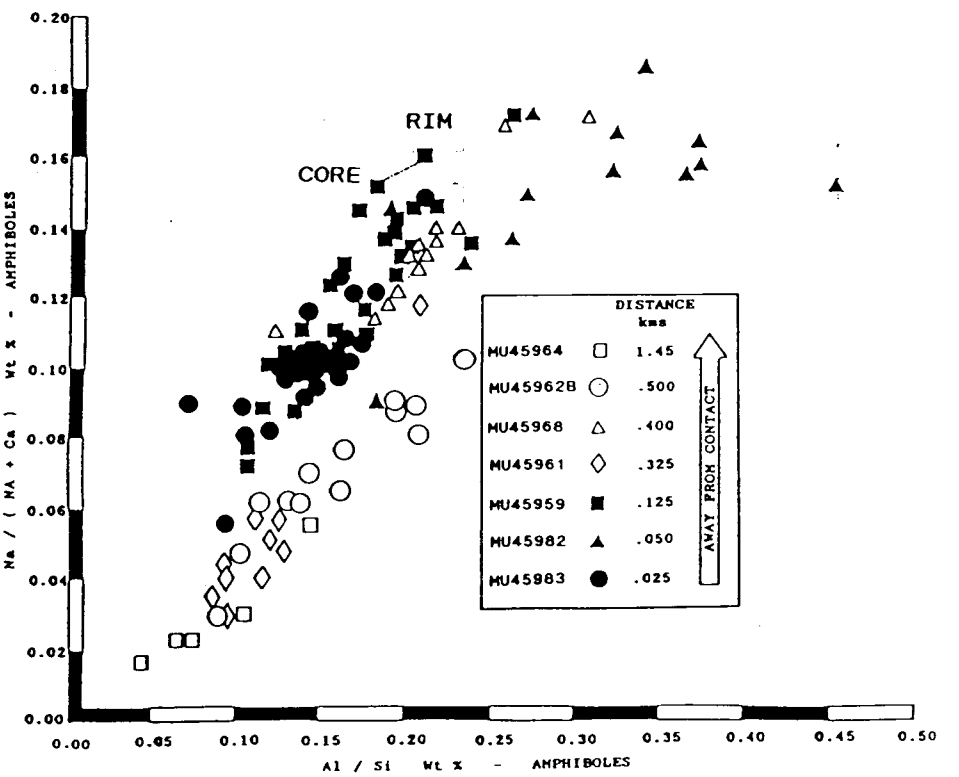

(producing small compositional ranges) and the highest grade is overprinted by an intermediate to low grade (producing the greatest compositional variation). This is shown diagramatically in figure 3.2.8 looking SSW along the studied area and revealling the proposed blind pluton.

As is apparent, a great deal more work is required to critically evaluate such a proposition of thermal overprinting and was not possible within the time constraints of this thesis. However, if this hypothesis proves correct then it can be concluded that this blind pluton is younger than both the Banalasta and Bendemeer adamellites.

## 3 . 2 . 3b ( iv ) : METAMORPHIC ZONATION

If the proposed intermediate grade thermal overprinting is removed, then it is possible to estimate three grade zones determined from colour, microstructural and compositional criteria.

### I. LOW GRADE ZONE : (0.5 to 1.5 km from contact) (upper albite-epidote facies)

This zone is characterised by amphiboles of a predominantly pale blue - green to pale yellow - green colour (table 3.2.3), a fibrous to ragged habit and the assemblage actinolitic hornblende, plagioclase, epidote, sphene and oxides.

The amphiboles plot in the actinolitic hornblende field (figure 3.2.4), have low alkali contents ( 1.5 wt % , figure 3.2.5), low titanium contents (generally 0.5 wt %, figure 3.2.6) and low sodic - aluminium exchange values ( 0.2 Al/Si wt % and 0.08 Na/(Na + Ca) wt %, figure 3.2.7). No metabasaltic samples were found at distances greater than 1.5 km and so purely regional assemblages cannot be determined.

### II. INTERMEDIATE GRADE ZONE : (0.1 to 0.5 km) (low to middle hornblende - hornfels facies)

This zone is characterised by pale olive green to strong blue - green amphiboles (table 3.2.3), ragged habits and the assemblage magnesio-hornblende, plagioclase and ilmenite. Compositionally they plot in the range from actinolitic - magnesio - hornblende through to their highest extreme of ferro - tschermakitic hornblende (figure 3.2.4), have intermediate alkali contents ( 1 - 2.5 wt %, figure 3.2.5), intermediate titanium contents ( 0.25 - 0.8 wt %, figure 3.2.6) and middle ranges for the sodic and aluminium exchange ( 0.07 - 0.16 Na/(Na + Ca) wt % and 0.10 - 0.30 Al/Si wt %, figure 3.2.7).

### III. HIGH GRADE ZONE : ( 0.1 km ) ( upper hornblende-hornfels facies)

The high grade zone will be discussed only for sample MU45982 (sample MU45983 closest to the contact will be discussed separately). This zone is characterised by brown - green to tan - brown amphiboles (table 3.2.3) of ragged to granular habit and the assemblage tschermakitic-hornblende, plagioclase,oxides and traces of K-feldspar.

Compositionally these amphiboles plot in the tschermakitic hornblende to ferro - tschermakite field (figure 3.2.4), have high alkali contents ( 2.2 wt %, figure 3.2.5), are high in titanium (1.1 - 1.5 wt %, figure 3.2.6) and have high sodic - aluminium exchanges values (0.12 - 0.17 Na/(Na + Ca) and 0.23 - 0.47 Al/Si wt %, figure 3.2.7).

Sample MU45983 is within 25m of the contact and contains amphiboles of only a brown - tan colour and plot in all diagrams consistantly within the field expected for the intermediate grade amphiboles. In addition veining is more abundant in this sample (as was observed for MU45964) and all except 5 amphiboles observed have ragged rims. No optical or compositional zoning of these amphiboles was detected. Their compositional character, habit and the presence of veining all suggest that in addition to retrograde reactions induced by the blind pluton, minor immediate contact zone metasomatism has occured to sufficently alter the amphibole composition. This contact metasomatism seems likely as those amphiboles closest to the veining tend to have the strongest pleochroic brown colours. Critically the colour of these magnesio - hornblendes have remained constant or with proximity to veining become stronger and would seem to be independent of titanium, alkali and magnesium contents. It is possible (although probe analyses did not permit the distinction) that hornblende colour associated with metasomatism is more heavily dependent upon Fe3+ and the proportion of ferric to ferrous iron as iron and not titanium is a key constituent in the vein minerals.

## 3 . 2 . 3b ( v ) : ZONED AMPHIBOLES :

9 zoned amphiboles were examined in two samples (MU45968 and MU45959 ) and the compositions for each ( both rim and core ) are given in table 3.2.5. All zoned amphiboles show a colour zonation with cores of lower grade colours ( blue - green to green ), rims of higher grade colours ( brown - green to brown - tan ) and are all ragged in appearance. All probed samples show increases in titanium, aluminium and alkali contents and associated decreases in magnesium and silica from rim to core (figures 3.2.9 and 10). The presence of this zoning may also suggest that these grains were once relict pyroxenes in the original basalt that have first altered to actinolitic hornblende at lower grades and then rimmed by magnesio to tschermakitic hornblendes at higher grades. Such a zonation would be consistant with the prograde metamorphic zonation outlined previously.

## 3 . 2 . 4 : CONCLUSION

The findings in this section are summarised in figure 3.2.11 and are briefly reviewed here. Although deformation twins and subgrain developement suggest that the intruding pluton not only thermally metamorphoses the surrounding metabasaltic rocks but also weakly deforms them, the metabasaltic plagioclase feldspars do not prove to be useful recorders of a metamorphic grade in the Bendemeer area. Conversely the amphiboles in the metabasaltic hornfelses are good indicators of metamorphic grade in the Bendemeer Adamellite's aureole based on the following criteria :

FIGURE 3.2.8 : AMPHIBOLE CLASSIFICATION DIAGRAM (Leake, 1968) FOR THE ZONED AMPHIBOLES IN THE BENDEMEER AUREOLE METABASALTC ( SAMPLES MU45968 & MU45959 )

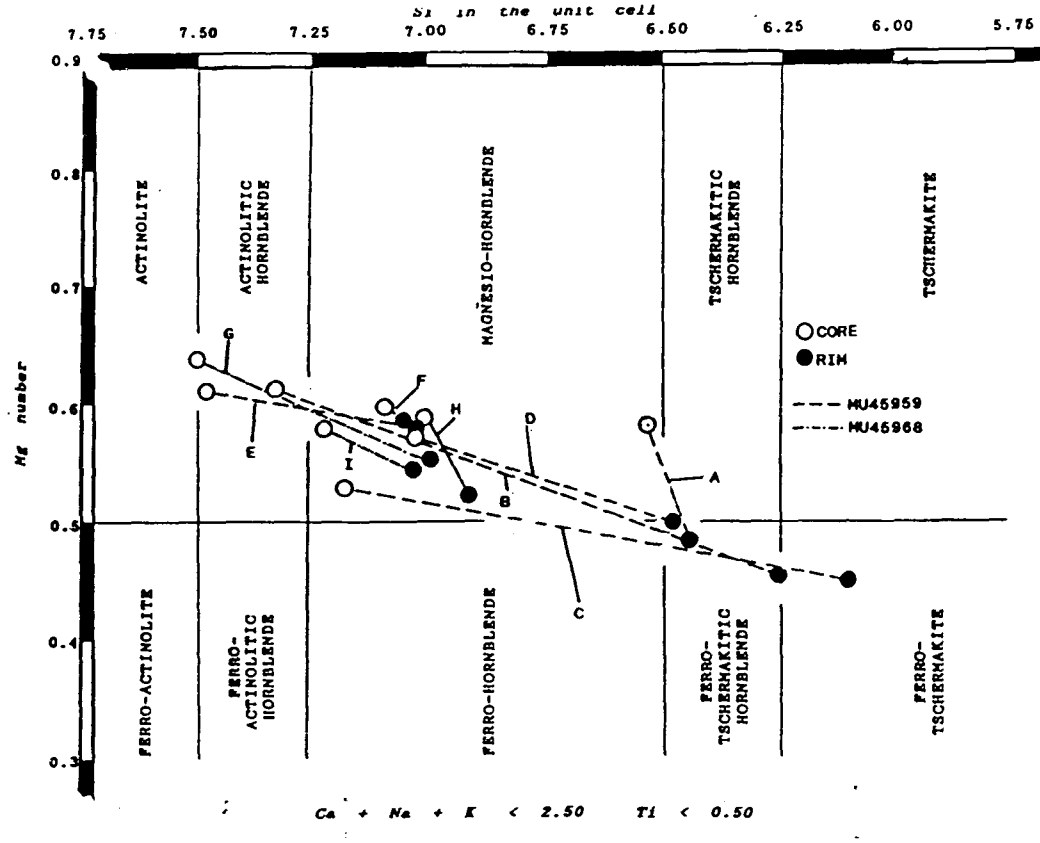


FIGURE 3.2.9 : PLOT OF TITANIUM AGAINST ALKALI CONTENTS FOR THE ZONED AMPHIBOLES FROM SAMPLES (MU45968 & MU45959)

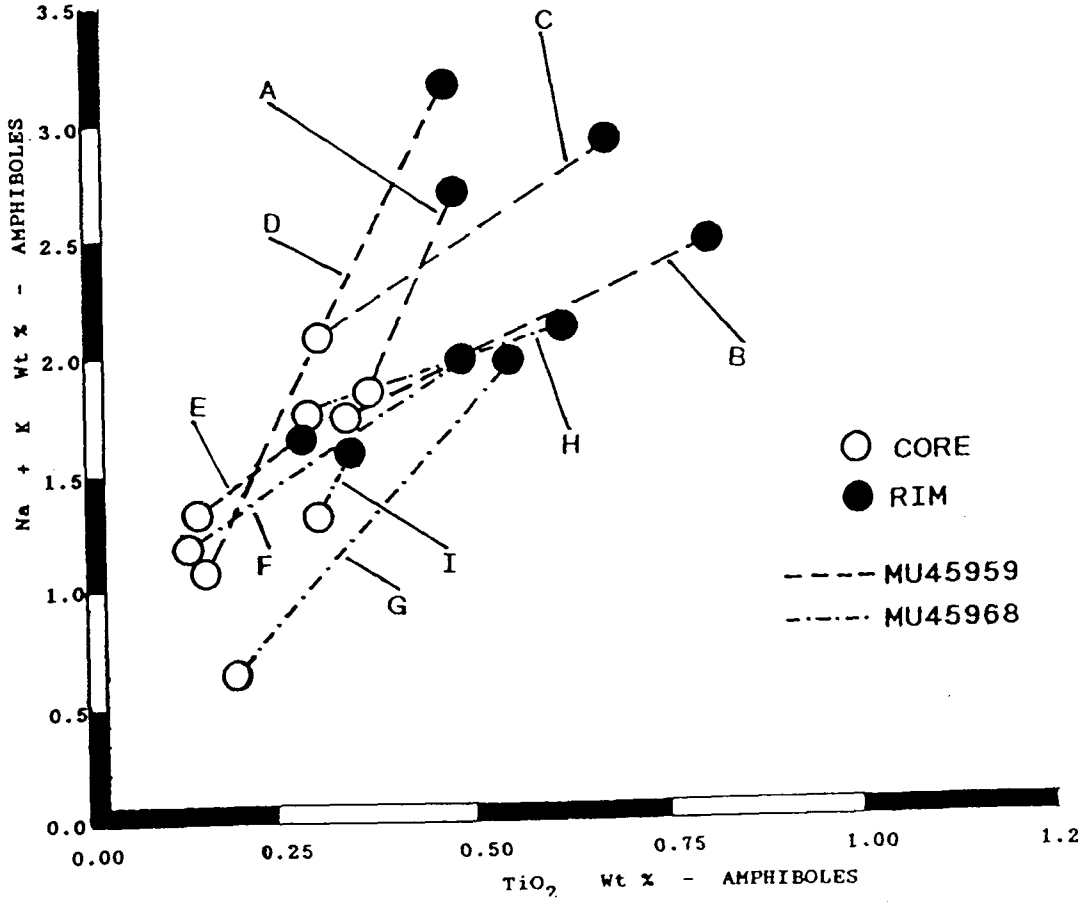

TABLE 3.2.5 : ZONED AMPHIBOLES FROM SAMPLES MU45959 ( A - E ) & MU45968 ( F - I )

| | A | | B | | C | | G | | H | | I | | D | | E | | F | |
|---|---|---|---|---|---|---|---|---|---|---|---|---|---|---|---|---|---|---|
| | CORE | RIM | CORE | RIM | CORE | RIM | CORE | RIM | CORE | RIM | CORE | RIM | CORE | RIM | CORE | RIM | CORE | RIM |
| | % | % | % | % | % | % | % | % | % | % | % | % | % | % | % | % | % | % |
| SiO2 | 47.68 | 42.21 | 46.67 | 42.80 | 46.24 | 39.73 | 50.91 | 45.65 | 48.12 | 44.15 | 48.40 | 46.65 | 49.83 | 40.62 | 50.66 | 47.09 | 48.15 | 46.20 |
| TiO2 | 0.35 | 0.47 | 0.33 | 0.85 | 0.29 | 0.70 | 0.18 | 0.51 | 0.27 | 0.66 | 0.27 | 0.29 | 0.14 | 0.46 | 0.14 | 0.31 | 0.13 | 0.50 |
| Al2O3 | 8.02 | 13.68 | 8.76 | 11.67 | 9.71 | 16.24 | 4.20 | 9.65 | 8.74 | 10.52 | 7.19 | 8.73 | 5.34 | 14.66 | 6.75 | 8.43 | 7.14 | 8.81 |
| Cr2O3 | 0.36 | 0.27 | 0.20 | 0.07 | 0.04 | 0.75 | 0.30 | 0.33 | 0.14 | 0.30 | 0.29 | 0.27 | 0.42 | 0.53 | 0.17 | 0.37 | 0.19 | 0.28 |
| FeO | 16.24 | 18.13 | 15.93 | 17.20 | 14.83 | 17.75 | 14.44 | 16.14 | 15.65 | 16.74 | 15.95 | 16.26 | 15.10 | 18.38 | 14.37 | 15.96 | 15.06 | 15.97 |
| MnO | 0.20 | 0.38 | 0.21 | 0.35 | 0.24 | 0.14 | 0.19 | 0.29 | 0.49 | 0.37 | 0.17 | 0.21 | 0.24 | 0.41 | 0.18 | 0.24 | 0.38 | 0.26 |
| MgO | 12.34 | 9.37 | 11.75 | 9.86 | 9.46 | 8.17 | 14.22 | 11.51 | 12.33 | 10.58 | 13.03 | 11.48 | 13.52 | 8.89 | 12.71 | 11.91 | 12.64 | 11.55 |
| CaO | 11.45 | 11.23 | 11.63 | 11.21 | 10.74 | 11.64 | 12.02 | 11.49 | 11.30 | 11.51 | 11.53 | 11.52 | 11.80 | 11.43 | 11.08 | 11.58 | 11.59 | 11.38 |
| Na2O | 1.53 | 2.41 | 1.60 | 2.28 | 1.96 | 2.58 | 0.63 | 1.87 | 1.63 | 1.90 | 1.21 | 1.58 | 1.06 | 2.88 | 1.30 | 1.56 | 1.21 | 1.84 |
| K2O | 0.11 | 0.31 | 0.10 | 0.20 | 0.17 | 0.24 | 0.02 | 0.13 | 0.09 | 0.19 | 0.17 | 0.04 | 0.10 | 0.24 | 0.02 | 0.12 | 0.05 | 0.11 |
| TOTAL | 98.28 | 97.46 | 97.18 | 96.19 | 99.28 | 97.94 | 97.11 | 97.57 | 98.76 | 96.92 | 98.21 | 97.03 | 97.55 | 98.48 | 97.38 | 97.57 | 96.54 | 96.90 |

FIGURE 3.2.10 : SUMMARY DIAGRAM FOR THE BENDEMEER AUREOLE METABASALTIC HORNFELS

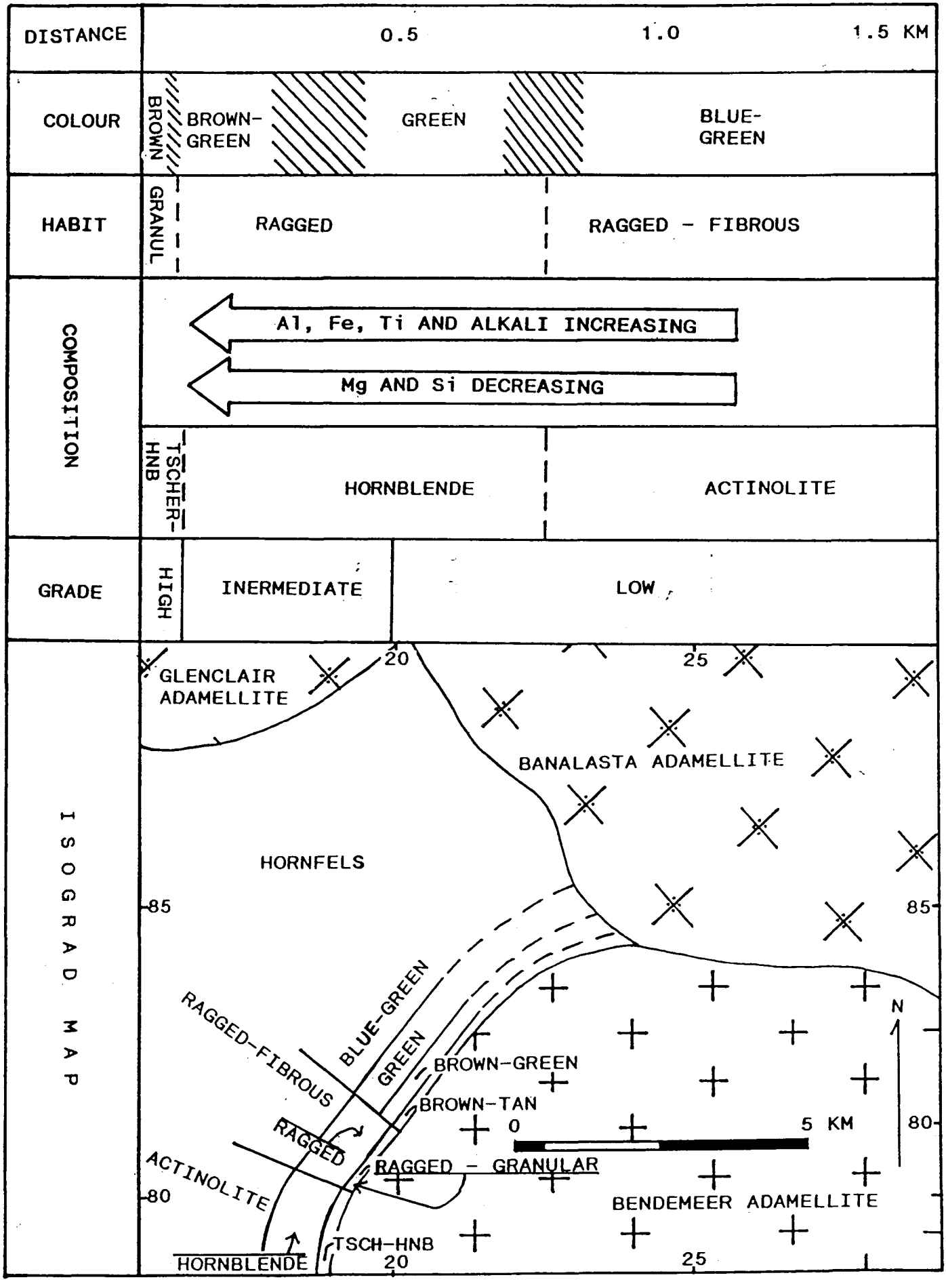

1. That the metamorphic zonation is by no means a simple one and departs from Binns' more classical zonation. It can however be estimated by removal of a proposed thermal overprinting induced by a blind pluton to the northwest.

2. After removal of the overprinting metamorphic effect, a gradation from low grade blue - green, ragged - fibrous actinolitic hornblende through green, ragged magnesio - hornblende to ragged - granoblastic, tan - brown tschermakitic hornblende can be estimated in the Bendemeer Adamellite's aureole.

3. Alkali content increases with grade in the amphiboles, again observed by Binns ( 1966 ) and confirmed to be present in the Bendemeer aureole, imply that mobilisation of alkalis has taken place under conditions of increasing contact metamorphic grade.

4. The presence of ilmenite in the lower grade metabasaltic assemblages implies titanium saturation of these amphiboles. The fact that titanium contents in the amphiboles then increases suggests that re-accomodation is occuring in the amphibole structure with increasing grade and that there is a link between amphibole colour and titanium contents in the non-metassomatised amphiboles and suggests the coupled substitution

$$MgSi \rightleftharpoons TiAl$$

5. Liou et al's ( 1974, 1983 ) thermometric calculations enables an estimate of aureole temperatures based upon the change from actinolite to hornblende at 475 - 550 degrees C. Thus at approxiamately 700m the temperature due to the intrusion is estimated at 520 degrees C. Additional application of Loomis's ( 1966 ) calculation for tan hornblende implies that immediate contact temperatures were as high as 620 - 650 degrees C.

6. That the zoned amphiboles confirm the prograde contact metamorphic reactions and the relationship of colour and grade.

# A . 3 . 3 : META-SEDIMENTS

## A . 3 . 3 . 1 : INTRODUCTION :

The meta-sediments in the Bendemeer Adamellite's aureole are largely cherts and siliceous pelites. Due to the limited mineralogical variation in the cherts and the fact that mineral assemblages in the meta-pelites show strong variation with metamorphic grade, the meta-pelites are used to define the main isograds within the aureole of the Bendemeer pluton.

## 3 . 3 . 2 : META-PELITES :

The pelitic rocks in the aureole of the Bendemeer Adamellite reveal metamorphic changes from low prehnite - pumpellyite facies rocks (outside the aureole) through the albite - epidote hornfels facies, to the upper hornblende hornfels facies (or Winkler's (1967) lower cordierite - K-feldspar hornfels facies).

Those rocks essentially outside the thermal aureole's effects ( 4km), have been regionally metamorphosed in the Carboniferous (Leitch, 1974) up to prehnite - pumpellyite facies (220 - 330 degrees celcius at 2 - 4kb pressure based on the regional facies' general delineation by Best,1982 and Turner, 1968). These regional metamorphic conditions have not been maintained at the time of the Permian granitoid intrusion and hence the conditions cited represent the upper limit of the regional metamorphism in the Permian.

A bulk rock analysis of 6 metapelitic samples has been performed by using the XRF technique and these are presented in table 3.3.1 and figure 3.3.1. The AFC diagram in figure 3.3.1 reveals that all the samples (excluding the highly siliceous MU45954) plot close to the cordierite field and confirm that these rocks are ideal for the foemation of cordierite at higher grades. This would account for the abundant cordierite porphyroblasts seen in these rocks at higher grade.

The non-contact metamorphosed pelitic rocks are very fine grained ( .005 mm), exhibit strong primary laminations and are often interlayered with the cherty layers. These pelites have a shalely appearance in handspecimen, are buff to mid-grey in colour and show a weak irregular discontinuous cleavage. With decreasing distance to the intrusive contact the rocks noticeably darken to a dark brown-grey to brown-black and increase in grainsize sufficently to discern individual grains on a microscopic scale (up to 0.05mm).

In hand specimen these pelitic rocks lose their laminated internal structure and become more massive, more typically hornfelsic in character, lose their discontinuous cleavage but maintain their interbanded nature right up to the intrusive contact. These changes in the rock's nature can be correlated with topography, the higher grades of

TABLE 3.3.1 : BULK ROCK ANALYSES FOR THE META-PELITES FROM XRF ANALYSIS. DISTANCES ARE IN KILOMETRES FROM THE BENDEMEER ADAMELLITE'S CONTACT.

| | TOWARDS INTRUSIVE CONTACT | | | | | |
|---|---|---|---|---|---|---|
| | MU45948 | MU45949 | MU45950 | MU45912 | MU45953 | MU45954 |
| DISTANCE | 3 | 2.5 | 2 | 1.75 | 1.25 | 1 |
| | % | % | % | % | % | % |
| SiO2 | 66.04 | 65.22 | 65.19 | 64.45 | 62.99 | 79.95 |
| TiO2 | 0.78 | 0.88 | 0.88 | 0.99 | 1.03 | 0.39 |
| Al2O3 | 15.45 | 14.07 | 14.48 | 15.32 | 16.04 | 8.83 |
| Fe2O3 | 1.29 | 1.34 | 1.53 | 1.80 | 1.59 | 2.84 |
| FeO | 3.80 | 5.04 | 5.48 | 4.74 | 5.46 | 1.41 |
| MnO | 0.08 | 0.11 | 0.10 | 0.13 | 0.13 | 0.19 |
| MgO | 1.85 | 2.07 | 2.18 | 2.31 | 2.50 | 1.33 |
| CaO | 4.76 | 3.04 | 2.59 | 2.36 | 3.96 | 0.21 |
| Na2O | 3.14 | 4.16 | 5.00 | 4.21 | 3.84 | 0.05 |
| K2O | 1.45 | 0.64 | 0.19 | 0.53 | 0.98 | 2.66 |
| P2O5 | 0.18 | 0.21 | 0.19 | 0.25 | 0.24 | 0.03 |
| H2O+ | 0.96 | 1.88 | 1.73 | 2.35 | 1.01 | 1.74 |
| H2O- | 0.10 | 0.07 | 0.05 | 0.07 | 0.04 | 0.19 |
| CO2 | 0.20 | 1.04 | 0.38 | 0.21 | 0.30 | 0.13 |
| TOTAL | 100.08 | 99.79 | 99.99 | 99.72 | 100.09 | 99.93 |

FIGURE 3.3.1 : A F C DIAGRAM FOR THE METAPELITIC WHOLE ROCK SAMPLES IN THE AUREOLE OF THE BENDEMEER PLUTON

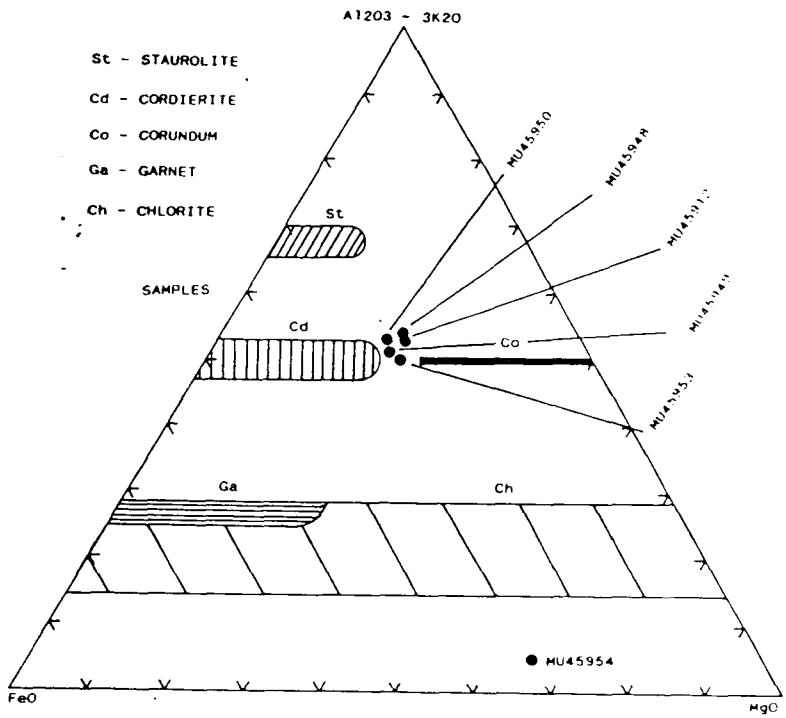

hornfelsic rocks commonly occuring at topographic highs (discussed later). Unlike the Walcha road Adamellite described by Teale (1974) no contact parallel schistosity is evident in the pelitic rocks although a moderately developed contact parallel matrix mineral orientation is observed in one contact sample (plate 3.3.1 right on the contact) with minor deflection around a cordierite porphyroblast (bottom left).

## 3 . 3 . 3 : ISOGRAD DELINEATION :

The delineation of the contact metamorphic isograds (figure 3.3.2 and 3) at varying distances from the Bendemeer Adamellite's contact, has been performed on samples examined in the area denoted in figure 3.3.2. The reason for this being that the main thrust of this study is to correlate hornfelsic isograds with the less typical isograds observed in the Banalasta Adamellite. Thus the variations in pelitic assemblages must be examined away from the influences of other plutons (such as the Moonbi Adamellite and the Banalasta Adamellite itself). Figure 3.3.1 shows the delineated isograds extrapolated to the Banalasta Adamellite's boundary and that the cordierite and Biotite isograds (based upon field observations and petrographic work) have been continued to show the approximate regional position of these isograds as they bend around both plutons' contacts. The isograds parallel to the Banalasta contact are less accurately placed and are established solely upon optical studies of thin sections observing the appearance or disappearance of particular index minerals.

The relationship of the mapped isograds relative to the topographic expression of the hornfels ridge (figure 3.3.4) reveals that in general the lowest contact grades (biotite and andalusite isograds) essentially show little control upon topography, whereas the most significant increase in topographic elevation occurs with the cordierite isograd. The topographic expression of the almandine-cordierite and K-feldspar-cordierite isograds are less apparent and are more likely controlled by their proximity to the topographically low Bendemeer Adamellite. The dips of the isograds are estimated and are based upon the contact parallel foliation measured in the Bendemeer Adamellite.

As was previously mentioned, the main thrust of this section has been to delineate the pelitic metamorphic zonation in order to correlate it with the Banalasta Adamellite's less conventional isograds. For this reason, it was not deamed profitable within the time constraints of the thesis to perform detailed studies on both the eastern and western aureoles. Thus the eastern aureole has only had the cordierite isograd delineated from field observations and petrographic examination.

### 1. BIOTITE ISOGRAD (table 3.3.2 and 3)

The crystallisation of very fine grained biotite occurs at approximately 3 km from the Bendemeer Adamellite's western contact. With increase in grade the grainsize and abundance of biotite increases and the microstructure becomes increasingly granoblastic ( .5 mm) in samples closer to the contact. The biotite isograd assemblages are given

FIGURE 3.3.2 : REGIONAL MAP OF THE CONTACT METAMORPHIC ISOGRADS TO THE WEST OF THE BENDEMEER ADAMELLITE.



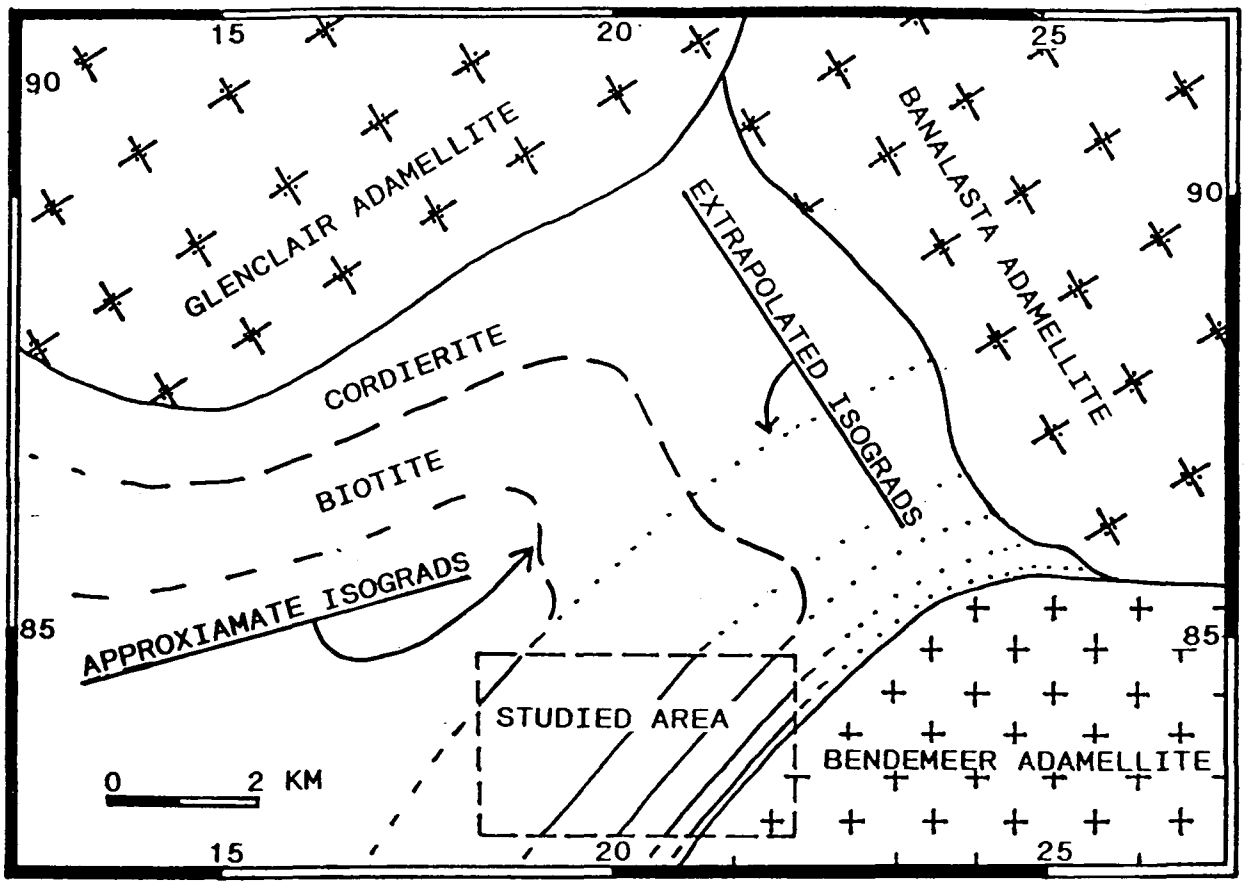


FIGURE 3.3.3 : ISOGRAD MAP OF THE BENDEMEER ADAMELLITE AUREOLE AWAY FROM THE CONTACT METAMORPHIC INFLUENCES OF BOTH THE BANALASTA AND MOONBI ADAMELLITES.

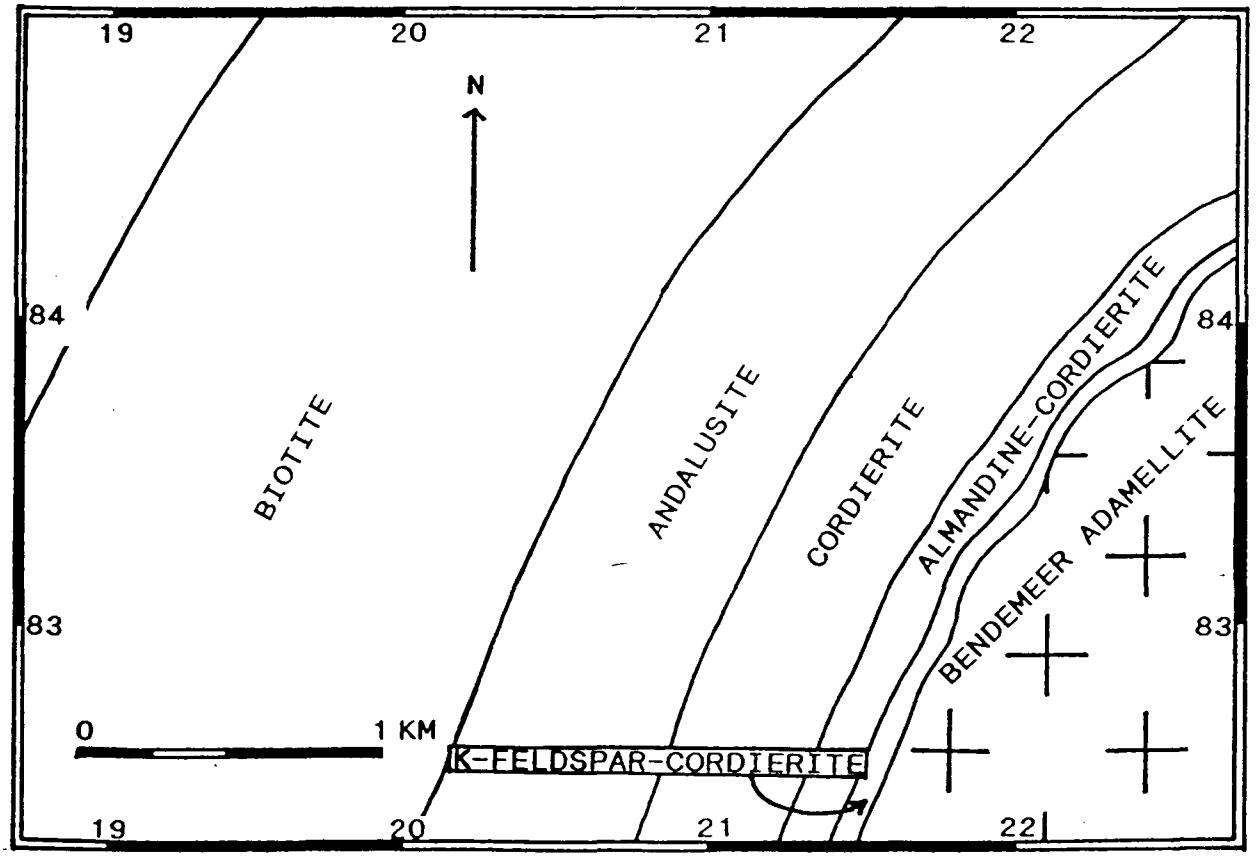

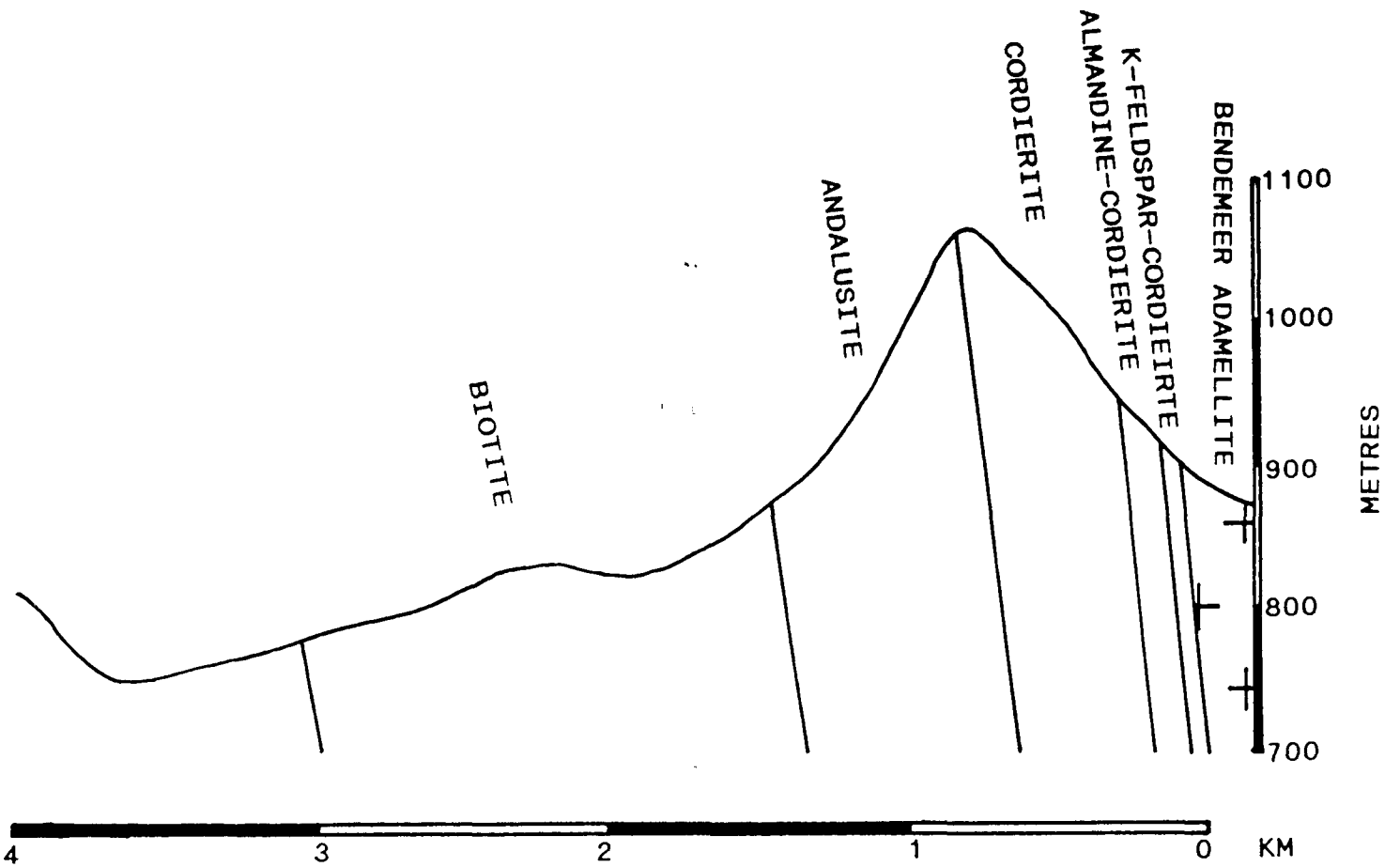


FIGURE 3.3.4 : TOPOGRAPHIC - ISOGRAD SECTION FROM FIGURE B, SHOWING THE GRADE RELATIONSHIPS IN THE HORNFELS RIDGE.
(DIPS BASED ON MEGACRYST FOLIATION DATA IN THE CONTACT OF THE BENDEMEER ADAMELLITE)

PLATE 3.3.1 : MATRIX FOLIATION IN A METAPELITE FROM THE IMMEDIATE CONTACT WITH THE BENDEMEER ADAMELLITE ( SHOWING MINOR DEFLECTION AROUND A CORDIERITE PORPHYROBLAST ) (MU45902)

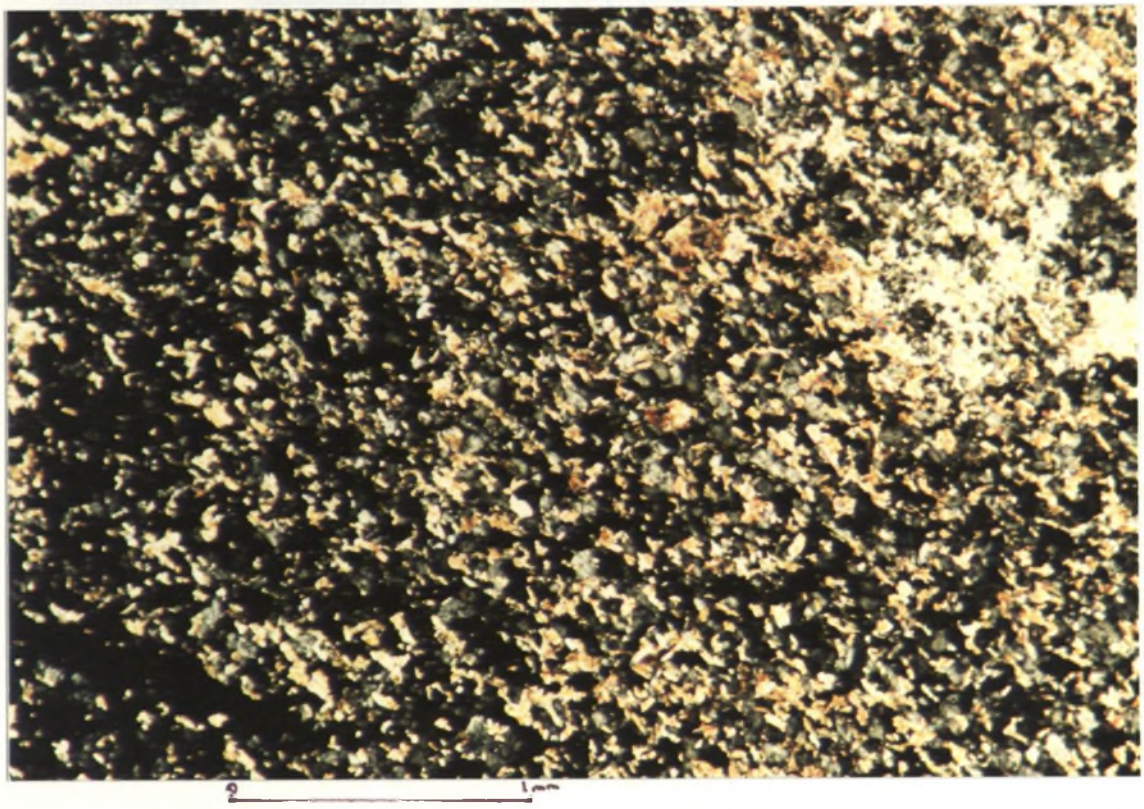


PLATE 3.3.2 : GRANOBLASTIC MICROSTRUCTURE TO THE METAPELITES IN THE AUREOLE OF THE BENDEMEER ADAMELLITE, SHOWING TYPICAL BIOTITE - QUARTZ ASSEMBLAGE (MU45954)

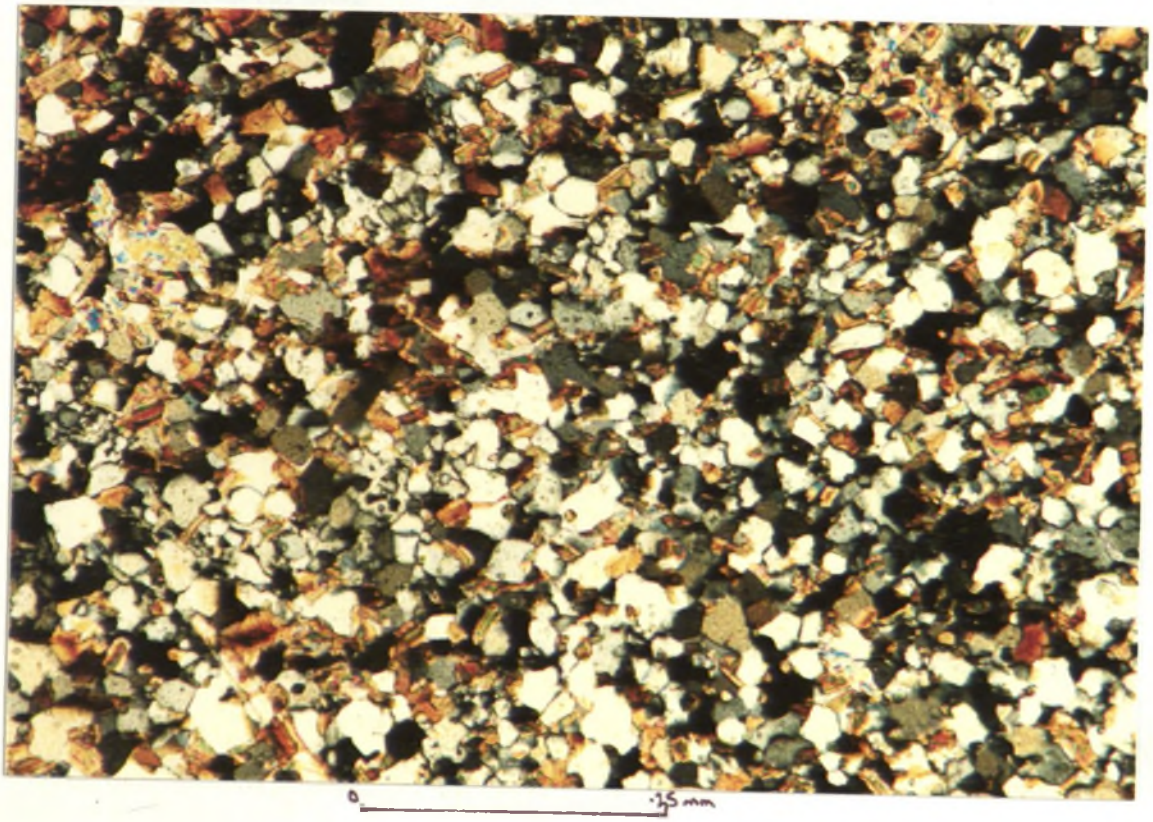

PLATE 3.3.3 : CORDIERITE PORPHYROBLAST IN THE METAPELITES SHOWING TYPICAL IRREGULAR OUTLINE AND HIGH INCLUSION ABUNDANCE (MU45963)

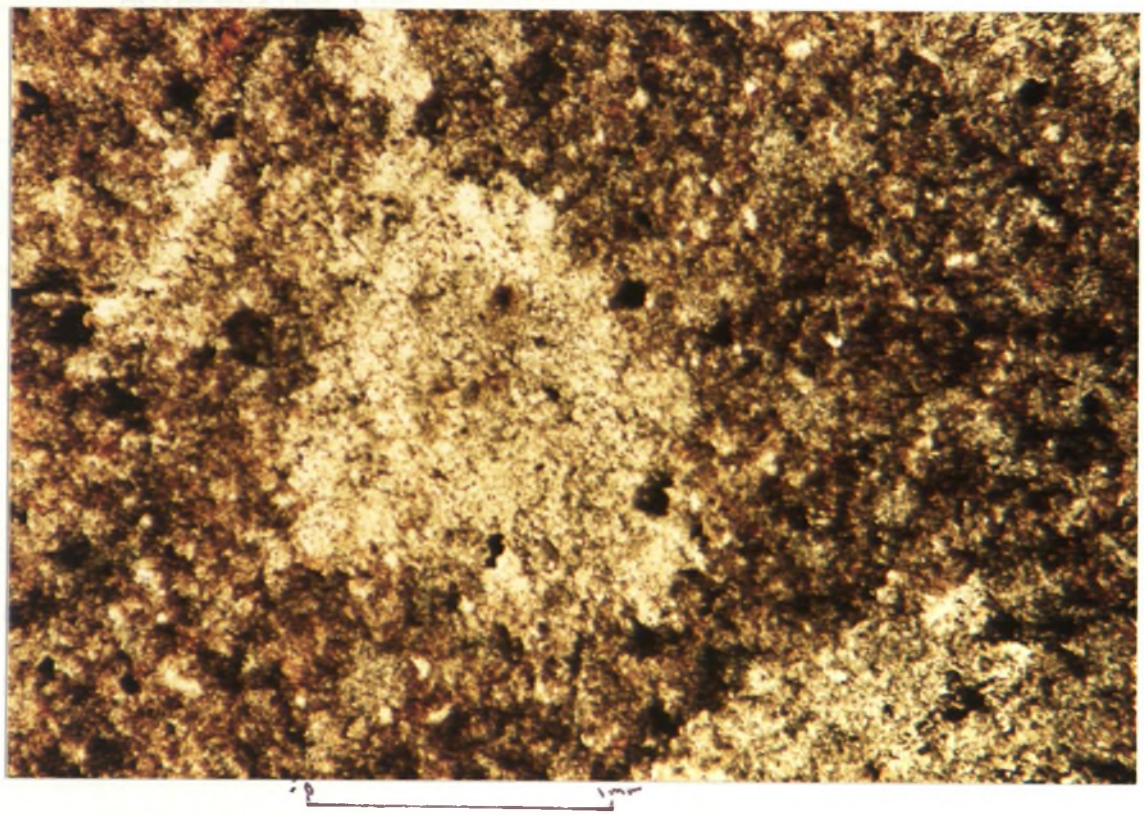

PLATE 3.3.4 : CLOSE UP OF THE GRANOBLASTIC MICROSTRUCTURE OF THE METACHERT UNITS CLOSE TO THE CONTACT OF THE BENDEMEER ADAMELLITE (MU45958)

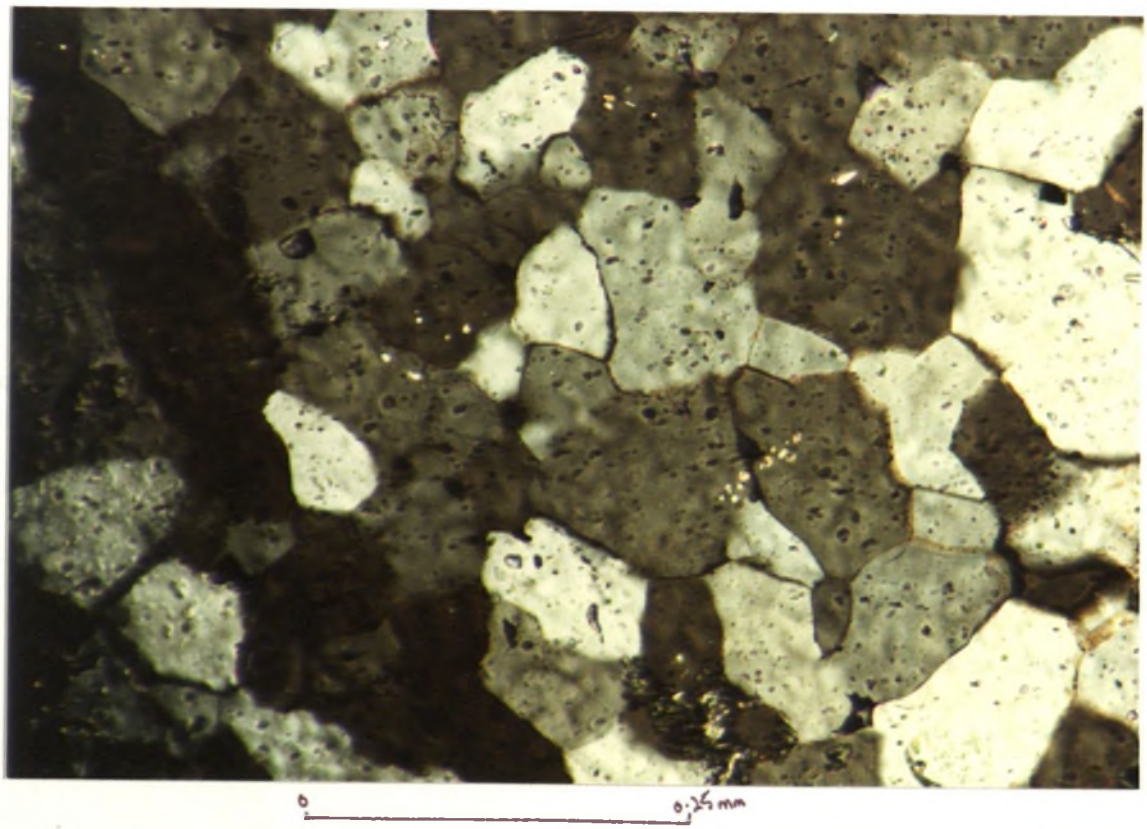

TABLE 3.3.2 : ASSEMBLAGES FOR THE GRADE ZONES DELINEATED IN THE METAPELITES FROM THE AUREOLE OF THE BENDEMEER ADAMELLITE

| ZONE AND DISTANCE | ASSEMBLAGE |
|---|---|
| *BIOTITE*<br><br>*( 3KM )* | *quartz + biotite :*<br>*-albite-chlorite-epidote-ilmenite*<br>*-muscovite-albite*<br>*-albite-epidote* |
| *ANDALUSITE*<br><br>*( 1.3KM )* | *quartz + biotite :*<br>*+-muscovite*<br>*-plagioclase ( An 27 )*<br>*-plagioclase-+andalusite* |
| *CORDIERITE*<br><br>*( 700M )* | *quartz - biotite :*<br>*-plagioclase*<br>*-cordierite-plagioclase* |
| *CORDIERITE*<br>*ALMANDINE*<br><br>*( 200M )* | *quartz - biotite :*<br>*-cordierite-plagioclase*<br>*-cordierite+-garnet(Almandine)*<br>*-plagioclase* |
| *CORDIERITE*<br>*K-FELDSPAR*<br><br>*( 70M )* | *quartz - biotite :*<br>*-cordierite-plagioclase-K-feldspar*<br>*-cordierite-K-feldspar*<br>*-plagioclase-cordierite* |

PROBE ANALYSES FOR THE RESPECTIVE ISOGRADS IN THE BENDEMEER ADAMELLITE'S AUREOLE

B) CORDIERITE ANALYSES ( MU45963 OCCURS AT THE MINIMUM DISTANCE FOR THE CORDIERITE ISOGRAD ON THE MAP IN FIGURE , MU45958 IS WITHIN 70M OF THE CONTACT IN THE K-FELDSPAR-CORDIERITE ZONE.

| | B I O T I T E | | ANDALUSITE | ALMANDINE | K-FELDSPAR |
|---|---|---|---|---|---|
| | MU45950 | MU45950 | MU45907 | MU457971 | MU45958 |
| | % | % | % | % | % |
| SiO2 | 34.31 | 35.27 | 35.84 | 36.78 | 62.22 |
| TiO2 | 2.75 | 2.67 | -- | 0.11 | -- |
| Al2O3 | 19.63 | 18.98 | 63.81 | 21.01 | 21.01 |
| FeO | 22.02 | 21.76 | 0.02 | 34.98 | -- |
| MnO | -- | -- | -- | 2.55 | -- |
| MgO | 7.31 | 7.94 | 0.01 | 3.51 | -- |
| CaO | 0.04 | 0.11 | -- | 1.25 | 0.33 |
| Na2O | 0.13 | 0.08 | 0.01 | -- | 2.14 |
| K2O | 8.41 | 7.98 | -- | -- | 13.15 |
| TOTAL | 94.60 | 94.75 | 99.73 | 100.19 | 98.85 |

| | C O R D I E R I T E S | | | | | | | |
|---|---|---|---|---|---|---|---|---|
| | MU45963 | | | | MU45958 | | | |
| | % | % | % | % | % | % | % | % |
| SiO2 | 47.93 | 49.19 | 47.46 | 48.11 | 49.46 | 45.44 | 47.90 | 47.87 |
| Al2O3 | 32.37 | 30.52 | 32.43 | 33.14 | 31.64 | 32.29 | 29.72 | 31.54 |
| FeO | 8.35 | 8.16 | 8.74 | 8.86 | 8.89 | 8.71 | 8.25 | 9.03 |
| MnO | 0.91 | 0.68 | 0.72 | 0.86 | 0.70 | 0.46 | 0.57 | 0.55 |
| MgO | 7.22 | 6.68 | 7.76 | 7.66 | 6.70 | 6.32 | 5.66 | 6.79 |
| Na2O | 0.24 | 0.30 | 0.20 | 0.30 | 0.07 | 0.50 | 1.34 | 0.23 |
| TOTAL | 97.02 | 95.53 | 97.31 | 98.93 | 97.46 | 93.72 | 93.44 | 96.01 |
| Mg # | 46.39 | 45.03 | 47.03 | 46.36 | 42.98 | 42.06 | 40.45 | 42.90 |

in table 3.3.2 and is typical of the albite-epidote hornfels facies (Vernon, 1976 and Speer, 1981) and two probe analyses are given in table 3.3.3. Chlorite is in lower abundance than in the regional metamorphic rocks further from the contact, suggesting a prograde reaction to biotite, although some biotites do show minor chloritic rims (suggestive of later retrogression). Utilising Turner's (1968) contact metamorphic crystallisation temperatures enables the biotite temperature at approximately 2 - 2.5 Kb to be estimated as 400 - 410 degrees C.

In addition this zone demarcates rocks with a truly hornfelsic structure (plate 3.3.2), whereas outside the biotite zone the siliceous meta-pelites have less sugary textures, are more shalely - phyllitic in appearance, and well joined and cleaved. This biotite zone being characterised by a very fine and even-grained appearance in hand specimens and thin section, unlike closer to the contact where cordierite porphyroblasts give the pelites a 'knotted' appearance in hand specimen similar to those observed near the Walcha Road pluton by Teale (1974) and Vernon (1987. in press).

## 2. ANDALUSITE ISOGRAD:

The first appearance of andalusite occurs at approximately 1.3 km from the Bendemeer Adamellite's contact. The andalusite was observed optically and probed in only one sample (table 3.3.3) where it occurs in very low abundance as small ( .05 mm) polygonal grains in the more quartz rich layers of the pelites. The extremely low abundances of andalusite is indicative of low Al2O3 and high silica in the pelites (Howarth 1973) and is most likely explained by the fact that these predominantly quartz - biotite hornfelses would have only localised traces of pyrophyllite and therefore conditions unfavourable for andalusite nucleation. The typical assemblages are given in table 3.3.2.

In hard specimen these rocks are even-grained, dark in colour and are coarser grained than those in the biotite zone. With close proximity to the cordierite isograd the rocks have a fine bleby appearance suggesting the nucleation and initial growth of cordierite 'knots'. The plagioclase observed was probed in one sample and gave a composition of An27 implying that albite has disappeared and more calcic feldspar appeared. The calcification of plagioclase feldspar may be accounted for by the disappearance of epidote and hence release of calcium in to the system. The temperature of the andalusite isograd has been estimated at between 500 and 515 degrees C based on Greenwood (1976), Turner (1968) and Vernon (1976).

## 3. CORDIERITE ISOGRAD:

The cordierite isograd can be placed at approximately 600 to 700 m from the Bendemeer pluton's western contact. It can be mapped to within 200m in the field by the appearance of dark 'knotted' patches of porphyroblastic cordierite

( 1mm) in the less silicic layers of the siliceous meta-pelites. Two main assemblages have been observed and are given in table 3.3.2.

The first appearance of these sub-circular to irregular shaped cordierites (plate 3.3.3) indicating the change from the albite-epidote facies to the hornblende hornfels facies (Turner 1968). Primary muscovite and chlorite were not observed at this stage, however, as was also found by Howarth (1973) some chlorite and muscovite are associated with cordierite rims, suggesting cordierite retrogression has occurred. He proposed that this retrogressive evidence suggested the reaction:

**cordierite + H2O = chlorite + muscovite + quartz**

With further increase in grade the modal proportion of cordierite increases with an associated slight decrease in Mg-number (from 45.54 at 400 m to 42.31 at 20 m from the contact) and MnO (.774 wt % to .6024 wt % at the same distances respectively) and an increase in sodium content (from .216 to .509 wt %) (see table 3.3.3). No compositional data was obtained for plagioclase in this zone, but the absence of epidote and the presence of cordierite might suggest that it has a calcic composition, as albite is out by this stage. Estimates of temperature at 2 - 3 kb of pressure are 530 - 560 degrees C based on Greenwood (1976), Winkler (1967) and Turner (1968).

## 4. CORDIERITE-ALMANDINE ISOGRAD:

This isograd has been estimated at approximately 200 - 220m from the Bendemeer pluton's contact and the assemblages are given in table 3.3.2.

Two fine grained almandine garnets were observed and one has been probed to provide compositional data (table 3.3.3). The almandine occurs in very low abundance as small granoblastic grains ( .05 mm) with minor inclusions of quartz and lesser biotite. Teale (1974) stated that almandine was only present in graphitic host rocks. The absence of any observed graphitic rocks in the western Bendemeer aureole (assuming Teale's observations are correct) would account for the extremely low abundances of almandine in the Bendemeer area.

The temperature of the cordierite - almandine isograd at pressures of 2 - 3 kb is in the range 560 - 580 degrees C (Naggar and Atherton, 1977 and Hsu, 1968).

## 5. CORDIERITE - K-FELDSPAR ISOGRAD:

This isograd has been based upon optically identified and analysed (table 3.3.3) metamorphic k-feldspar in the meta-pelites within 70 m of the contact and the assemblage is given in table 3.3.2.

FIGURE 3.3.5 : SUMMARY DIAGRAM FOR THE METAPELITES IN THE AUREOLE OF THE BENDEMEER ADAMELLITE

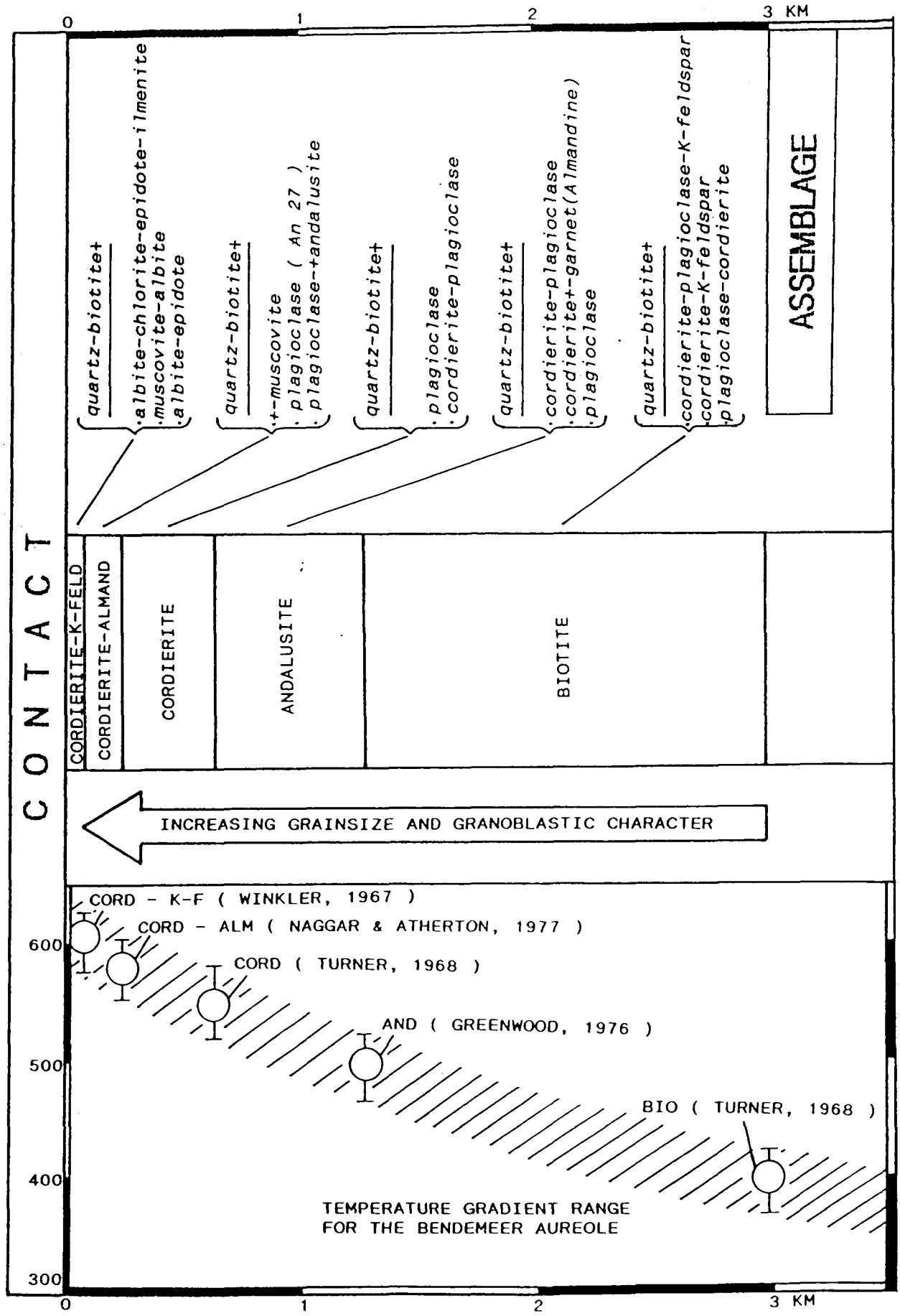

Biotite is less abundant in this zone, but is coarser grained (up to .1mm). No chlorite is observed and cordierite porphyroblasts are also coarser grained (up to 1.5mm), more abundant and more subtly iron rich (Mg-number = 42.31) in this zone (see MU45958 in table 3.3.3). Some minor retrograde rections have occurred and where secondary muscovite is present it occurs as fine fibrous overgrowths rimming cordierite, k-feldspar and less commonly biotite. No significant deflection of matrix foliation around the cordierite porphyroblasts is observed at this grade (except right on the contact, plate 3.3.1) and may imply that thermal effects favourable for continued cordierite growth have outlasted any weak deformational effects in these rocks induced by the small ( 10km diameter) Bendemeer pluton, unlike those observed in the much larger Walcha Road Adamellite's aureole (Teale, 1974 and Vernon, 1987.in press). The presence of cordierite and K-feldspar places the immediate contact zone in the upper Hornblende Hornfels facies (or Winkler's ( 1967 ) lower cordierite - K-feldspar hornfels facies) and therefore temperatures in the order of 600 - 630 degrees C (Winkler, 1967; Vernon, 1976; and Best, 1982).

## 3 . 3 . 4 : META - CHERTS :

Due to their limited mineralogical variation the silica rich meta-sediments prove not to be as useful grade indicators as the meta-pelites do. However, there is a marked increase in grainsize with increasing contact metamorphic grade (from .01 mm at 3 km from the contact to up to .5 mm within 20 m of the contact). In addition the microstructure of these siliceous rocks becomes increasingly granoblastic with grade until at 20 m from the contact the meta - cherts are predominantly even grained and have good polygonal grain shapes (plate 3.3.4).

## 3 . 3 . 5 : SUMMARY :

A summary of the metamorphic zonation in the western Bendemeer aureole for the metasediments is given in figure 3.3.5. The metasediments reveal distinct changes from regional metamorphic rocks through the albite - epidote hornfels and hornblende hornfels facies, up to the lower cordierite - K-feldspar hornfels facies. The much larger Walcha Road pluton records a weak emplacement induced deformational matrix foliation (Teale, 1974 and Vernon, 1987. in press). No such foliation is evident in the Bendemeer Adamellite's aureole (except in the immediate few centimetres of the contact, plate 3.3.1). This would suggest that although a weak deformation has been recorded elsewhere in the Bendemeer Adamellite's aureole, it has been insufficent in strength to significantly affect the meta-pelites and hence they record purely thermal metamorphic changes.

# A. CHAPTER 4: CONTACT METAMORPHISM OF THE BANALASTA ADAMELLITE

## 4. 1 : POTASSIUM FELDSPAR STRUCTURAL STATE

### 4. I. I : INTRODUCTION

Potassium feldspar may be classified as a polymorphic mineral as it contains a continous series of structural state polymorphs. The structural state is controlled by an order - disorder reaction in which aluminium in the K-feldspar migrates into more stable structural sites as temperature or deformation increases (Vernon, 1976). Monoclinic sanidine is the disordered polymorph in the K-feldspar system, annealling of this over time or subjecting it to strain results in the migration of aluminium into T1o sites directly from T1m, T2o and T2m sites (ordering), disordering simply being the reverse migration upon heating the K-feldspar. The migration to a more ordered state is an attempt by the K-feldspar to attain lower free energy and higher configuration entropy. When conditions are favourable for this ordering the microcline that forms always shows cross-hatch twinning (Ribbe, 1975). This aluminium migration dictates the degree of movement away from monoclinic symmetry, which will be referred to as triclinicity.

Observations of K-feldspar disordering in the Banalasta Adamellite within the aureole of the Walcha Road Adamellite (Flood, 1971) prompted this study and the initial findings (which revealed that first ordering and then disordering transformations were mappable towards later intrusive contacts) have resulted in a detailed examination of potassic feldspar changes within a contact metamorphic aureole.

The ordering of magmatic orthoclase (monoclinic) to microcline (triclinic) with increasing grade of regional metamorphism has been noted by many authors: Eskola (1951); Karamata (1961); and Smithson (1963) but the studies of Steiger & Hart (1967) and Wright (1967) were the first to show that a continous microcline to orthoclase disordering occurs in the K-feldspars of pegmatites from the Pre-Cambrian Boulder Granite (Sierra Nevada) where it is intruded by Tertiary Eldora Quartz-Monzonite stocks. These changes in structural state were shown to be dependent upon temperature, pressure, time and individual crystal surface areas by Eggleton (1980) and the transition from triclinic to monoclinic K-feldspar occuring between 400 - 500 degrees C (Steiger & Hart,1967; Wright 1967; Stormer,1975; Olatunji,1976 and Eggleton, 1980).

Perhaps the simplest method of determining the structural state of alkali feldpsars is the triclinicity index proposed by Orville (1963) which is 12.5 x ($d1\bar{3}1$ - d131). This triclinicity value ranges from unity for maximum

microcline (MM, ordered and triclinic) to zero for orthoclase (Or, disordered and monoclinic) (Orville,1963). This value will be refered to as triclinicity and the term isocline will be used for equal triclinicity contours on a map.

Utilising the $1\bar{3}1$ - 131 x-ray diffraction peak traces, Steiger and Hart produced mixes of varying proportions of pure orthoclase and pure maximum microcline in order to estimate microcline - orthoclase ratios from field samples (figure 4.1.l) A similar mix series has been produced from pure orthoclase and pure near maximum microcline (triclinicity = 0.833) for the two field areas studied in this thesis. These mix series are important in that they suggest for field samples that order - disorder transformations are commonly incomplete, with residuals of the unstable phase commonly present in minor abundance.

Another method proposed by Tilling (1968) and Wright (1967 & 1968) allows alkali feldspar composition and the structural state to be measured by plotting the $2\theta$ ($\bar{2}04$) value against the $2\theta$ ($\bar{0}60$) value and plotting the $2\theta$ ($\bar{2}01$) value directly against OrAb composition thus enabling feldspar composition to be determined directly from $2\theta$ values.

## 4.l.2. TRICLINICITY OBSERVATIONS (figure 4.l.2 & 3, map 2 & 3)

Measurement of triclinicity for 88 perthitic K-feldspar separates ( given in appendix 2 ) from the Carboniferous Banalasta Adamellite reveals a number of changes with decreasing distance from the contacts of the Bendemeer and Looanga Adamellites (figures 4.l.2 and 3).

Furthest from these contacts (7 - 20 km to the north and north-west) five samples (three Pringles Adamellite, one Glenclair Adamellite and one Tilmunda Granite, sample locations shown in figure 4.l.2) were collected in from the contacts of adjacent S-type plutons that comprise the bulk of the southern section of the Bundarra Plutonic Suite and their measured triclinicities have been tabulated below :

| PLUTON | TRICLINICITY |
|---|---|
| l.Average regional Banalasta Adamellite | .36 |
| 2.Average Pringles Adamellite | .49 |
| 3.Glenclair Adamellite | .53 |
| 4.Tilmunda Granite | .58 |

FIGURE 4.1.1 : MIXING TRACES FOR NEAR MAXIMUM MICROCLINE ( TRICLINICITY = 0.833 ) AND PURE ORTHOCLASE AS AN ESTIMATE OF THE PROPORTIONALITY OF MICROCLINE TO ORTHOCLASE IN THE BANALASTA ADAMELLITE'S COMPOSITIONAL TRAVERSES ( EACH 100 % MIX IS EQUAL TO 0.01 GRAMS ).

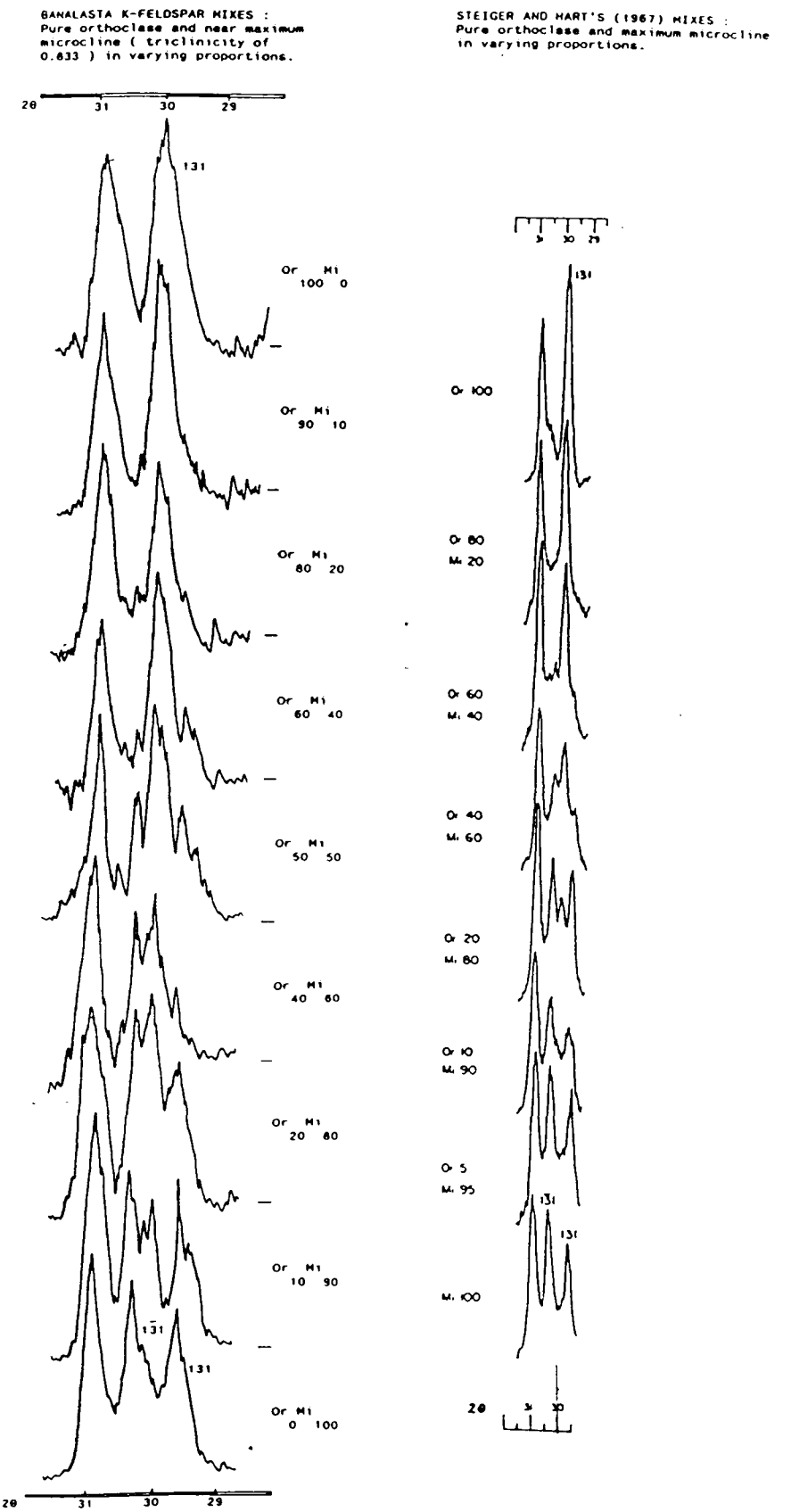

FIGURE 4.1.2 : ISOCLINAL MAP OF THE MICROCLINE BEARING SOUTHERN BUNDARRA SUITE PLUTONS IN THE BENDEMEER AREA.

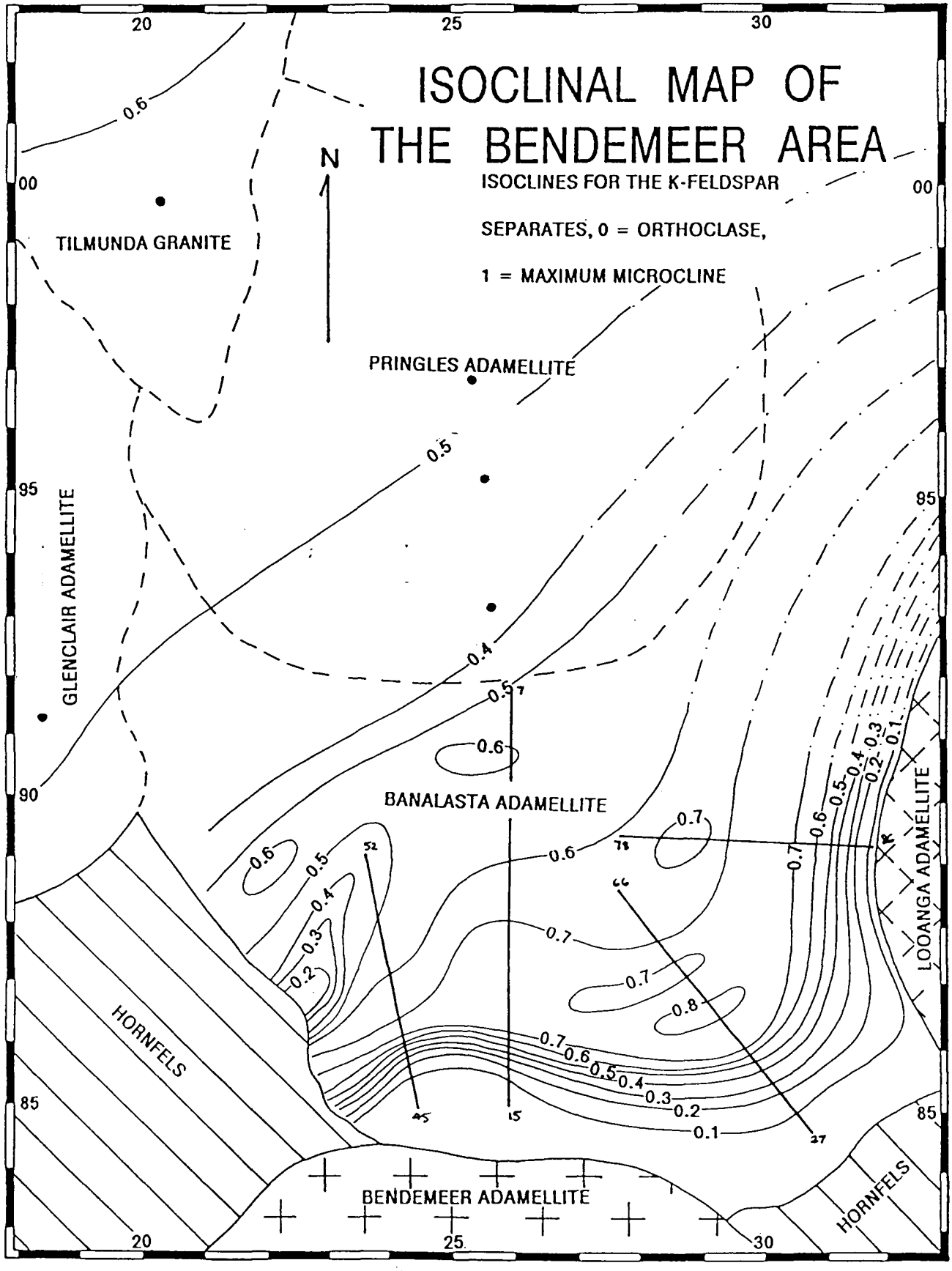

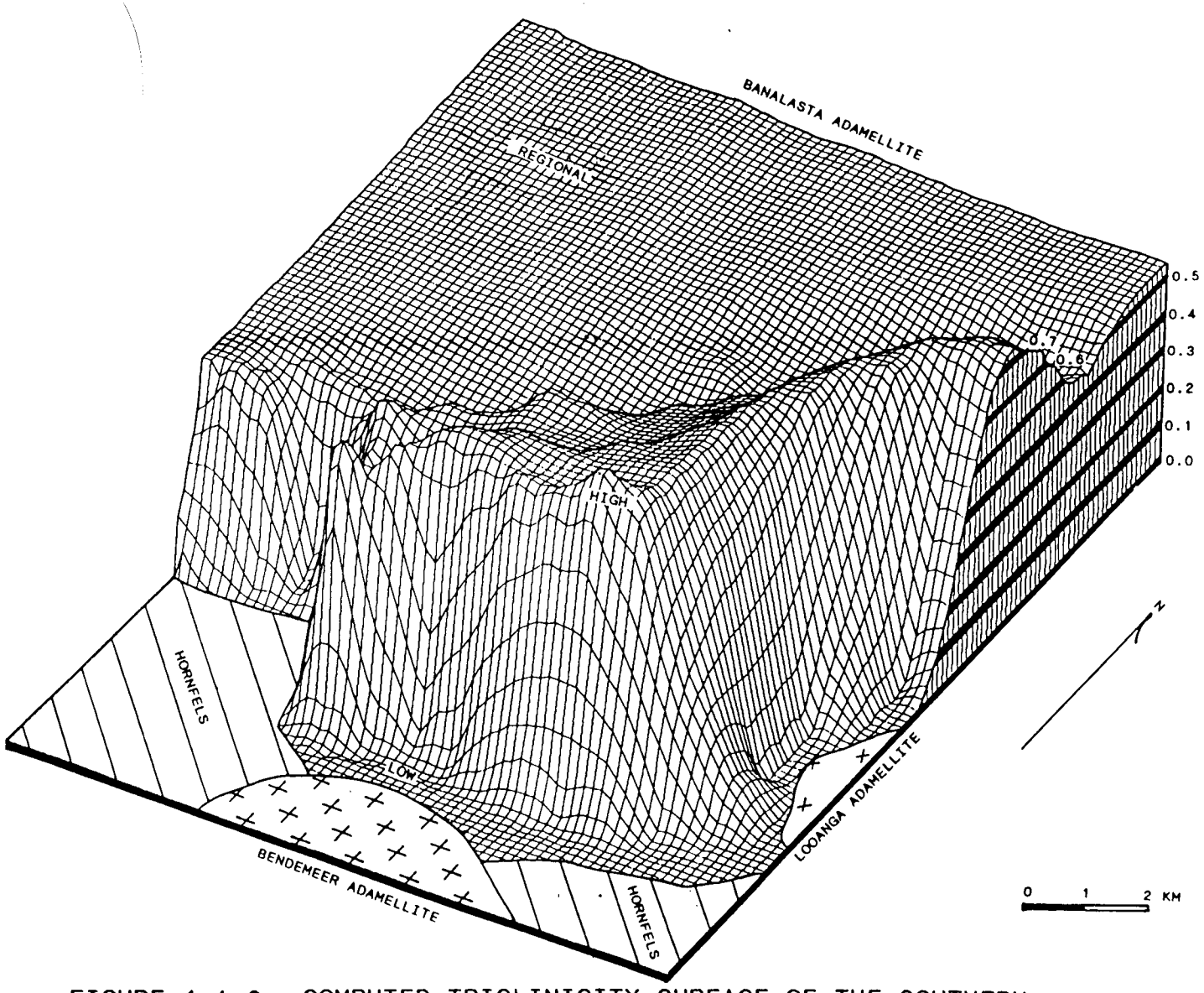


FIGURE 4.1.3 : COMPUTED TRICLINICITY SURFACE OF THE SOUTHERN BUNDARRA SUITE PLUTONS IN THE BENDEMEER AREA.

These triclinicity values show a regional fluctuation about an intermediate microcline mean (0.36 - 0.58) that is continuous throughout the southern Bundarra Suite Plutons. It is proposed that these triclinicities from both the Banalasta Adamellite and the surrounding S-type plutons record minor post- emplacement deformation of these plutons prior to the Permian I-type intrusions. With decreasing distance to the contact a gradual increase in triclinicity from an average of 0.4 to a maximum of 0.83 occurs over a distance of approxiamately 4 kms.

Still closer to the contacts the triclinicity drops abruptly from 0.83 to 0.0 within 1 km. This abrupt change between the high triclinicity zone and the low triclinicity zone immediately adjacent to the later plutons is a very recognisable metamorphic isograd.

The width of the low triclinicity zone is different for the Bendemeer and Looanga plutons. This width difference may be induced by a number of factors :

(i) It may be a function of the contact shapes and dips. The Bendemeer pluton is known to dip inwards at steep angles. This inclined contact may produce the 'apparent' greater thickness of the low triclinicity zone of the Bendemeer pluton. However, no such foliation dip data was obtained from the Looanga pluton to confirm such a cause of the width difference.

(ii) An alternative is that the Looanga intruded towards the end of a regional deformation phase, resulting in microcline being present in the Looanga pluton and therefore a suggested weak reordering of the low triclinicity zone.

(iii) Another possibility is based on the observation that no two plutons show identical contact aureoles, the aureole itself being dependent upon the diameter of the pluton, temperature gradients after emplacement and contact shapes and dips. The character of the Yarrowyck Granodiorite's triclinicity pattern in the aureole of the Gwydir River Adamellite (discussed in part.B) is quite different again and may confirm that although the features of a high and low triclinicity zone are common, their character is determined by the temperature and strains induced by the later intruding pluton.

Another anomalous low triclinicity area is observable in the Banalasta Adamellite on its southeastern margin between the Bendemeer and Looanga plutons. However the proximity to the Walcha Road pluton ( 3km away) may account for this if this larger pluton's thermal effects extend this far into the surrounding area. The placing of the contact metamorphic isograds on the Walcha road pluton's eastern margin by Teale (1974) and in the eastern Bendemeer aureole by Howarth (1973) would suggest that this is possible.

FIGURE 4.1.4 : ARLEMONT TRICLINICITY CONTOURS, SURFACE AND DIAGRAM OF THE PROPOSED BLIND PLUTON

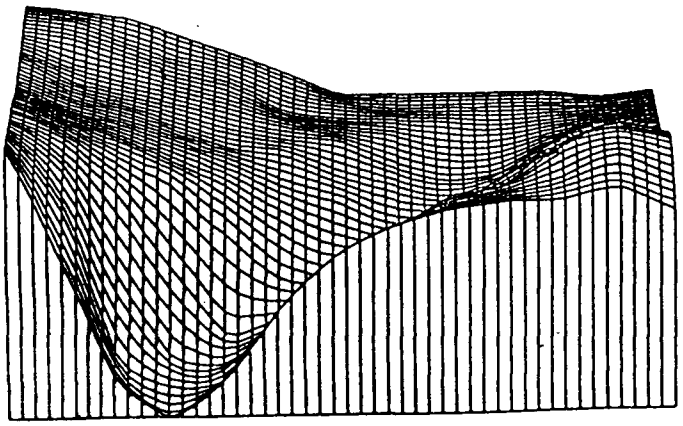

ARLEMONT TRICLINICITY SURFACE

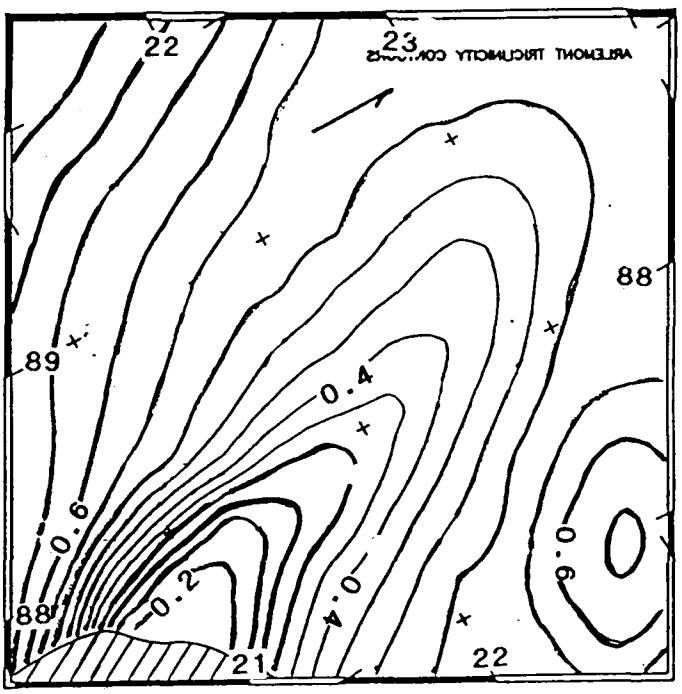


ARLEMONT TRICLINICITY CONTOURS
PROPOSED BLIND PLUTON AT DEPTH, h
AND DIAMETER, d.

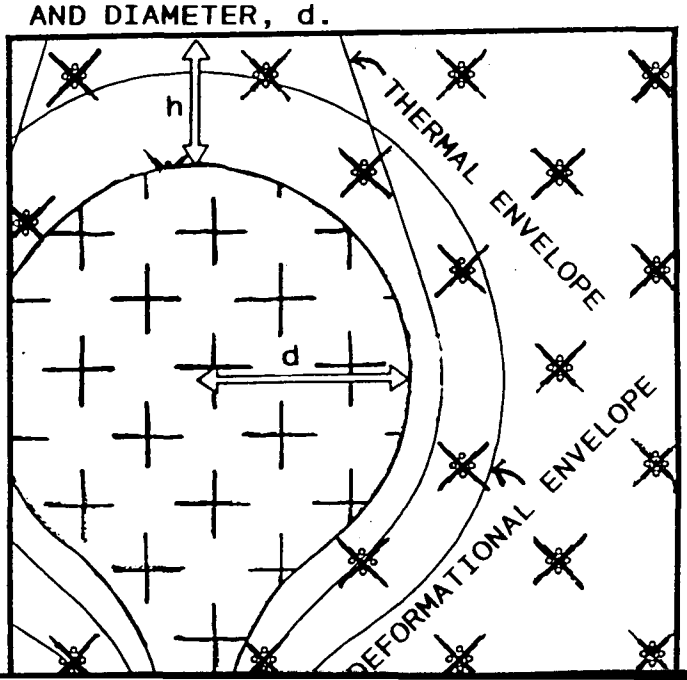

The additional low triclinicity area near the property of Arlemont (Map 2, figure 4.1.4) may also be due to thermal effects. In this area, the otherwise broad (2000m wide) high triclinicity zone (parallel to the contact of the Bendemeer Adamellite) is reduced to only 200m width and adjacent to this is an area of unusually low triclinicity (0.1 - 0.3) (figure 4.1.4) in the vicinity of the Arlemont homestead.

A number of mineralogical and microstructural features observed in thin-section also occur unexpectedly in this area. In particular low abundances of perthite occuring as stringer and bleb styles (Deer et al,1966); recovery and recrystallisation of quartz and misoriented subgrains and deformation twins in plagioclase can be observed. These are all characteristics similar to the high grade zone discussed in chapter 4.2 and would imply thermal annealling due to a localised heat source. This would suggest the existance of a blind pluton (figure 4.1.4) below the south western margin of the Banalasta Adamellite and that the triclinicity analytical method may be useful in detecting blind plutons or adjacent but non-truncating plutons and their age relationship.

The thermal effects and associated causes of the high triclinicity zone will be discussed later after first evaluating the main zones within the Banalasta Adamellite.

## 4 . 1 . 3 : DELINEATION OF THREE TRICLINICITY ZONES :

The K-feldspar triclinicity values (plotted on figure 4.1.5 and map 2) and the observations outlined in section 4.1.2 can be used to divide the metagranite into three metamorphic zones.

The first zone of intermediate triclinicity extends away to the N and NW for many 10's kms, is considered to reflect the general triclinicity of the Bundarra Suite Plutons and has a similar triclinicity to the "unaffected zone" of the Boulder Creek area described by Steiger & Hart (1967).

The next zone has the highest triclinicity and is also sub - parallel to the contacts of the younger plutons, the width varying from 1500 to 2500 m. This high triclinicity zone is characterised by an orthoclase to microcline ordering which has been discussed by previous workers (Eskola,1951; Karamata,1961 and Smithson,1965) in a regional metamorphic context but not as a function of contact metamorphic effects, although Flood (1971) did propose that microcline in the Banalasta Adamellite could be caused by minor post - crystallisation deformation. This zone has not been previously recognised as Flood (1971) considered this to be the regional character of the suite.

The third is the low triclinicity zone of 200m to 1000m width that is closest to the contacts of the two Upper Permian plutons. The recognition of this low triclinicity zone is not new. Steiger & Hart (1967) and Wright (1967) both identified an orthoclase zone adjacent to the later intrusive stocks of the Eldora Quartz-Monzonite, a similar

disordering being observed by Flood (1971) in the Banalasta Adamellite where it is within the aureole of the Walcha Road pluton 10km to the NNE of Bendemeer.

The boundaries between these three triclinicity zones are as follows :

1) MAXIMUM MICROCLINE TO ORTHOCLASE TRANSITION : This boundary between the highest and lowest triclinicity zones is marked by an abrupt change in triclinicity as near maximum microcline is disordered to orthoclase ( represented by the 0.3 to 0.6 isoclines closest to the later intrusive contacts ).

2) REGIONAL INTERMEDIATE TO MAXIMUM MICROCLINE TRANSITION : This boundary from regional triclinicities of 0.4 to outer contact triclinicities of 0.8 is a more gradual change that takes place over distances of 1.5 to 3 kilometres .

On the basis of these triclinicity zones, 17 samples from four traverses (figure 4.1.2) were then x-rayed again for the $\bar{2}04$, 060, $\bar{2}01$ peaks (Wright,1967), to examine whether the alkali feldspar composition for these zones changes in the contact aureole (figures 4.1.5 to 8). [ 1 ]

## 4 . 1 . 3a : INTERMEDIATE TRICLINICITY DOMAIN ZONE.

This zone ( 3-4 kms from the adjacent later intrusive contacts) is characterised by a mix of microcline with intermediate triclinicity values (0.3 to 0.5) and orthoclase. Most K-feldspar grains have both cross-hatch twinned and untwinned domains, a moderate degree of sericitization and the zone delineated by the gentle triclinicity gradient that increases towards the high triclinicity zone.

Compositionally this zone features intermediate microcline - low to intermediate albite (IM-LIA) microperthitic alkali feldspar and compositions of Or80-97 Ab20-3 and a K-feldspar proportion of Mi70-90Or10-30 (figures 4.1.6 to 8).

## 4 . 1 . 3b : HIGH TRICLINICITY ZONE :

This zone, from 1.5 to 4 kms from the later intrusive contacts, is characterised by K-feldspar that is highly ordered microcline (triclinicity = 0.6 to 0.83), the highest value occuring where the high triclinicity zone of the Looanga pluton intersects the high triclinicity zone of the Bendemeer pluton (figure 4.1.2 and map 2). It is delineated on the proximal side by the microcline to orthoclase transition and on its outlying margin by the line demarcating the shallow triclinicity gradient up to the high triclinicity ridge (see figure 4.1.2 & 3,map 2 & 3).

---

[1] all sample numbers refered to in figures 4.1.5 to 8 are preceded by the prefix MU458nn i.e. 66 = MU45866

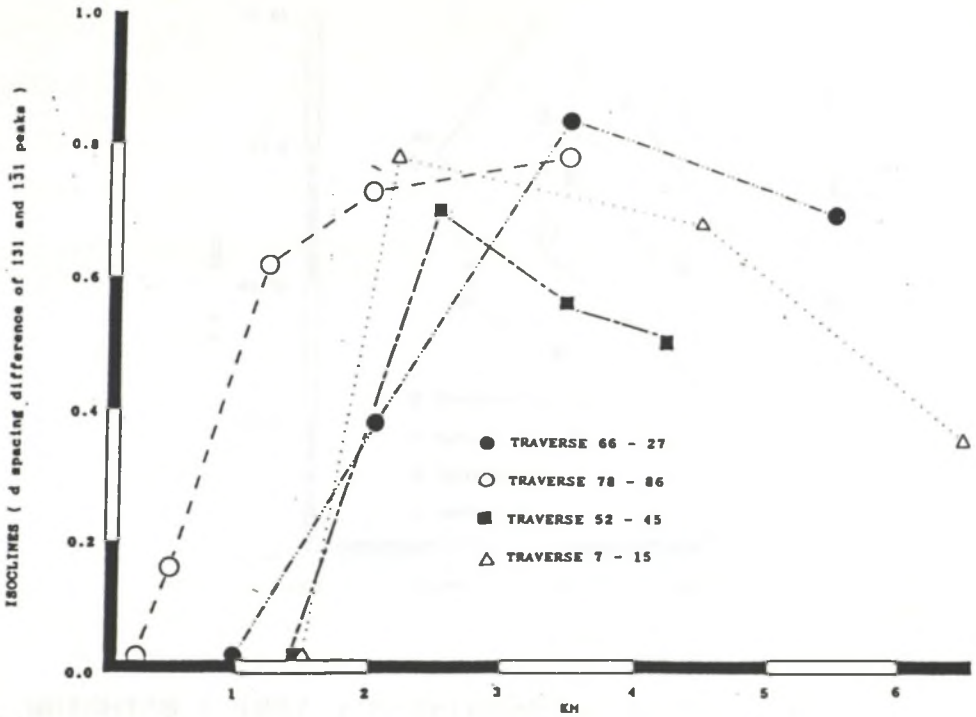


FIGURE 4.1.5 : ISOCLINES ( TRICLINICITY VALUES ) FOR THE 4 COMPOSITIONAL TRAVERSES IN THE BANALASTA ADAMELLITE

FIGURE 4.1.6 : K-FELDPSAR COMPOSITIONS ON THE 4 TRAVERSE LINES, EXPRESSED AS A POTASSIC - SODIC ENDMEMBER %

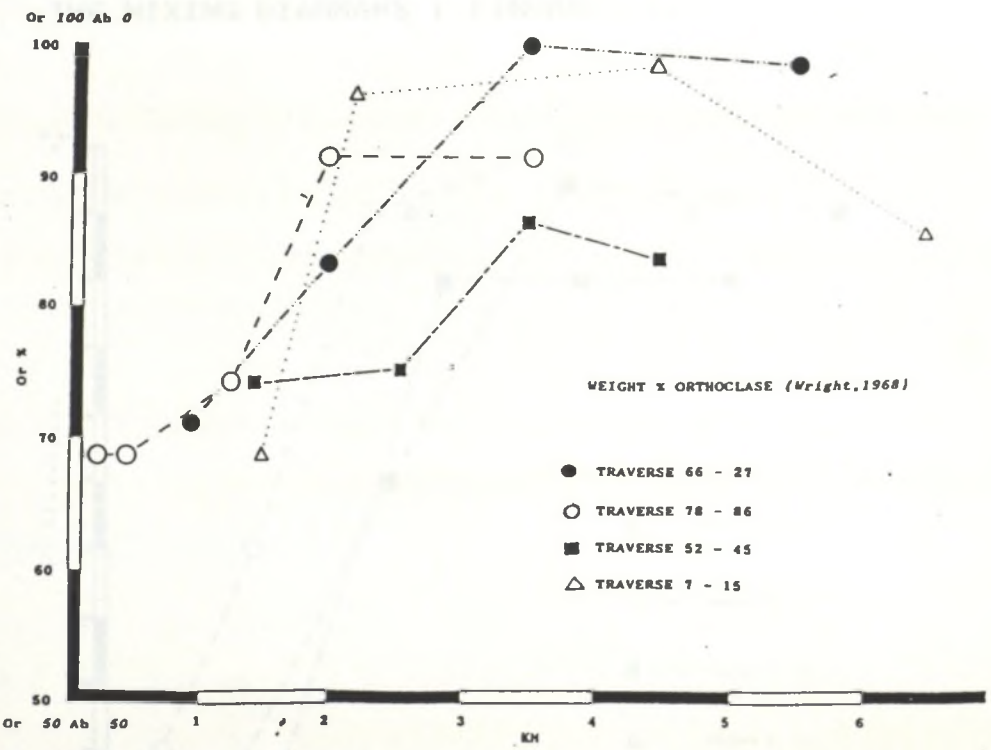

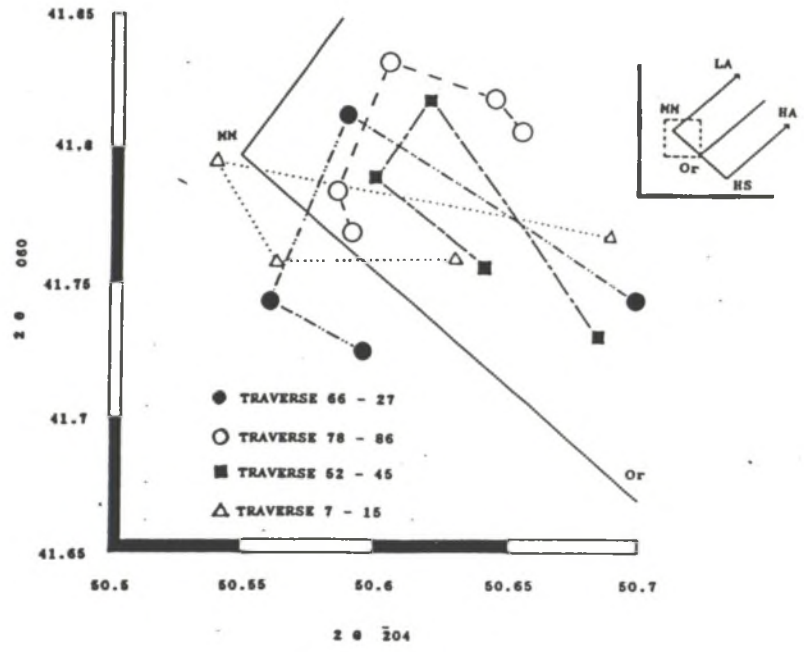


FIGURE 4.1.7 : WRIGHT'S ( 1967 ) K-FELDSPAR COMPOSITIONAL NOMENCLATURE FOR THE BANALASTA TRAVERSES.

FIGURE 4.1.8 : PERCENTAGE MICROCLINE FOR THE BANALASTA K-FELDSPAR COMPOSITIONAL TRAVERSES, BASED ON ESTIMATES FROM THE MIXING DIAGRAMS ( FIGURE ).

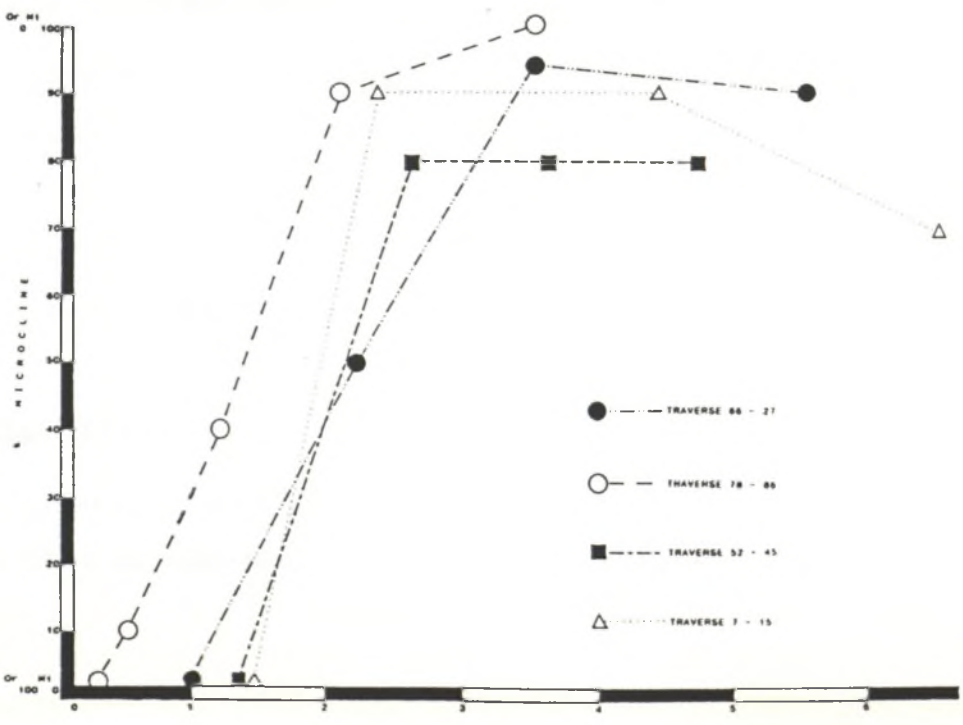

The K-feldspars in this high triclinicity zone have obvious cross-hatch twinning, a higher abundance of replacement style microperthite (Deer,Howie and Zussman,1969) and a high abundance of sericite replacing the feldspars.

The plot of 2θ's for the 060-$\bar{2}$04 peaks (figure 4.1.7) and the 2θ value for the $\bar{2}$01 peak, expressed as an Ab% (figure 4.1.6) demonstrates that in the four traverses this zone is characterised by near maximum microcline - low albite microperthitic alkali feldspar with composition of the K-feldspar host of Or 97-100 Ab 3-0 and a K-feldspar proportion of Mi95-100 Or0-5 (figure 4.1.8).

## 4 . 1 . 3c : LOW TRICLINICITY ZONE :

This zone of 250m to 1500m width is characterised by K-feldspar that is disordered (monoclinic) orthoclase (0.0 triclinicity) and less abundant low triclinicity microcline ( 0.2 triclinicity). Examination of thin sections of 6 samples within this zone reveals only minor patches of grid twinning in otherwise simple twinned orthoclase feldspar, fine stringer-bleb microperthite and a moderate abundance of sericitic replacement.

Plots of the 2θ values of (060) vs ($\bar{2}$04) (figure 4.1.7) indicate an orthoclase - intermediate albite microperthitic alkali feldspar composition.

The position of the 201 peak (Wright,1967) for potassium feldspar indicates the K-feldspar composition is Or70 Ab30 (figure 4.1.6). Thus the closest zone to the Permo-Triassic intrusions contains the most disordered (0.0 to 0.2 triclinicity) and the most albite rich (Or70 Ab30) alkali feldspar separates which lie towards the orthoclase - intermediate albite end of Wright's (1968) alkali exchange series, with a K-feldspar proportion of Mi0-5Or95-100 (figure 4.1.8).

## 4 . 1 . 4 : A MODEL FOR THE BANALASTA ADAMELLITE'S TRICLINICITY

The determination of a number of domains is by no means a new feature in K-feldspar analysis, Steiger and Hart (1967) and Wright (1968) outlined three distince zones in the Boulder Creek area due to the microcline to orthoclase transition. Tilling (1968) determined three similar zones and explained them by pluton cooling inducing an orthocalse to intermediate microcline ordering and later contact re-heating causing a microcline to orthoclase disordering. However, in the Banalasta pluton the maximum microcline ridge is not effectively explained by any of these previous models.

## 4 . 1 . 4a : DEFORMATION EFFECTS :

A monoclinic orthoclase to triclinic microcline ordering due to increasing deformational strain effects has been documented by Eskola (1951), Karamata (1961), Smithson (1963) and Nillsen and Smithson (1965). Initial

observations would seem to suggest that the rise to a high triclinicity ridge in the Banalasta Adamellite may correlate with increasing strains and less importantly temperature conditions caused by the deformational emplacement forces induced by the Permo-Triassic plutons, with the greatest triclinicities (and therefore deformation) occuring at the intersection of the two pluton's high triclinicity zones.

## 4 . 1 . 4b : THERMAL EFFECTS

The disordering of microcline to orthoclase has been explained by thermal (contact) metamorphism by Hart (1961), Steiger & Hart (1967), Wright (1967), Tilling (1968) and Gorbatschev (1972). This transition zone is a function of temperature (400 - 500 degrees Celcius), the width of the transition zone being a function of the temperature distribution) and the later intrusive contact shape and diameter (Steiger & Hart,1967).

The microcline to orthoclase disordering on the S and E margins of the Banalasta Adamellite is caused by this thermal (contact) metamorphic effect and the associated temperature increase with decreasing distance to the contact (based upon Wright's (1967) calculations (figure 4.1.9)) is shown in figure 4.1.10. This thermally induced disordering may also explain the low triclinicities in the Arlemont area (section 4.1.4) and on the Banalasta pluton's southeastern margin possibly due to the Walcha Road pluton's thermal aureole.

## 4 . 1 . 4c : DEFORMATIONAL - TEMPERATURE RELATIONSHIPS :

The implications of the thermal and deformational zones outlined by triclinicity and compositional data suggests increases in deformation (due to an increased strain), induced by the emplacement forces of the two I-type intrustions. This triclinicity variation being caused by an ordering of a predominantly intermediate microcline pluton to maximum microcline by increased stresses (associated with the rise of the I-type granitoids). Contemporaneous with this, disordering of microcline to orthoclase due to increased thermal conductivity adjacent to the emplacing granitoids results in the low triclinicity zone. The modelled triclinicity surface for these features is shown in figure 4.1.3 and map 2.

Eggleton (1980) states that temperature, pressure and deformation are all physical controls that determine the degree of order-disorder (pressure and deformation tending to enhance ordering and temperature tending to enhance disordering). If Eggleton's findings are coupled with Wright (1967) and Stormer's (1975) geothermometric calculations then it might be possible to construct strain - temperature relationships associated with the intrusion of the Bendemeer and Looanga Adamellites into the Banalasta Adamellite.

If, when the Bendemeer and Looanga plutons intruded the Banalasta Adamellite, the contact zones became increasingly strained and the contact temperature increased to 600 degrees C (figure 4.1.10) (which compares

FIGURE 4.1.9 : CONTACT, TRANSITIONAL AND HIGH TRICLINICITY TEMPERATURE ESTIMATES : AFTER WRIGHT ( 1967 )

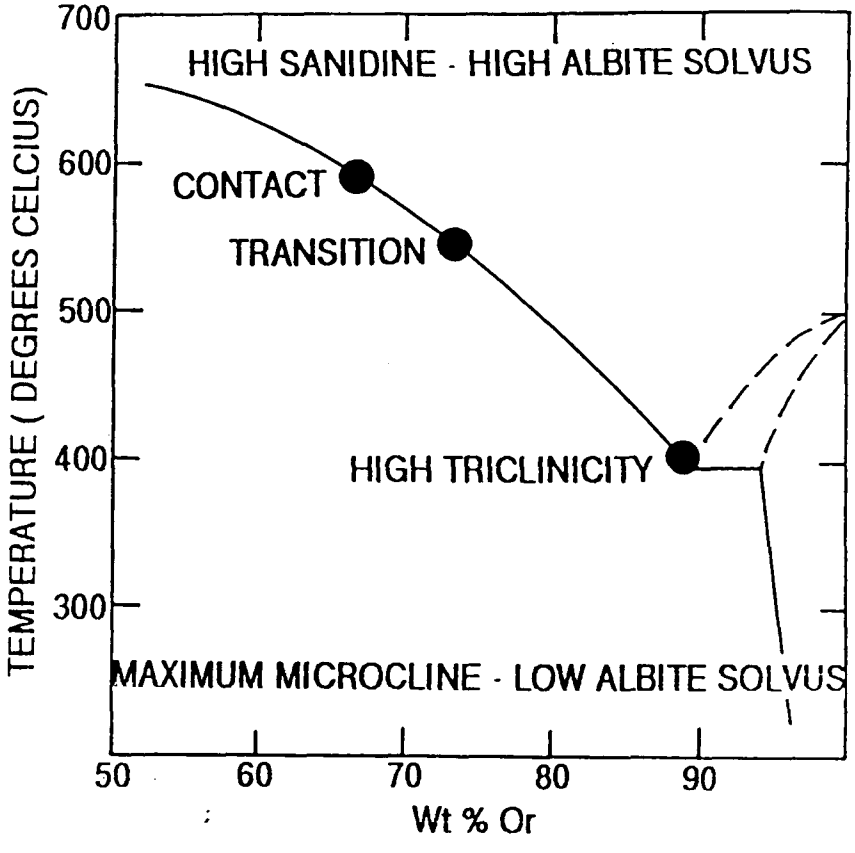


FIGURE 4.1.10 : TEMPERATURE VS DISTANCE FROM CONTACT FOR THE BANALASTA ADAMELLITE IN THE BENDEMEER ADAMELLITE'S AUREOLE.

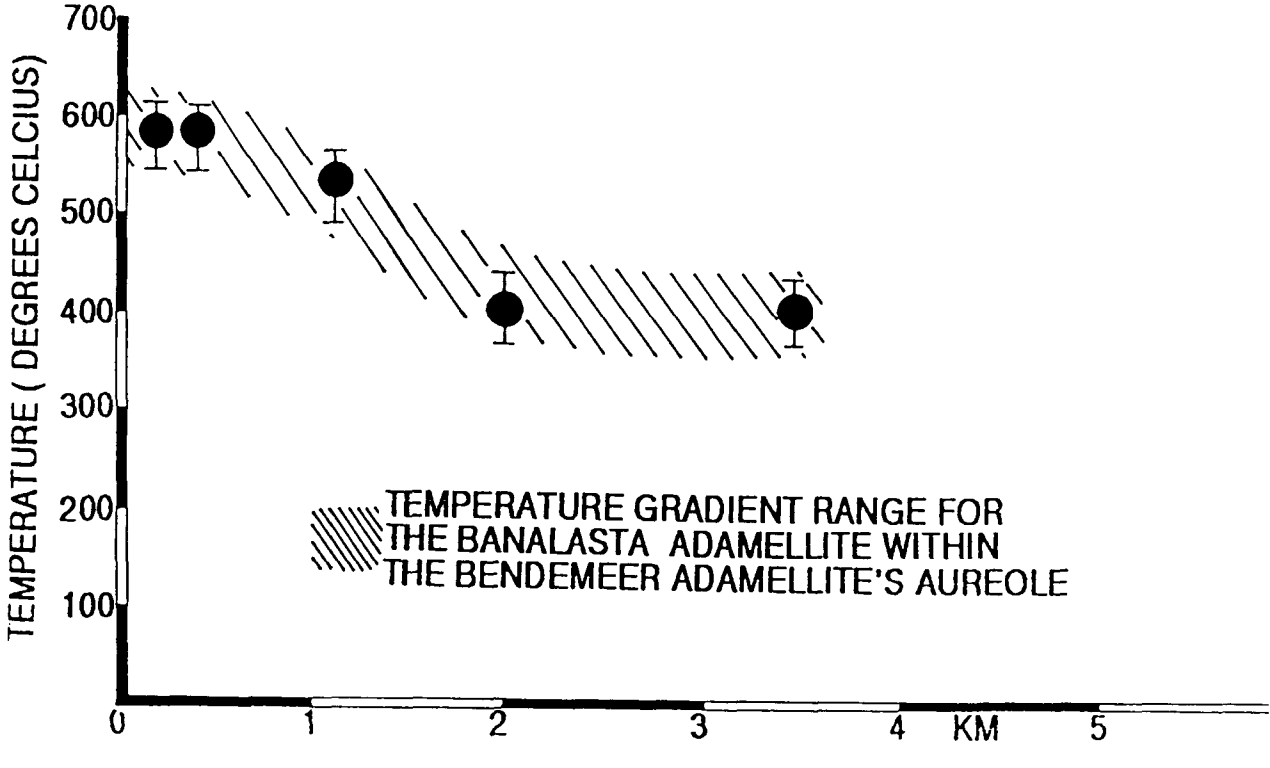

FIGURE 4.1.11 SUMMARY DIAGRAM OF POTASSIC FELDSPAR VARIATIONS WITH DECREASING DISTANCE TO THE LATER INTRUSIVE CONTACTS ( PERTHITE STYLES HAVE BEEN INCLUDED TO EMPHASISE THE OrAb - PERTHITE CORRELATION )

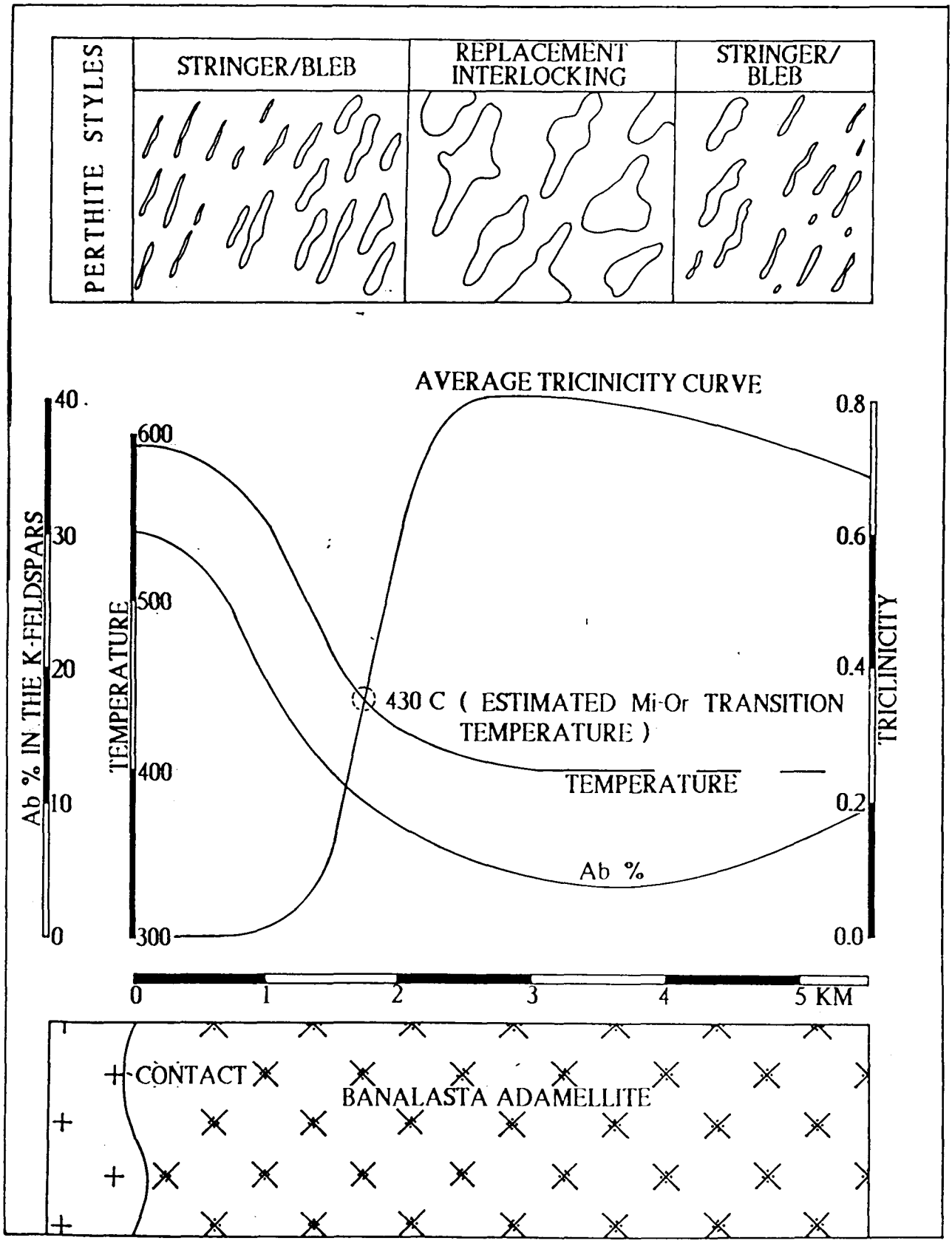

favourably with contact temperatures in the hornfelsic rocks (chapter 3.3)), Then the implications of the increased strain and temperature when coupled with the high and low triclinicity zones, are as follows:

(i) High emplacement induced stresses from the Permian granitoids have resulted in a wide (up to 3 km) deformation aureole. This aureole is evident in the ordering of the K-feldspars and has produced the documented high triclinicity zone marginal to the intruding plutons. Further evidence for this deformation is seen in the microstructural and intergrowth responce of the Banalasta Adamellite's minerals, described in chapter 4.2.

(ii) contemporaneous with the higher deformational strain the contact temperatures within 1 to 1.5 km of the emplacing plutons lies above the orthoclase - microcline inversion temperature (based on figures 4.1.9 and 10 and equals in the Bendemeer area approxiamately 430 +-10 C). These high contact temperatures (up to a maximum of 590 degrees C , figure 4.1.10) have induced thermal disordering of the K-feldspars and hence the low triclinicity zone adjacent to the later intrusives. Few deformation microstructures and lower abundances of solid-state intergrowths are observed in this zone. This can be explained if strain rates are low during emplacement (Griggs et al, 1960) and hence recovery and recrystallisation processes continuously anneal out the higher strain features expected in this zone.

These triclinicity observations confirm that high-level granitoid emplacement is at least weakly syndeformational as concluded by Vernon (1987) on porphyroblast - matrix relationships in contact aureoles. The triclinicity progression of order-disorder is summarized in figure 4.1.11 and includes the correlated perthite observations.

# A . 4 . 2 : MICROSTRUCTURAL RESPONSE

## 4 . 2 .1 : INTRODUCTION

Petrographic studies of samples from the Banalasta Adamellite have revealed a microstructural zonation within the pluton that correlates with the three triclinicity zones outlined in section 4.1. All samples are coarse grained and some contain K-feldspar megacrysts. The major minerals of K-feldspar, plagioclase, quartz and the micas have been examined microstructurally as well as the myrmekite and perthite intergrowths. The zones will be referred to as regional, low and high grade and correlate with the regional, high triclincity and low triclinicity zones respectively.

## 4 . 2 . 2 : POTASSIUM FELDSPAR

In addition to the compositional and structural state changes of the potash feldspars in the Banalasta Adamellite, three distinct textural zones can also be recognised within the contact aureole of the Bendemeer Adamellite.

### (i) regional zone : ( 2 - 3 km from intrusive contacts)

The majority of K-feldspar grains in this zone show gradational patches of both orthoclase and cross-hatch twinned microcline. The patches of microcline twinning were commonly observed throughout the grains, however noticeably higher concentrations predominated in the interstitial areas of the k-feldspar grains. This is shown in plate 4.2.1, and the interstitial microcline areas of the orthoclase grain may be accounted for by the fact that higher stresses induced by a regional deformational episode are likely to occur at the more irregular (higher energy) grain boundaries. Some sericitic and perthitic replacement occurs but is of low abundance compared to the other two zones.

### (ii) low grade zone : (1.5 - 3 km from intrusive contacts)

The K-feldspar in this zone is characterised by a higher proportion of microcline twins evenly distributed thoughout the grains (plate 4.2.2). The K-feldspars show a high proportion of sericite and perthite (the perthite being a mixture of string and interlocking styles, plate 4.2.2) and more numerous marginal intergrowths of myrmekite. The microclines commonly are interstitial ( except in the case of the megacrysts ) and contain granoblastic inclusions of biotite, quartz, plagioclase and white-mica. Some patches of orthoclase are visible which grade smoothly into microcline. These areas may suggest remnants of once disordered orthoclase or the initiation of the disordering process seen in the thermal zone.

PLATE 4.2.1 : ORTHOCLASE - MICROCLINE PATCHES IN K - FELDSPAR FROM THE LOW GRADE ZONE ( NOTE THAT THE MICROCLINE CROSS - HATCH TWINNING CONCENTRATES IN THE NARROWER INTERSTITIAL AREAS OF THE GRAIN ) ( MU45808 )

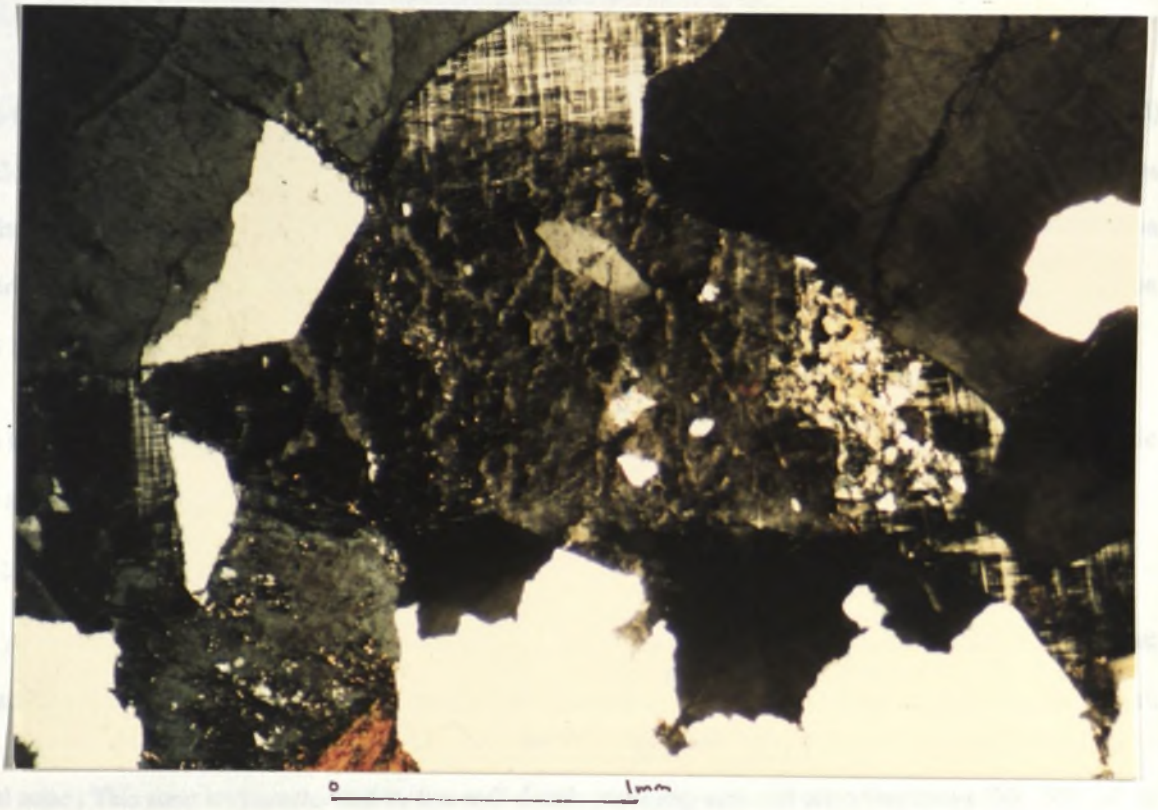


PLATE 4.2.2 : COARSE STRINGER AND INTERLOCKING PERTHITE STYLES AND COMPLETE GRID TWINNING OF INTERMEDIATE GRADE MICROCLINE ( MU45861 )

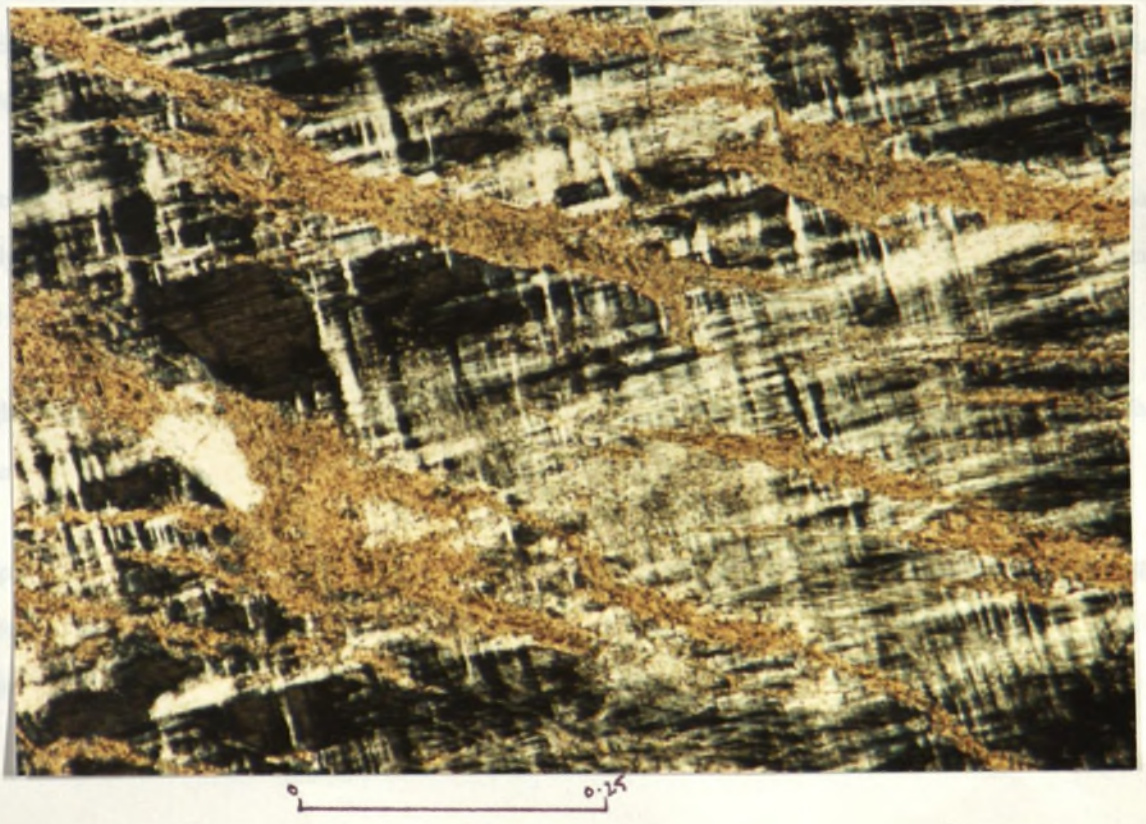

(iii) high grade zone: ( -1.5 km of intrusive contact)

The K-feldspars in this zone are characterised by predominantly orthoclase. Subgrain development (plate 4.2.3) in the K-feldspar has been observed and is due to grain boundary migration (along serrated margins). Minor patches of microcline twinning do occur, commonly near grain boundaries and imply that the microcline - orthoclase transition is characterised by varying proportions of microcline and orthoclase (as has been outlined compositionally in section 4.1) and is potentially controlled by areas of residual high stress.

The K-feldspar close to the contact also shows high abundance of alteration to sericite. However perthitic exsolution and myrmekitic developement are significantly lower in abundance.

## 4 . 2 . 3 : PLAGIOCLASE

In general throughout the Banalasta Adamellite, plagioclase occurs as coarse grains and less abundant megacrysts. Multiple twinning (both growth and deformation) is common throughout as well as sericitic replacement.

(i) regional zone : This zone is characterised by few well developed subgrains and misorientations (30 - 50% of the area of the grains). In addition the zone is characterised by undisrupted primary magmatic grains with predominantly growth and only minor deformational twinning. No subgrain development is observed and more typical granitic microstructures with variable angle grain boundaries occur.

(ii) low grade zone : This zone is characterised by plagioclases with high proportions of misorientations, internal subgrain development and rotation (rotation being from sub-parallel to as much as 80 degrees (plate 4.2.4) and up to 60 - 75% of the area of grains show rotational subgrains).

Minor rim subgrain development of plagioclase is evident and suggests processes of grain size reduction (potentially due to deformational effects). Large scale kink bands in plagioclase twins are also evident and in some cases bent twins are observable (photograph not processed by Kodak).

Higher abundances of sericitic replacement of the plagioclase grains occurs in this zone (plate 4.2.5). The abundance of misoriented subgrains was observed to decrease further into the Banalasta Adamellite.

(iii) high grade zone : Plagioclase in this zone is characterised by lower abundances of misoreintations in the large grains ( less than 30% of the area of the plagioclase grains show the dislocations and subgrain development). In addition there is a high proportion of grain boundary recovery within this zone, annealling and the developement of

PLATE 4.2.3 : RECRYSTALISATION AT A SUTURED GRAIN BOUNDARY BETWEEN TWO K-FELDSPAR GRAINS (MU45843)

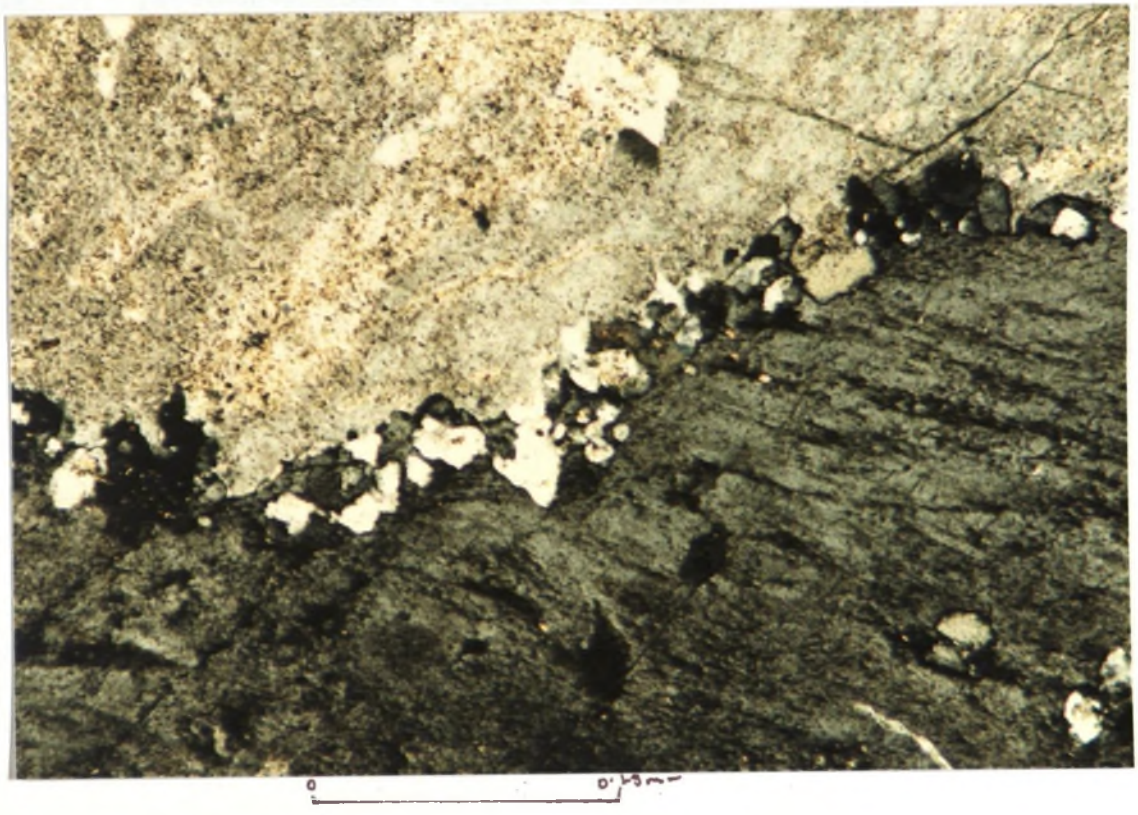


PLATE 4.2.4 : PLAGIOCLASE MISORIENTATIONS ( MU45848 )

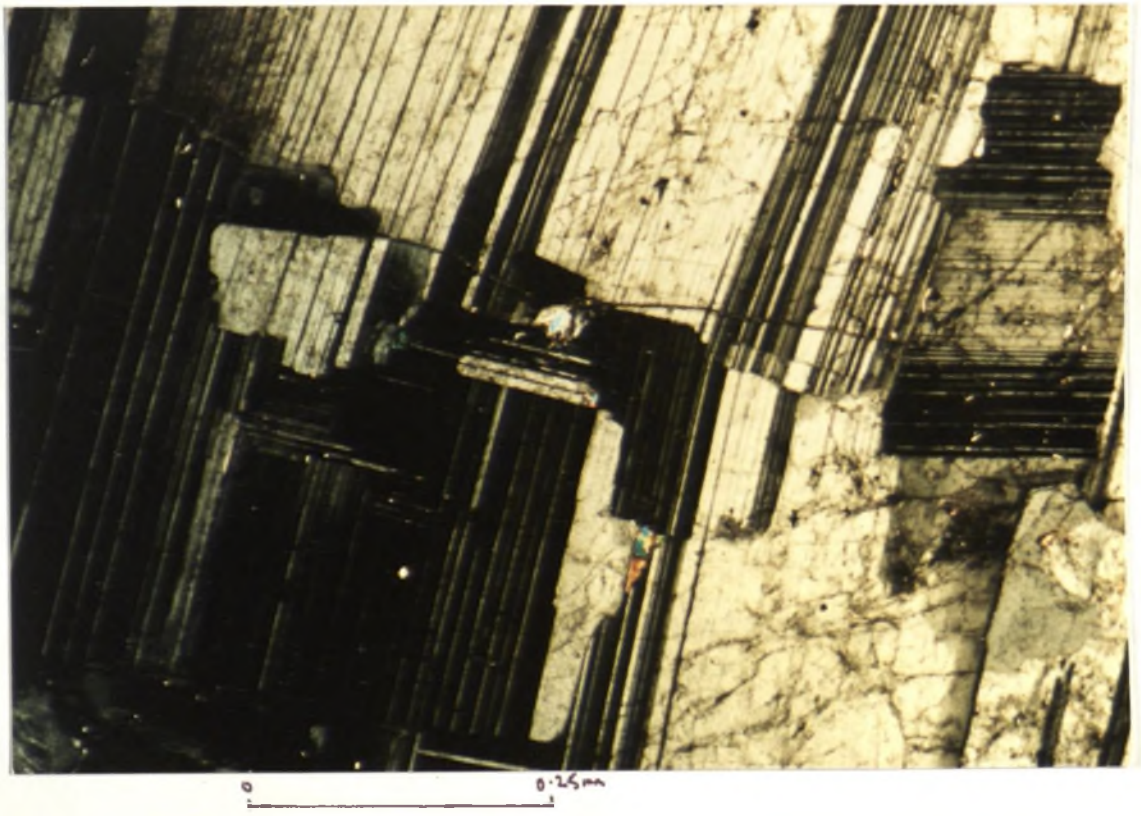

PLATE 4.2.5 : SERICITIC REPLACEMENT OF PLAGIOCLASE ( MU45882 )

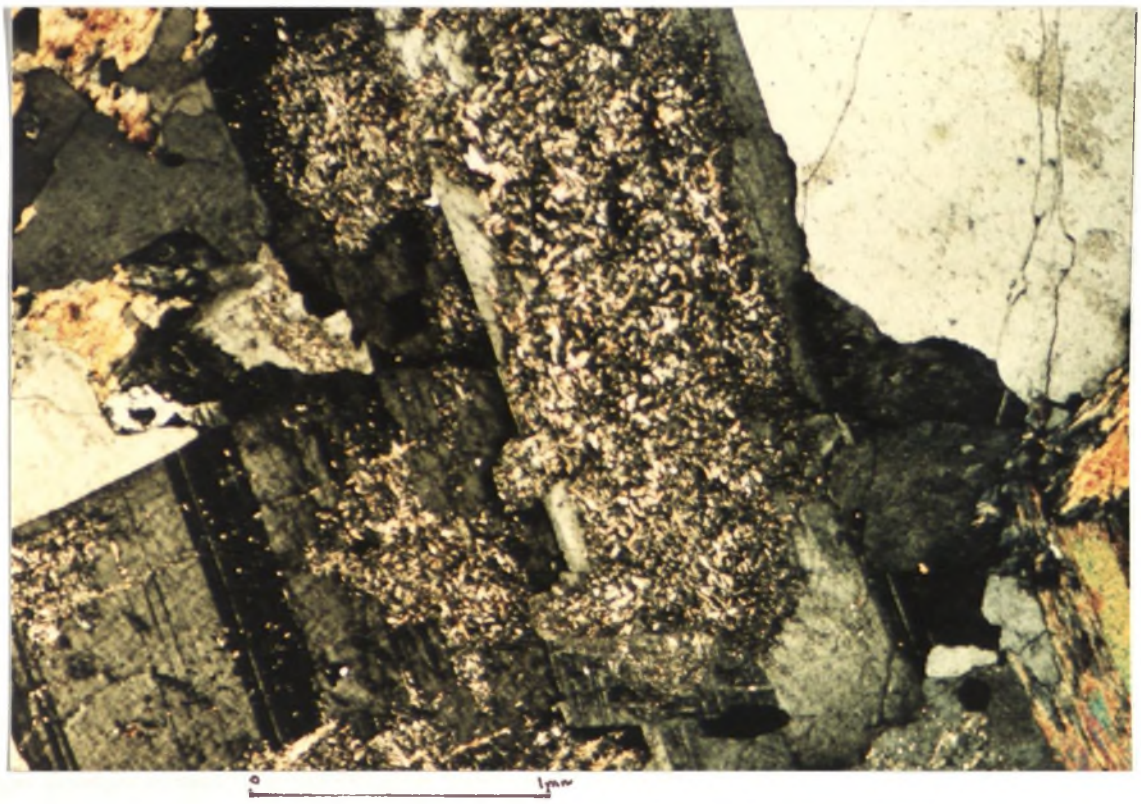


PLATE 4.2.6 : BANDED EXTINCTION IN A LARGE QUARTZ GRAIN ( MU45813 )

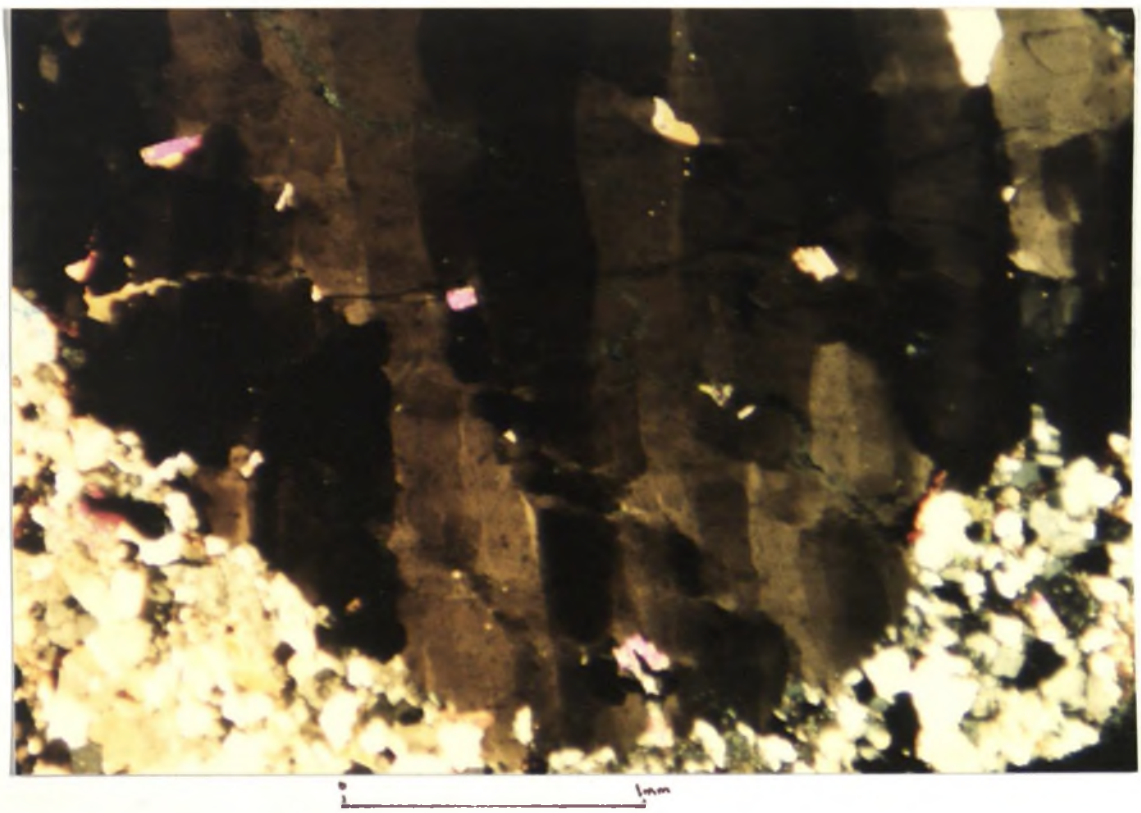

a granoblastic texture to the finer grains. Replacement has occurred within plagioclase grains showing finer grained albitic margins where in contact with potash feldspar and sericitic replacement is evident in a number of grains, but is in lower abundance than in the low grade zone.

### 4 . 2 . 4 : QUARTZ

In hand specimen the quartz grains are medium to coarse grained throughout the study area, with the largest grains being up to 2 cm across. (i) regional zone : The quartz grains in this zone show little straining and show low abundances of banded extinction (20 - 40% of the area of all grains) with almost no sutured (corrugated) grain boundaries. Undulose extinction is common but is more typically gradational thoughout the grains. The grains themselves in this lowest grade zone tend to have more late stage magmatic interstitial microstructures with typical undulose and complete extinction being common.

(ii) low grade zone : Polygonal grains are more common in this zone not only in the finer recrystallised grains but also in the larger grains, suggesting significant grain boundary migration under high stress conditions. Extinction bands are more common (up to 80 - 100% of the area of all grains) and they are almost always sharp and commonly sub-parallel throughout each thin-section (plate 4.2.6). Internal bulge nucleation and internal planes of migration are evident by sutured ( Vernon, 1976) to highly sutured sharp internal bands (plate 4.2.7), separating areas of differing undulosity within grains. The subgrain development is near to completion in a number of grains, forming granoblastic areas of quartz aggregates. Some fine granoblastic quartz associated with plagioclase subgrains near partially replaced potash feldspar megacrysts suggest subgraining and polygonization of once myrmekitic intergrowths. The quartz subgrains appear to be in discontinous trails suggestive of 'ghost' vermicules with plagioclase grains distributed around and between these trails. The quartz and plagioclase aggregates have crude rim outlines adjacent to the replaced K-feldspar and in one slide, the larger plagioclase subgrains possibly show different extinction directions in one area (plate 4.2.8) suggestive of a once larger (now misoriented) myrmekite rim.

(iii) high grade zone : This zone is characterised by low abundances of linear extinction bands with sub-gradational boundaries between bands and moderately large grains ( up to 1.5 cm in places). Quartz grain annealling was observed, sutured quartz grain boundaries, although common, are now characterised by recovery and recrystallisation and hence numerous very fine granoblastic subgrains, at once sutured grain boundaries are observable (plate 4.2.9). In addition a lower percentage and a gradational nature to the undulose bands (by comparison with the low grade zone ) suggest a degree of annealling and healing of the dislocations developed in the quartz grains.

PLATE 4.2.7 : SUTURED GRAIN BOUNDARIES IN QUARTZ AND THE INITIATION OF RECRYSTALISATION (MU45859)

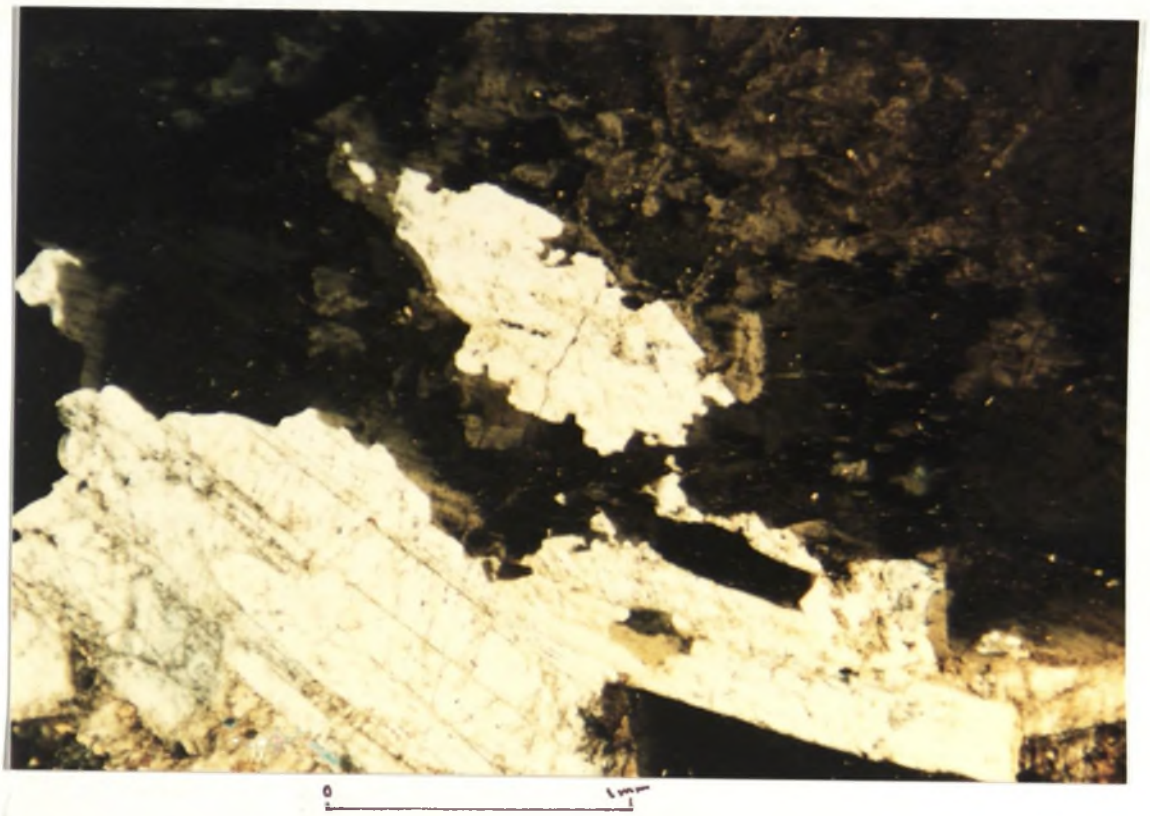


PLATE 4.2.8 : RIM MYRMEKITE AND MISORIENTED AREAS SHOWN BY THE SODIC FELDPSAR'S DIFFERENT EXTINCTION DIRECTIONS ( MU45810 )

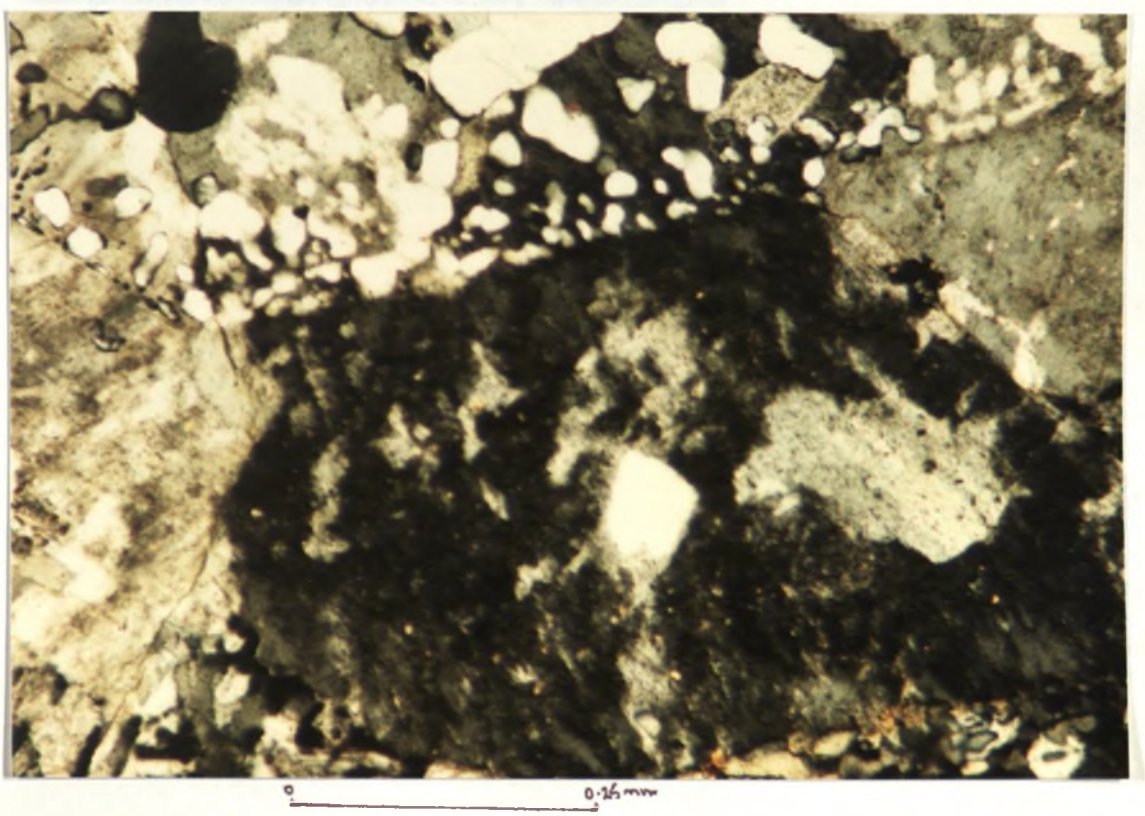

PLATE 4.2.9 : QUARTZ RECRYSTALISATION AT A SUTURED GRAIN BOUNDARY (MU45866)

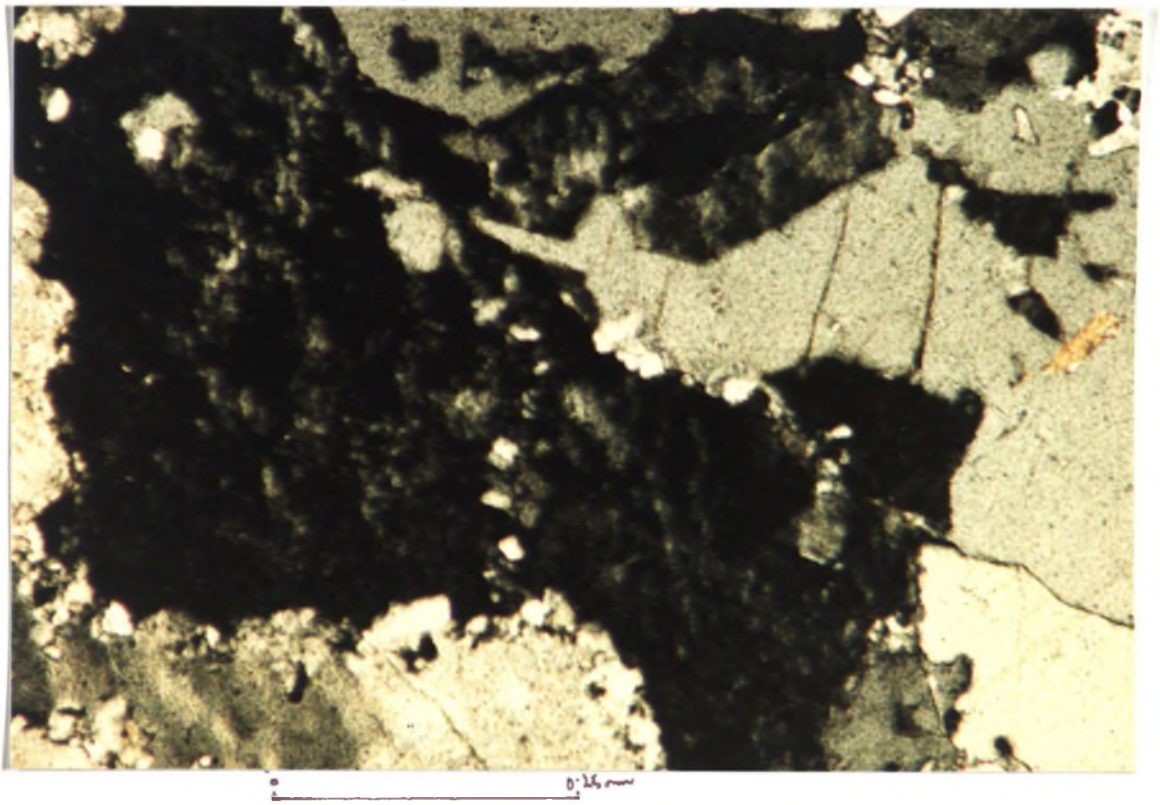

PLATE 4.2.10 : BENT 001 CLEAVAGE PLANES IN BIOTITE AND THE OCCURANCE OF PRIMARY MUSCOVITE ( MU45866 )

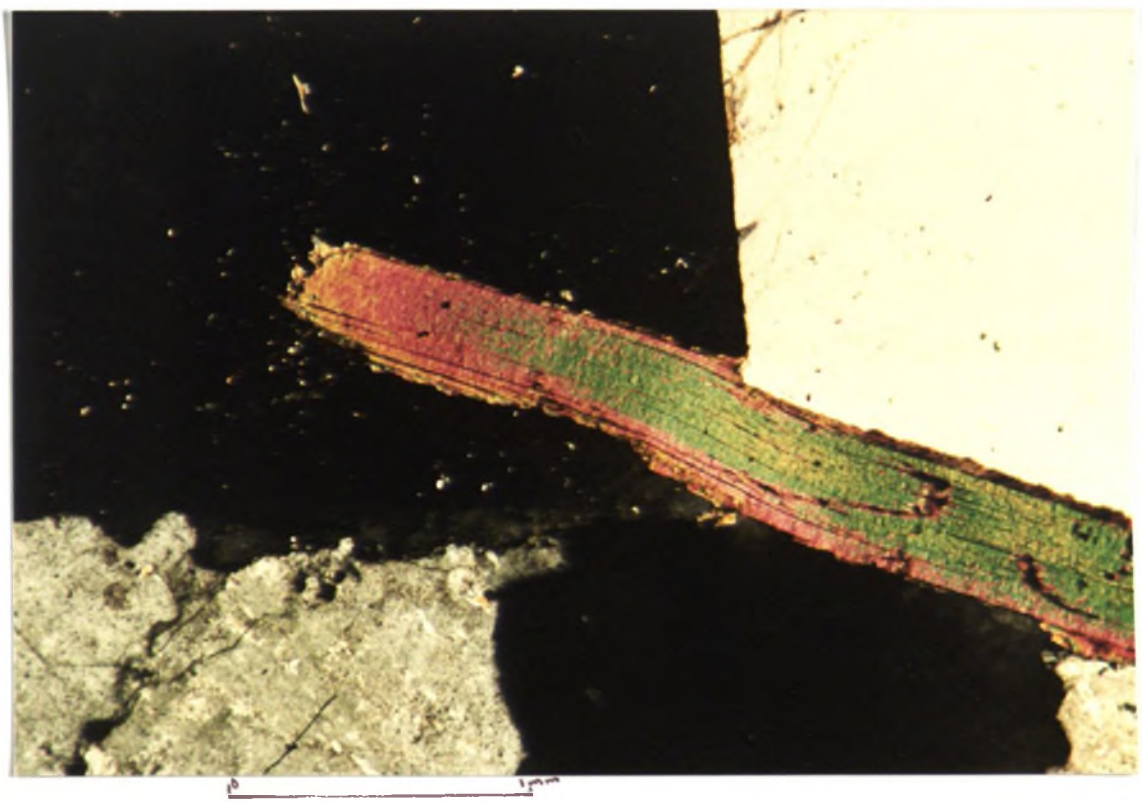

## 4 . 2 . 5 : MICAS

Micas are a minor constituent of the Banalasta Adamellite with biotite ( modally less than 8%, Chappell(1978)) being the most abundant variety and of magmatic origin, muscovite being in minor abundance and being partially of secondary origin and sericitic white mica being a replacement product in the feldspars and cordierites.

(i) regional zone : Muscovite and biotite are both present in this zone, whereas sericite is a fairly minor constituent. The micas are all unkinked and no evidence of bending is observable. Generally the micas are in typical granitic-igneous textural relationships to other grains.

(ii) low grade zone : Biotite in this zone is characterised by a higher abundance of broad kinked and bent grains and subgrains. The bent 001 planes observed in both plates 4.2.10 & 11 are only very gentle warps and suggest that the deformation that induced these features was weak.

(iii) high grade zone : Closest to the contact the biotites exhibit minor kinking and bending. Where kinking does occur these kink bands are often sub-parallel to the quartz extinction bands noted above. A number of areas show large biotite grains (of uniform extinction) possibly being replaced by quartz and secondary biotite intergrowths. Recrystallisation was observed although not common and suggests that large grains have undergone grainsize reduction.

## 4 . 2 . 6 : MYRMEKITE

Myrmekite intergrowths are present as minor constituents in all samples, but show some variation in style and abundance in each zone.

(i) regional zone : This zone is characterised by high abundances of primary myrmekitic intergrowths occuring as thin rims and minor lobes within k-feldspar grains and may have been induced by a weak regional deformational episode. Phillips ( 1974 ) suggesting that bulbous myrmekite tends to be associated with a deformed host rock.

(ii) low grade zone : Myrmekite in this zone is in higher abundance and occurs in thick lobes and rims to the extent that in some places it has completely engulfed the potash feldspar. Plates 4.2.13 & 14 show this complete supplanting of K-feldpsar by myrmekite and an additional interesting phenomenon where the myrmekitic intergrowths have been crystallographically controlled parallel to the growth directions on each face of the original magmatic sector-zoned K-feldspar. Previous studies of sector zoned K-feldspars have postulated that the sector zoning is due to crystallographic control of the acceptance of inclusions (Vaniman, 1978). However, no inclusions were observed in

PLATE 4.2.11 : BENT 001 CLEAVAGE IN BIOTITE ( MU45848 )

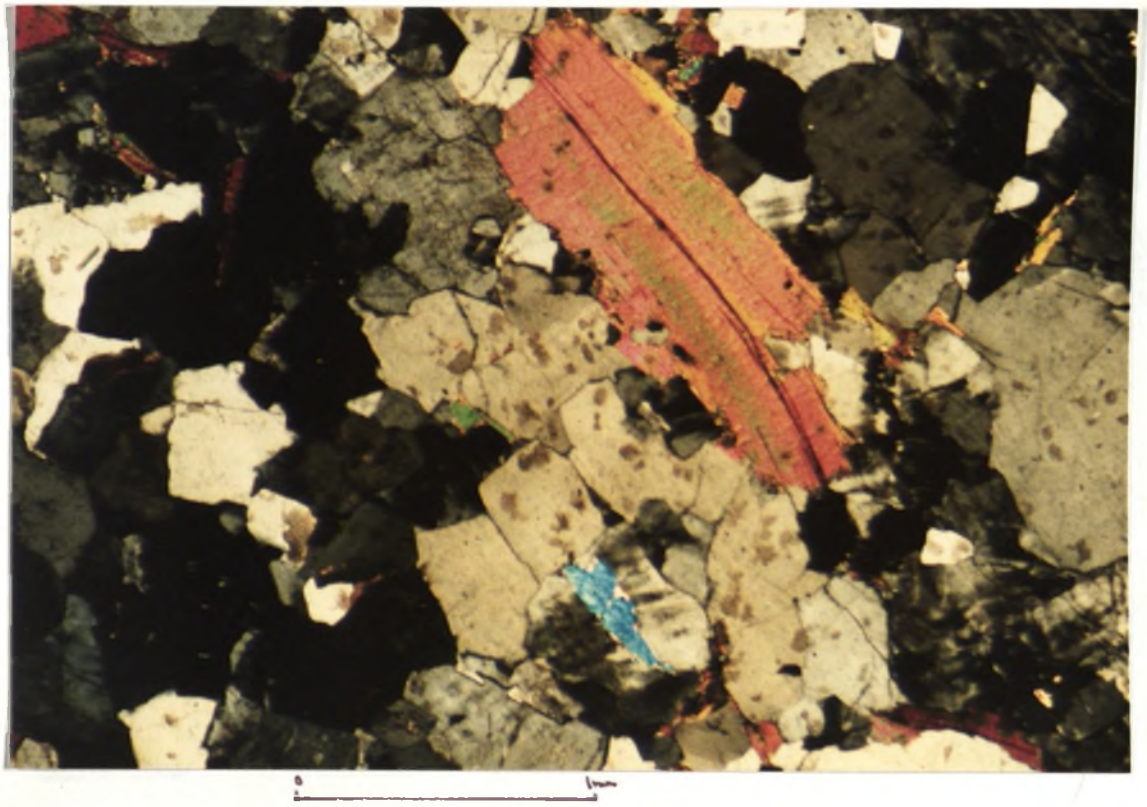

PLATE 4.2.12 : THIN ( < 0.1 mm ) RIM MYRMEKITE ON A FELDSPAR GRAIN ( MU45815 )

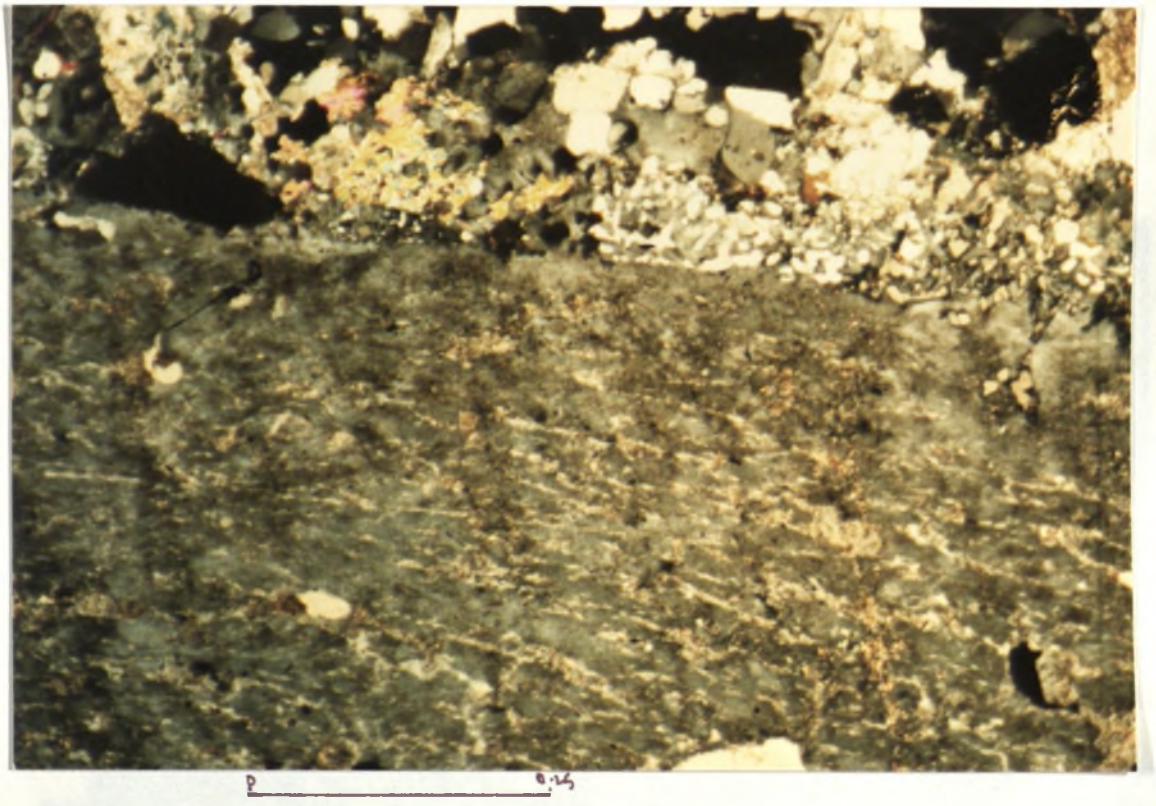

PLATE 4.2.13 : COMPLETE ENGULFING OF ORIGINALLY SECTOR ZONED K-FELDSPAR BY MYRMEKITE ( MU45869 )

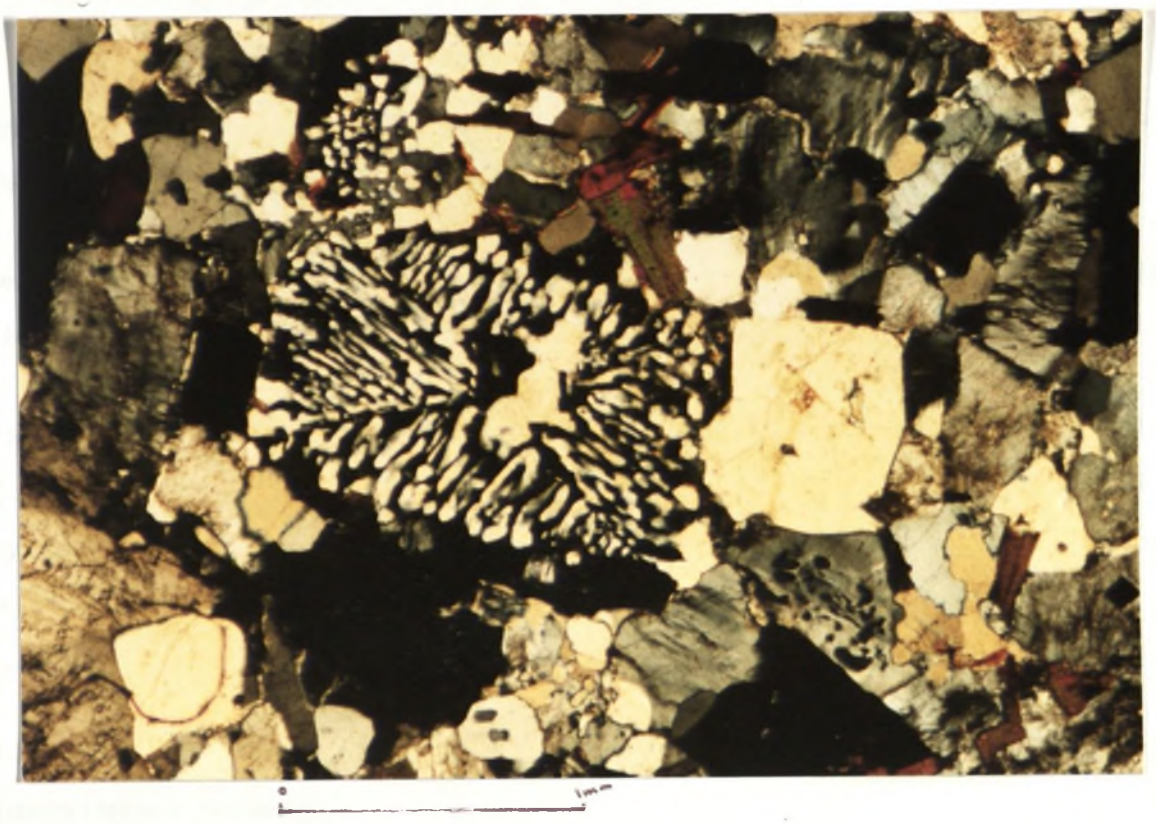

PLATE 4.2.14 : CLOSE UP OF MYRMEKITE PSEUDOMORPHING OF THE SECTOR ZONED K-FELDSPAR, SHOWING HIGH ANGULAR RELATIONSHIPS BETWEEN THE VERMICULES IN ADJACENT SECTORS. ALL VERMICULES WITHIN EACH SECTOR BEING ESSENTIALLY PARALLEL ( MU45869 )

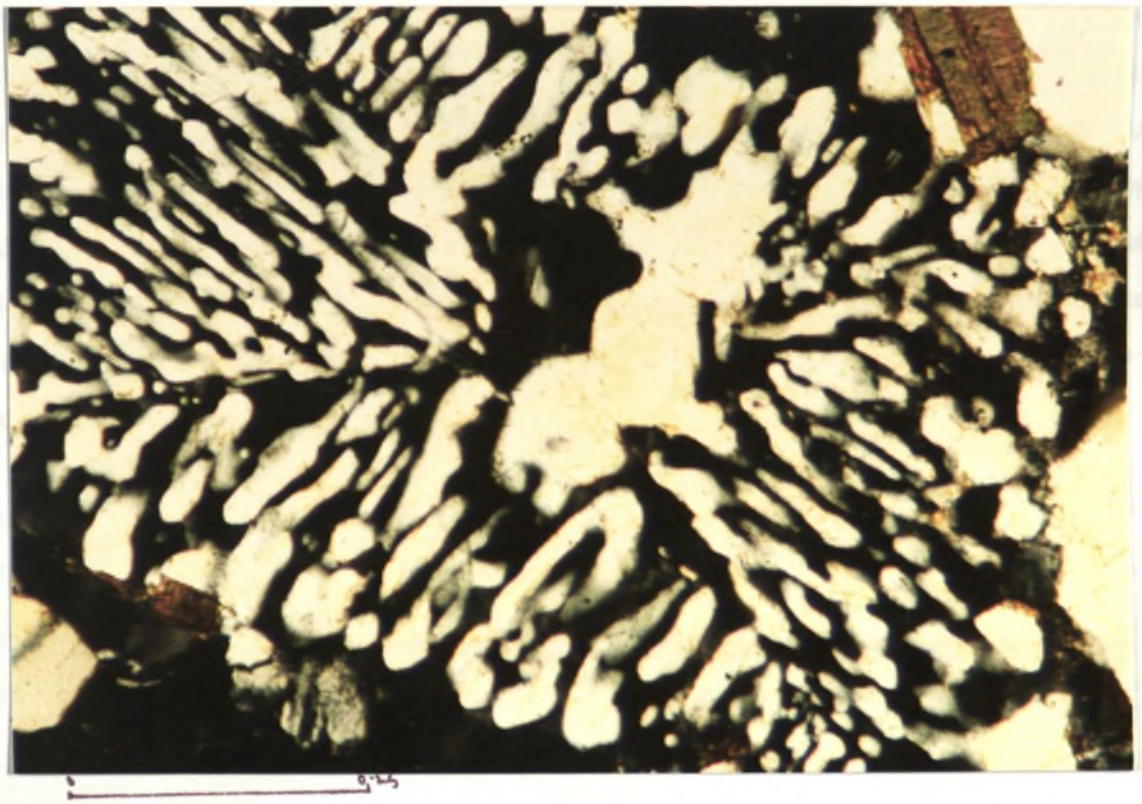

this sample and may suggest that this zoning is common but is not always detectable optically. Further work is required to confirm this but is outside the scope of this thesis.

As mentioned earlier, subgraining of the myrmekite into different oriented intergrowth grains has possibly also occured in this zone.

These higher abundances and varying morphologies of myrmekite in this zone suggest that deformation (Phillips, 1974) and the effects of stress (Phillips and Carr, 1973) have been more intense here than elsewhere.

(iii) high grade zone : Within this zone myrmekite is much finer grained and occurs as lobes and thin rims (plate 4.2.12), ( .1 mm) on a number of plagioclase grain margins. Where myrmekite is associated with k-feldspar it is commonly adjacent to areas of remnant microcline suggesting that there may be a relationship between the persistance of microcline and the development of myrmekite in contact metamorphism.

### 4 . 2 . 7 : PERTHITE

The K-feldspars in the Banalasta Adamellite are all perthitic or microperthitic and display a variability in the different contact metamorphic zones.

(i) regional zone : This is pre-dominated by stringer style perthitic lamellae and low abundances of perthite in most grains ( 15 % of the average area of grains) and is consistant throughout the regional zone.

(ii) low grade zone : Perthite within this zone comprises up to 35 % of the area of the K-feldspar grains on average and is represented by an equal modal mix of replacement interlocking and stringer styles (Deer et al, 1966) (plate 4.2.2). The fact that the perthite is in higher abundance and has a higher degree of replacement character suggests strongly that there is a relationship between the perthite and the higher stresses observed in this zone. Replacement in some grains has continued to the extent that the potassium feldspar grain is almost completely pseudomorphed by perthitic and sericitic growths. In one sample (plates 4.2.15 & 16) perthite planes are observed to bend and kink about misorientation planes within a microcline feldspar ( cross - hatch twinning in these photos is not obvious due to the stage being oriented to accentuate the perthite ). Plate 4.2.16 suggests that this perthite deformation post-dated the increased exsolving processes in this zone.

(iii) high grade zone : Perthite within this zone is predominantly of the form of stringers and bleby lamellae (Deer et al ,1966). Minor replacement style perthite does occur but is in very low abundance. The perthite itself forms less than 10 % of the area of K-feldspar grains in this contact zone. Perthitic lamellae in one sample show deflection in towards a strain-free round quartz inclusion, suggesting preferential growth of lamellae towards low energy interfaces

PLATE 4.2.15 : DEFORMATION OF STRINGERS AND INTERLOCKING PERTHITE ABOUT MISORIENTATION PLANES IN K-FELDSPAR ( MU45864 )

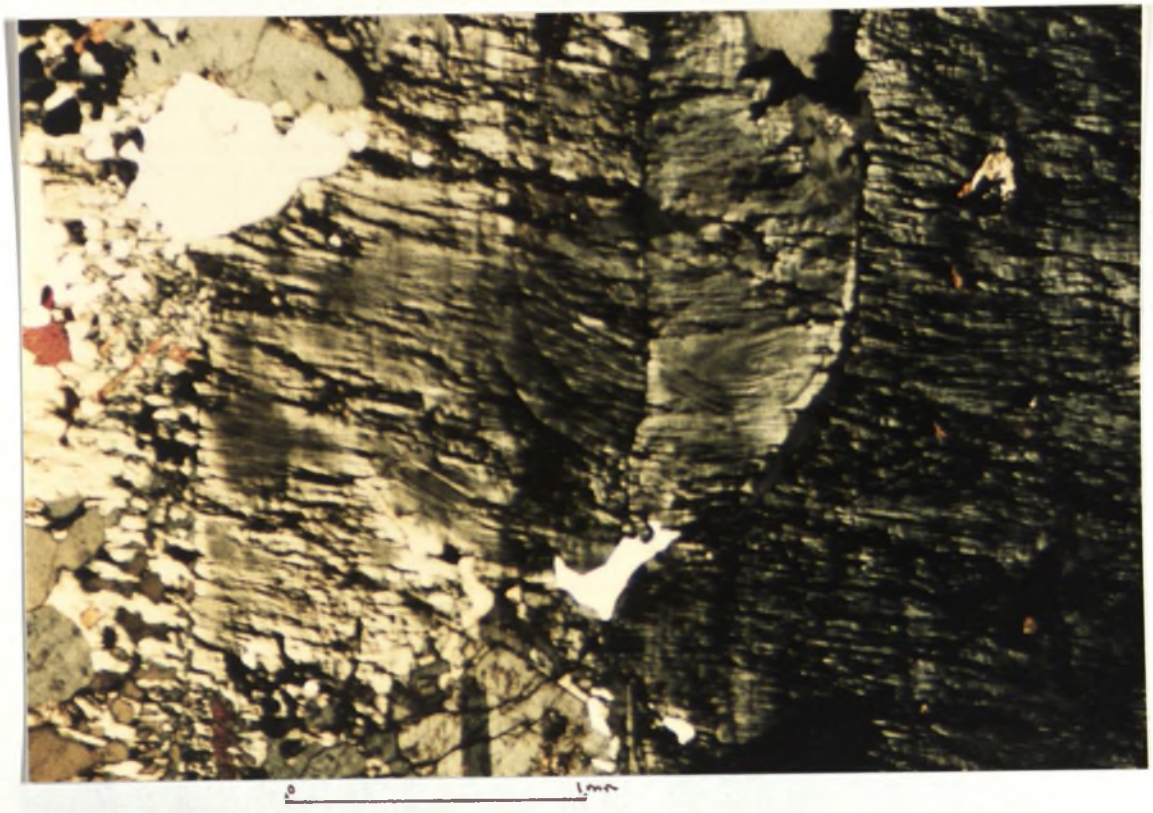

PLATE 4.2.16 : CLOSE UP OF THE BENT PERTHITE LAMELLAE SHOWING INTENSIFICATION OF BENDING TOWARDS THE MISORIENTATION PLANE ( MU45864 )

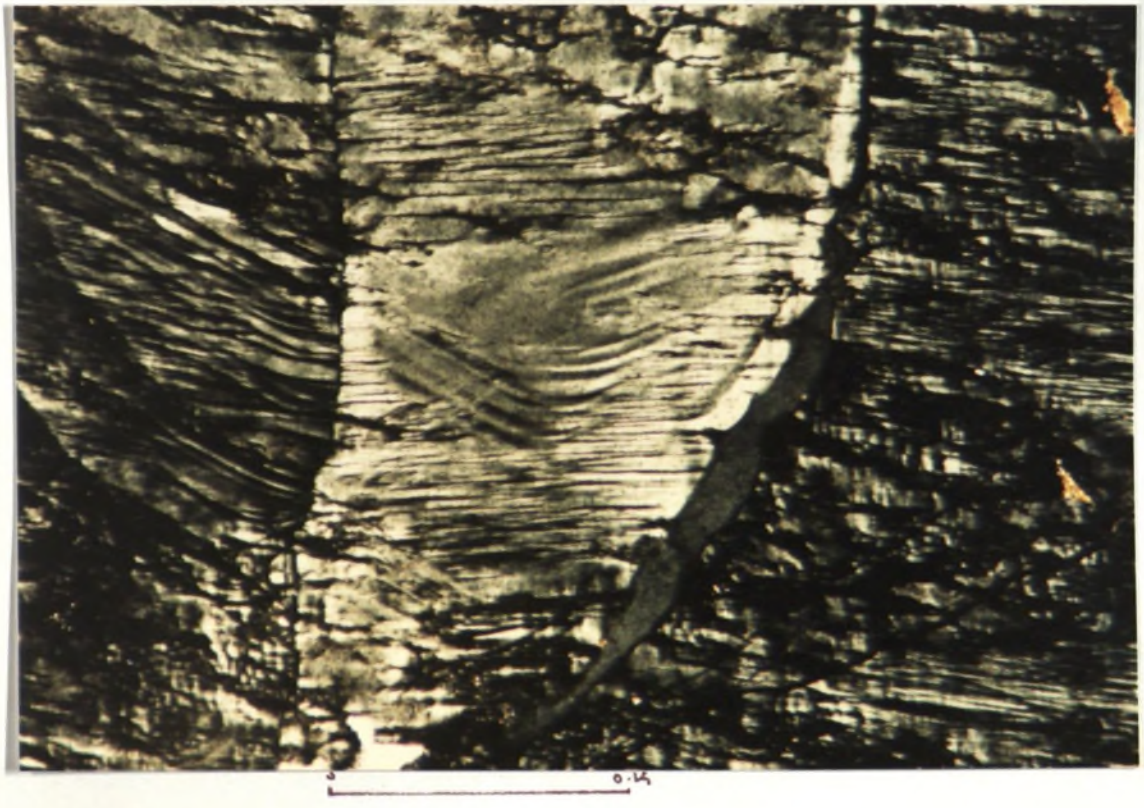

PLATE 4.2.17 : PERTHITE DEFLECTION IN TOWARDS QUARTZ INCLUSION. NOTE THE GRANOBLASTIC CHARACTER OF THE QUARTZ AND THE 90 DEGREE RELATIONSHIP BETWEEN THE QUARTZ BOUNDARY AND THE PERTHITE LAMELLAE ( MU45882 )

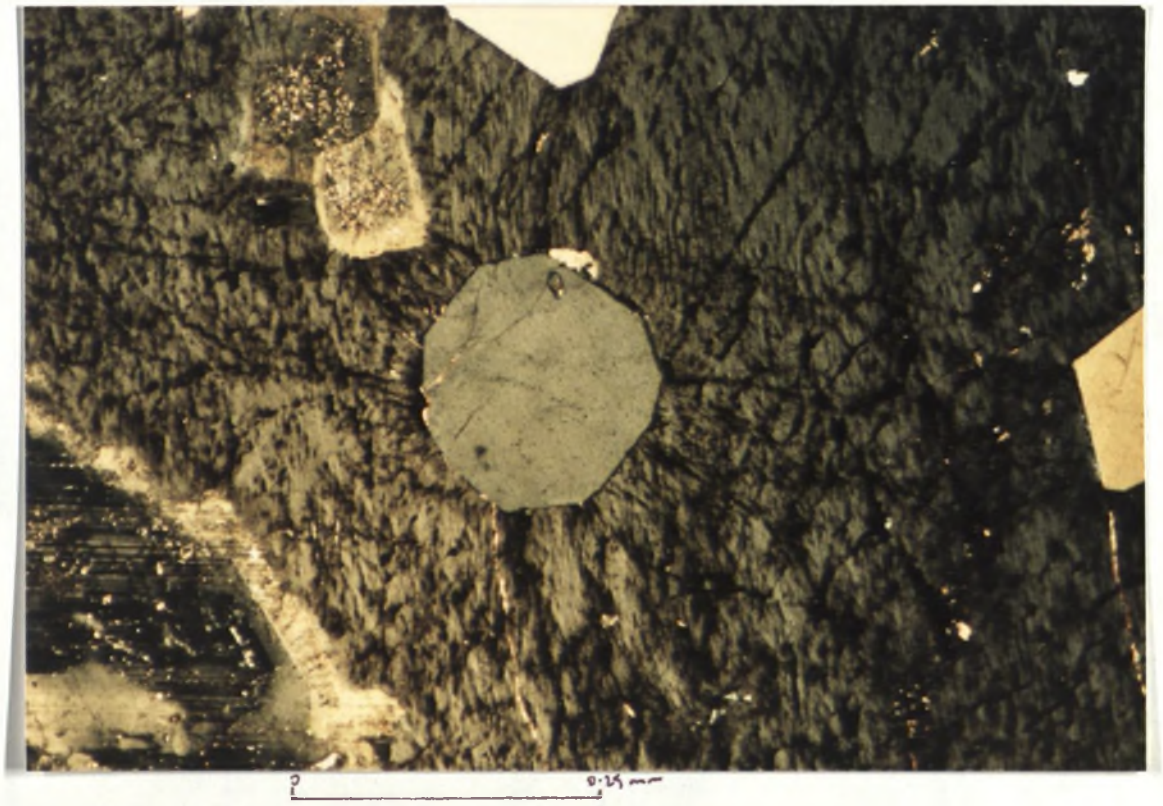

FIGURE 4.2.1 : SUMMARY DIAGRAM OF THE MAIN MICROSTRUCTURAL OBSERVATIONAL DIFFERENCES BETWEEN EACH GRADE ZONE.

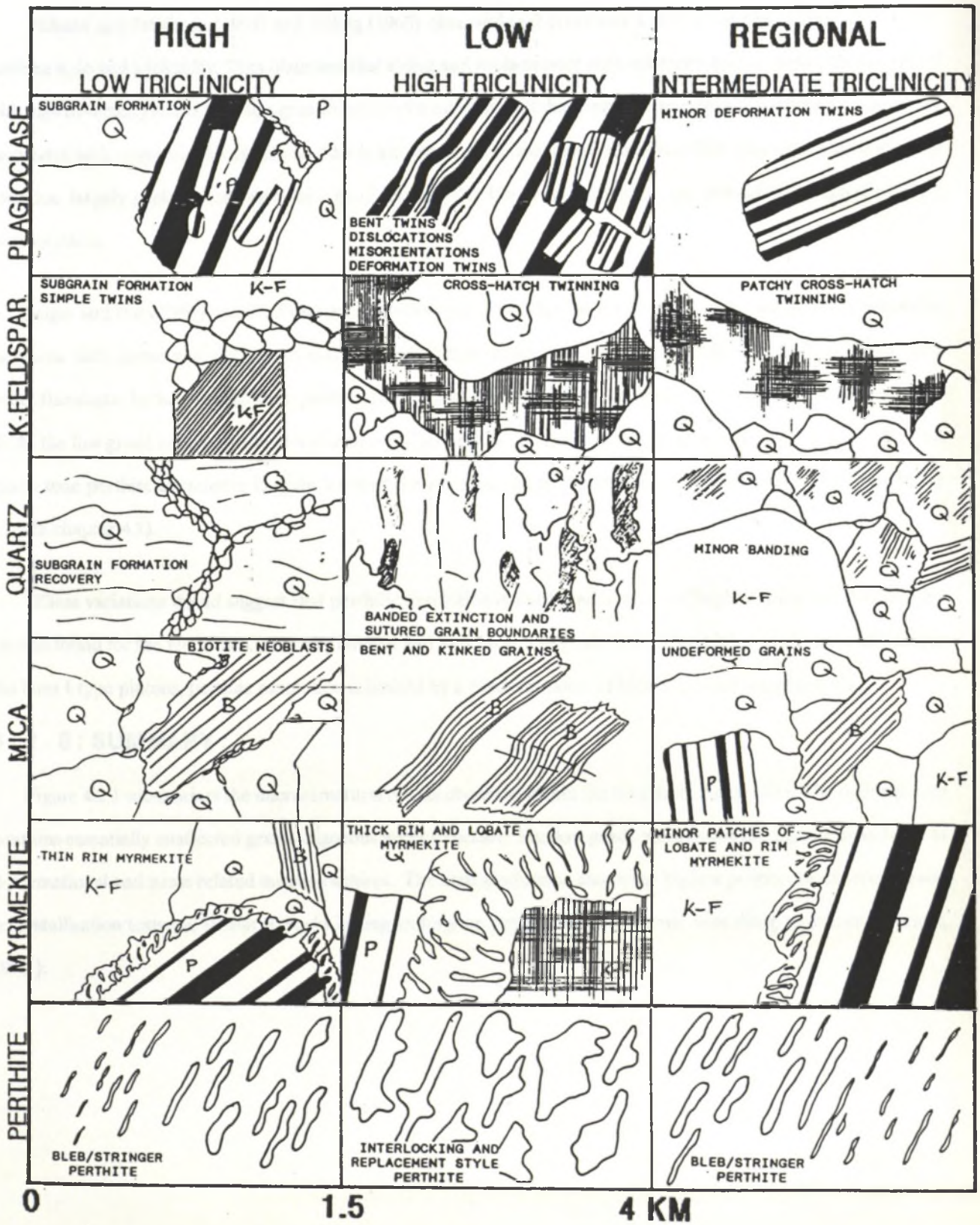

(plate 4.2.17). In some extreme cases strings of perthite extend right across grains and are commonly sub-parallel to cleavage. Where microcline twins have remained the perthite seems to be more concentrated and in two cases was of a bleby to replacement form.

Nilssen and Smithson (1965) and Tilling (1968) observed that there was a strong correlation between micro - perthite style and triclinicity. They observed that string and replacement style microperthite is commonly associated with high triclinicity values (due to a greater extent of unmixing) and that stringers and blebs of perthite are commonly associated with lower triclinicity values. This is also observed in the Banalasta Adamellite where the high triclinicity zone has largely replacement style microperthite and the low triclinicity zone has primarily stringer-bleb style microperthite.

Steiger and Hart(1967) recorded that perthitization and actual lamellae width decreases and Or-Ab composition increases with decreasing distance from the contact. These again were both observed in x-ray and optical analyses in the Banalasta. In the regional zone perthite abundances are low and Ab contents for the K-feldspars are up to 20 %. In the low grade zone perthite abundance is higher and Ab contents of the K-feldspars are 0 - 5 %. In the high grade zone perthite abundance is again low and the Ab contents of the associated K-feldspars is 30 % (see figure 4.1.6 in chapter 4.1).

These variations would suggest that perthitic exsolution is enhanced in zones of higher stress and deformation (as was found for the Herefoss Granite by Nilssen and Smithson, 1963) whereas in the higher grade zone adjacent to the later I-type plutons, perthite exsolution is limited by a predominance of higher contact temperatures.

## 4 . 2 . 8 : SUMMARY :

Figure 4.2.1 summarises the microstructural trends observed within the Banalasta Adamellite. The regional zone contains essentially unaffected granitic igneous microstructure. The low grade zone shows the highest abundance of deformational and stress related microstructures. The high grade zone shows the highest proportion of recovery and recrystallisation textures, similar to rocks having undergone predominantly thermal annealling processes ( Vernon, 1976 ).

# A . 4 . 3 : CORDIERITE MEGACRYST ACCESSORY PHASE

## 4 . 3 . 1 : INTRODUCTION

The presence of cordierite in the Banalasta Adamellite documented first by Shaw & Flood (1975) was suggested by them to be restite cordierite with euhedral magmatic cordierite overgrowths. Observation of other cordierite bearing eastern Australian S-type plutons by Baker (1940), Phillips et al (1981) and Clemens et al (1981) shows such euhedral, inclusion poor, high sodium ( .7 wt %), intermediate Mg-number (.5 - .6) cordierites are common. Speer (1981) and Phillips et al (1981) have argued that the aforementioned characteristics along with grainsizes (5 - 20mm) similar to the other mierals in the S-type granitoids strongly suggests emplacement stage magmatic crystallisation.

## 4 . 3 . 2 : MINERALOGY AND MICROSTRUCTURE

Eleven magmatic cordierites from samples 300m to 6km from the Banalasta Adamellite's contact with the Bendemeer Pluton (figure 4.3.1) show near complete to complete replacement (plate 4.3.1) unlike the fresh cordierites observed further to the north by Shaw and Flood (1975) (plate 4.3.2, sample supplied by Flood,1988). The main replacement product is pinite (typical of altered cordierite) and consists of a chloritic - muscovite fine grained mix (Deer et al, 1967). These minerals give the pseudomorphs a characteristic yellow-green colouration in thinsection and a dark green appearance in hand specimen. The alteration products are not observed to penetrate past the original cordierite's grain boundaries except where the cordierite pseudomorph abutts a biotite aggregate.

The fact that fresh cordierites were observed by Shaw & Flood (1975) further north of the study area, suggests that the developement of these pseudomorphs may be localised and related to the contact metamorphic effects in the vicinity of the later I-type plutons. With decreasing distance to these later intrusives, the replacement products lose their fine grained character and show an increases in grainsize (up to 2mm for muscovite within 300m of the Bendemeer Adamellite) and an increase in the abundance of replacement muscovite. Chlorite is not observed within 2.0km of the contact.

At 1.7km from the Bendemeer Adamellite, extremely fine growths ( .01mm) of andalusite were observed (MU45858) and have been examined by electron microprobe analysis, enabling the andalusite isograd to be located (figure 4.3.1). Within 600m of the Bendemeer pluton's contact, chemically and microstructurally different fresh cordierite occurs and has been probed (table 4.3.1), this cordierite has 0.39 wt% sodium and an Mg-number of 41.5, which is more typical of metamorphic cordierite (Leake, 1960). These cordierites occur as up to 1mm diameter granoblastic grains within the psuedomorphed magmatic cordierite and show faint sector and lenticular lamellae twinning. These cordierites contain abundant muscovite inclusions of finer grainsize than the adjacent muscovite grains, consistant with continued muscovite grain growth (up to 2mm) after formation of this metamorphic cordierite

PLATE 4.3.1 : ANHEDRAL CORDIERITE GRAIN FROM THE BANALASTA ADAMELLITE, SHOWING PSUEDOMORPHING BY FINE GRAINED REPLACEMENT PRODUCTS OF MUSCOVITE, CHLORITE AND PINITE.

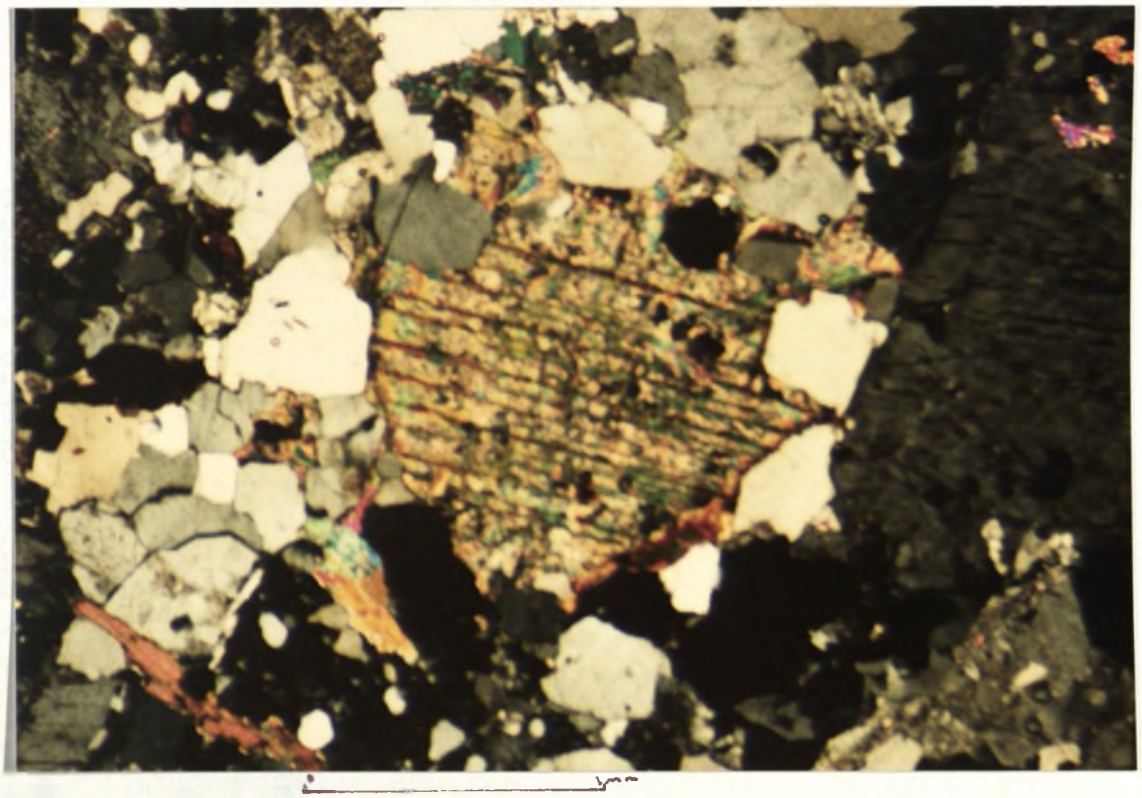

PLATE 4.3.2 : FRESH CORDIERITE FROM NORTH OF THE STUDY AREA COLLECTED BY FLOOD AND SHAW (1975).

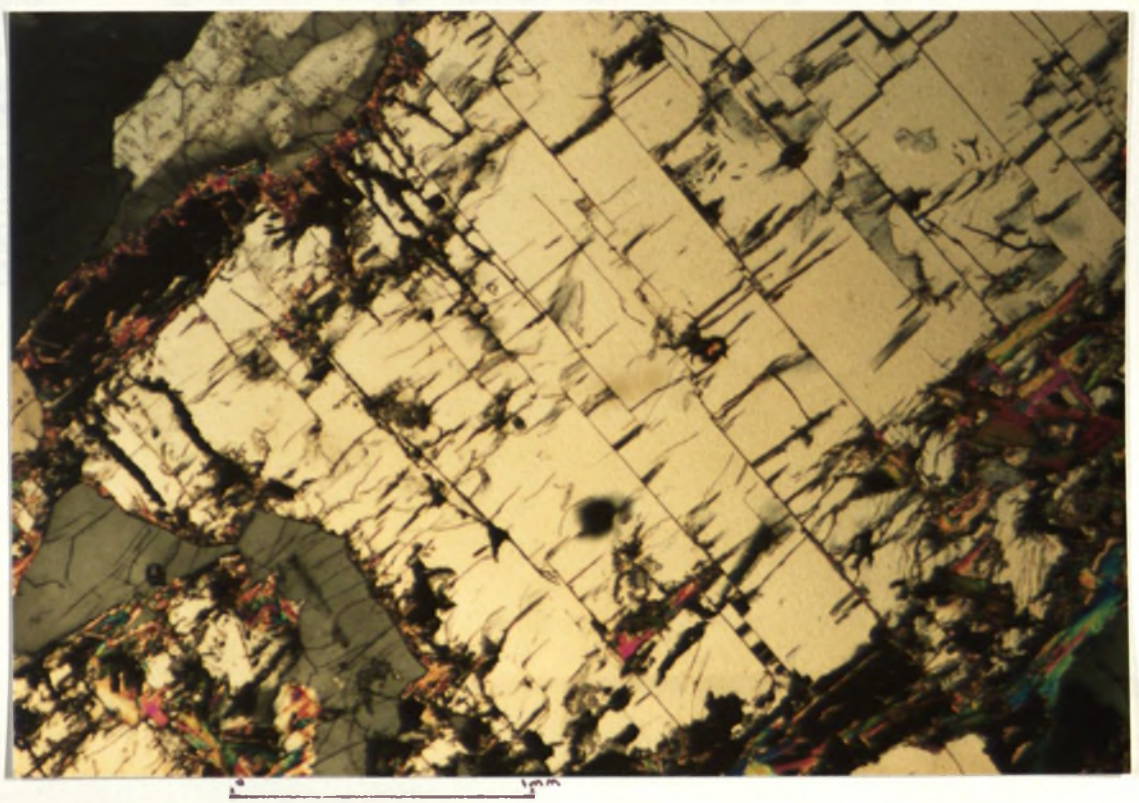

TABLE 4.3.1 : ANALYSES OF CORDIERITES IN THE BANALASTA ADAMELLITE. SAMPLES MU8400 AND MU8401 ARE ANALYSES PERFORMED BY FLOOD AND SHAW ( 1975 ) ON MAGMATIC ZONED INCLUSION POOR EUHEDRAL CORDIERITES. SAMPLE MU 45843 IS AN ANALYSIS OF THREE GRANOBLASTIC, INCLUSION RICH CORDIERITES CONTAINED WITHIN A PSEUDOMORPHED EUHEDRAL MAGMATIC CORDIERITE GRAIN.

| | MU 8400 | | MU 8401 | | | MU 45843 | | |
|---|---|---|---|---|---|---|---|---|
| | CORE | MARGIN | CORE | MARGIN | | | | |
| | % | % | % | % | | % | % | % |
| SiO2 | 48.57 | 48.70 | 48.46 | 47.53 | SiO2 | 49.34 | 49.36 | 49.31 |
| Al2O3 | 33.36 | 33.38 | 33.39 | 33.18 | Al2O3 | 32.82 | 33.33 | 33.54 |
| FeO | 9.53 | 9.13 | 9.63 | 11.37 | FeO | 8.24 | 8.77 | 8.71 |
| MnO | 0.11 | 0.17 | 0.14 | 0.33 | MnO | 0.08 | 0.14 | 0.11 |
| MgO | 7.58 | 7.67 | 7.37 | 6.41 | MgO | 3.90 | 2.46 | 3.31 |
| Na2O | 0.77 | 0.85 | 0.92 | 0.76 | Na2O | 0.48 | 0.35 | 0.34 |
| K2O | 0.08 | 0.10 | 0.09 | 0.02 | K2O | 0.14 | 0.07 | 0.01 |
| TOTAL | 100.00 | 100.00 | 100.00 | 100.00 | TOTAL | 95.00 | 95.06 | 95.46 |
| Mg # | 58.70 | 59.90 | 57.70 | 50.10 | Mg # | 45.80 | 38.30 | 40.40 |

FIGURE 4.3.1 : MAP OF THE BANALASTA ADAMELLITE'S ANALYSED CORDIERITE SAMPLES AND THE MINIMUM DISTANCES FOR THE METAMORPHIC ANDALUSITE AND CORDIERITE ISOGRADS.

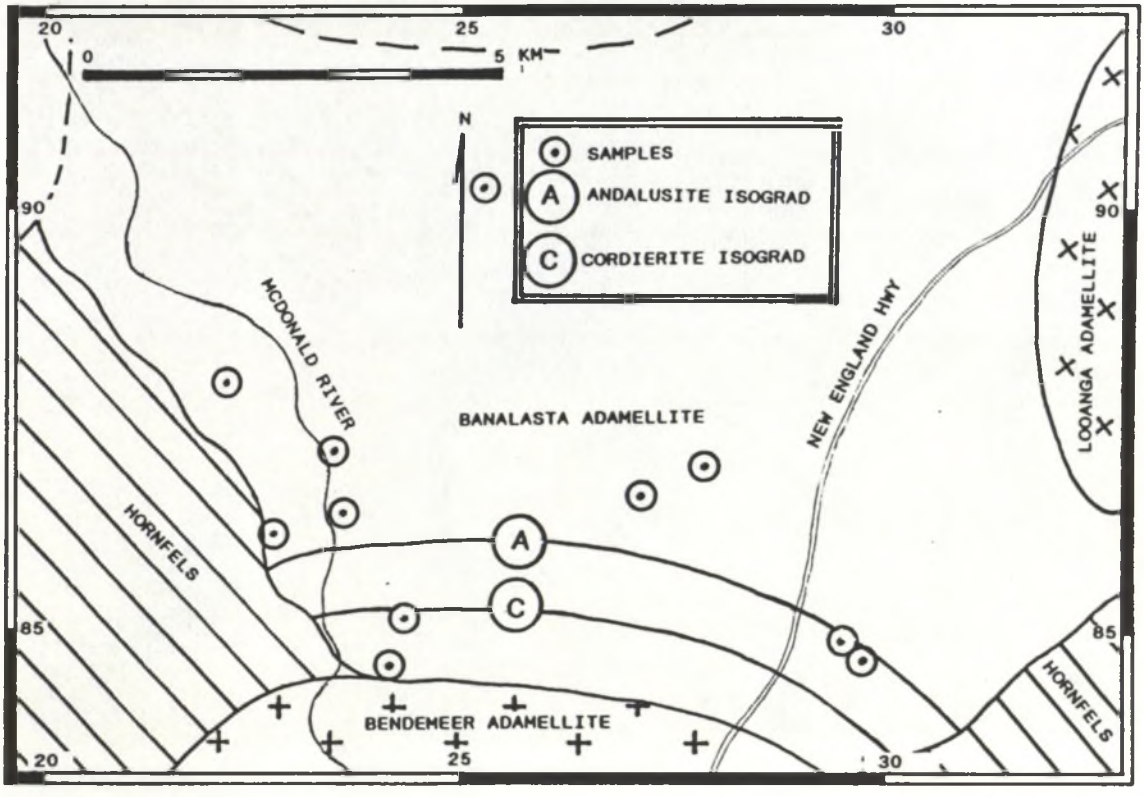


PLATE 4.3.3 : METAMORPHIC GRANOBLASTIC CORDIERITE WITHIN A PSEUDOMORPHED MAGMATIC CORDIERITE GRAIN. THE METAMORPHIC CORDIERITE PRESERVES WHITE MICA INCLUSIONS OF FINER GRAINSIZE THAN THE SURROUNDING WHITE MICA.

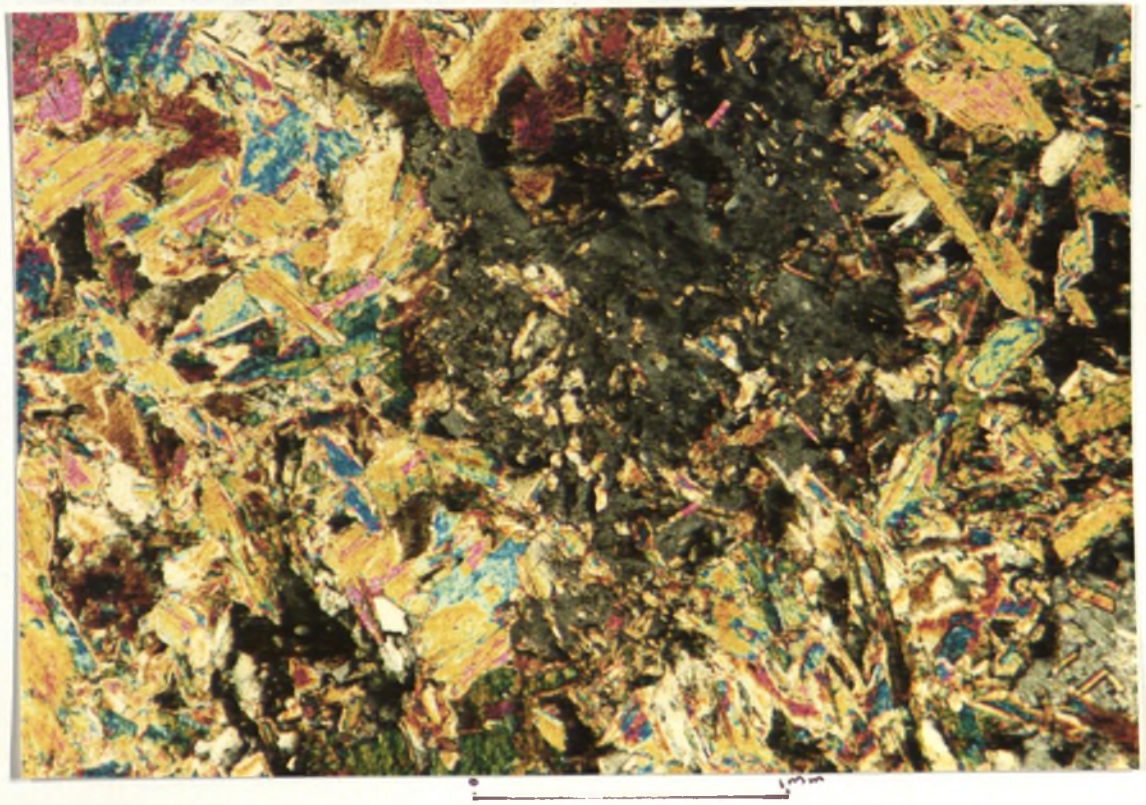

PLATE 4.3.4 : GARNET INCLUSION WITHIN A PSEUDOMRPHED CORDIERITE
( PPL : MU 45856 )

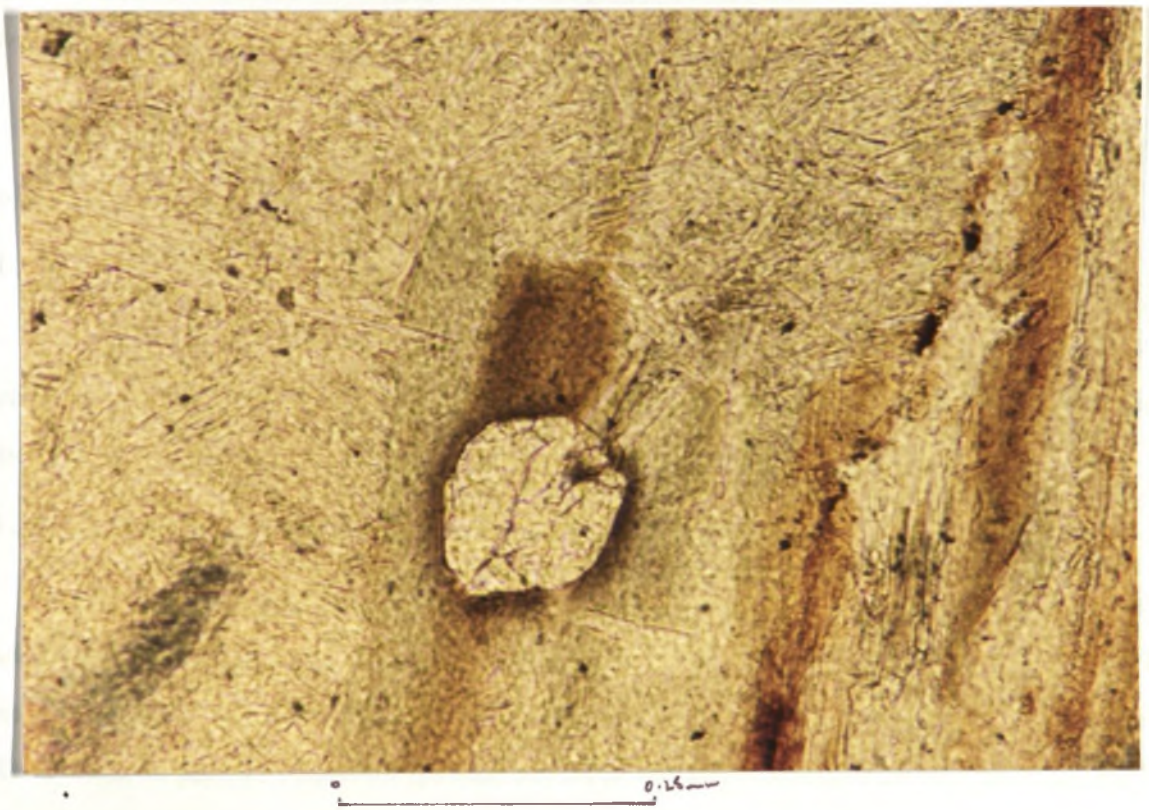


PLATE 4.3.5 : SAME GARNET INCLUSION AS IN THE ABOVE PLATE UNDER CROSSED POLARS.

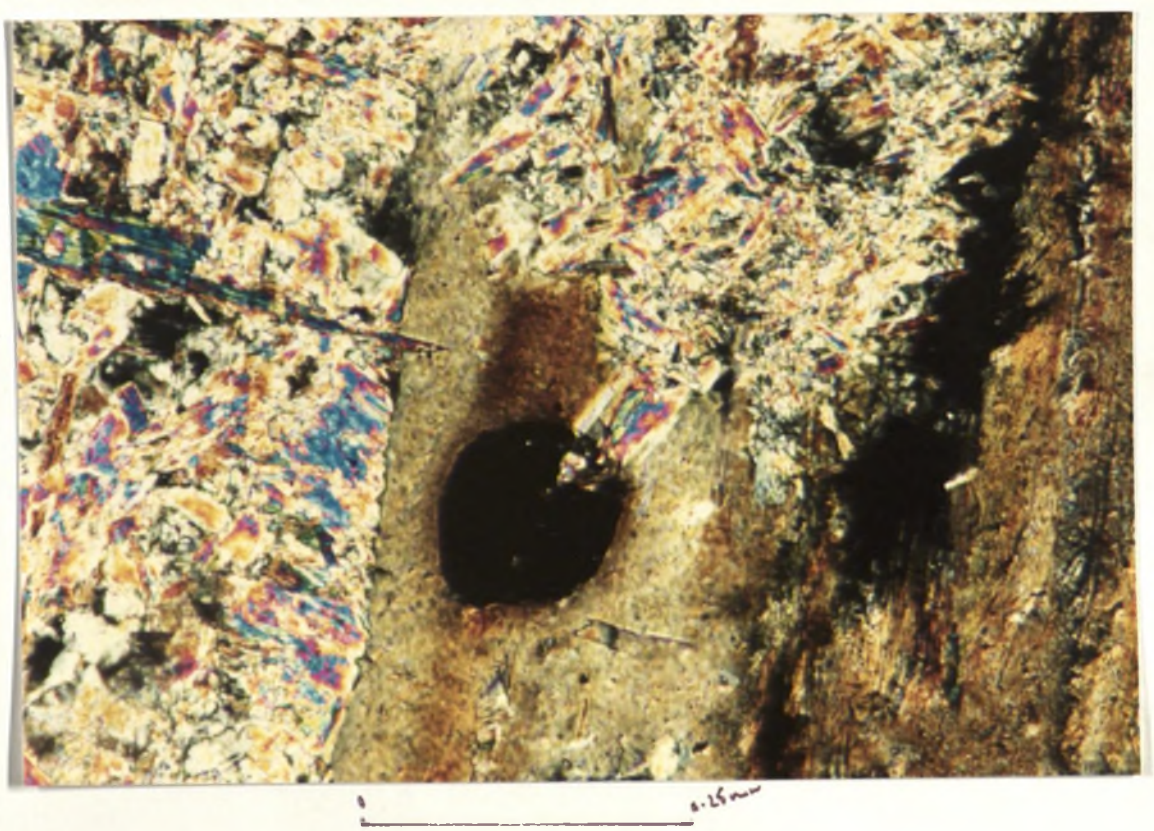

(plate 4.3.3). These granoblastic cordierites show no alteration and based upon the above examination a contact metamorphic origin for this granoblastic cordierite seems certain.

The recognition of the contact metamorphic cordierite enables the minimum distance for a cordierite isograd to be delineated within the Banalasta Adamellite (figure 4.3.1)

## 4 . 3 . 3 : INCLUSIONS

The magmatic cordierites are generally inclusion poor, but biotite, muscovite and some minor quartz inclusions are present in low abundance. In addition, tourmaline inclusions were observed and in one slide a fine grained ( .4mm) garnet inclusion occurred (based on optical observations, plate 4.3.4 and 5).

## 4 . 3 . 4 : CONCLUSIONS

The euhedral, inclusion poor cordierites of similar grainsize to other major constituent minerals for the Banalasta Adamellite, with Mg-numbers .501 and sodium wt % .76 suggest these are magmatic in origin. The initial pseudomorphous replacement of the cordierite by pinite, muscovite and chlorite is due to localised retrogressive affects within the Banalsta Adamellite (possibly associated with emplacement of the later I-type plutons). However, the increase in replacement product grainsize and the introduction of andalusite and metamorphic cordierite are all proposed to be induced by contact metamorphic affects by the adjacent Bendemeer Adamellite.

# A . CHAPTER 5 : SUMMARY

The contact metamorphism induced by the Bendemeer Adamellite upon the surrounding 'country rocks' has been tabulated in figure A.5.1 and on the basis of this summary a contact metamorphic zonation can be established.

## A . 5 . 1 : METAMORPHIC ZONATION

### 5 . 1 . 1 : REGIONAL ZONE ( 4 - 5 km from contact)

This zone is unmodified by the contact metamorphic effects of the intruding Bendemeer pluton. No hornfelsic rocks are evident and the Banalasta Adamellite shows typical igneous microstructures, contains unaltered cordierite and has microcline with intermediate triclinicity values and orthoclase consistent with the regional values of the Bundarra suite plutons.

### 5 . 1 . 2 : LOW GRADE ZONE ( 1.5 to 4 km from contact)

The only mineralogical changes in the hornfelsic rocks of this zone is the incoming of metamorphic biotite and the beginnings of a grainsize increase in the cherts. No metamorphic effects were observed in the metabasalts.

The most significant changes that delineate this zone occur in the Banalasta Adamellite. The K-feldspar records increases in triclinicity (up to 0.833), large amounts of exsolved albite (Or90-100) and the disappearance of monoclinic orthoclase. Associated with this are high abundances of replacement and interlocking perthite which show bent and misoriented lamellae. Other microstructural features are higher abundances of thick rimmed and lobate myrmekite, banded extinction and sutured subgrains in quartz, kinked and bent biotite and misoriented and kinked deformational twins in plagioclase. The magmatic cordierite in this zone is completely replaced by a pinite - chlorite - muscovite mix. The K-feldspar and microstructural changes induced in this zone are all features common to strained and deformed granitic rocks and imply that pluton emplacement has produced an outer cold deformation envelope.

### 5 . 1 . 3 : HIGH GRADE ZONE ( 1.5 km from contact)

This zone records contact metamorphic changes in all the country rocks. The microcline to orthoclase transition zone (occurring at between 400 and 500 degrees celcius) correlates with metamorphic andalusite in both the Banalasta Adamellite and the metapelites and suggests temperatures close to 500 degrees celcius occur at the outer margin of this zone.

K-feldspar in the metagranite has low to zero triclinicities and contains higher proportions of unexsolved albite (Or70) which is reflected in the low abundance of perthite lamellae. Myrmekite, is also in low abundance occuring as thin rims and minor lobes. No evidence exists for an annealing out of myrmekite and therefore would suggest that

FIGURE A.5.1 : SUMMARY DIAGRAM FOR THE CORRELATED METAGRANITE AND HORNFELS CONTACT METAMORPHIC EFFECTS OBSERVED WITHIN THE AUREOLE OF THE BENDEMEER ADAMELLITE

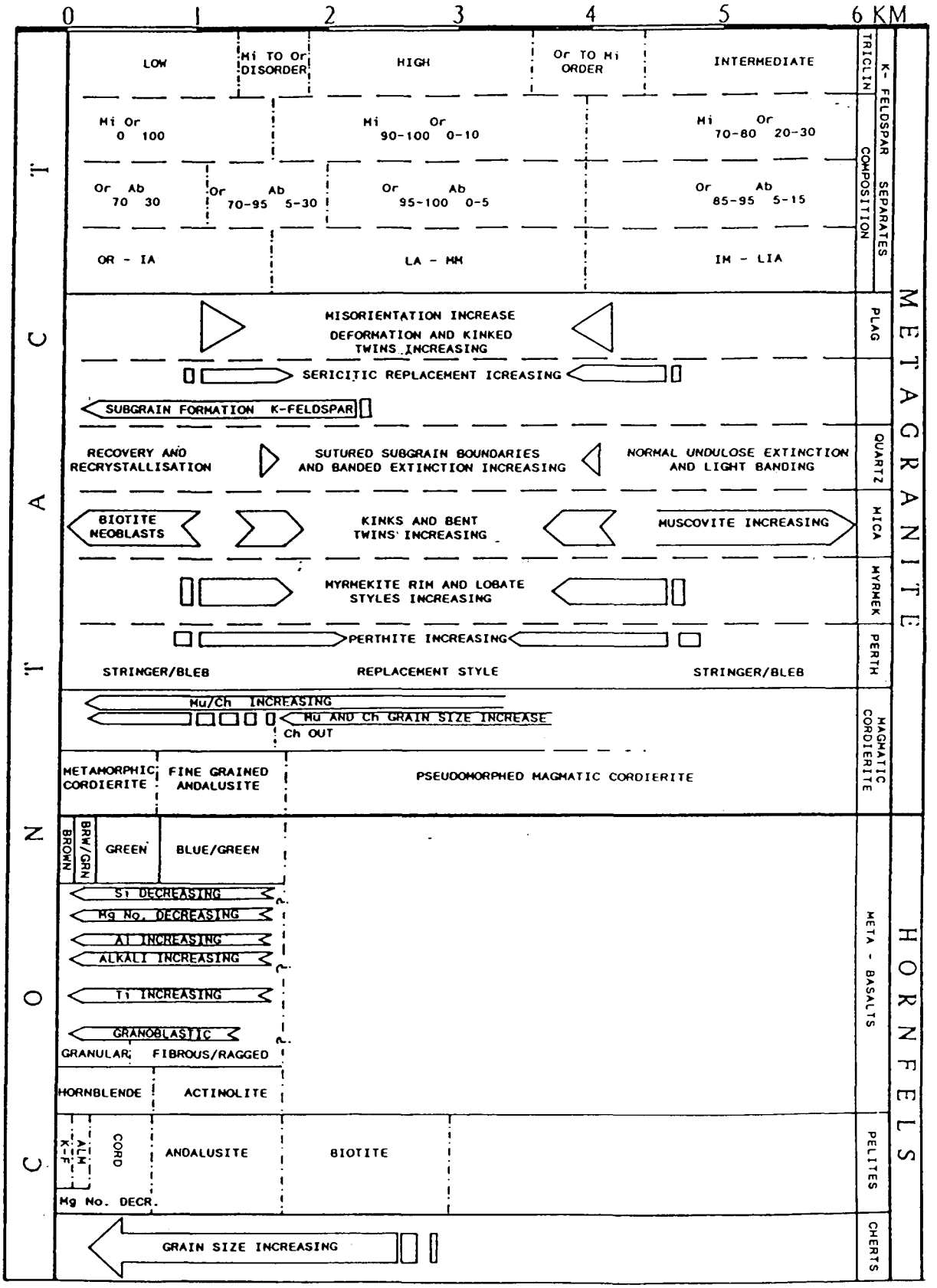

although the same strains are present in the high grade zone, the higher temperatures may result in conditions unfavourable for myrmekite formation. If this is correct then it has important ramifications upon the temperature and strain conditions favourable for myrmekite formation. However, further work is required to evaluate such implications.

Microstructurally, the metagranite shows high abundances of subgrains, recovery and recrystallisation in K-feldspar, quartz, plagioclase and biotite. The pseudomorphed cordierites are characterised by a coarsening of the replacement muscovite grainsize and the nucleation and growth of metamorphic andalusite (in very low abundance) and metamorphic cordierite.

Although the andalusite isograd is poorly constrained in both the metasediments and the metagranite, the position of the first appearance of andalusite and metamorphic cordierite in both rock types is very similar. These isograds suggest immediate contact temperatures of 620 - 650 degrees celcius.

Coinciding with the cordierite isograd is the hornblende isograd in the metabasalts and associated increases in titanium and alkali contents in the metabasaltic amphiboles with grade, along with a progression from blue-green, fibrous-ragged actinolitic hornblende to brown granoblastic tschermakitic hornblende.

Thus the metagranite records both an outer deformation and an inner thermal envelope induced by the later granitoid emplacement while the hornfelsic rocks enable a fine subdivision only of the inner envelope.

This metamorphic zonation will be addressed in Part C where comparison is made with a similar metamorphic zonation observed for the I-type, orthoclase bearing Yarrowyck Granodiorite discussed in part B.

# B. CONTACT METAMORPHISM OF A WEAKLY DEFORMED I-TYPE GRANODIORITE IN THE AUREOLE OF THE I-TYPE GWYDIR RIVER ADAMELLITE, N.S.W.

## B . CHAPTER 1 : INTRODUCTION

This part extends the findings made in the Bendemeer Area (Part A) by examining the contact metamorphism of the Permian I-type orthoclase bearing Yarrowyck Granodiorite in the aureole of the Gwydir River Adamellite. The Gwydir River Adamellite's aureole is also mapped in the surrounding low grade regionally metamorphosed Devonian to Carboniferous Sandon Beds (Leitch, 1974) and the Kurrajong park Volcanics (believed to be early Permian by Brown, 1986).

The Yarrowyck area (30 km west of Armidale) was chosen on the basis that it differed from the Bendemeer area insomuch as the metagranite (the Yarrowyck Granodiorite) is an I-type (unlike the S-type Banalasta Adamellite) and was believed to be orthoclase rather than microcline bearing. Initial examination revealed that the K-feldspar in this pluton is indeed predominatly orthoclase, but that it also contains minor low triclinicity microcline and is pervasively deformed by microshears.

The study is in the same format as part A, but simply presents the findings and omits the details of previous studies already referred to in part A. The results of this study are correlated and summarised, to be used for a comparison of both I and S-type contact metamorphosed metagranites and their emplacement implications for the New England Batholith.

# B . CHAPTER 2 : REGIONAL GEOLOGY

## B . 2 . 1 : METAMORPHIC ROCKS

The metasedimentary country rocks in the Yarrowyck area include both the Devonian to Carboniferous (Ishiga, 1988; Brown, 1986) Sandon Beds (Leitch, 1975) and the Early Permian Kurrajong Park Volcanics (Brown, 1986). The older Sandon Beds comprise undifferentiated conglomerates, turbiditic arenites, pelites, cherts, jaspers and minor metabasalts. The younger Kurrajong Park volcanics comprise a mix of volcanoclastic conglomerates and sandstones, breccias, minor pepperites, crystal ashflow tuffs and rhyolites (Joyce, 1964 and Brown, 1986). The occurence of pepperitic textures (plates 2.1 and 2.2a) in some of the volcanic rocks has been related to the Balala Dyke Swarm by Joyce (1964), although interbedding with surrounding volcanogenic rocks observed by the author would more strongly suggest a primary origin in water saturated, poorly consolidated sediments.

The author has observed two main kilometre scale fold structures in the northern and southern hornfels (figure B.3.1a and 1b), both of which are synclinal structures trending NNW and plunging to the south.

The intrusion of the Uralla Plutonic suite granitoids and the Balala Dyke Swarm in the later Permian has truncated these low grade regionally metamorphosed rocks and produced upper hornblende-hornfels facies contact metamorphism.

## B . 2 . 2 : YARROWYCK GRANODIORITE

The Yarrowyck Granodiorite is a medium grainsize, even grained, hornblende - biotite I-type pluton that shows a subtle gradational zoning from a more felsic margin to a mafic core (Ransley, 1970). Only near the northern margin does it contain a small area of phenocrystic K-feldspars up to 1 cm in length. To the south the Yarrowyck Pluton intrudes the Balala Granodiorite as well as the Sandon Beds and the Kurrajong Park Volcanics. The pluton itself is intruded by the Balala Dyke Swarm, the Uralla Granodiorite and the Gwydir River Adamellite.

Although the Yarrowyck pluton shows a weak to moderate contact parallel foliation within 300 m of its margins, observable only on stained, sawn slabs (figs.B.2.1 and 2), this foliation is not evident at distances of greater than 600 m in from the contact. Outcrop style is most commonly as flat whalebacks (plate 2.2b). CIPW norms and modal abundances for the pluton are given in table 2.1 from data supplied by Flood & Shaw (1988, pers. comm.).

Although, Ransley (1970) mapped the Balala Dyke Swarm intruding the Yarrowyck Granodiorite no mention was made of this pluton being deformed. Small scale (up to 2 cm wide and 10 m long) dextral (and less commonly sinistral) shear zones are found to be ubiquitous in the Yarrowyck Granodiorite. The shear zones formed after

PLATE B.2.1 : PEPPERITIC TEXTURES IN A MEMBER OF THE KURRAJONG PARK VOLCANICS. NOTE ANGULAR NATURE OF BRECCIATED CLASTS

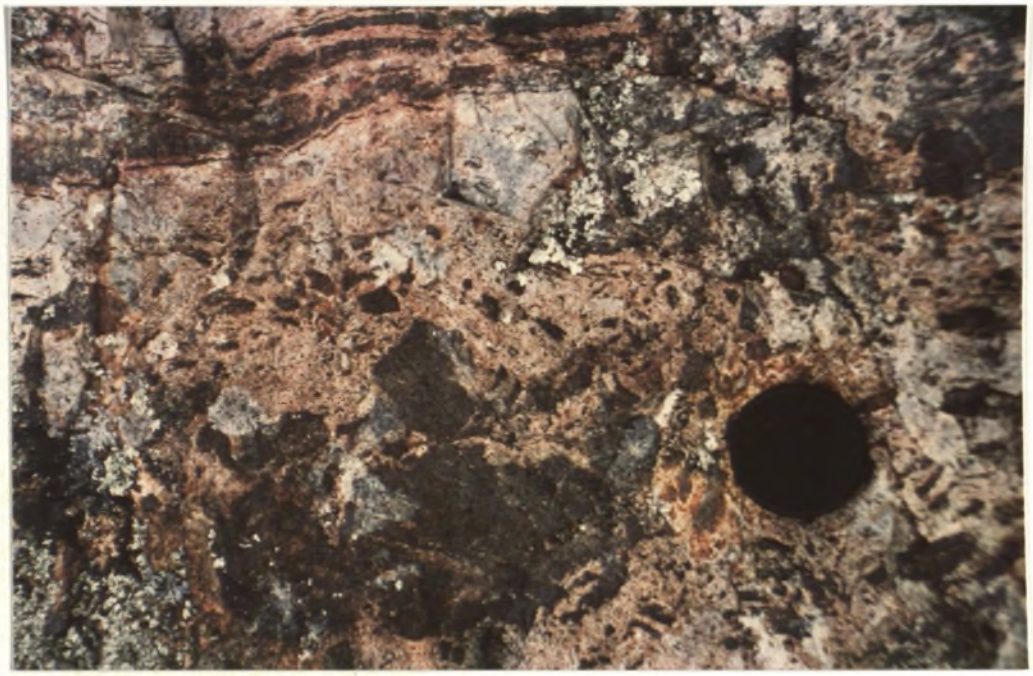

PLATE B.2.2a : PEPPERITIC UNIT SHOWING PARTIAL JIGSAW FIT OF CLASTS AND FLOW BANDING EVIDENT IN THE LARGER BLOCKS

FIGURE B.2.1 : ROSE DIAGRAM OF MEASUREMENTS OF STRIKE IN THE YARROWYCK GRANODIORITE ON ITS SOUTHERN MARGIN ( MU46150, NEAREST CONTACT DIRECTION SHOWN )

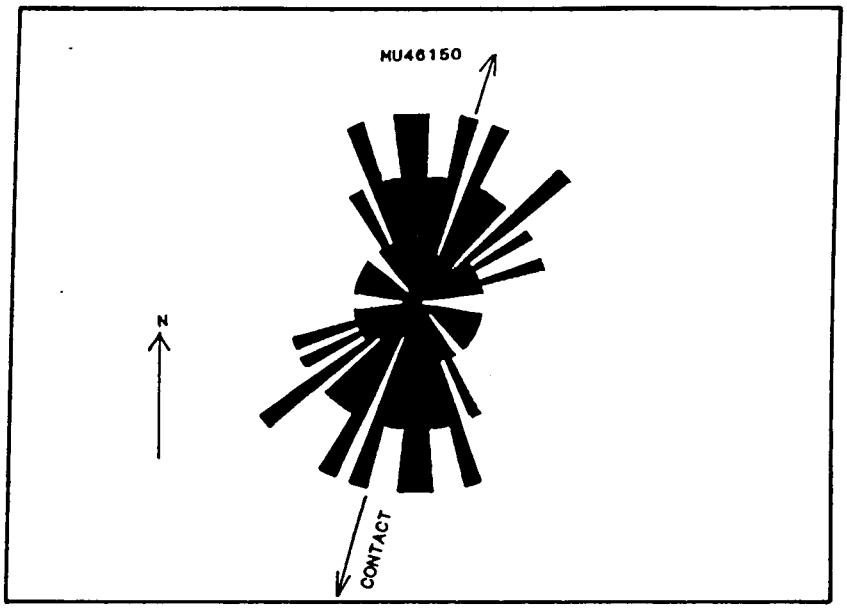


FIGURE B.2.2 : FOLIATION MEASUREMENT FOR THE YARROWYCK PLUTON NEAR THE NORTHERN MARGIN ( MU46157, CONTACT DIRECTION SHOWN )

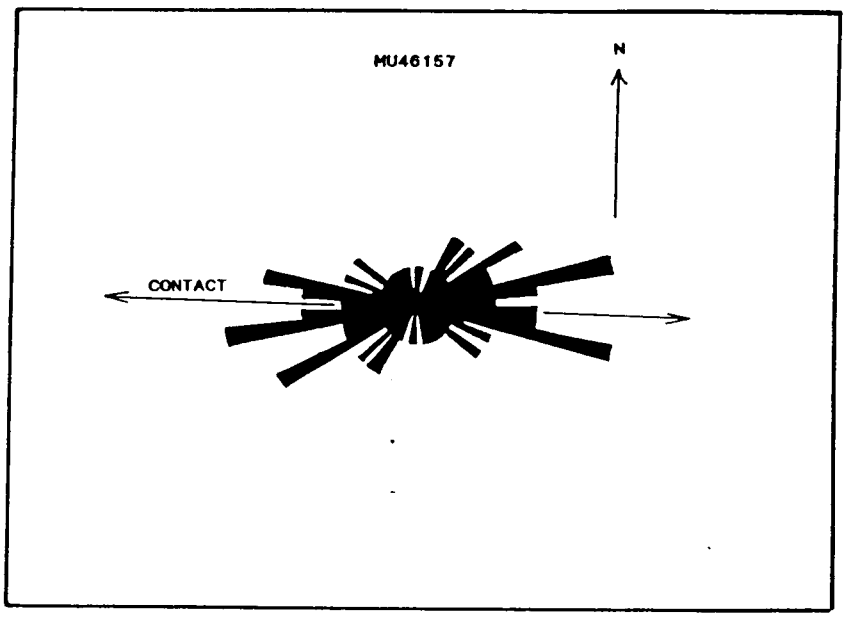

PLATE B.2.2b : CHARACTERISTIC OUTCROP STYLE OF THE YARROWYCK GRANODIORITE OCCURING AS BROAD, LOW WHALEBACKS

PLATE B.2.3 : SHEAR ZONES IN THE YARROWYCK GRANODIORITE DISPLACING AND APLITE DYKE.

TABLE 2.1 : CIPW NORM ( WEIGHT PERCENTAGE ) AND MODAL ABUNDANCES FOR THE YARROWYCK GRANODIORITE AND THE GWYDIR RIVER ADAMELLITE ( after Shaw & Flood )

| | A N A L Y S E S | | | |
|---|---|---|---|---|
| SAMPLE | Y13 | Y14 | GW11 | GW12 |
| | % | % | % | % |
| SiO2 | 68.63 | 68.19 | 69.76 | 68.83 |
| TiO2 | 0.53 | 0.46 | 0.48 | 0.56 |
| Al2O3 | 14.25 | 15.40 | 14.08 | 14.27 |
| Fe2O3 | 0.40 | 0.40 | 0.40 | 0.40 |
| FeO | 2.66 | 2.73 | 2.39 | 2.74 |
| MnO | 0.09 | 0.10 | 0.06 | 0.07 |
| MgO | 1.74 | 1.12 | 1.47 | 1.68 |
| CaO | 2.87 | 2.93 | 2.55 | 2.86 |
| Na2O | 3.16 | 3.87 | 3.00 | 3.02 |
| K2O | 4.48 | 3.75 | 4.70 | 4.50 |
| P2O5 | 0.18 | 0.14 | 0.16 | 0.18 |
| TOTAL | 98.99 | 99.09 | 99.05 | 99.11 |

| | C I P W N O R M S | | | |
|---|---|---|---|---|
| SAMPLE | Y13 | Y14 | GW11 | GW12 |
| Q | 23.46 | 21.93 | 25.71 | 24.36 |
| ORTHO | 26.47 | 22.16 | 27.77 | 26.59 |
| AB | 26.37 | 32.73 | 25.37 | 25.54 |
| AN | 11.47 | 13.58 | 11.08 | 12.10 |
| DI | 1.31 | 0.03 | 0.43 | 0.75 |
| HY | 7.53 | 6.88 | 6.82 | 7.71 |
| MT | 0.58 | 0.58 | 0.58 | 0.58 |
| IL | 1.01 | 0.87 | 0.91 | 1.06 |
| AP | 0.42 | 0.32 | 0.37 | 0.42 |
| TOTAL | 98.99 | 99.09 | 99.05 | 99.11 |

| | M O D A L A B U N D A N C E S | | | |
|---|---|---|---|---|
| SAMPLE | Y13 | Y14 | GW11 | GW12 |
| QTZ | 25.77 | 24.33 | 28.00 | 26.87 |
| PLAG | 31.98 | 41.49 | 30.51 | 31.59 |
| K-F | 25.57 | 20.25 | 26.99 | 25.16 |
| BIO | 8.07 | 8.93 | 8.43 | 9.10 |
| HNB | 8.05 | 4.31 | 3.53 | 6.83 |
| TOTAL | 99.44 | 99.30 | 99.45 | 99.55 |

PLATE B.2.4 : CENTIMETRE SCALE DISPLACEMENT OF AN APLITIC DKYE BY THE SHEAR ZONES IN THE YARROWYCK GRANODIORITE

PLATE B.2.5 : CENTIMETRE SCALE DISPLACEMENT OF IGNEOUS ENCLAVE BY SHEAR ZONES IN GRANODIORITE

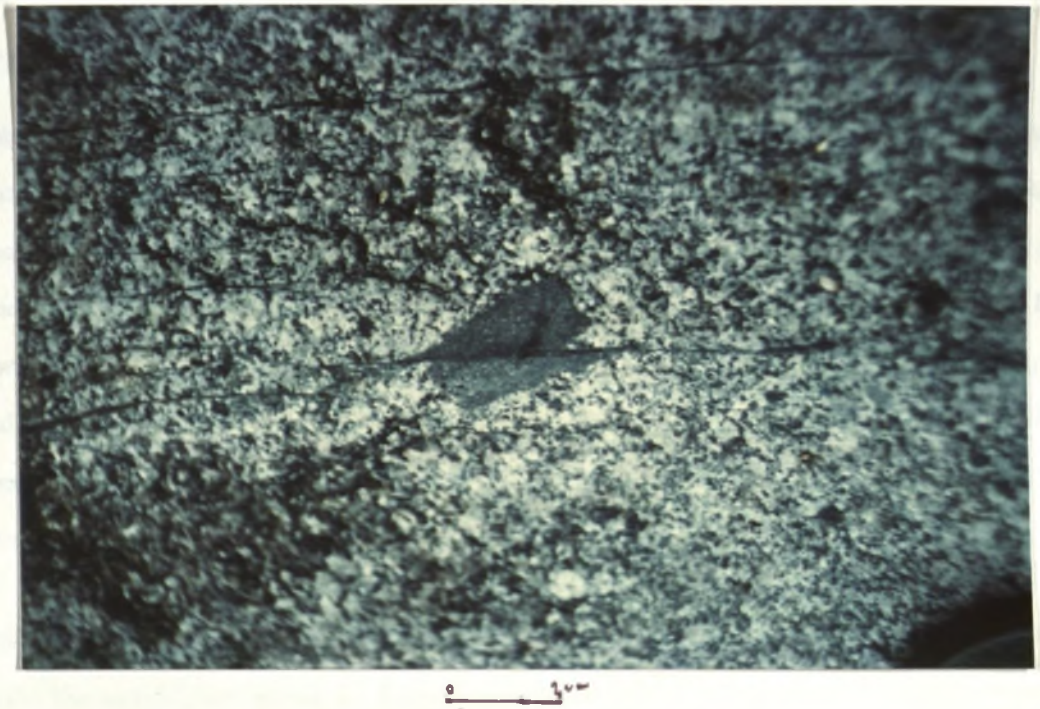

complete crystallisation of the pluton and only show brittle deformation. They are easily observed in the field by narrow ( 5mm wide) dark bands of chlorite and phyllosilicates. Displacement ranges from less than a centimetre to a up to 3 metres. These shears are evident only in the Yarrowyck Granodiorite and offset aplite dykes (plates 2.3 & 4) microgranitoid enclaves (plate 2.5) and in one locality appears to truncate one of the Balala dykes (plate 2.6). However, it has been observed elsewhere by the author that these shear zones are also truncated by the dykes. This would suggest that deformation and the emplacement of the Balala Dyke Swarm were contemporaneous and that there may be an order to dyke emplacement before and after shearing.

## B . 2 . 3 : BALALA DYKE SWARM

The Yarrowyck Granodiorite, the Balala Granodiorite and the immediately surrounding metasedimentary and metavolcanic rocks have been pervasively intruded by the extensive Balala Dyke Swarm. The dykes in this large swarm range from andesitic to rhyolitic in composition (Joyce, 1964 and Ransley, 1970) and are generally 3 m wide, up to 200 m long (maximum) and trend generally 280 to 330 degrees. The author has observed that within the Yarrowyck Granodiorite, the most abundant dykes are rhyolites (showing minor flow banding) and dark andesites, porphyritic in plagioclase (plate 2.7), containing areas of extensive magmatic vermicular intergrowths (plate 2.8), whereas in the hornfelsic rocks, rhyolite predominates. The dykes intruding the Yarrowyck Granodiorite occur in clusters, which on average are 50 - 250 m apart and the dykes within clusters are 10 - 20 m apart. The dykes can be mapped by airphoto intepretation as they outcrop as low linear exposed ridges (plate 2.9).

The dyke swarm is intruded by the Myanbah Leuco - adamellite and the Gwydir River Adamellite, as demonstrated by both the regional distribution of dykes and field evidence of truncation at both the plutons' contacts.

## B . 2 . 4 : MYANBAH LEUCOADAMELLITE

The Myanbah pluton (Ransley, 1970) is a medium grained biotite leucoadamellite. It intrudes the Sandon beds, the Kurrajong Park Volcanics and the Balala Dyke Swarm and is itself intruded by the Gwydir River Adamellite. It consists of subequal amounts of quartz, plagioclase and K-feldspar and contains minor biotite as the only ferromagnesian mineral (plate 2.10). Some debate exists as to its delineation (Ransley, 1970; and Brown , 1986). Both Ransley and Brown differ (by as much as 1 km) in their placing of its contacts. This is perhaps because Ransley mapped onto uncontrolled photo mosaics and Brown used Ransley's boundaries as a guide with only limited field checking. The author has walked the complete perimeter of the contact and believes its boundaries to be those shown on map 4 (these boundaries are accurate to within 10 m).

The Myanbah leucoadamellite truncates the Balala Dyke Swarm and is undeformed. The author believes this stock post-dates the Yarrowyck Granodiorite, the Balala Dyke Swarm and the regional dextral shear deformation.

PLATE B.2.6 : YARROWYCK SHEAR ZONE DISPLACING A MEMBER OF THE BALALA DYKE SWARM.

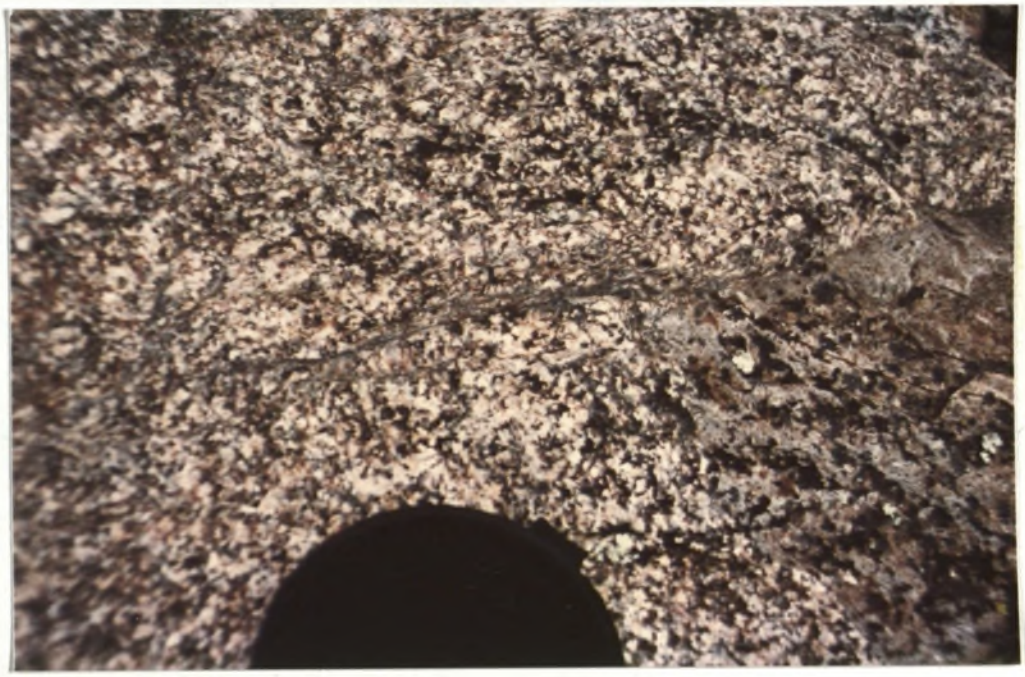

PLATE B.2.7 : PLAGIOCLASE PHENOCRYSTS IN ANDESITIC DYKE FROM THE BALALA DYKE SWARM.

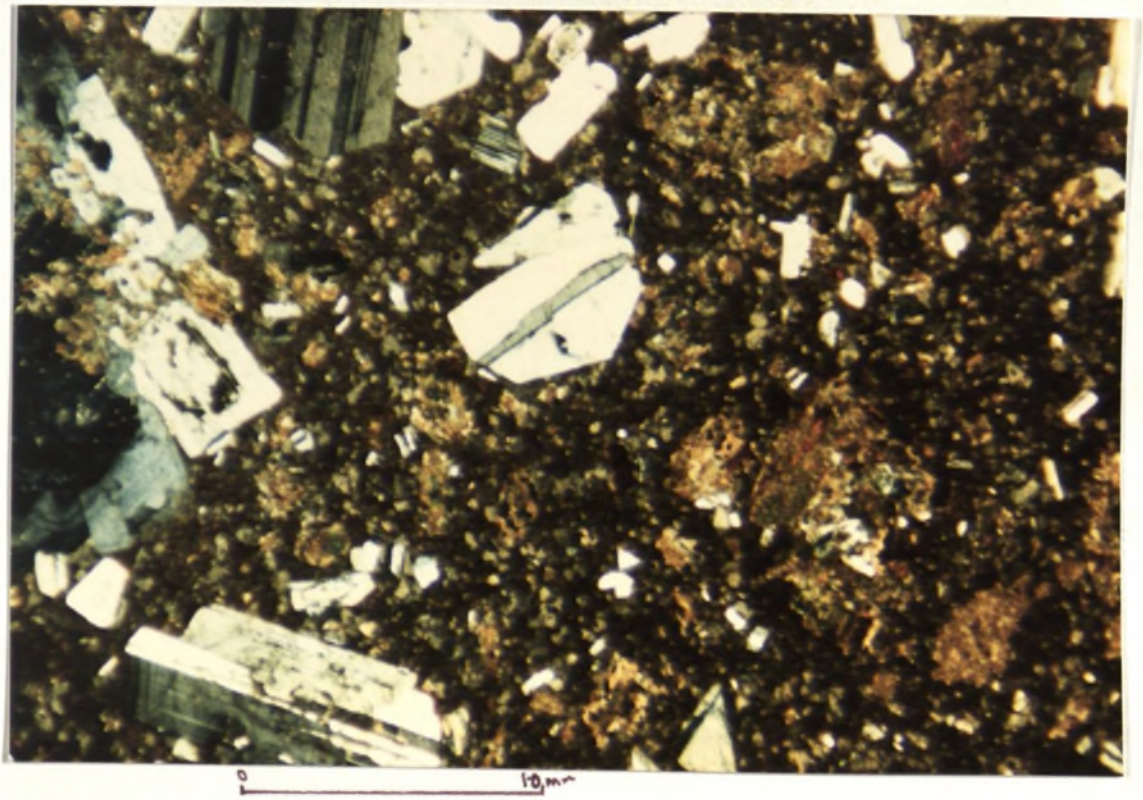

PLATE B.2.8 : FINE GRAINED WELL DEVELOPED VERMICULAR INTERGROWTHS EVIDENT IN MANY OF THE BALALA DYKES IN THE YARROWYCK AREA

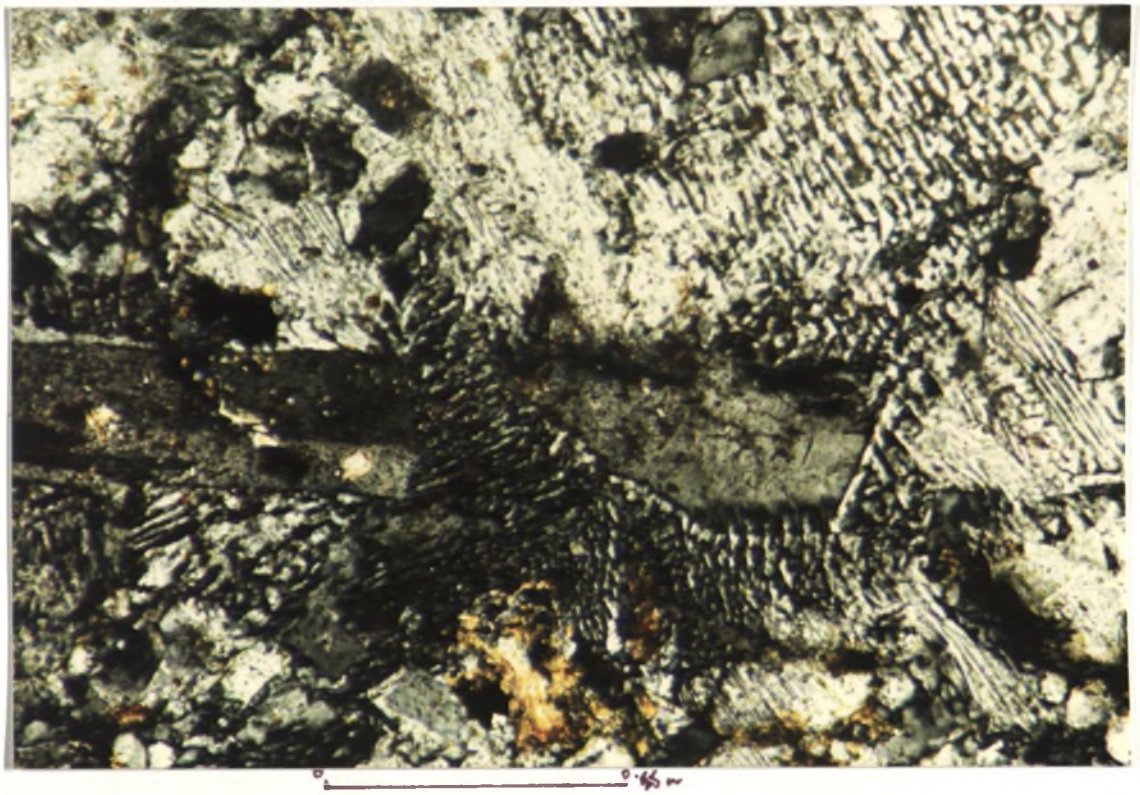

PLATE B.2.9 : OUTCROP STYLE OF THE BALALA DYKE SWARM AS LOW LYING EXPOSED ROCK RIDGES, EITHER IN SITU OR AS TRAILS OF FLOAT

PLATE B.2.10 : CLOSE UP OF THE MYANBAH LEUCOADAMELLITE SHOWING A MORE MAFIC IGNEOUS ENCLAVE, AND THE STRONGLY LEUCOCRATIC CHARACTER OF THE PLUTON.

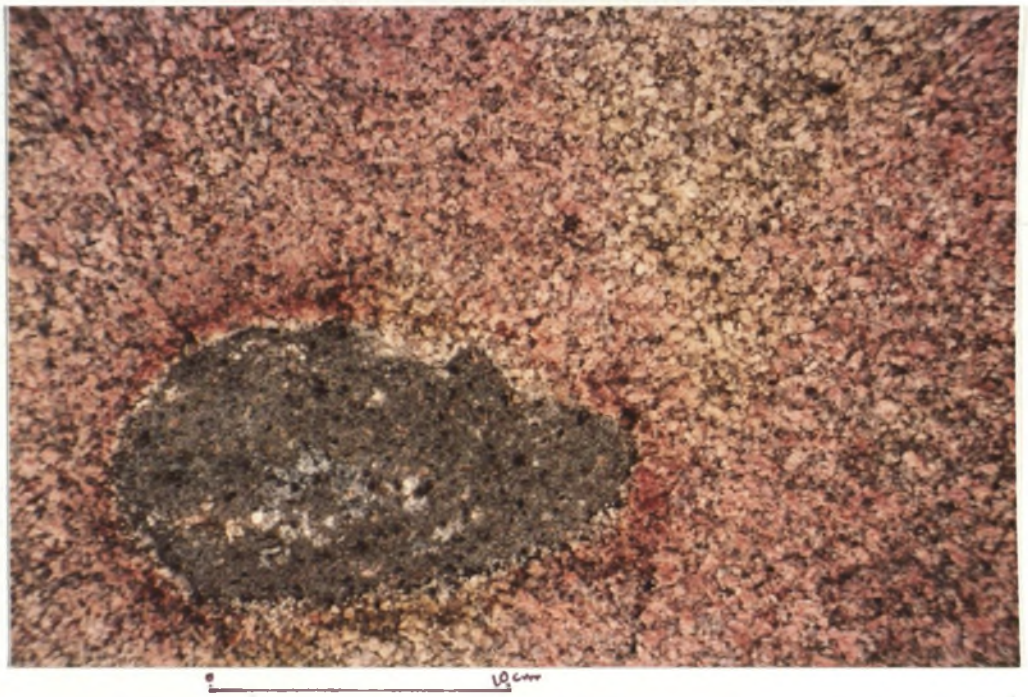


PLATE 2.11a : CLOSE UP OF THE MEGACRYSTIC GWYDIR RIVER PLUTON

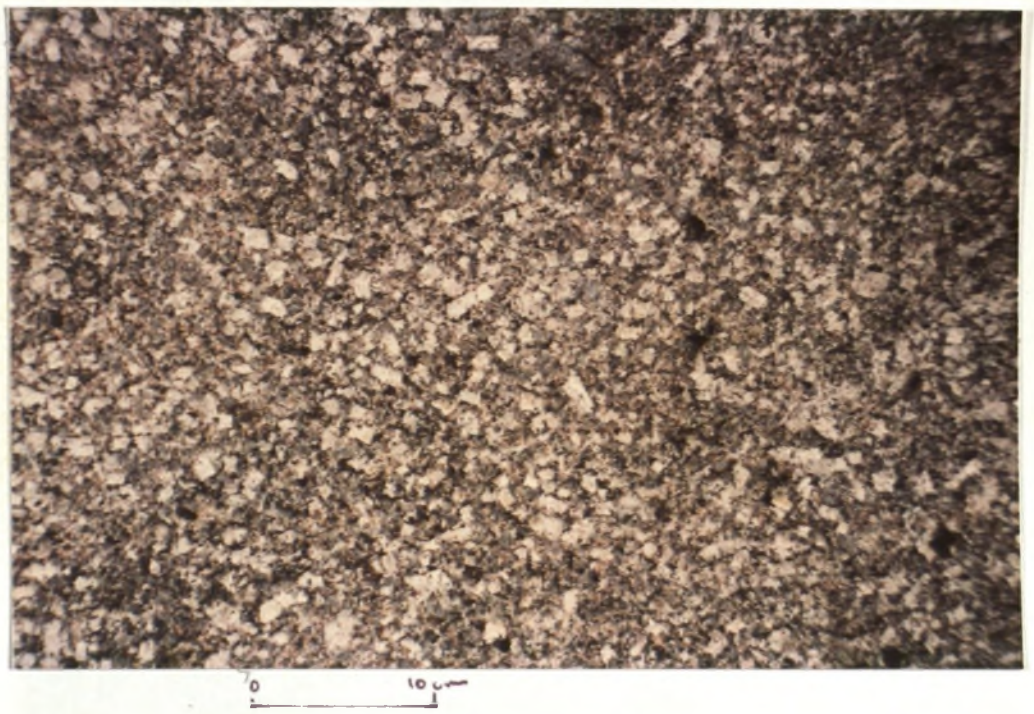

PLATE B.2.11b : MICROGRANITOID ENCLAVE IN THE GWYDIR RIVER ADAMELLITE

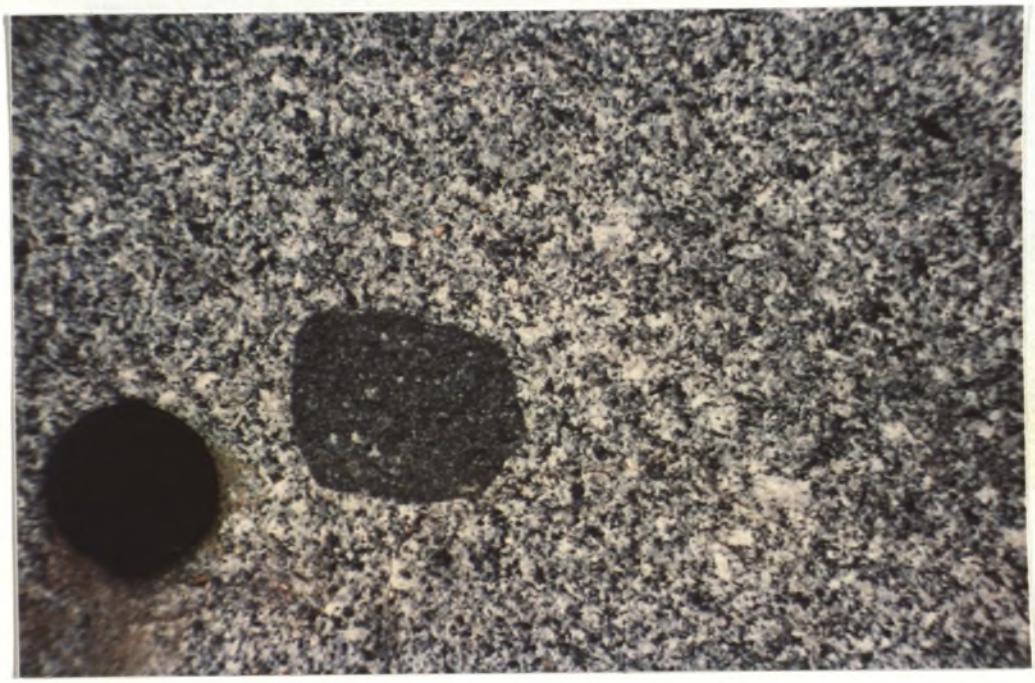

PLATE B.2.12 : CONTACT OF THE MYANBAH LEUCOADAMELLITE WITH THE GWYDIR RIVER ADAMELLITE. FOLIATIONS OBSERVED IN GWYDIR RIVER PLUTON ( EMPHASISED BY BLACK LINES ) PARALLEL THE CONTACT ON BOTH MARGINS.

PLATE B.2.13 : CLOSE UP OF THE MYANBAH LEUCOADAMELLITE - GWYDIR RIVER ADAMELLITE CONTACT, SHOWING MINERAL BANDING IN THE GWYDIR RIVER PLUTON PARALLEL TO THE CONTACT

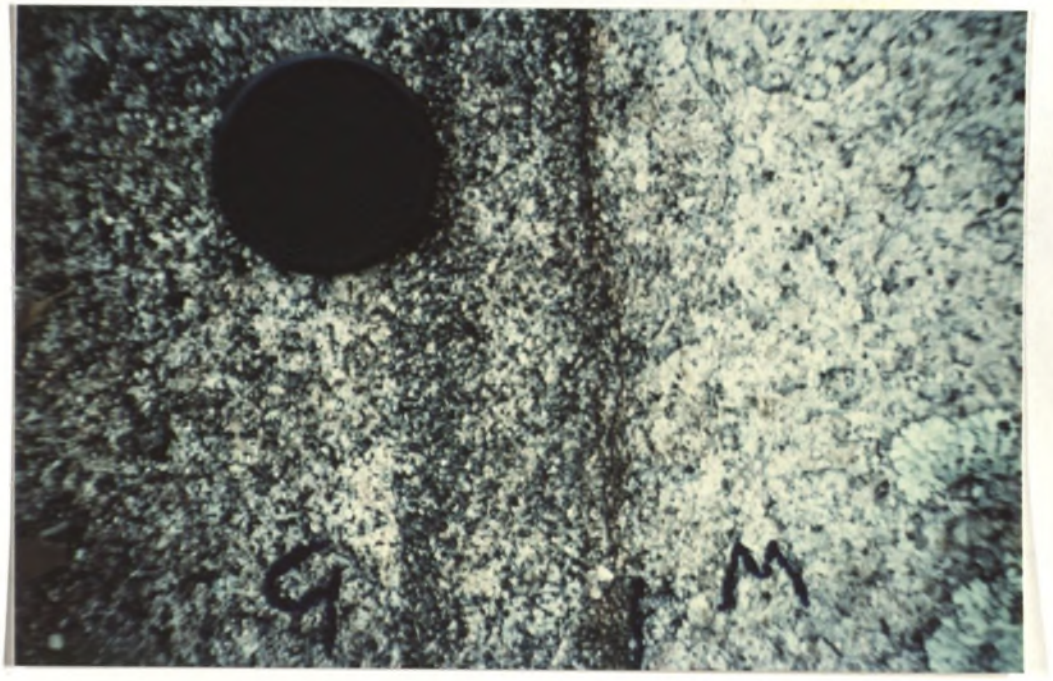

FIGURE B.2.3 : GWYDIR RIVER ADAMELLITE'S CONTACT PARALLEL MEGACRYST AND ENCLAVE ALLIGNMENTS FOR SAMPLE MU46390 ON THE PLUTON'S SOUTH WESTERN MARGIN

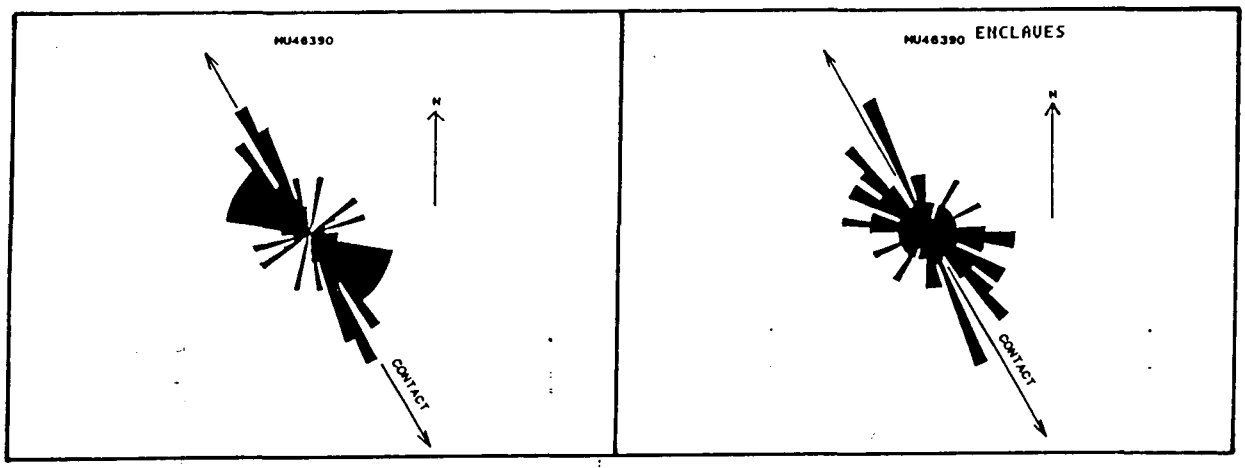


FIGURE B.2.4 : MEGACRYST ALLIGNMENT MEASURMENTS FOR SAMPLES MU46387 ( CONTACT DIRECTIONS AS SHOWN )

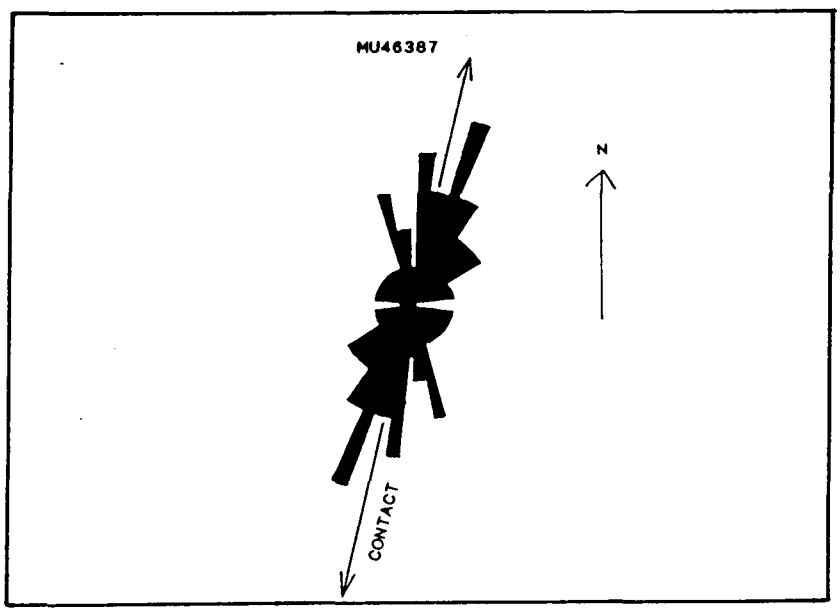

FIGURE B.2.5 : MEGACRYST AND ENCLAVE DIP MEASUREMENTS FOR SAMPLE MU46392 ON THE GWYDIR RIVER ADAMELLITE'S EASTERN MARGIN

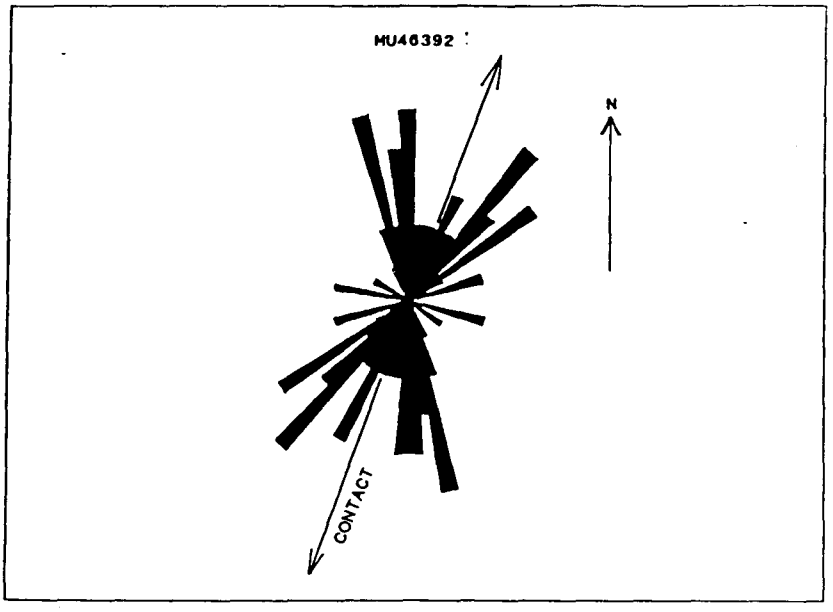


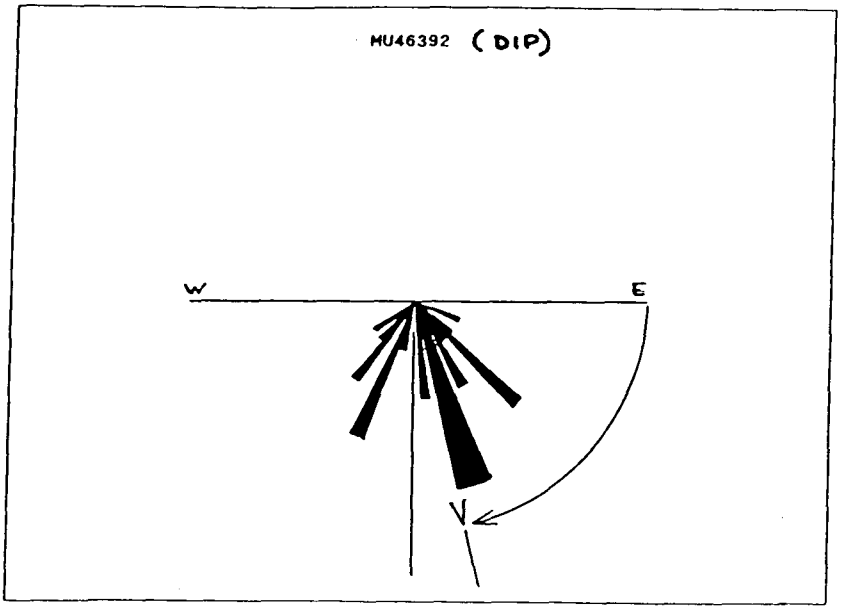

## B . 2 . 5 : GWYDIR RIVER ADAMELLITE

This is a coarse, K-feldspar - plagioclase porphyritic (plate 2.11a) biotite-hornblende I-type adamellite. Ransley (1970) proposed a finer grained, less porphyritic core although samples examined in this study would suggest that any zonation is slight. CIPW norms and modal abundances for this pluton are given in table 2.1 (after Shaw & Flood).

The pluton contains microgranitoid enclaves (plate 2.11b) concentration near the margin. Ransley (1970) also observed meta-sedimentary enclaves near the contact. The Gwydir River Adamellite can be seen to intrude the Myanbah Leucoadamellite evident where megacrysts and mineral banding parallel the contact (plate 2.12). This would imply that the Gwydir River Adamellite is the youngest pluton in the area.

Measurements of the long axes of megacrysts and xenoliths in the Gwydir River Adamellite (figures 2.3 and 4) reveal a strong margin parallel foliation dipping out from the contact at 74 degrees (figure 2.5). This foliation consistantly truncates the weak margin parallel foliation in the Yarrowyck Granodiorite.

# B . CHAPTER 3 : HORNFELS

## B . 3 . 1 : STRUCTURE

The Sandon Beds and Kurrajong Park Volcanics are of Devonian to Carboniferous and Early Permian age respectively (Ishiga, 1988; Cuddy, 1978; and Brown, 1986). Leitch et al (1974) described the Sandon Beds as a multiply deformed, thick series of cherts, mudstones, basalts and conglomerates that appear to have undergone a similar regional and thermal metamorphism to those Woolomin Beds observed in the Bendemeer Area (Brown, 1986). Cuddy (1978) suggested two main deformation periods : the first resulting in minor thrust faulting and gently southward plunging upright open folds under an E-W compression, the second producing a steepening of plunges and a tightening of folds to a close style. The Kurrajong Park Volcanics, consisting of rhyolites, crystal and lithic tuffs and pepperites, unconformably overlie the Sandon Beds but are folded with them, suggesting that they at least were deposited prior to the last deformation (Cuddy, 1978; Brown, 1986).

The hornfels in the Yarrowyck area are divisible into two aureole areas :

The North-eastern Sandon Beds (map 4 and fig B.3.1a ) are bordered by the Yarrowyck Granodiorite and the Gwydir River Adamellite. A large 2 km wide syncline was mappable in the field, with two small ( m wide) parasitic folds on its eastern and western limbs (based on long and short limb vergence relationships). This close, synusoidal syncline trends due north and its fold axis plunges approximately 50 degrees to the south (based on readings taken in its nose to the north of the Gwydir River pluton ). No folds were observed in outcrop and the division of Cuddy's (1978) D1 and D2 fold phases was not possible. However, the moderate plunges correlate with the steepening of once gentle fold plunges and might suggest that both D1 and D2 are present.

Rhyolite Dykes from the Balala Dyke Swarm pervasively intrude this area but are undeformed.

The South-western Sandon Beds and Kurrajong Park Volcanics (map 4 and fig B.3.1b ) are bordered to the east by the Yarrowyck Granodiorite and to the north by both the Gwydir River Adamellite and Myanbah Leucoadamellite. Field mapping shows that both metasedimentary formations have folds with moderate plunges. Figure 1b cuts through the western limb of a predominantly SSE trending synclinal structure. However, this section has been drawn through the inflection point of this fold where it appears to swing to the east, further east it swings back sub-parallel to its original trend. No plunge has been determined and the later intrusives have truncated the synclines nose and eastern limb.

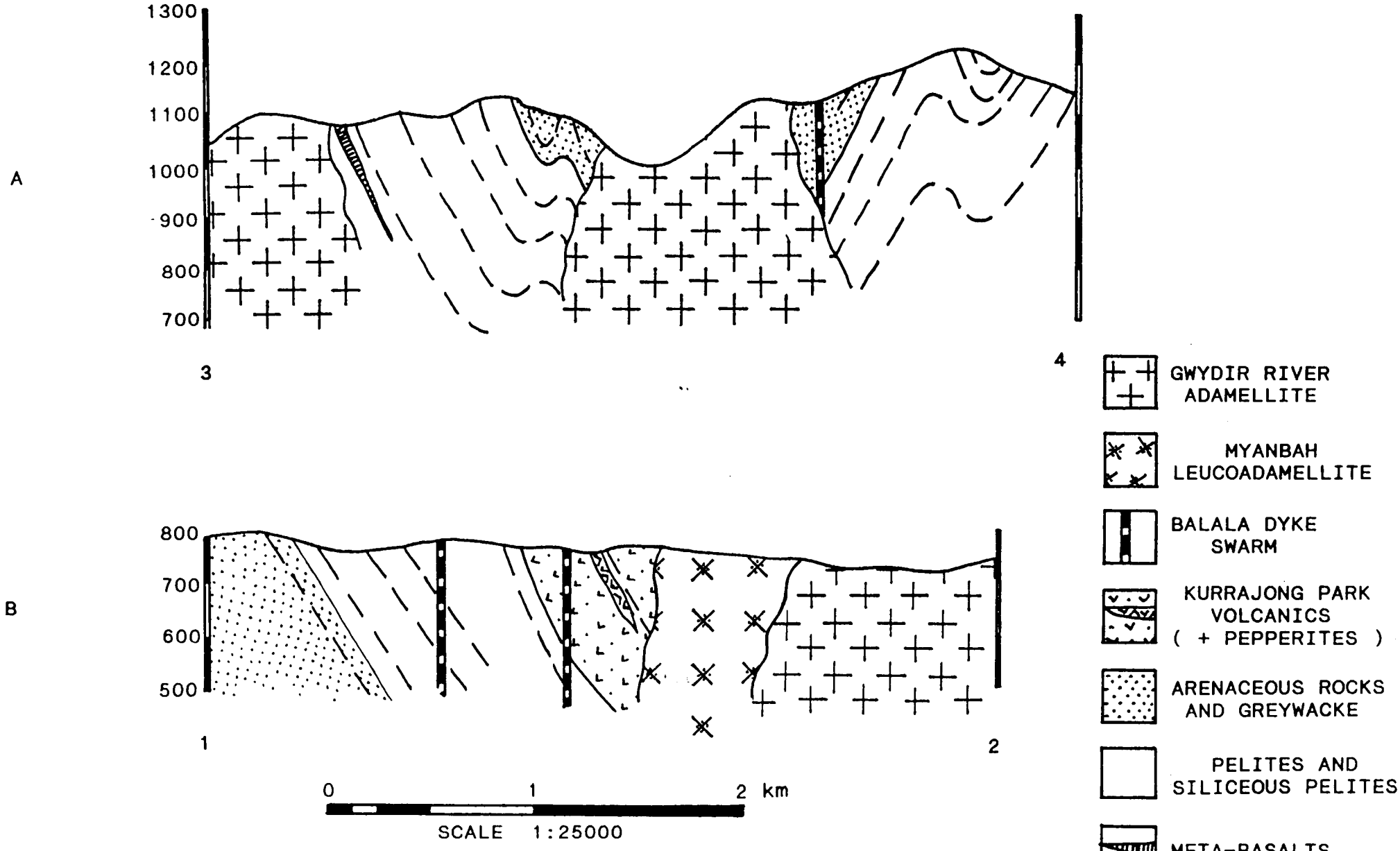


FIGURE B.3.1 STRUCTURAL CROSS-SECTIONS FOR THE YARROWYCK AREA; a) NORTHERN SANDON BEDS, b) SOUTHERN SANDON BEDS AND KURRAJONG PARK VOLCANICS. DIPS ON GRANITE CONTACTS ARE BASED ON DIP MEASUREMENTS OF THE MARGIN PARALLEL FOLIATION OBSERVED IN THE GWYDIR RIVER ADAMELLITE.

What can be concluded for both areas of hornfelses is that they show folds of 100s metres to kilometre scales that maintain their structural continuity right up to the sharp intrusive contacts. No strong evidence of 'shouldering aside' has been observed and only minor areas of stoped blocks ( 30m) occur and these are consistent with passive low strain emplacement imposing little deformation.

# B . 3 . 2 : META-BASALTS

## 3 . 2 . 1 : WHOLE ROCK ANALYSIS

Whole rock analyses and CIPW norms of 7 metabasaltic samples (collected in the northern aureole of the Gwydir River Adamellite, figure 3.2.3) obtained by microprobe analysis of melted and quenched rock powders using the methods of Gulson (1967) and Reed (1970) (see appendix 1) are presented in table 3.2.1 and plotted in figures 3.2.1 and 2. The normative mineral plot (figure 3.2.1) shows that these metabasalts plot as alkali olivine basalts, although plotting close to the tholeiitic boundary. The presence of long laths of plagioclase similar to those seen in the Bendemeer metabasalts suggests a once variolitic fabric. These basalts are all believed to be from the same or associated units, see figure 3.3.3. The concordant nature with surrounding marine sediments, the extensive outcrop and the presence of possibly quenched samples suggests that these units might have once been sills or flows in the marine sediments. As no contacts were exposed and much of the outcrop may has been rotated due to soil creep a more detailed evaluation of the emplacement of these basalts was not possible.

Plotting these samples on an AFC diagram (figure 3.2.2) confirms these samples to be basaltic composition (Winkler, 1976). These samples plot with a high degree of geochemical uniformity regardless of grade and imply that no significant metasomatism seems to have occurred around the Gwydir River Adamellite. In addition they consist primarily of amphibole, plagioclase, oxides and minor sphene. No veining was observed in these rocks.

## 3 . 2 . 2 : PLAGIOCLASE

Plagioclase occurs as elongate laths in all samples and has a porphyritic character in a generally finer grained ground mass, although close to the contact this porphyritic character is lost as coarser grained metamorphic amphibole develops and minor metamorphic granoblastic plagioclase forms.

No variation in the magmatic plagioclase has been observed except for the rims becoming less euhedral and more ragged with grade (plate 3.2.3). No granoblastic plagioclase is observed at lower grades (plates 3.2.1 & 2) but can be seen closer to the contact (plate 3.2.3). This appearance of granoblastic plagioclase is represented graphically in figure 3.2.4 where the proportion of amphibole to plagioclase decreases with distance from the contact. Microprobe analyses of the metabasaltic plagioclases are presented in table 3.2.2 and reveals no observable compositional trend with grade.

FIGURE 3.2.1 : METABASALTIC NORMATIVE MINERAL PLOT OF SAMPLES MU46271 TO MU46277 (after Irvine & Baraga, 1971)

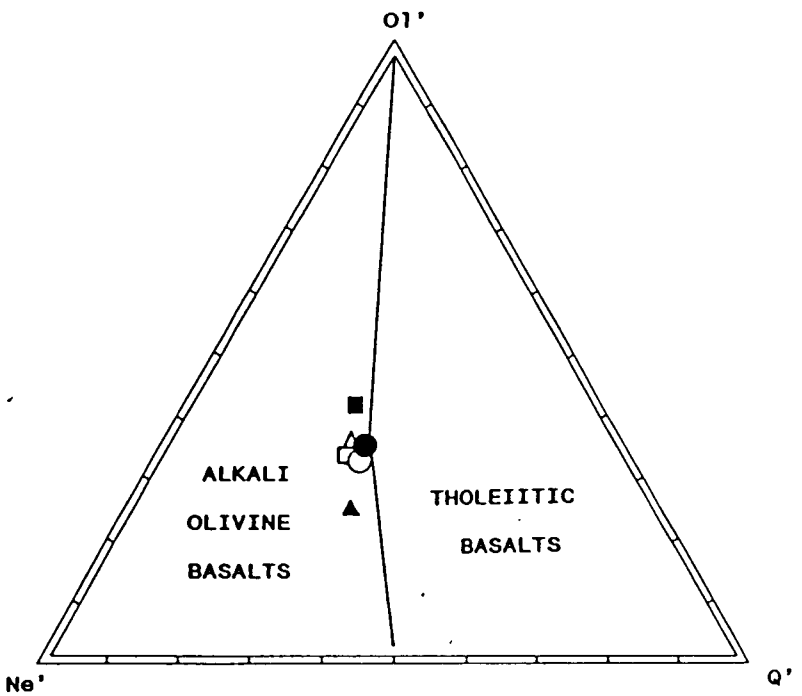


FIGURE 3.2.2 : A F C DIAGRAM OF THE YARROWYCK AREA METABASALTIC SAMPLES

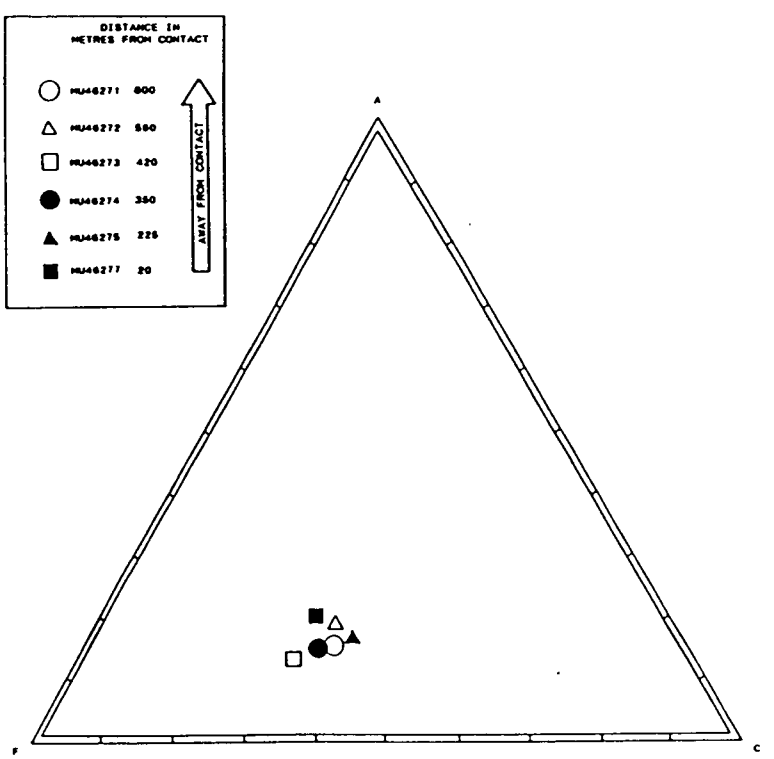


A F C DIAGRAM FOR THE BULK ROCK COMPOSITIONS OF THE YARROWYCK AREA META-BASALTIC HORNFELS

TABLE 3.2.1 : WHOLE ROCK ANALYSES AND CIPW NORMS FOR THE 7 METABASALTIC SAMPLES IN THE AUREOLE OF THE GWYDIR RIVER ADAMELLITE

| SAMPLE | MU46277 | MU46275 | MU46274 | MU46273 | MU46272 | MU46271 |
|---|---|---|---|---|---|---|
| SiO2 | 50.03 | 51.53 | 50.28 | 49.82 | 50.22 | 50.65 |
| TiO2 | 0.95 | 1.03 | 1.08 | 1.10 | 1.13 | 1.01 |
| Al2O3 | 14.18 | 15.27 | 14.80 | 14.77 | 16.59 | 15.07 |
| Fe2O3 | 1.63 | 1.40 | 1.47 | 1.49 | 1.50 | 1.57 |
| FeO | 8.95 | 7.77 | 8.17 | 8.25 | 8.33 | 8.70 |
| MnO | 0.05 | 0.20 | 0.26 | 0.21 | 0.21 | 0.18 |
| MgO | 8.77 | 6.47 | 8.31 | 7.92 | 9.87 | 7.34 |
| CaO | 12.38 | 12.83 | 12.30 | 12.02 | 12.21 | 13.16 |
| Na2O | 2.59 | 3.45 | 3.08 | 3.32 | 2.84 | 2.85 |
| K2O | 0.28 | 0.25 | 0.15 | 0.24 | 0.34 | 0.17 |
| TOTAL | 99.79 | 100.20 | 99.80 | 99.14 | 100.24 | 100.70 |
| Q | 0.00 | 0.00 | 0.00 | 0.00 | 0.00 | 0.00 |
| Or | 1.27 | 1.48 | 0.89 | 1.42 | 2.01 | 1.00 |
| Ab | 22.36 | 28.43 | 26.05 | 25.64 | 24.02 | 24.11 |
| Ne | 0.00 | 0.41 | 0.00 | 1.32 | 0.00 | 0.00 |
| An | 25.93 | 25.44 | 26.11 | 26.68 | 31.51 | 27.82 |
| Di | 29.04 | 31.28 | 28.40 | 28.48 | 23.80 | 30.67 |
| Hy | 4.56 | 0.00 | 0.84 | 0.00 | 5.24 | 2.90 |
| Ol | 12.15 | 9.18 | 13.33 | 13.35 | 9.35 | 10.01 |
| Mt | 2.38 | 2.03 | 2.13 | 2.16 | 2.17 | 2.28 |
| Il | 2.00 | 1.96 | 2.05 | 2.09 | 2.15 | 1.92 |
| TOTAL | 99.79 | 100.20 | 99.80 | 99.14 | 100.24 | 100.70 |

FIGURE 3.2.3 : AREA MAP SHOWING SAMPLE LOCATIONS FOR THE 6 METABASALTIC SAMPLES FROM THE YARROWYCK AREA

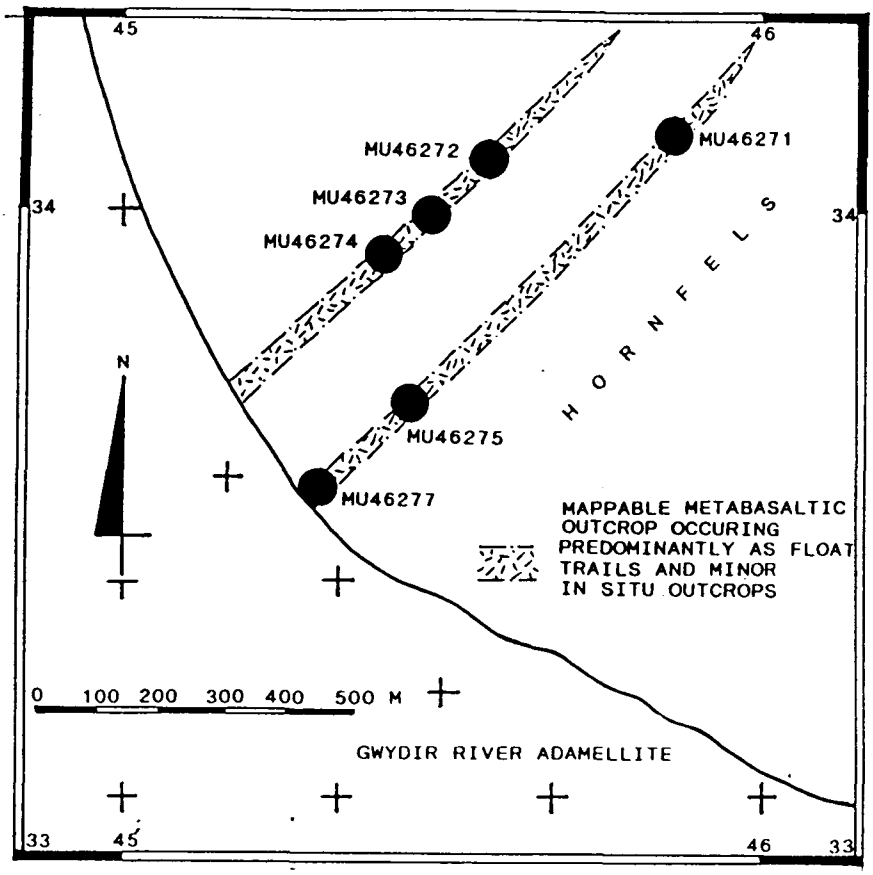


FIGURE 3.2.4 : PLOT OF HORNBLENDE / PLAGIOCLASE PROPORTIONS AGAINST DISTANCE FROM THE CONTACT OF THE GWYDIR RIVER ADAMELLITE

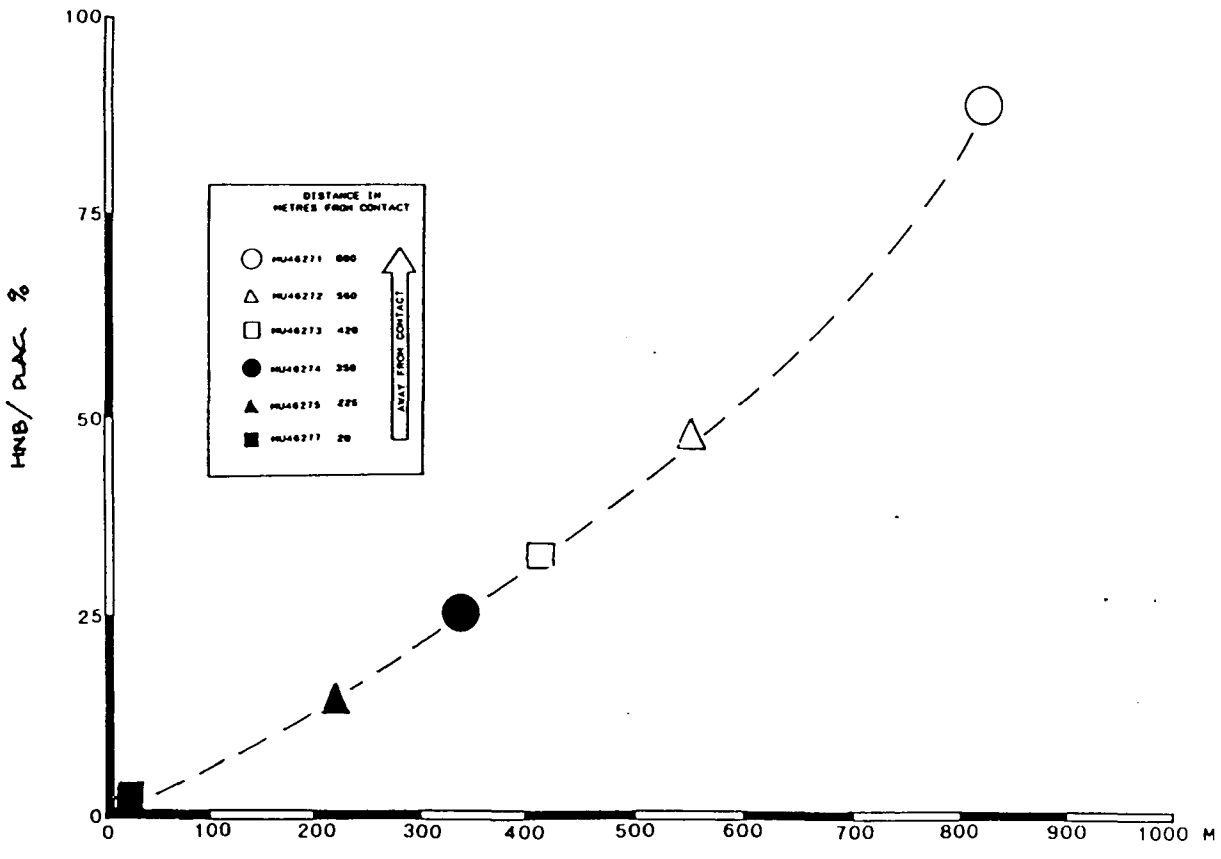

TABLE 3.2.2 : PLAGIOCLASE ANALYSES FOR THE YARROWYCK AREA METABASALTIC SAMPLES

| | MU46277 | MU46277 | MU46275 | MU46275 | MU46275 | MU46275 |
|---|---|---|---|---|---|---|
| | % | % | % | % | % | % |
| SiO2 | 43.65 | 53.51 | 53.52 | 52.29 | 49.76 | 53.89 |
| Al2O3 | 37.11 | 26.25 | 27.72 | 30.02 | 31.84 | 25.78 |
| CaO | 16.43 | 14.35 | 9.72 | 12.47 | 15.23 | 11.99 |
| Na2O | 5.03 | 6.51 | 6.99 | 5.72 | 3.17 | 8.13 |
| K2O | 0.03 | 0.19 | 0.49 | 0.13 | 0.09 | 0.25 |
| TOTAL | 102.26 | 100.81 | 98.45 | 100.63 | 100.10 | 100.00 |

| | MU46274 | MU46274 | MU46273 | MU46272 | MU46272 | MU46271 |
|---|---|---|---|---|---|---|
| | % | % | % | % | % | % |
| SiO2 | 54.92 | 51.81 | 49.31 | 54.26 | 53.13 | 57.57 |
| Al2O3 | 23.52 | 24.61 | 35.99 | 29.22 | 29.77 | 28.05 |
| CaO | 10.48 | 13.31 | 11.23 | 12.57 | 13.59 | 10.22 |
| Na2O | 5.62 | 8.97 | 5.26 | 5.03 | 4.73 | 6.84 |
| K2O | 0.18 | 0.06 | -- | 0.09 | 0.11 | 0.06 |
| TOTAL | 94.72 | 101.75 | 101.79 | 101.17 | 101.35 | 102.73 |

PLATE 3.2.1 : COLOURLESS TO VERY PALE BLUE - GREEN FIBROUS - RAGGED ACTINOLITIC HORNBLENDE ( MU46271 )

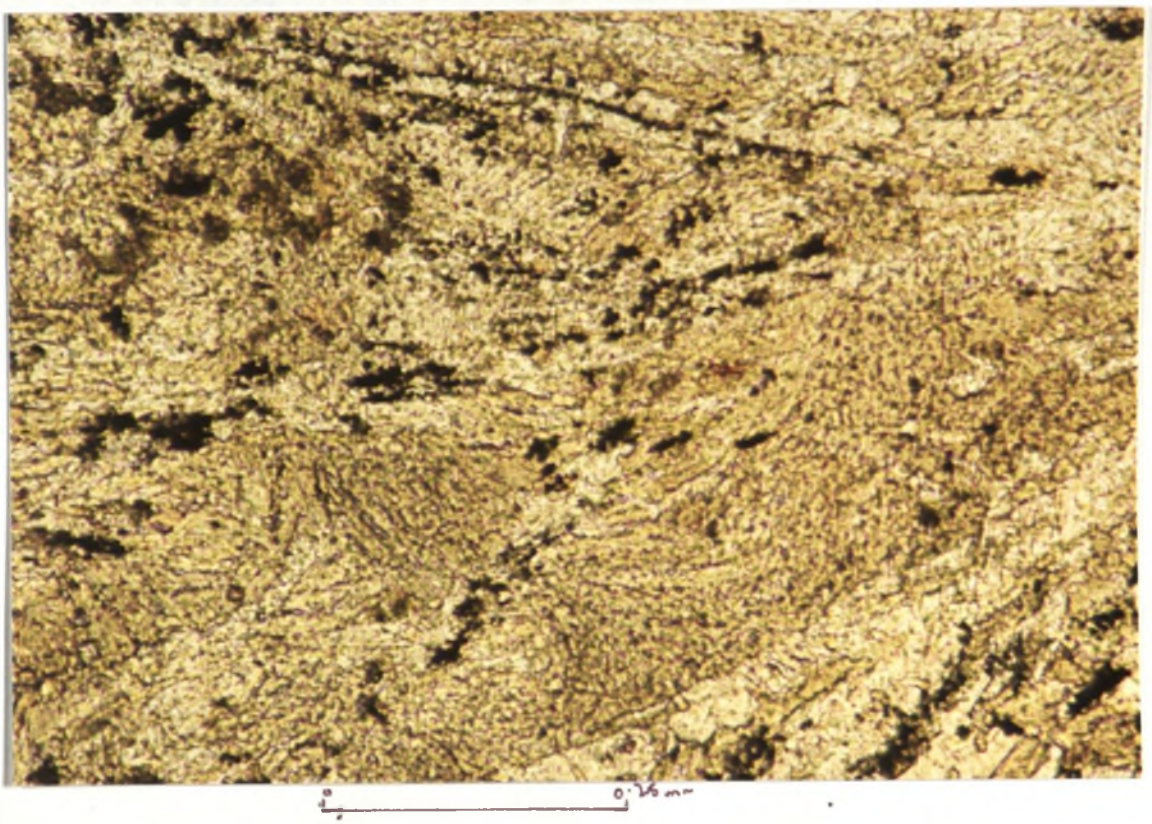

PLATE 2.3.2 : BLUE - GREEN TO GREEN, RAGGED MAGNESIO-HORNBLENDE ( MU46274 )

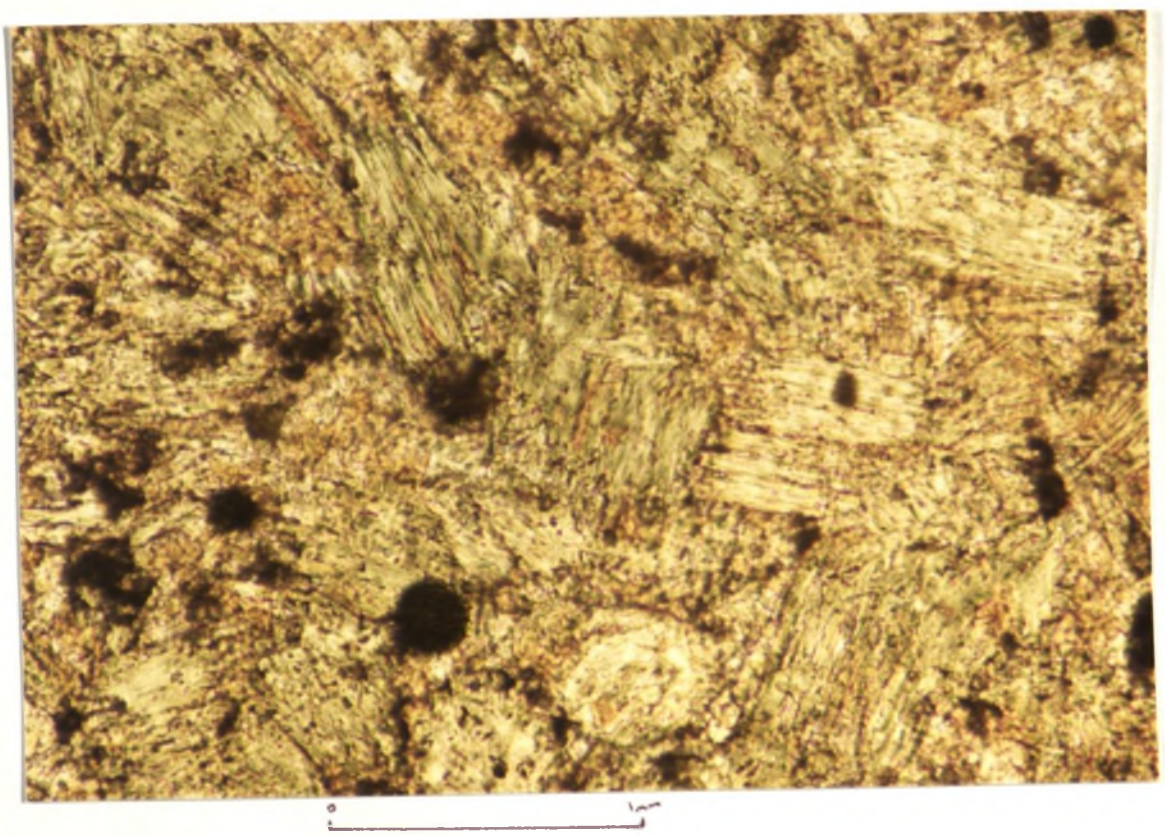

PLATE 3.2.3 : OLIVE - GREEN TO BROWN, RAGGED TO GRANULAR TSCHERMAKITIC HORNBLENDE ( MU46277 )

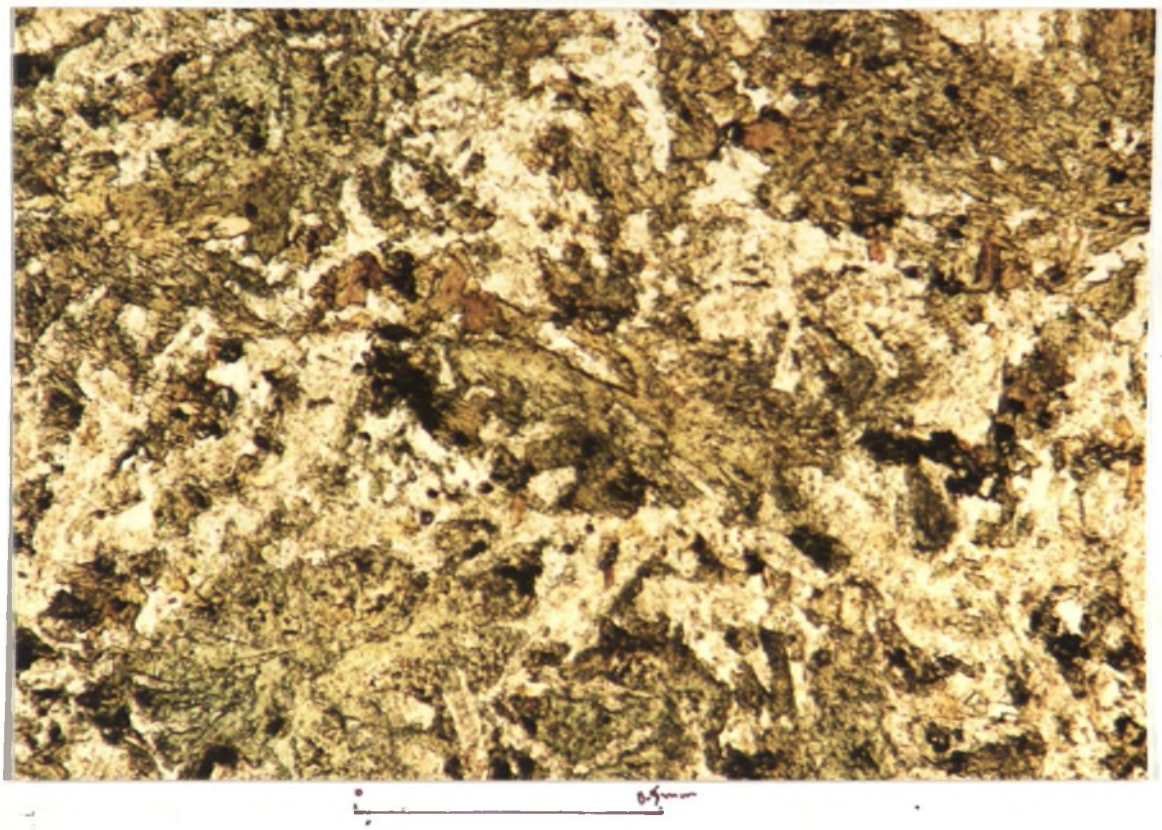

TABLE 3.2.3 : AMPHIBOLE COLOURS FOR THE 3 ABSORPTION DIRETIONS FROM THE 6 METABASALTIC SAMPLES IN THE YARROWYCK AREA

| | MU46271 | MU46272 | MU46273 | MU46274 | MU46275 | MU46277 |
|---|---|---|---|---|---|---|
| A | PALE YELLOW TO COLOURLESS | PALE YELLOW GREEN | PALE YELLOW GREEN | YELLOW GREEN | YELLOW GREEN | YELLOW GREEN |
| B | PALE YELLOW - GREEN TO GREEN | GREEN | GREEN | OLIVE GREEN | OLIVE GREEN | OLIVE GREEN - TAN |
| C | PALE BLUE GREEN | BLUE - GREEN | BLUE - GREEN | STRONG BLUE - GREEN | DEEP GREEN | GREEN BROWN - OLIVE |
| DIST | 800 | 560 | 420 | 350 | 225 | 20 |

## 3 . 2 . 3 : AMPHIBOLE

### 3 . 2 . 3 a ) Microstructural variation

Binns (1966) outlined a microstructural progression with grade for metabasalts in the Moonbi Adamellite's aureole, from a fibrous-ragged habit, through primarly ragged to a granular habit closest to the intrusive contact. An essentially similar progression can be observed in the metabasalts from the Gwydir River Adamellite's aureole. Furthest from the contact (800 m) a fibrous to ragged habit can be observed (plate 3.2.1, MU46271) progressing into a predominantly ragged habit at 350 m (plate 3.2.2, MU46274) and finally into a ragged, partially granoblastic phase closest to the contact (20 m, plate 3.2.3, MU46277).

### 3 . 2 . 3 b ) Colour variation

A colour progression with grade has been outlined also by Binns (1966) for contact metamorphosed basalts in the aureole of the Moonbi Adamellite. This same colour progression occurs in the amphiboles of the metabasalts in the aureole of the Gwydir River Adamellite. Table 3.2.3 outlines this progression for the different absorption directions (alpha, beta, and gamma) of each sample at varying distances from the intrusive contact. At 800 m from the contact the amphiboles are a pale blue-green to yellow-green in colour (plate 3.2.1, table 3.2.3, MU46271), closer to the contact (350 m) the amphiboles are a stronger blue-green to green in colour (plate 3.2.2, table 3.2.3, MU46274) and within 20 m of the contact the amphiboles are a strong olive-green to brown colour (plate 3.2.3, table 3.2.3, MU46277). The presence of the olive-green to brown amphiboles suggests a maximum grade of upper hornblende hornfels facies (Loomis, 1966).

### 3 . 2 . 3 c ) : Compositional variation

The colour and microstructural trends in the amphiboles from the Gwydir River pluton's aureole have been used as the basis for a compositional examination of these amphiboles. Twenty amphiboles were analysed from the six metabasaltic samples and are listed in table 3.2.4 and plotted in figures 3.2.5 to 8. All four plots reveal continuous chemical progressions in the calcic amphiboles with increasing grade. Using Leake's (1968) classification of calcic amphiboles by plotting silica in the unit cell against the Mg-number of the amphibole (figure 3.2.5) reveals that the amphiboles change from actinolite and actinolitic-hornblende at the lowest grades through magnesio-hornblende and up to tschermakitic - hornblende at the highest grades.

The additional plots of Na + K, Ti and sodic-aluminium exchange (figures 3.2.6 to 8) show continuous progressions from the low titanium-low alkali actinolitic amphiboles at the lowest grades up to titanium and alkali enriched tschermakitic hornblendes at the highest grade. These changes are the same as those observed by Binns (1966) at Moonbi.

TABLE 3.2.4 : AMPHIBOLE MICROPROBE ANALYSES FOR THE 6 METABASALT SAMPLES.

| | MU46271 | | MU46271 | | MU46271 | | MU46271 | |
|---|---|---|---|---|---|---|---|---|
| | % | SF | % | SF | % | SF | % | SF |
| SiO2 | 52.46 | 7.529 | 51.21 | 7.402 | 49.80 | 7.178 | 48.47 | 7.026 |
| TiO2 | 0.38 | 0.041 | 0.52 | 0.057 | 0.70 | 0.076 | 1.40 | 0.152 |
| Al2O3 | 3.83 | 0.647 | 4.74 | 0.806 | 6.17 | 1.048 | 7.38 | 1.259 |
| FeO | 12.38 | 1.486 | 13.02 | 1.575 | 14.63 | 1.764 | 16.53 | 2.004 |
| MnO | 0.38 | 0.046 | 0.39 | 0.048 | 0.45 | 0.055 | 0.28 | 0.035 |
| MgO | 15.42 | 3.300 | 14.99 | 3.231 | 14.22 | 3.055 | 12.07 | 2.607 |
| CaO | 12.65 | 1.945 | 11.99 | 1.857 | 11.96 | 1.847 | 12.02 | 1.866 |
| Na2O | 0.64 | 0.179 | 0.96 | 0.270 | 1.19 | 0.333 | 1.48 | 0.417 |
| K2O | 0.23 | 0.043 | 0.28 | 0.051 | 0.34 | 0.063 | 0.38 | 0.070 |
| TOTAL | 98.38 | 15.216 | 98.11 | 15.297 | 99.47 | 15.419 | 100.00 | 15.430 |

| | MU46272 | | MU46272 | | MU46272 | | MU46271 | |
|---|---|---|---|---|---|---|---|---|
| | % | SF | % | SF | % | SF | % | SF |
| SiO2 | 47.27 | 6.925 | 49.28 | 6.963 | 47.04 | 6.914 | 49.30 | 7.058 |
| TiO2 | 1.49 | 0.164 | 1.38 | 0.146 | 1.38 | 0.153 | 1.29 | 0.139 |
| Al2O3 | 7.68 | 1.324 | 6.56 | 1.091 | 8.01 | 1.387 | 6.87 | 1.157 |
| FeO | 15.80 | 1.936 | 12.34 | 1.458 | 15.17 | 1.865 | 13.77 | 1.648 |
| MnO | 0.51 | 0.062 | 0.28 | 0.034 | 0.27 | 0.033 | 0.38 | 0.045 |
| MgO | 11.87 | 2.592 | 12.61 | 2.655 | 11.60 | 2.541 | 13.44 | 2.867 |
| CaO | 12.42 | 1.949 | 14.24 | 1.962 | 13.44 | 2.116 | 11.69 | 1.672 |
| Na2O | 1.66 | 0.472 | 1.61 | 0.441 | 1.29 | 0.366 | 3.56 | 0.841 |
| K2O | 0.46 | 0.087 | 0.17 | 0.031 | 0.44 | 0.082 | 0.18 | 0.033 |
| TOTAL | 99.17 | 15.501 | 98.47 | 14.781 | 98.66 | 15.457 | 100.47 | 15.460 |

TABLE 3.2.4 : AMPHIBOLE MICROPROBE ANALYSES FOR THE 6 METABASALT SAMPLES ( CONTINUED ).

| | MU46273 | | MU46273 | | MU46273 | | MU46274 | |
|---|---|---|---|---|---|---|---|---|
| | % | SF | % | SF | % | SF | % | SF |
| SiO2 | 47.82 | 6.995 | 46.55 | 6.844 | 46.83 | 6.810 | 46.74 | 6.813 |
| TiO2 | 1.34 | 0.147 | 1.53 | 0.170 | 1.30 | 0.145 | 1.80 | 0.198 |
| Al2O3 | 7.82 | 1.339 | 8.36 | 1.448 | 8.96 | 1.552 | 8.80 | 1.510 |
| FeO | 14.01 | 1.704 | 14.34 | 1.763 | 14.20 | 1.747 | 15.28 | 1.863 |
| MnO | 0.35 | 0.042 | 0.36 | 0.043 | 0.33 | 0.041 | 0.30 | 0.036 |
| MgO | 13.44 | 2.914 | 12.28 | 2.693 | 11.64 | 2.554 | 11.73 | 2.548 |
| CaO | 11.88 | 1.851 | 12.69 | 1.899 | 12.08 | 1.874 | 12.47 | 1.849 |
| Na2O | 1.77 | 0.499 | 1.90 | 0.543 | 2.17 | 0.609 | 2.01 | 0.568 |
| K2O | 0.21 | 0.038 | 0.24 | 0.045 | 0.24 | 0.029 | 0.27 | 0.051 |
| TOTAL | 98.63 | 15.529 | 98.25 | 15.548 | 97.45 | 15.361 | 99.41 | 15.436 |

| | MU46274 | | MU46274 | | MU46274 | | MU46275 | |
|---|---|---|---|---|---|---|---|---|
| | % | SF | % | SF | % | SF | % | SF |
| SiO2 | 45.36 | 6.664 | 46.01 | 6.758 | 45.93 | 6.721 | 44.69 | 6.663 |
| TiO2 | 1.84 | 0.202 | 1.81 | 0.199 | 1.62 | 0.179 | 1.49 | 0.167 |
| Al2O3 | 10.74 | 1.847 | 8.73 | 1.509 | 9.48 | 1.634 | 10.34 | 1.815 |
| FeO | 14.43 | 1.763 | 15.72 | 1.931 | 14.80 | 1.812 | 13.90 | 1.734 |
| MnO | 0.30 | 0.037 | 0.32 | 0.040 | 0.35 | 0.043 | 0.27 | 0.034 |
| MgO | 11.13 | 2.423 | 11.68 | 2.558 | 11.99 | 2.616 | 11.98 | 2.662 |
| CaO | 12.32 | 1.876 | 12.26 | 1.870 | 12.44 | 1.890 | 11.67 | 1.864 |
| Na2O | 2.27 | 0.519 | 2.34 | 0.554 | 2.06 | 0.583 | 2.07 | 0.597 |
| K2O | 0.23 | 0.043 | 0.28 | 0.527 | 0.29 | 0.057 | 0.23 | 0.044 |
| TOTAL | 97.73 | 15.374 | 99.16 | 15.946 | 98.95 | 15.535 | 96.63 | 15.580 |

TABLE 3.2.4 : AMPHIBOLE MICROPROBE ANALYSES FOR THE 6 METABASALT SAMPLES ( CONTINUED ).

| | MU46275 | | MU46275 | | MU46277 | | MU46277 | |
|---|---|---|---|---|---|---|---|---|
| | % | SF | % | SF | % | SF | % | SF |
| SiO2 | 46.34 | 6.789 | 46.35 | 6.550 | 43.32 | 6.402 | 45.19 | 6.341 |
| TiO2 | 1.47 | 0.161 | 1.67 | 0.198 | 1.15 | 0.128 | 1.54 | 0.175 |
| Al2O3 | 10.32 | 1.780 | 9.27 | 1.541 | 11.93 | 2.076 | 10.37 | 1.761 |
| FeO | 14.13 | 1.731 | 16.97 | 2.086 | 14.75 | 1.824 | 15.84 | 1.961 |
| MnO | 0.34 | 0.043 | 0.24 | 0.030 | 0.28 | 0.035 | 0.25 | 0.033 |
| MgO | 10.99 | 2.400 | 10.49 | 2.298 | 11.52 | 2.538 | 11.16 | 2.301 |
| CaO | 12.17 | 1.910 | 12.27 | 1.882 | 12.53 | 1.883 | 11.97 | 1.768 |
| Na2O | 2.26 | 0.543 | 1.98 | 0.564 | 2.80 | 0.678 | 1.87 | 0.532 |
| K2O | 0.22 | 0.042 | 0.64 | 0.120 | 0.36 | 0.067 | 0.59 | 0.098 |
| TOTAL | 98.25 | 15.399 | 99.88 | 15.269 | 98.68 | 15.631 | 98.58 | 14.970 |

FIGURE 3.2.5 : PLOT OF Si IN THE UNIT CELL AGAINST Mg - NUMBER
( after Leake, 1968 )

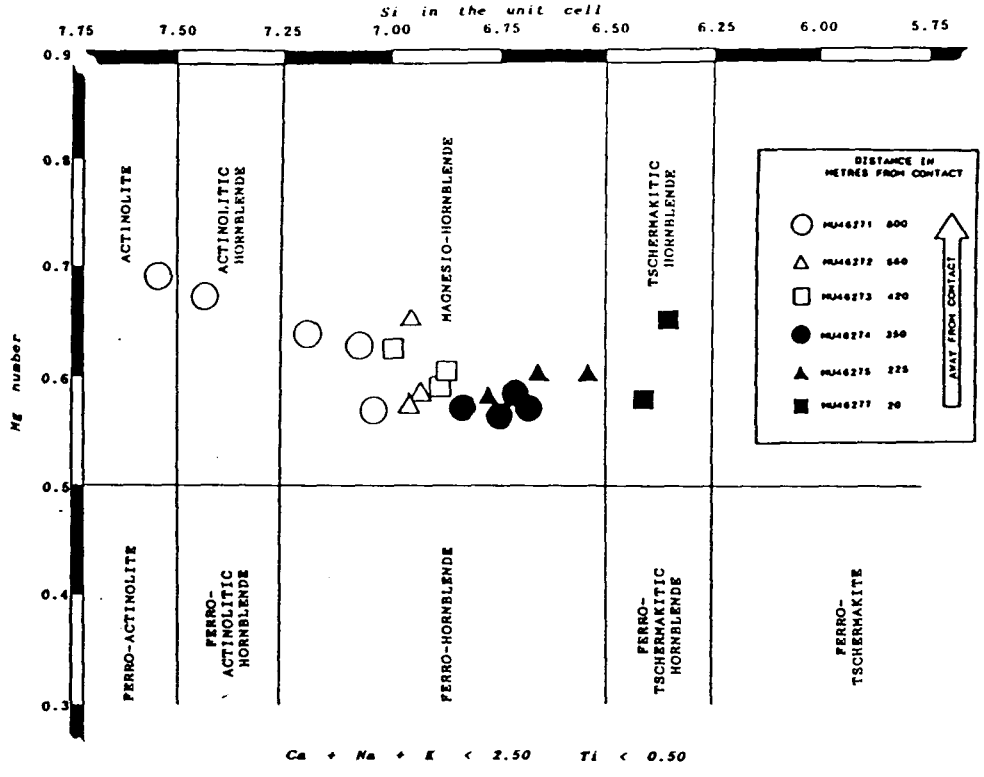


FIGURE 3.2.6 : PLOT OF NET ALKALI AGAINST ALUMINIUM - NET ALKALI
( Sobolev, 1970 )

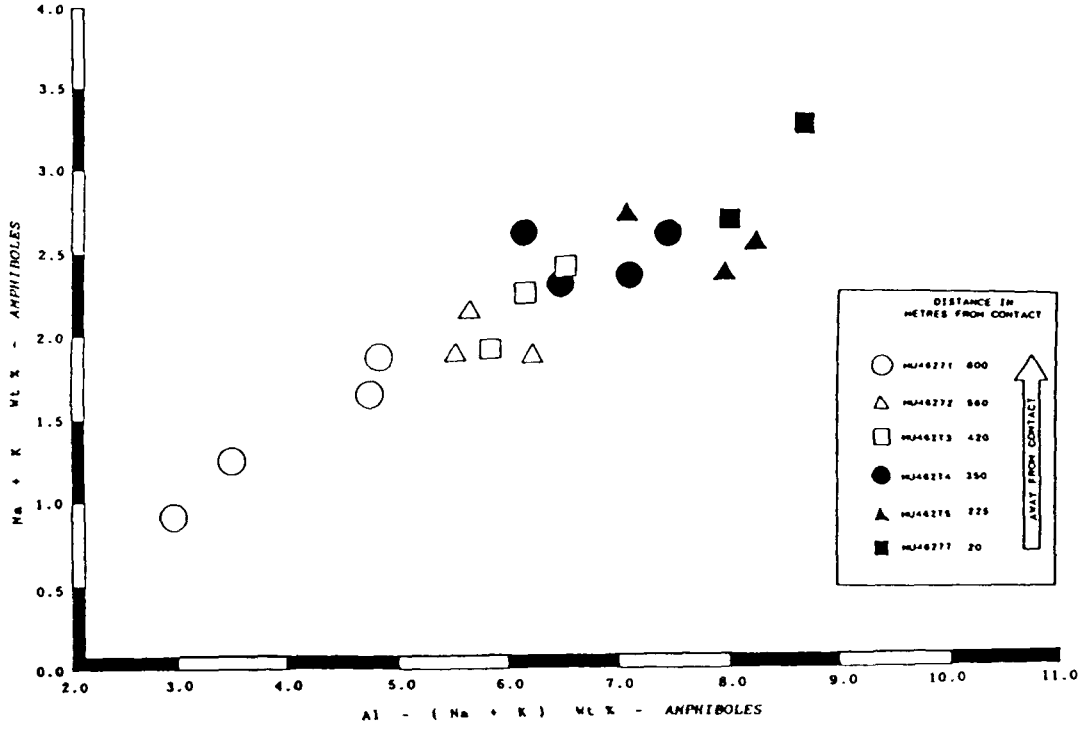

FIGURE 3.2.7 : PLOT OF Wt % ALKALI VERSUS TITANIUM (Leake, 1968)

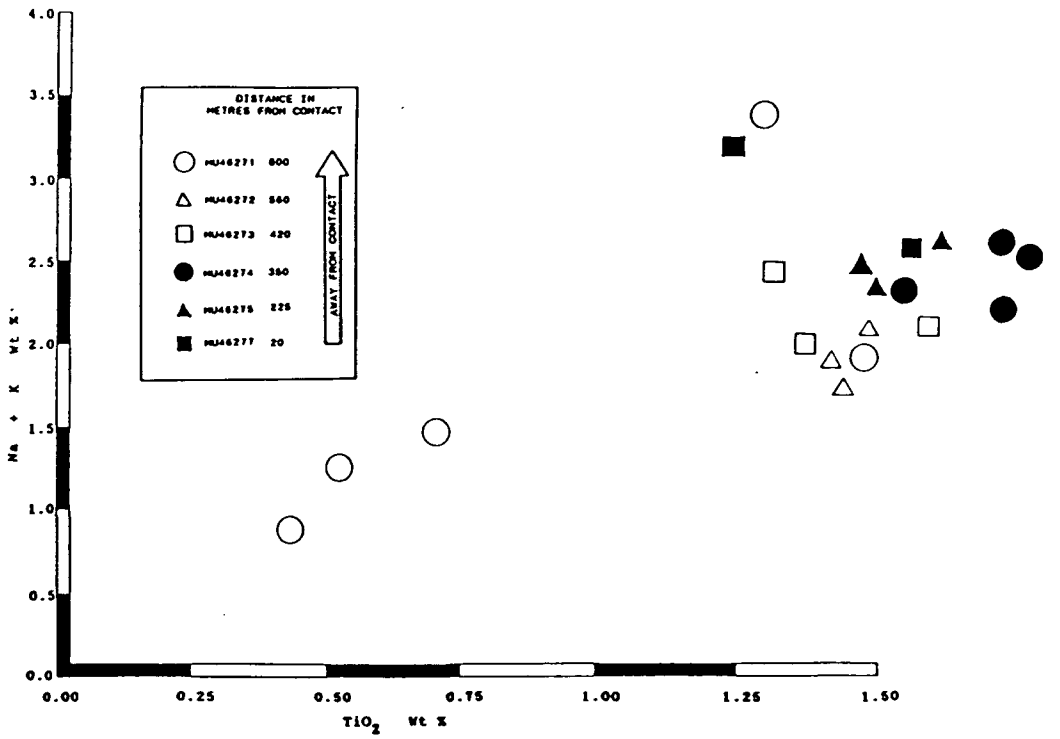


FIGURE 3.2.8 : PLOT OF SODIC/CALCIC EXCHANGE AGAINST ALUMINIUM/ SILICA EXCHANGE ( Leake, 1968; Sobolev, 1970 )

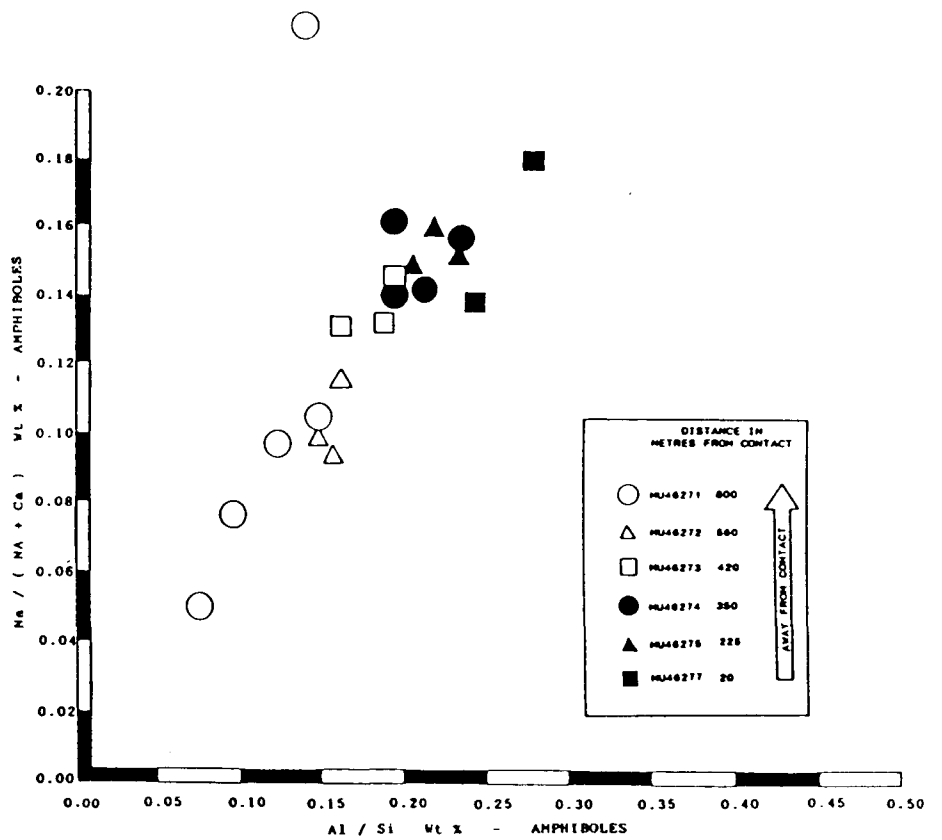

FIGURE 3.2.9 : SUMMARY DIAGRAM FOR THE AMPHIBOLES FROM THE METABASLTIC SAMPLES IN THE AUREOLE OF THE GWYDIR RIVER ADAMELLITE

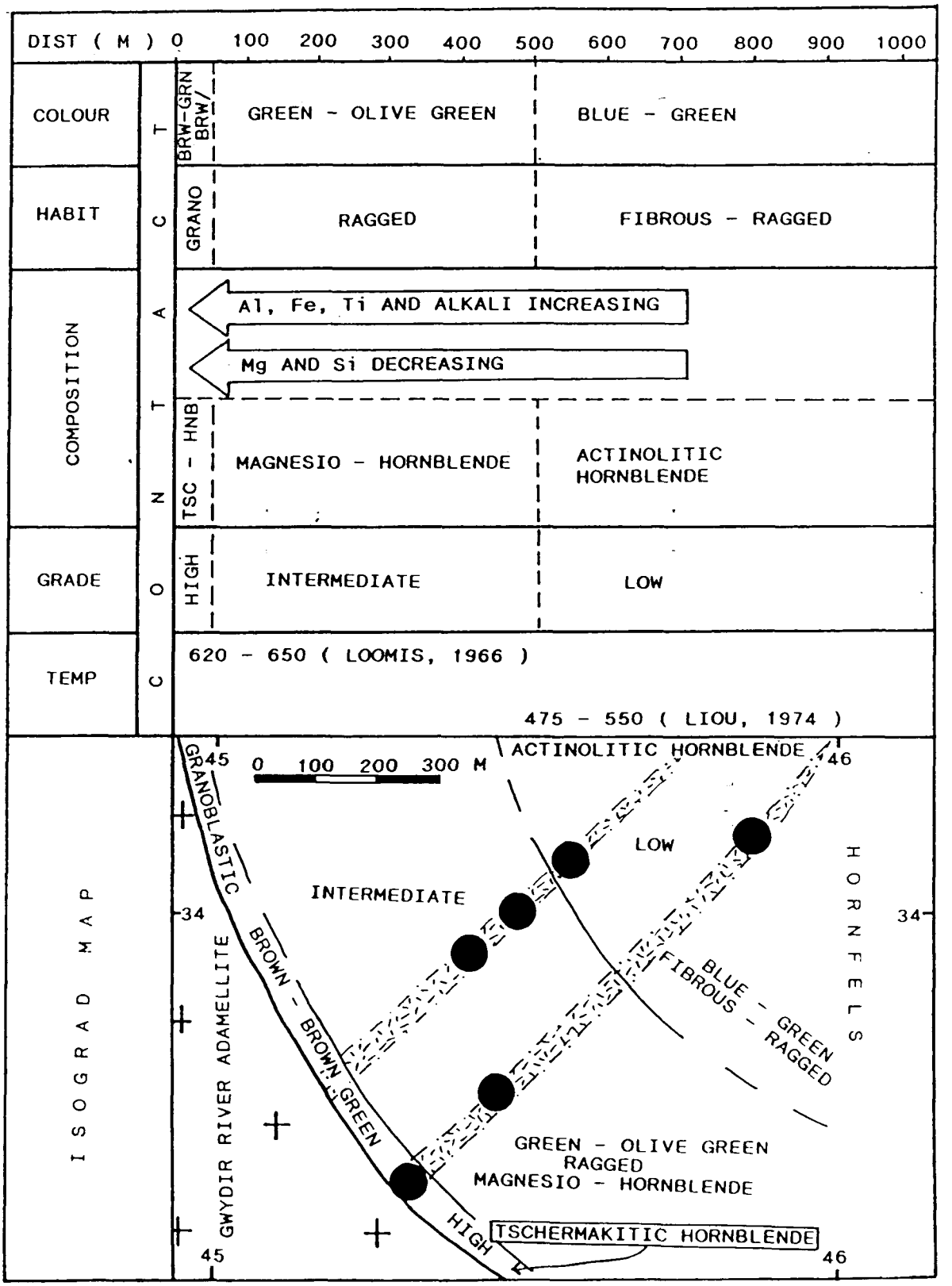

## 3 . 2 . 4 : CONCLUSION:

Plagioclase in the contact metamorphosed basalts in the Yarrowyck area shows little observable change with grade althought the appearance of metamorphic plagioclase has been noted. However, changes in metamorphic amphibole microstructure, colour and composition, like those defined by Binns (1966), can be delineated and are summarised in figure 3.2.9. Applying Liou et al's (1974, 1983) and Loomis' (1966) thermometric calculations suggests aureole temperatures of 475 - 550 degrees celcius at 400 - 500 m (actinolite - hornblende transition) and immediate contact temperatures of 620 - 650 degrees celcius (brown - tan hornblende, see summary figure 3.2.9).

# B . 3 . 3 : METASEDIMENTS

## 3 . 3 . 1 : META-PELITES

The pelitic rocks in the hornfels ridges around the Gwydir River and Yarrowyck plutons are very fine grained ( .01 mm ) shalely to sub - phyllitic and have been regionally metamorphosed in the Carboniferous to the lower prehnite - pumpellyite facies (Leitch, 1974). (This facies being 220-330 degrees C at 2-4 Kb pressure; Best, 1982 and Turner, 1968). They show a discontinuous cleavage, weakly developed laminations and their bedding varies from sharp to gradational with the greywacke units. Flame structures were observed in the field extending from the pelitic layers into a fine to medium grained subangular conglomeritic arenite. These turbiditic bedding structures are observed right up to the contact with the Gwydir River Adamellite.

Within the contact aureoles of the Gwydir River and Yarrowyck plutons, these rocks gradually become more massive in appearance, darker in colour to a dark brown-grey-black and lose their weak lamination, becoming more typically hornfelsic and crystalline in appearance.

Table 3.3.1 shows three XRF analyses of the metapelites which are plotted on an AFM diagram in figure 3.3.1. The diagram shows that the samples lie between the cordierite-chlorite fields and are chemically suitable for cordierite forming reactions. All three samples come from the area delineated in figure 3.3.2 (dashed outline).

## 3 . 3 . 2 : ISOGRAD DELINEATION

Contact metamorphic isograds have been delineated at varying distances from the Gwydir River Adamellite in the area shown in figure 3.3.2, based on optical and probe data (table 3.3.2 ) and the assemblages given in table 3.3.3. The area was chosen as it contained good outcrop and is far enough away from the Yarrowyck Granodiorite as to reveal only the highest grades induced by the Gwydir River Adamellite. The isograds from this known area have been extrapolated to the contact of the Yarrowyck Granodiorite to aid correlation with the less conventional isograds recorded in the Yarrowyck Pluton (see chapters 4.1 & 4.2). The approximated isograds shown on figure 3.3.2 for the Yarrowyck Granodiorite's aureole are only based on a petrographic study of samples and will not be discussed in detail. The south western aureole has not been studied as (like the Bendemeer area) time constraints only permitted the metamorphic zonation of the northern part of the Gwydir River Adamellite's aureole to be established.

The section in figure 3.3.3 reveals that, although the hornfelsic rocks sit topographically higher than the adjacent pluton, no apparent relationship exists between topographic elevation and the grade of contact metamorphism. It is possible, however, that a topographic - grade relationship is masked in this area by the ubiquitous felsic dykes that outcrop and these may act as a stronger topographic control. Figure 3.3.2 only shows five dykes in order to provide

TABLE 3.3.1 : BULK ROCK ANALYSES FOR THE METAPELITES IN THE AUREOLE OF THE GWYDIR RIVER ADAMELLITE.

| | MU46254 | MU46276 | MU46250 |
|---|---|---|---|
| | % | % | % |
| SiO2 | 69.84 | 64.58 | 65.21 |
| TiO2 | 0.69 | 0.91 | 1.12 |
| Al2O3 | 13.05 | 15.46 | 13.77 |
| Fe2O3 | 1.81 | 1.36 | 1.23 |
| FeO | 3.54 | 4.72 | 5.41 |
| MnO | 0.19 | 0.08 | 0.28 |
| MgO | 1.45 | 2.13 | 2.62 |
| CaO | 2.61 | 3.33 | 4.03 |
| Na2O | 3.98 | 4.31 | 2.86 |
| K2O | 0.82 | 0.87 | 1.47 |
| P2O5 | 0.09 | 0.11 | 0.19 |
| H2O+ | 1.16 | 1.78 | 1.42 |
| H2O- | 0.27 | 0.03 | 0.19 |
| CO2 | 0.29 | 0.31 | 0.26 |
| TOTAL | 99.79 | 99.98 | 100.06 |

FIGURE 3.3.1 : AFM DIAGRAM FOR THE 3 ANALYSED META-PELITES FROM THE GWYDIR RIVER ADAMELLITE'S AUREOLE.

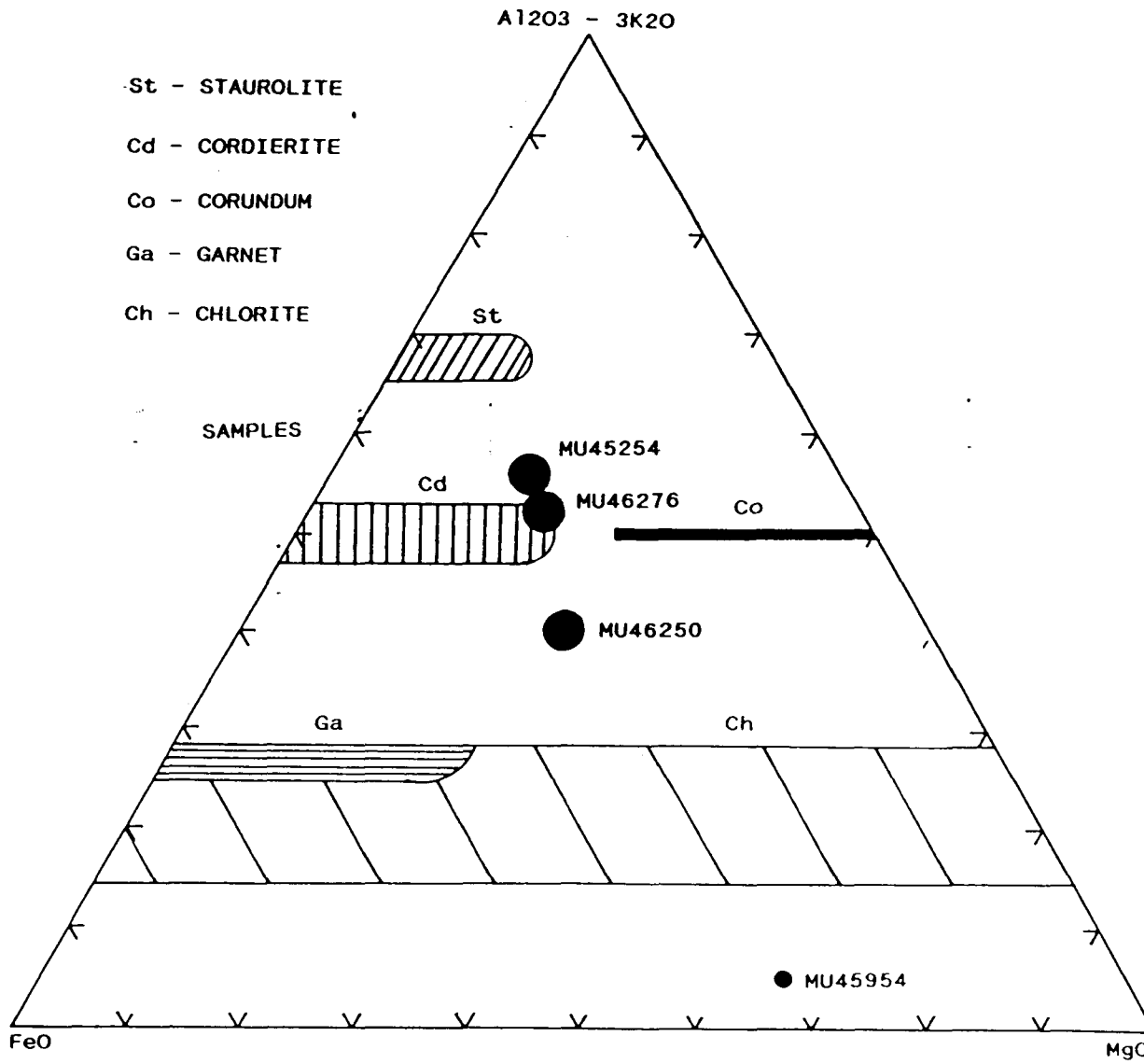

FIGURE 3.3.2 : ISOGRAD MAP FOR THE NORTH EASTERN AUREOLE OF THE GWYDIR RIVER ADAMELLITE

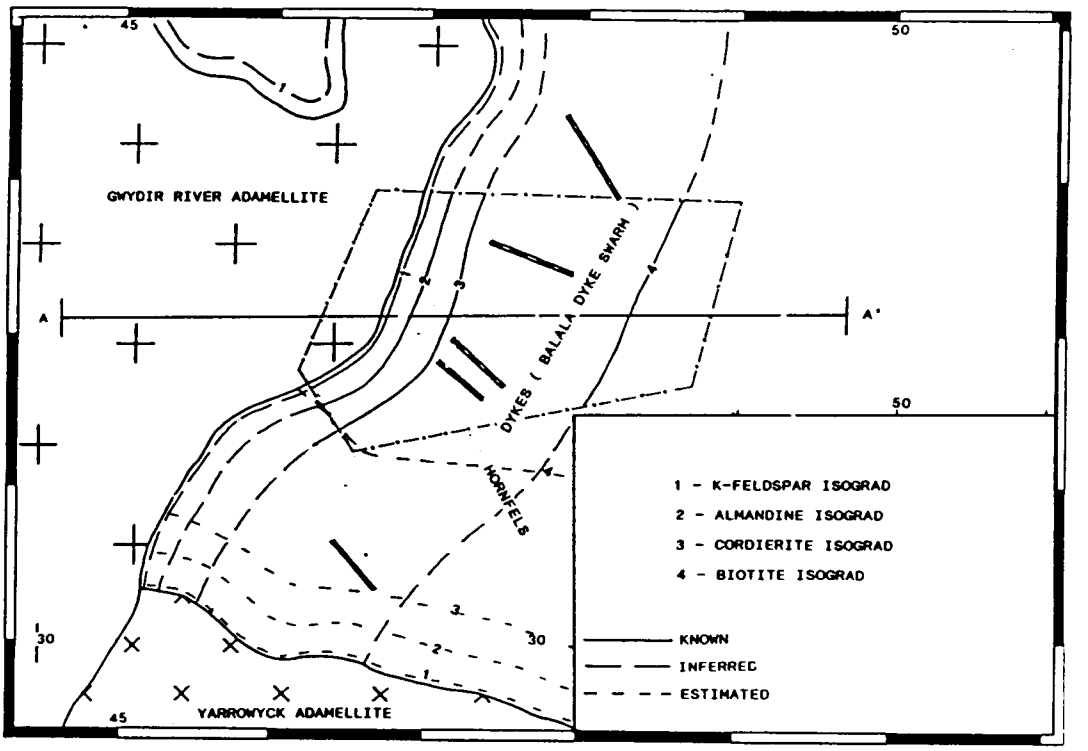


FIGURE 3.3.3 : SECTION A - A' REVEALING THAT NO SIGNIFICANT GRADE - TOPOGRAPHIC RELATIONSHIP EXISTS WITHIN THIS AUREOLE.

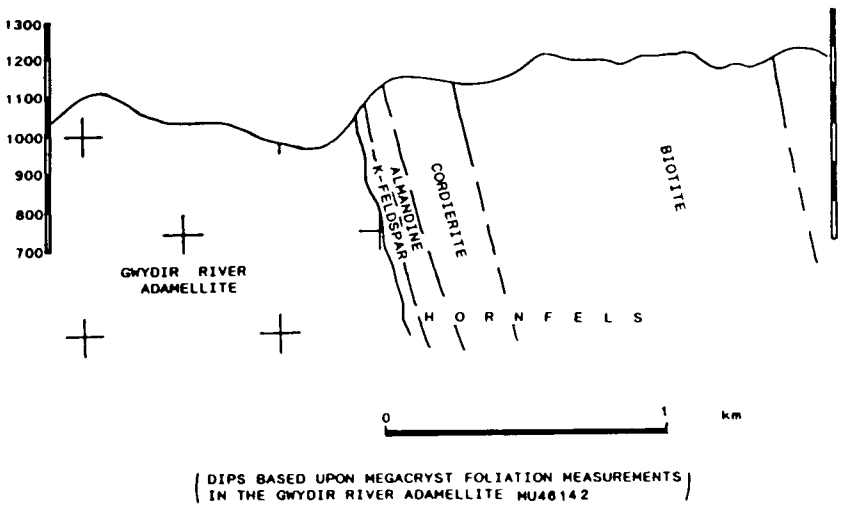


( DIPS BASED UPON MEGACRYST FOLIATION MEASUREMENTS IN THE GWYDIR RIVER ADAMELLITE MU46142 )

a general trend in this area. However, they are considerably more numerous than this (with a spacial density of up to 2-3 dykes per 100 m).

All the following isograd descriptions will refer to figure 3.3.2 and tables 3.3.2 and 3.

## 1 : BIOTITE ZONE :

Fine-grained ( .05 mm) granoblastic-stubby biotite has been observed up to 1.5 km from the Gwydir River Adamellite's contact. With proximity to the contact this grainsize increases up to a maximum of .25mm. The presence of albite and chlorite at this grade suggests the albite-epidote hornfels facies (Vernon,1976; and Speer, 1981) and a temperature range for the biotite isograd has been estimated by Turner (1968) as 400 - 410 degrees C.

## 2. CORDIERITE ZONE :

The cordierite isograd has been mapped at approximately 400 m from the Gwydir River pluton's contact. No 'knotted' appearance was observed associated with the cordierite zone and unlike the Bendemeer aureole the position of the cordierite isograd could not be inferred from field observations. The cordierites occur as irregular shaped porphyroblasts ( 1 mm ) in the pelitic rocks ( plate 3.3.1 ) and are inclusion rich. The appearance of cordierite according to Turner (1968) indicates the change to lower hornblende hornfels facies and temperature estimates by Greenwood (1976) and Winkler (1967) place this zone in the range 525 to 560 degrees celcius. Plagioclase of An 21 in this zone would infer the disappearance of albite.

## 3. CORDIERITE-ALMANDINE ZONE :

The isograd for this zone is at approximately 150 m from the Gwydir River pluton's contact. Garnet is in extremely low abundance and only one grain was positively identified and probed (table 3.3.2 ), giving an almandine ( 75 % almandine ) composition. Estimates of the temperature range for the cordierite- almandine isograd by Naggar and Atherton ( 1977 ) and Hsu ( 1968 ) suggest a range of 560 - 580 degrees celcius at 2 - 3 kb pressure.

## 4. CORDIERITE - K-FELDSPAR ZONE :

The cordierite-K-feldspar isograd is located approximately 40 m from the contact. In this zone biotite and quartz are still the most abundant constituent minerals. The K-feldspars occur as fine granoblastic grains ( .1 mm) in the generally biotite-quartz-rich matrix. Phillips and Wall ( 1981 ) accounted for the presence of K-feldspar in the Bonnie Doon area, Victoria by the reaction :

**muscovite + biotite + quartz = cordierite + k-feldspar + H20**

TABLE 3.3.2 : ELECTRON MICRPROBE ANALYSES OF THE MAIN INDEX MINERALS IN THE AUREOLE OF THE GWYDIR RIVER PLUTON

| | B I O T I T E | | ALMANDINE | K - F E L D S P A R | |
|---|---|---|---|---|---|
| | MU46251 | MU45252 | MU46206 | MU46205 | MU46205 |
| | % | % | % | % | % |
| SiO2 | 35.67 | 36.21 | 37.21 | 62.89 | 64.33 |
| TiO2 | 3.10 | 2.43 | -- | -- | -- |
| Al2O3 | 21.40 | 19.98 | 20.34 | 20.01 | 21.81 |
| FeO | 19.52 | 21.06 | 33.60 | 0.02 | -- |
| MnO | 0.39 | -- | 1.41 | -- | -- |
| MgO | 7.13 | 8.21 | 4.12 | -- | 0.01 |
| CaO | -- | 0.03 | 1.76 | 0.26 | 0.22 |
| Na2O | 0.10 | 0.19 | 0.03 | 0.75 | 0.91 |
| K2O | 8.51 | 8.53 | 0.01 | 16.12 | 12.70 |
| TOTAL | 95.93 | 97.64 | 98.48 | 100.05 | 99.98 |

| | C O R D I E R I T E | | | | |
|---|---|---|---|---|---|
| | MU46205 | MU46206 | MU46250 | MU46250 | MU46250 |
| | % | % | % | % | % |
| SiO2 | 53.96 | 52.90 | 53.72 | 50.00 | 50.41 |
| Al2O3 | 28.50 | 28.44 | 26.48 | 30.48 | 29.15 |
| FeO | 8.74 | 8.68 | 8.35 | 8.90 | 8.14 |
| MnO | 1.36 | 0.96 | 0.65 | 0.52 | 0.67 |
| MgO | 5.90 | 5.90 | 5.92 | 6.33 | 6.92 |
| Na2O | 0.19 | 0.34 | 0.25 | 0.22 | 0.28 |
| TOTAL | 98.21 | 97.22 | 95.69 | 96.64 | 95.78 |
| Mg | 54.70 | 55.20 | 55.80 | 55.90 | 56.40 |

TABLE 3.3.3 : ASSEMBLAGES FOR THE GRADE ZONES DELINEATED IN THE METAPELITES FROM THE AUREOLE OF THE GWYDIR RIVER ADAMELLITE

| ZONE AND DISTANCE ( M ) | ASSEMBLAGE | |
|---|---|---|
| *BIOTITE* | *quartz + biotite* | *- albite-+chlorite* |
| | | *- muscovite-chlorite* |
| *( 1.5 KM )* | | *- muscovite-albite* |
| *CORDIERITE* | *quartz + biotite* | *- muscovite-plagioclase (An 21) - cordierite* |
| *( 400 M )* | | *- cordierite-plagioclase* |
| | | *- cordierite-muscovite* |
| *CORDIERITE ALMANDINE* | *quartz + biotite* | *- plagioclase* |
| | | *- cordierite-+garnet* |
| | | *- plagioclase-muscovite* |
| *( 150 M )* | | |
| *CORDIERITE K-FELDSPAR* | *quartz + biotite* | *- cordierite-plagioclase-K-feldspar* |
| | | *- cordierite-plagioclase* |
| | | *- plagioclase* |
| *( 40 M )* | | |

PLATE 3.3.1 : CORDIERITE PORPHYROBLAST IN THE METAPELITES FROM THE AUREOLE OF THE GWYDIR RIVER ADAMELLITE ( MU46250 )

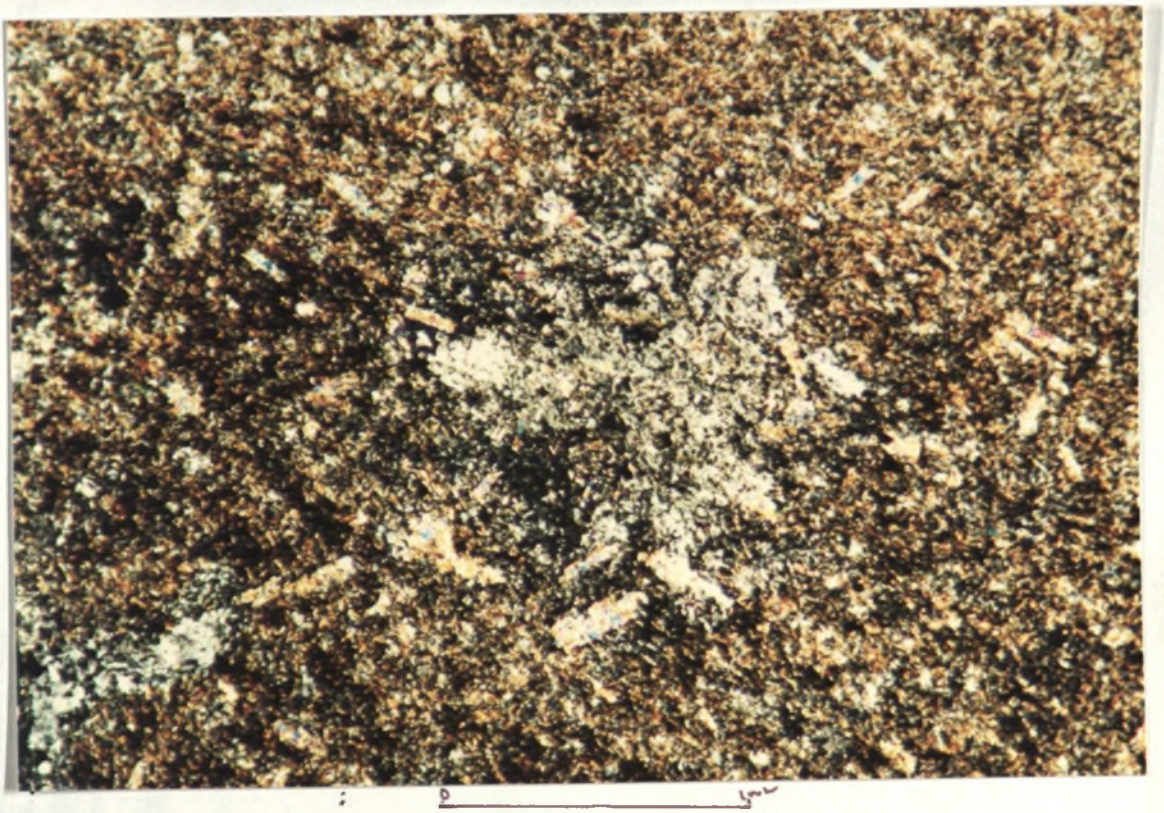

PLATE 3.3.2 : GRANOBLASTIC QUARTZ GRAINS IN THE PSAMMITIC BEDS ( MU46252 )

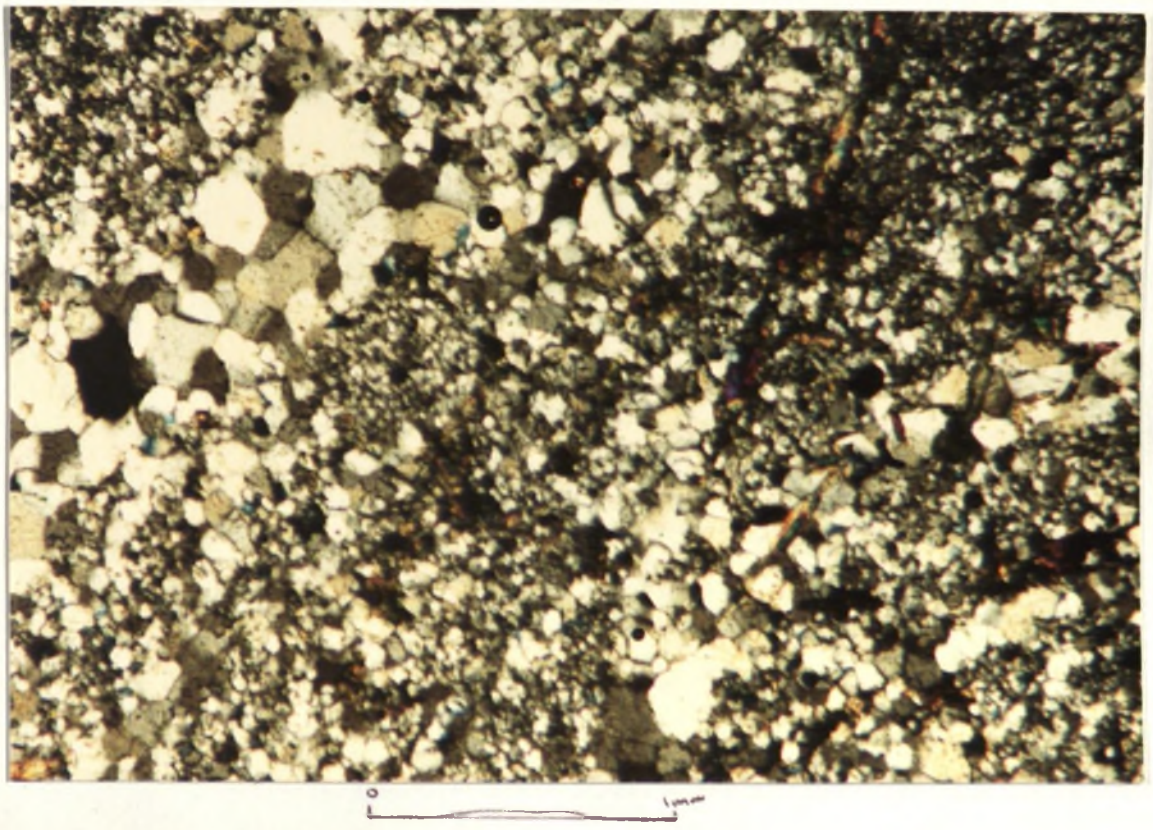

FIGURE 3.3.4 : SUMMARY DIAGRAM FOR THE METAPELITES IN THE AUREOLE OF THE GWYDIR RIVER ADAMELLITE.

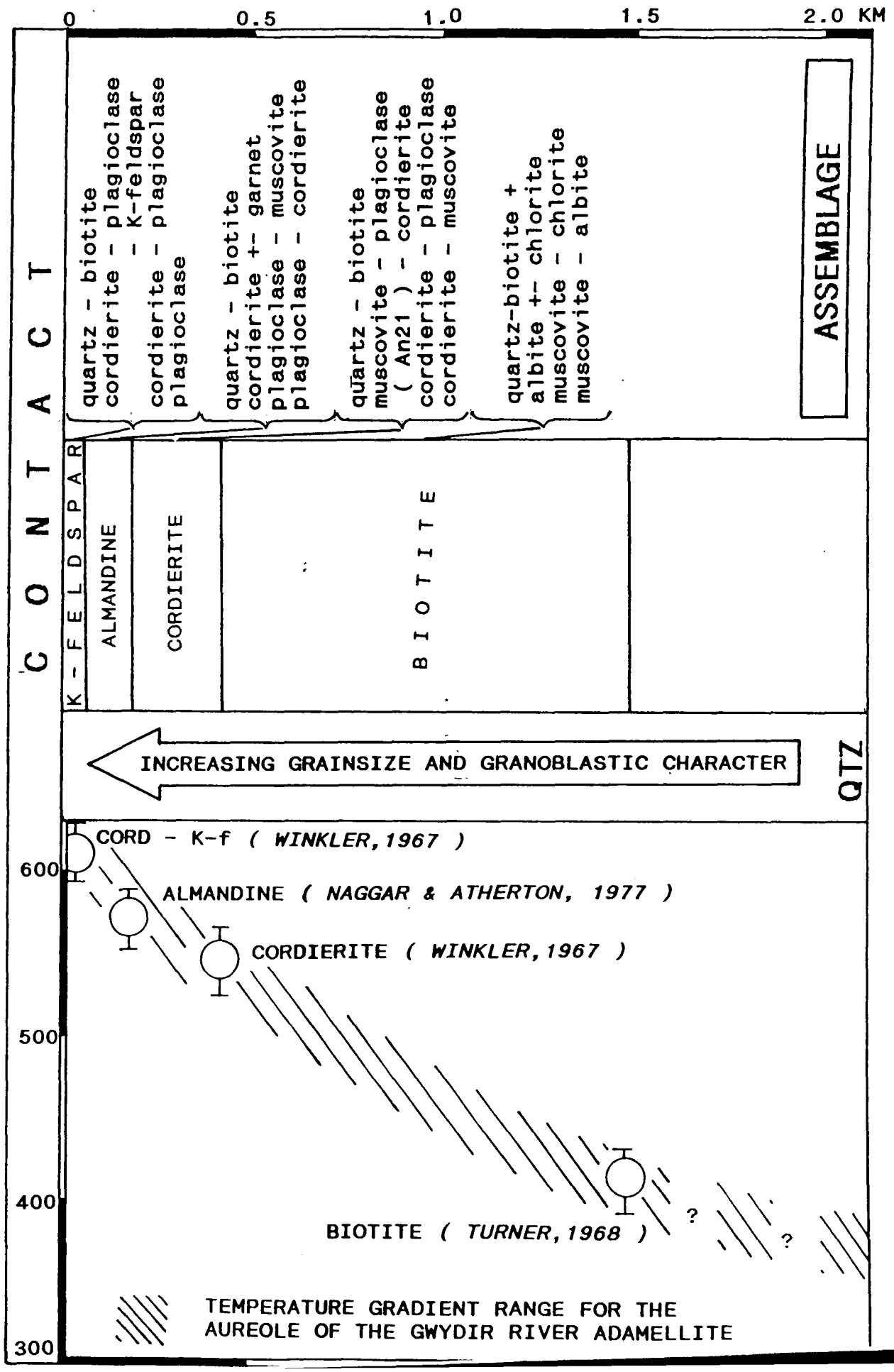

If this reaction is applicable for the cordierite - k-feldspar zone in the aureole of the Gwydir River pluton, then using Winkler's ( 1967 ) temperature estimates for this reaction, could place the immediate contact temperatures in the range 590 - 620 degrees C.

## 3 . 3 . 3 : ARENACEOUS METASEDIMENTS

Although the psammitic rocks contain biotite and less abundant muscovite, they do not seem to show the same metamorphic mineral index progression as the pelites. They do however show an obvious microstructural variation with grade. At the lowest grades the arenites have primary sedimentary microstructures but with contact metamorphic grade, the arenites become increasingly granoblastic with recrystallised polygonal quartz of variable grainsize (proportional to the original psammitic larger grain size, plate 3.3.2 ).

## 3 . 3 . 4 : SUMMARY

The metamorphic zonation of both pelitic assemblages and the arenaceous meta-sediments is outlined in figure 3.3.4 with the estimated temperature gradient with distance.

# B . CHAPTER 4 : CONTACT METAMORPHISM OF THE YARROWYCK GRANODIORITE

## B . 4 . 1 : K-FELDSPAR TRICLINICITY AND COMPOSITION

### 4 . 1 . 1 : TRICLINICITY OBSERVATIONS :

Measurements of triclinicity (Orville, 1963) for 77 microperthitic K-feldspar separates from the Permian Yarrowyck Granodiorite reveal a number of changes in structural state with decreasing distance to the younger Gwydir River intrusive contact (figure B.4.1a & b and maps 5 & 6).

Furthest from the contact with the Gwydir River Adamellite ( 1.0 km) the Yarrowyck Granodiorite has triclinicity values that lie between 0.0 and 0.3. A number of localised intermediate to high triclinicity areas were observed (0.5 to 0.7) at distances of 3 - 4 km from the contact (see maps 5 and 6) but these values are from samples known to contain microshear zones and will be discussed separately, as they are not characteristic of the overall Yarrowyck Granodiorite prior to contact metamorphism by the Gwydir River Adamellite.

With decreasing distance to the contact the generally low triclinicity of the Yarrowyck Granodiorite changes abruptly to high triclinicity within 500-1000m of the Gwydir River Adamellite (figure B.4.2) [1]. This zone of high triclinicity parallels the contact of the Gwydir River Adamellite from the Yarrowyck Granodiorite's northern to south western boundaries. This abrupt increase in triclinicity occurs over a distance of only 200 m. Within 350 m of the Gwydir River Adamellite's contact an abrupt drop occurs (figure B.4.2) from the high triclinicity zone (0.7 - 0.8) to zero triclinicity within 200 m of the Gwydir River intrusive contact. This change occurs over a distance of only 100 - 200m (see maps 5 and 6). The zero triclinicity zone also parallels and runs the length of the Gwydir River Adamellite's contact.

Triclinicity observations on a much smaller (centimetre) scale were made on 5 K-feldspar separates from an oriented sawn slab containing a shear zone in the regional triclinicity zone. Separates were made at increasing distances from this shear zone (figure B.4.7 and 8). Furthest from the shear,

---

[1] all sample numbers used in figures B.4.2 to 5 are preceded by MU461nn e.g38 = mu46138.

FIGURE B.4.1 : a) SKETCH MAP OF THE YARROWYCK GRANODIORITE TO SHOW COMPOSTIONAL TRAVERSES.
b) THREE DIMENSIONAL COMPUTED TRICLINICITY SURFACE FOR THE YARROWYCK GRANODIORITE

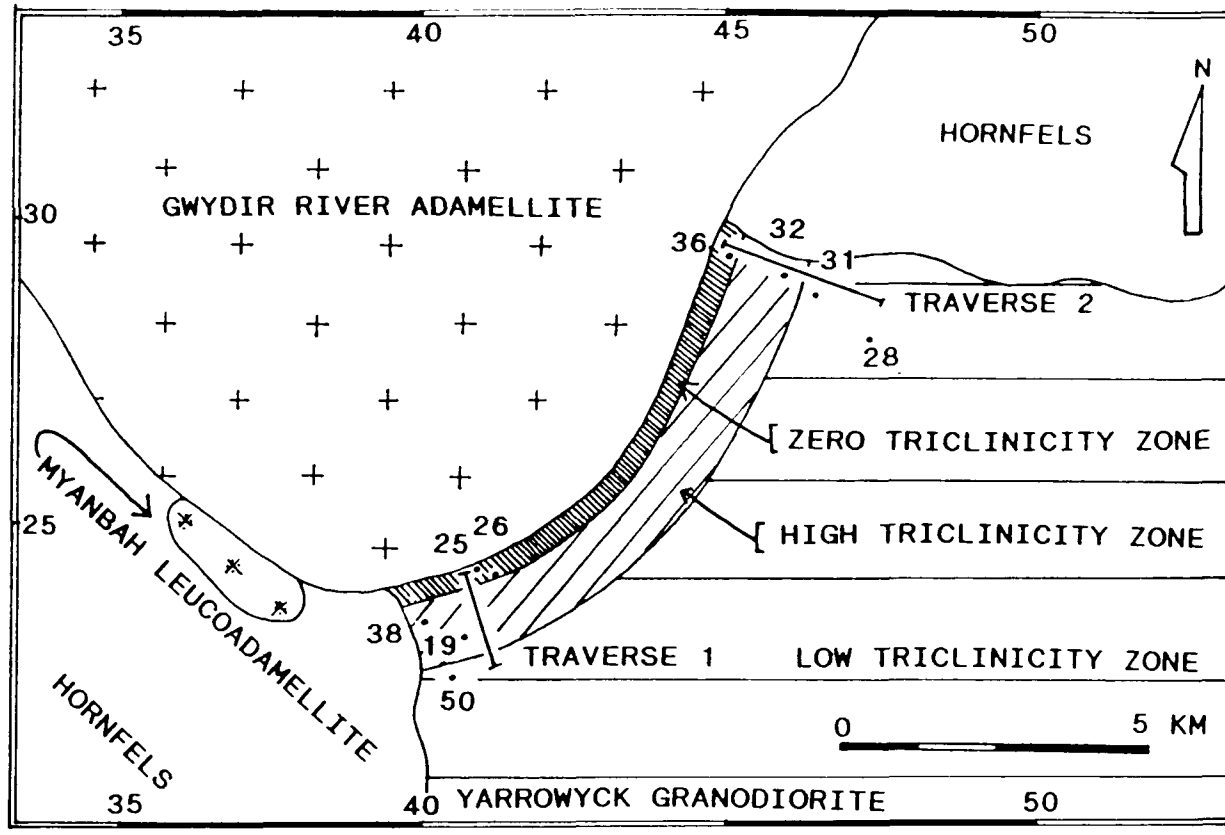


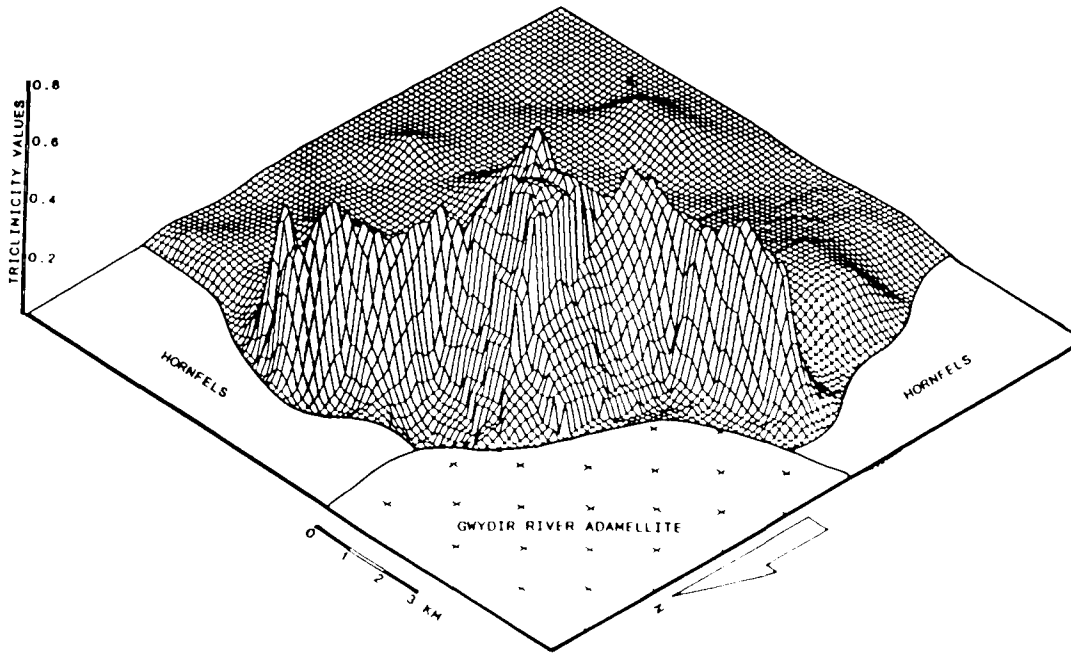

FIGURE B.4.2 : TRICLINICITY AGAINST DISTANCE FROM THE GWYDIR RIVER ADAMELLITE'S CONTACT FOR THE TWO TRAVERSES

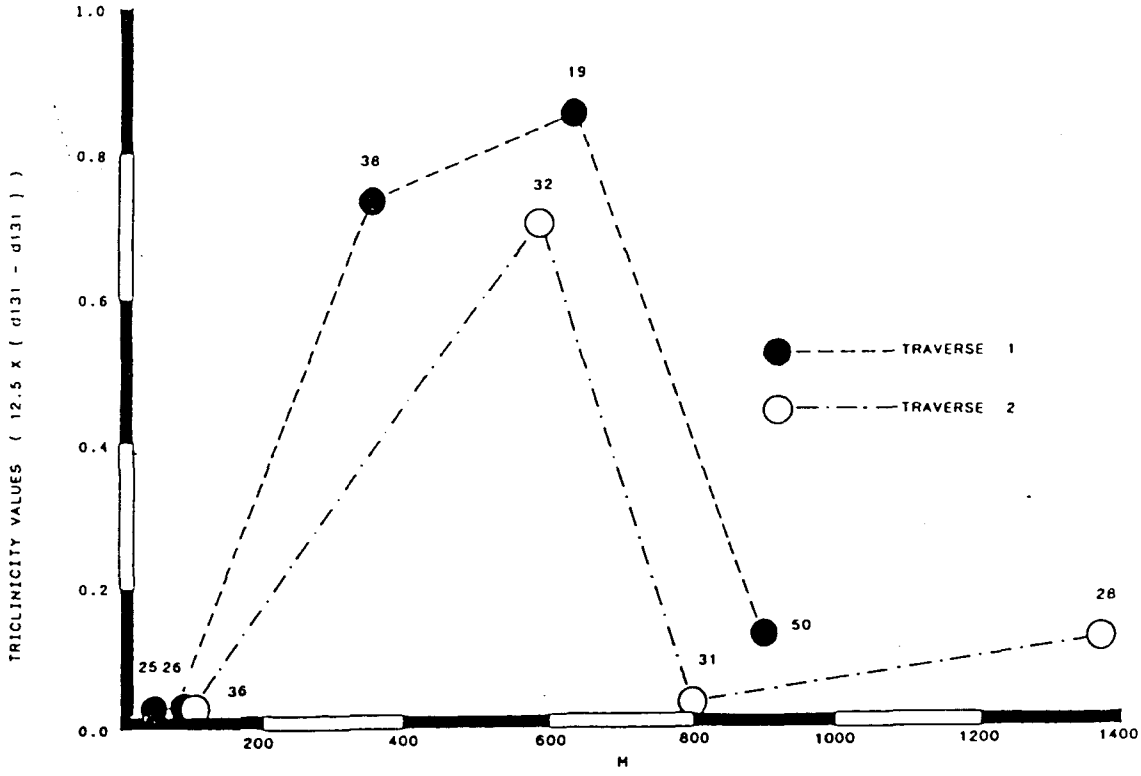


FIGURE B.4.3 : ALKALI EXCHANGE PATHS ( WRIGHT, 1968 ) FOR THE TWO COMPOSITIONAL TRAVERSES

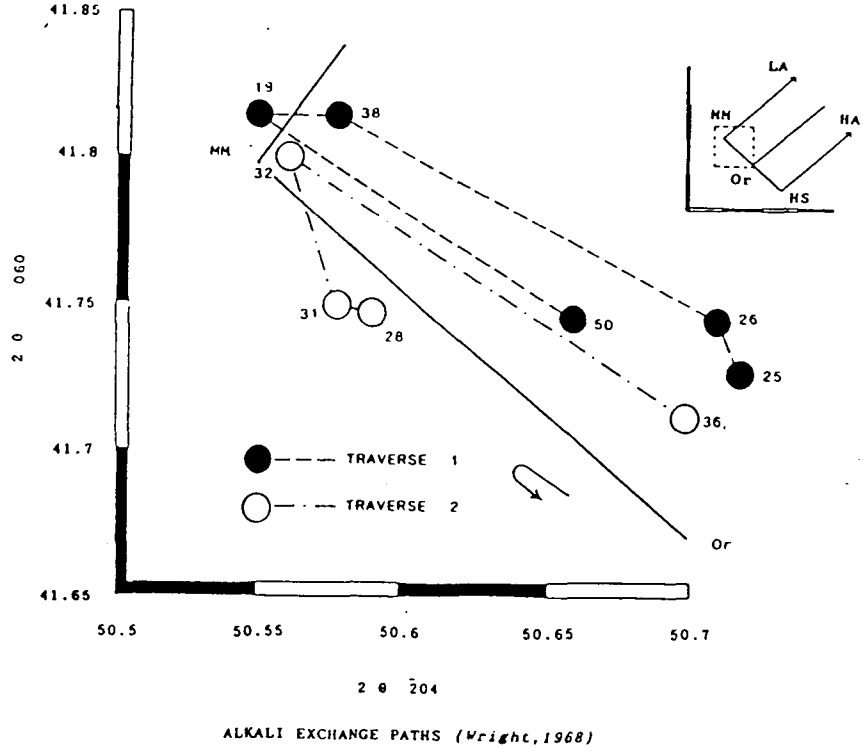

triclinicity values are comparable to those found throughout the Yarrowyck Granodiorite (0.0 - 0.2, at distances 1.5 km from the Gwydir River Adamellite's contact). However, within 5 cm of the shear zone the triclinicity shows a marked increase to a maximum triclinicity value of 0.5 on the shear plane itself. This microshear zone is discussed later.

## 4 . 1 . 2 : TRICLINICITY ZONAL DIVISIONS :

The triclinicity variation within the metagranite can be divided into 3 metamorphic zones (regional, high and low) and, defined in this way, are very similar to those documented in the Banalasta Adamellite, although zone widths are different. The Banalasta Adamellite has a high triclinicity zone from 1.5 to 4 km from the younger pluton's contact and a low triclinicity zone within 1 km of the contact. The Yarrowyck Adamellite however has a high triclinicity zone from 500 to 1000 m and a low triclinicity zone within 200m of the Gwydir River Adamellite's contact.

On the basis of these triclinicity zones, 9 K-feldspar samples from two traverses (figure B.4.1a) were then x-rayed again for the $\bar{2}04$, 060, $\bar{2}01$ peaks (expressed as an Ab %, Wright, 1967) (figures B.4.3 and 4) and estimated for their microcline - orthoclase mix proportions (figure B.4.5) based on the mix series developed for near maximum microcline (triclinicity = 0.833) from the Banalasta Adamellite. Thus an examination of composition change in the Yarrowyck Granodiorite's alkali feldspars wihtin the contact aureole of the Gwydir River Adamellite, is also undertaken.

The regional zone ( 1.0 km from the Gwydir River Adamellite's contact) may be delineated by K-feldspars consistantly containing a subequal mix of microcline with low triclinicity ( 0.3) and orthoclase. The zone is characterised by low triclinicity microcline - low to intermediate albite (LM - LIA) microperthitic K-feldspar (fig. B.4.3), with a composition of Ab 2-20 (fig. B.4.4) and a predominance of orthoclase (Mi 0 - 30 Or 70 - 100) (figure B.4.5).

The high triclinicity zone from 500 up to 1000m from the later intrusive contact is characterised by highly ordered microcline (triclinicity = 0.7 - 0.82). The plot of 2θ's for the 060, $\bar{2}04$ and $\bar{2}01$ reveal this zone to contain near maximum microcline - low albite (MM - LA) microperthitic K-feldspar (figure B.4.3) containing a composition of Ab 0 -10 (figure B.4.4) and estimates from the mixing series reveal a microcline - orthoclase proportion of Mi 80 - 100 Or 0 - 20(figure B.4.5).

The zero to very low triclinicity zone adjacent to the contact with the Gwydir River Adamellite and of width 100 - 350m is characterised by a mix of highly disordered microcline (triclinicity 0.2) and orthoclase (triclinicity = 0.0). Plots of the 2θ values of 060 vs $\bar{2}04$ and $\bar{2}01$ indicate an orthoclase-intermediate albite (Or - IA) microperthitic

FIGURE B.4.4 : ALBITE CONTENT IN COMPOSITIONAL ORTHOCLASE AGAINST DISTANCE FROM THE CONTACT

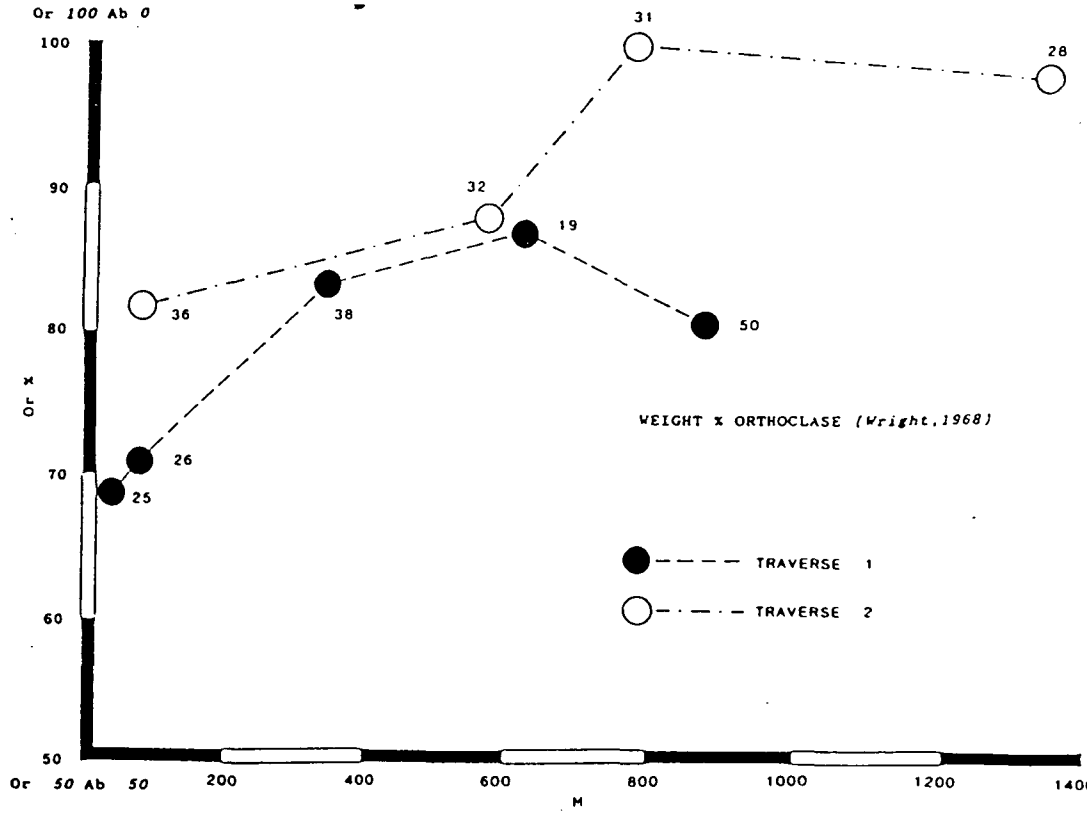


FIGURE B.4.5 : ESTIMATED MICROCLINE TO ORTHOCLASE PROPORTION AGAINST DISATNCE FROM THE CONTACT, BASED ON THE NEAR MAXIMUM MICROCLINE - ORTHOCLASE MIX SERIES PROPOSED IN PART A.

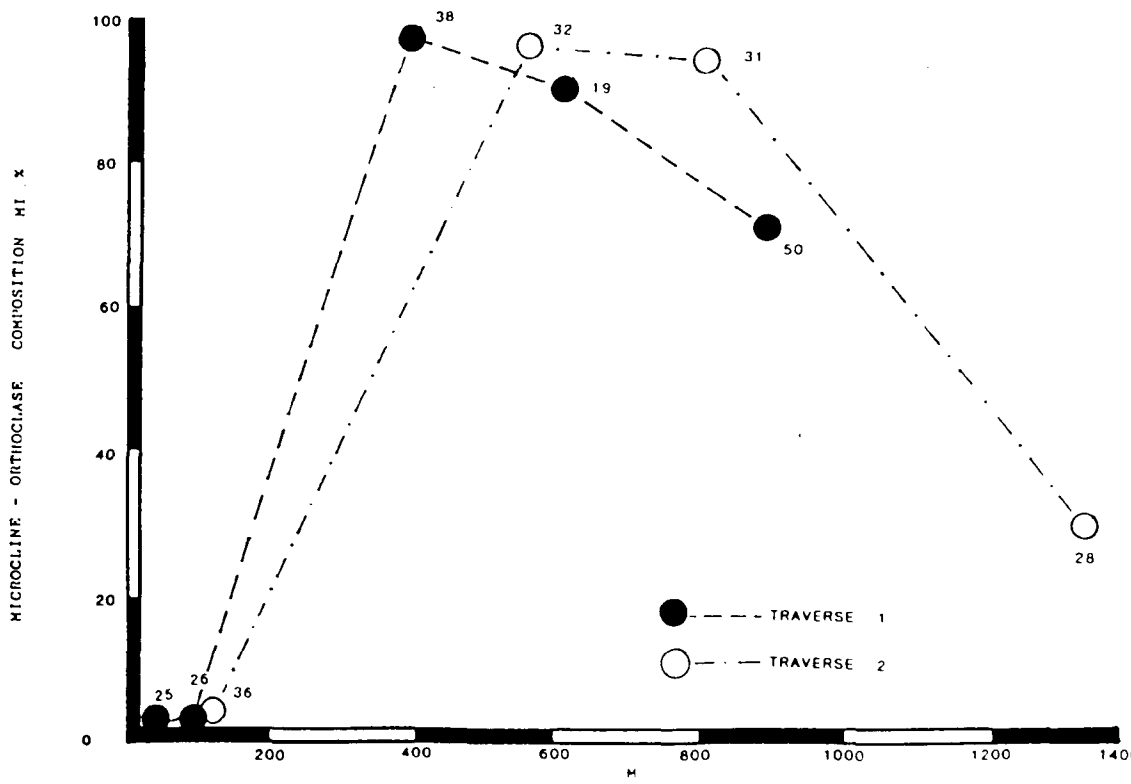

FIGURE B.4.6 : SUMMARY DIAGRAM FOR K-FELDSPARS IN THE YARROWYCK GRANODIORITE.
( ESTIMATE OF TEMPERATURE TAKEN FROM Or % VS TEMPERATURE PLOT IN A.4.1 )

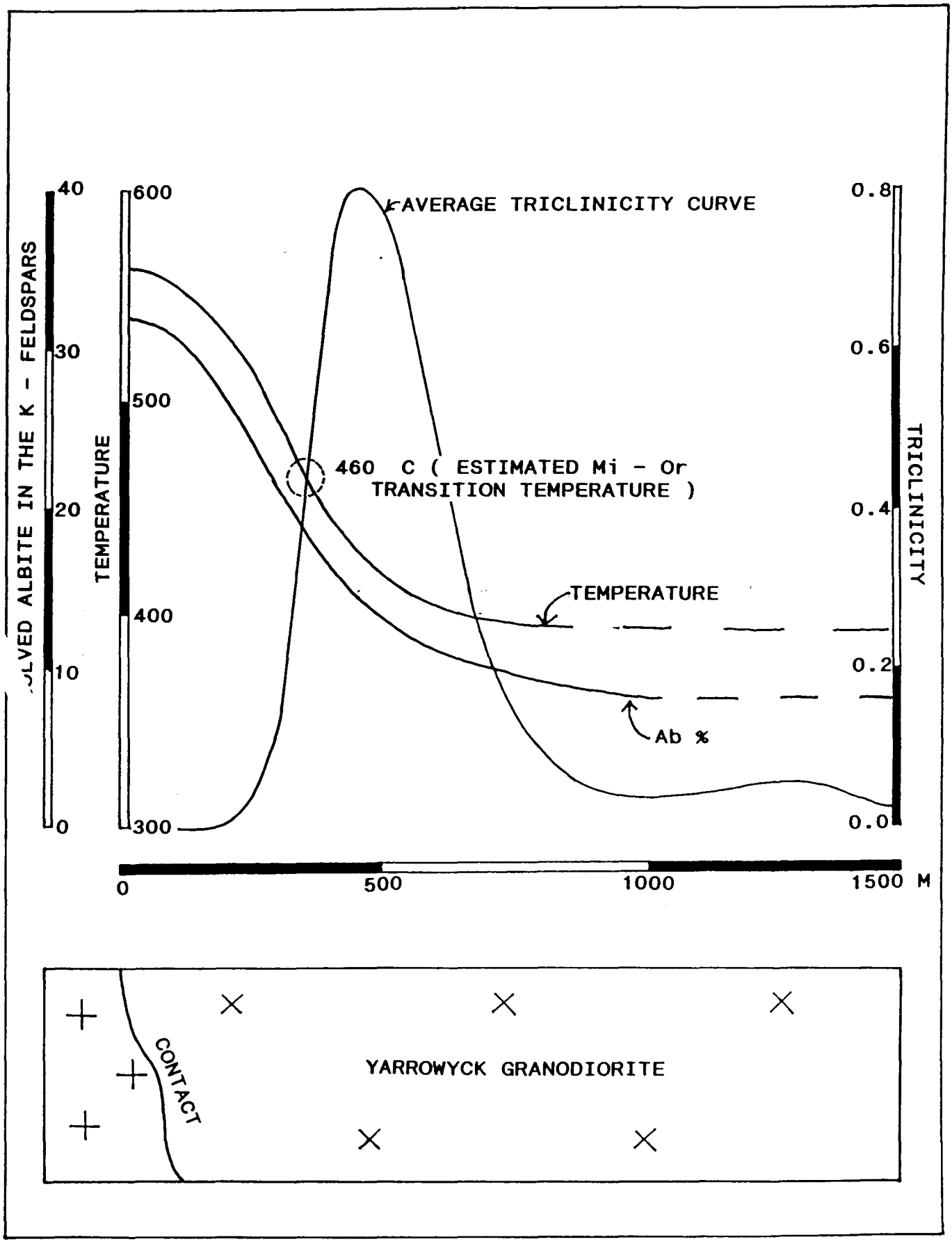

K-feldspar (figure B.4.3) containing compositions of Ab 30-20 (fig. B.4.4) and an estimated K-feldspar proportion of Mi 0 Or 100 (figure B.4.5).

## 4 . 1 . 3 : MODELLING OF THE YARROWYCK GRANODIORITE'S TRICLINICITY :

The rise to a narrow high triclinicity zone in the Yarrowyck Granodiorite may correlate with increasing strain (and less importantly temperature) during emplacement of the Gwydir River Adamellite. Likewise the disordering of microcline to orthoclase is caused by the thermal (contact) metamorphic effects as outlined by Hart (1961), Steiger and Hart (1967), Wright (1967), Tilling (1968) and Gorbatchev (1972). This disordering due to higher temperatures would not reveal the high strains in this zone as found in the colder high triclinicity zone.

An originally orthoclase bearing granodiorite developed a localised low triclinicity microcline-orthoclase mix due to post-crystallisation deformation (evident by the pervasive microshear zones in the Yarrowyck pluton (fig. B.4.7 )). With the emplacement of the Gwydir River Adamellite this regional triclinicity was ordered (in a narrow zone parallel to the later intrusives contact) to near maximum microcline due to strains accompanying the intrusion of the Gwydir River Adamellite. The contemporaneous thermal disordering of microcline to orthoclase caused by higher temperatures closer to the contact, resulted in continual annealling out of the emplacement induced strain. As outlined in Part A, the deformational effects favour high triclinicities, whereas the penecontemporaneous thermal annealling (at temperatures above 400 degrees celcius : Wright, 1968) closer to the contact favours low to zero triclinicity, thus producing the zones observed. This triclinicity history is summarised in figure B.4.6.

## 4 . 1 . 4 : TRICLINICITY VERSUS DISTANCE FROM A SHEAR ZONE

As has been mentioned 5 K-feldspar separates at varying distances from a shear zone in a sawn slab were measured for triclinicity (figures B.4.7 and 8). The triclinicity increases with proxixity to the shear zone and this would confirm the four anomalous triclinicity values observed in the regional zone which are all samples containing such shear zones. If these shear-related samples are omitted the resulting triclinicity map would show a much higher degree of uniformity in the regional triclinicity zone.

The observation of triclinicity being a function of proximity to a shear zone is not new, Gorbatchev (1972) observed a high triclinicity value in his specimen (J65/138T) which had been subjected to strong post-intrusive shearing deformation. Nilssen and Smithson (1965) observed that for the Herefoss Granite, many of the samples containing mostly maximum microcline were found along fault zones. In addition both Binns (1966) and Flood (1971) observed a common association of maximum microcline with shear zones. This is true of the Yarrowyck Granodiorite, however only intermediate microcline was observed, although one sample (containing a shear zone) had a triclinicity value of 0.72. This intermediate microcline may be due to the shear zones being very narrow ( 2 cm maximum) and only

FIGURE B.4.7 : SKETCH OF THE SAWN, ORIENTED SLAB CONTAINING THE MICROSHEAR ZONE, SHOWING SAMPLE SPACING.

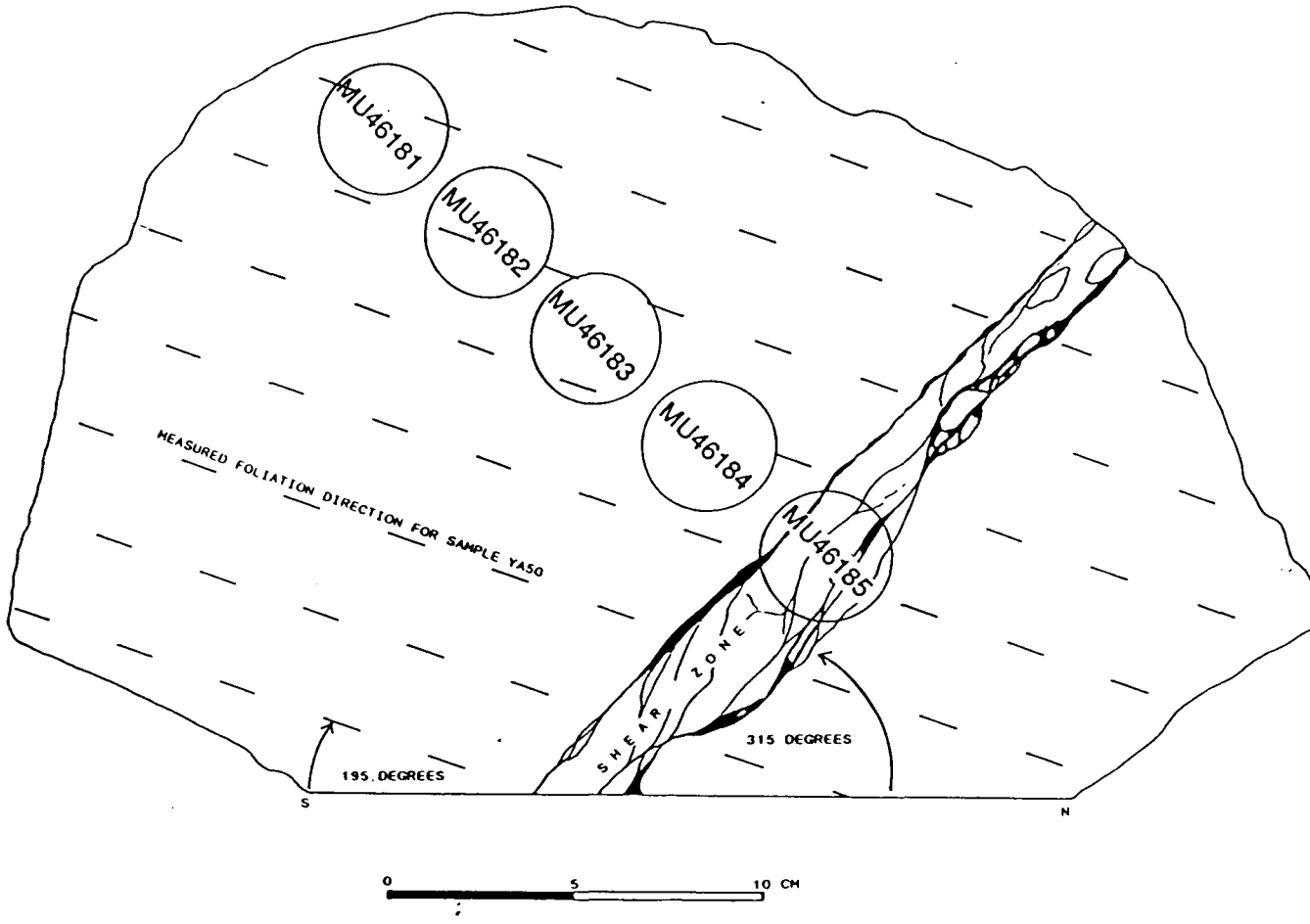


FIGURE B.4.8 : TRICLINICITY VERSES DISTANCE FROM THE SHEAR ZONE IN THE YARROWYCK GRANODIORITE.

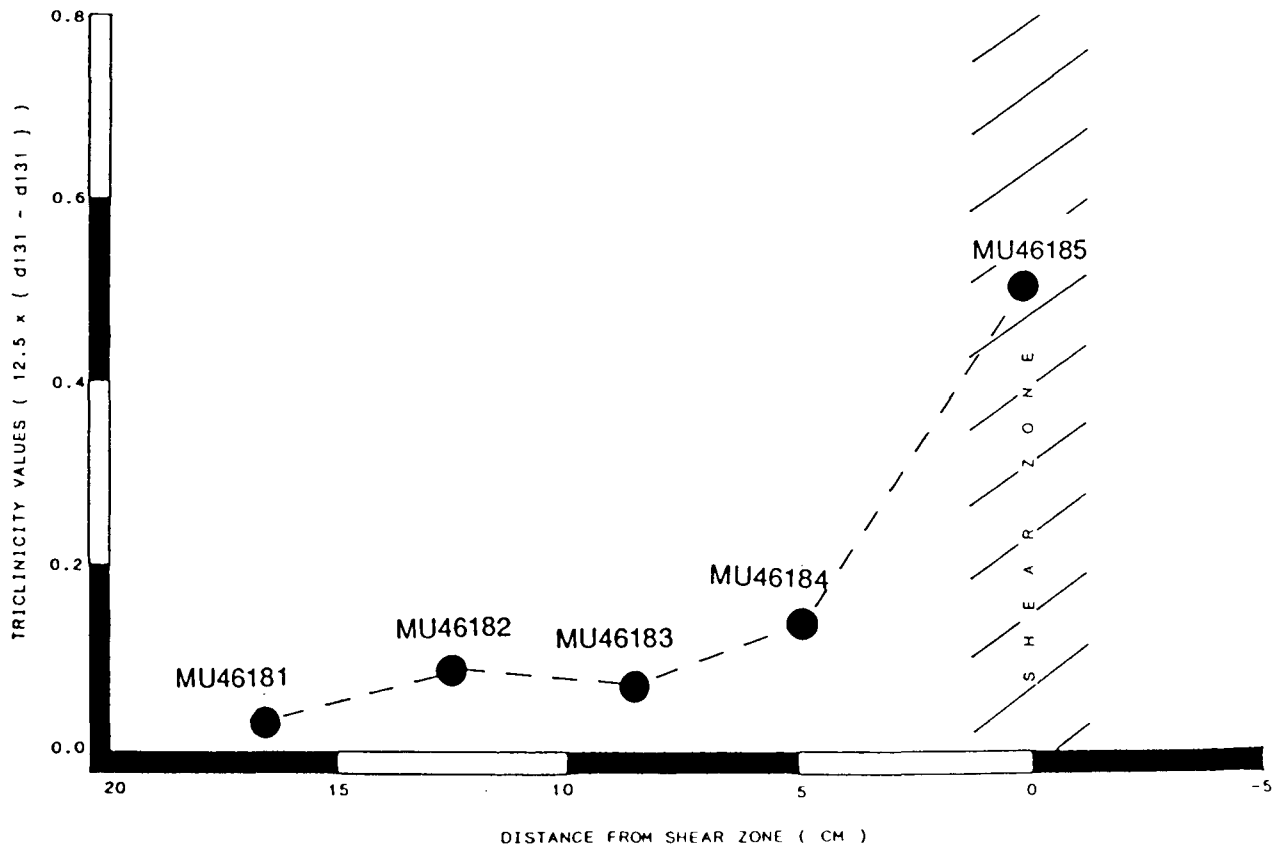

displacing small distances ( 3 m maximum) whereas those faults observed by others are on a kilometre scale. However, it is significant that even such small shear zones of limited displacement are sufficient to induce a K-feldspar ordering in the sheared granodiorite. These microshear zones prove to be of interest and would be worthy of further investigation at a later date, however this investigation arose as a sideline to the main aims of this thesis and has not been pursued due to time constraints.

# B . 4 . 2 MICROSTRUCTURAL RESPONSE OF THE YARROWYCK GRANODIORITE

## 4 . 2 . 1 : INTRODUCTION

A petrographic study of the Yarrowyck Granodiorite reveals a microstructural zonation that (like the Banalasta Adamellite, part A) correlates well with the triclinicity zonation outlined in the previous section. The same nomenclature of regional ( 1000m from the Gwydir River Adamellite's contact), low (350 - 1000m) and high ( 350m) grade metamorphic zonation is used here and corresponds to the regional, high and zero triclinicity zones outlined in the preceeding section.

## 4 . 2 . 2 : POTASSIUM FELDSPAR

Furthest from the contact in the regional zone, all the K-feldspars are either orthoclase or faintly twinned low microcline and occur as interstitial grains in a typical magmatic granitoid microstructure. Closer to the contact in the low grade zone, microcline is abundant and shows cross-hatch twinning throughout the grains, although plate 4.2.1 also shows an untwinned domain suggestive of incomplete ordering. Closest to the contact in the high grade zone, potassium feldspars are all orthoclase and no residual areas of crosshatch twinning were observed. The most significant microstructural variation in the K-feldspars in this high grade zone is recrystallisation along pre-existing grain boundaries which is absent in other zones. Plates 4.2.2 - 4 depict a number of areas where fine grains have crystallised at grain margins. Plate 4.2.2 shows recrystallised grain development between two orthoclase grains, where once sutured grain boundaries have resulted in reoriented bulge nucleated new grains. Plate 4.2.3 emphasises that this recrystallisation is not only marginal to K-feldspar grains but has occured within the large grains themselves.

## 4 . 2 . 3 : PLAGIOCLASE

Plagioclase in the Yarrowyck Granodiorite occurs as subhedral medium size grains (1 - 5 mm), shows simple and multiple growth twins, typical igneous microstructures and an absence of misorientations and deformation twins. The low grade zone reveals higher abundances of misoriented and rotated grains (plate 4.2.5) and deformation twins (plates 4.2.6 and 7). Only very limited rim recrystallisation and suturing was observed, and can be seen in plates 4.2.6 and 7 on the margins of the deformed plagioclases. No bent or kinked twins were detected. These features may well suggest that although this zone has been deformed enough to induce the ordering of the K-feldspar, the deformation has had little effect upon the plagioclase feldspars.

The highest grade zone shows some deformation twins (plate 4.2.2), but is essentially characterised by rim recovery and recrystallisation of grains. In both plates 4.2.2 and 3 recrystallised grains are present adjacent to twinned plagioclase grains. The fact that some deformation features do exist in this zone but are in low abundance compared

PLATE 4.2.1 : ORDERED MICROCLINE SHOWING CROSSHATCH TWINNING AND AN UNTWINNED DOMAIN ( TOP RIGHT ) ( MU46103 )

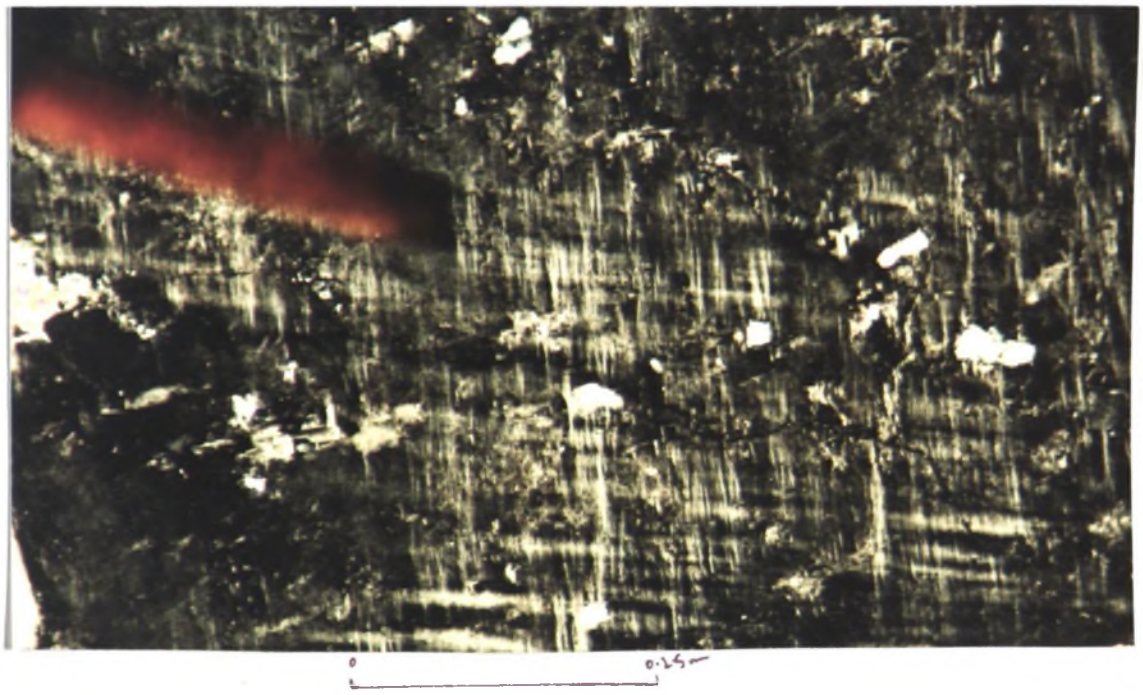

PLATE 4.2.2 : RECRYSTALLISATION AT ONCE SUTURED ORTHOCLASE GRAIN BOUNDARIES, RESULTING IN REORIENTED BULGE NUCLEATED GRAINS. ( MU46135 )

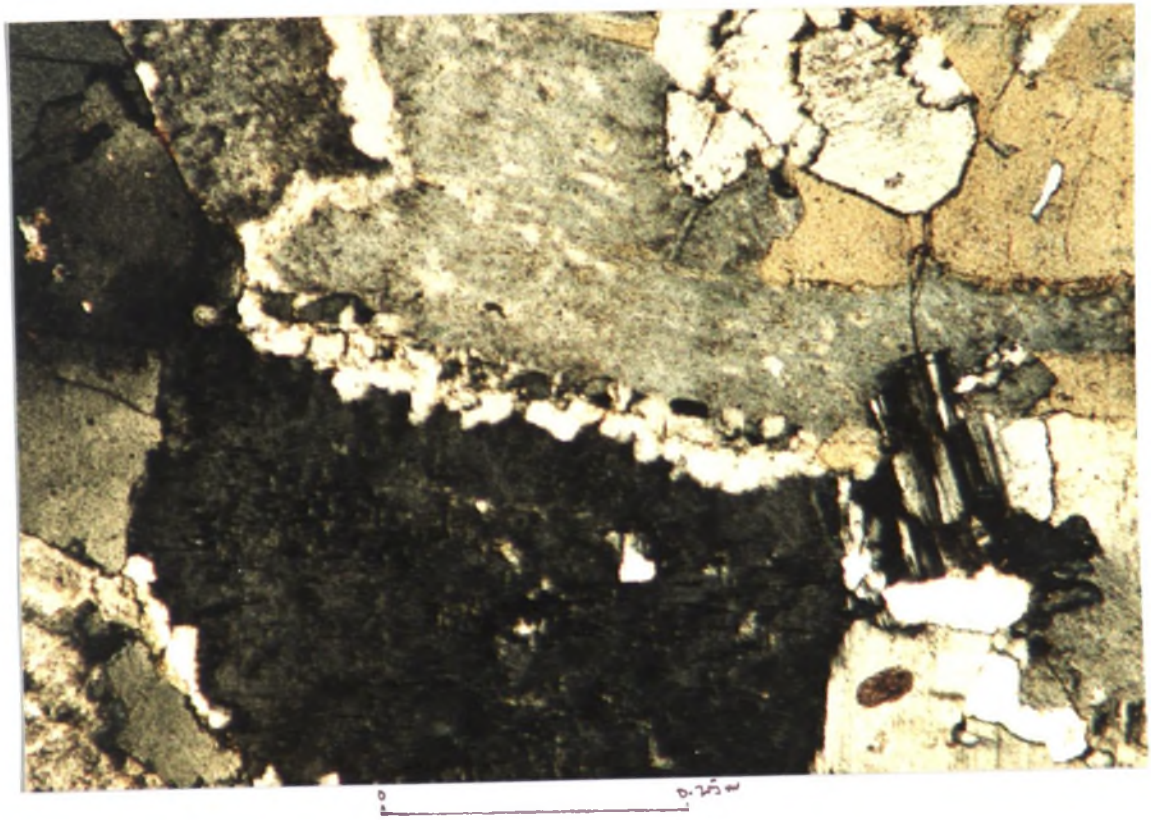

PLATE 4.2.3 : INTERNAL K-FELDSPAR RECRYSTALLISATION PLANE PARALLEL TO PERTHITE LAMELLAE, PLAGIOCLASE INCLUSIONS SHOWING SUTURED GRAIN BOUNDARIES ALSO. ( MU46135 )

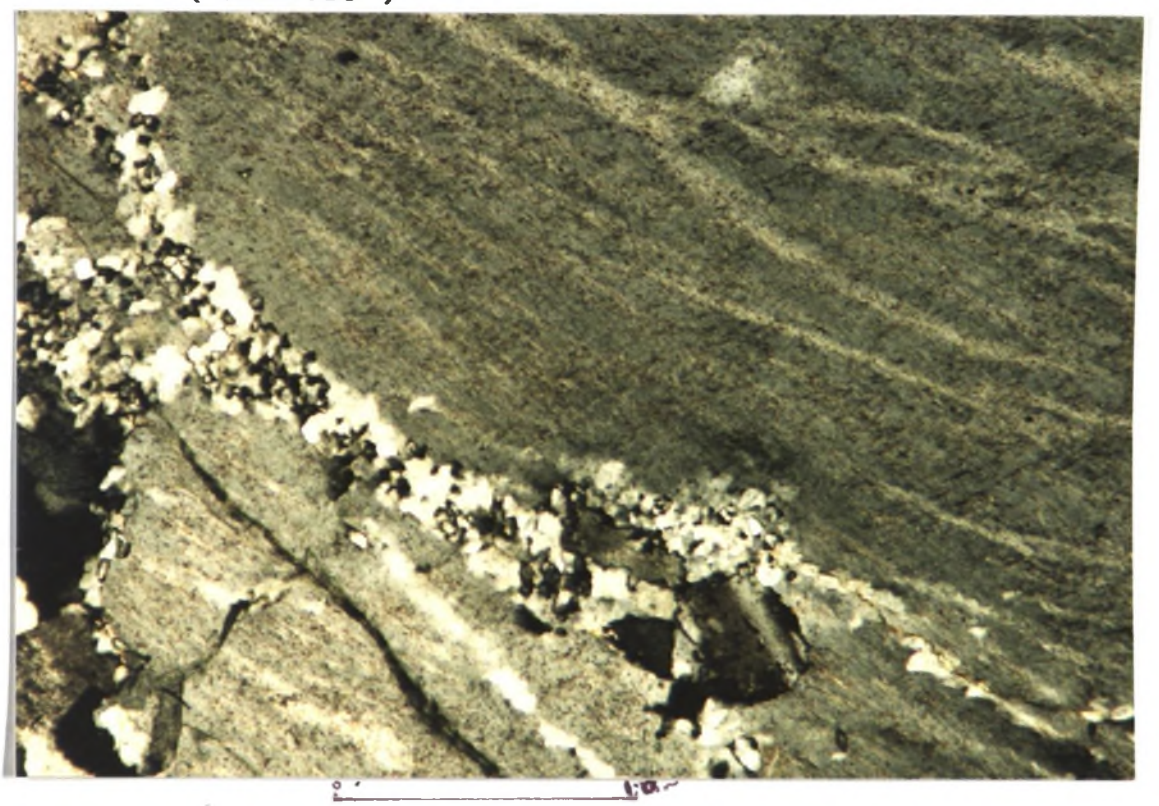

PLATE 4.2.4 : K-FELDSPAR RIM RECRYSTALLISATION SHOWING LOCALLY WELL DEVELOPED THICK RIMS ( 1/3 THE GRAIN RADIUS ) ( MU46126 )

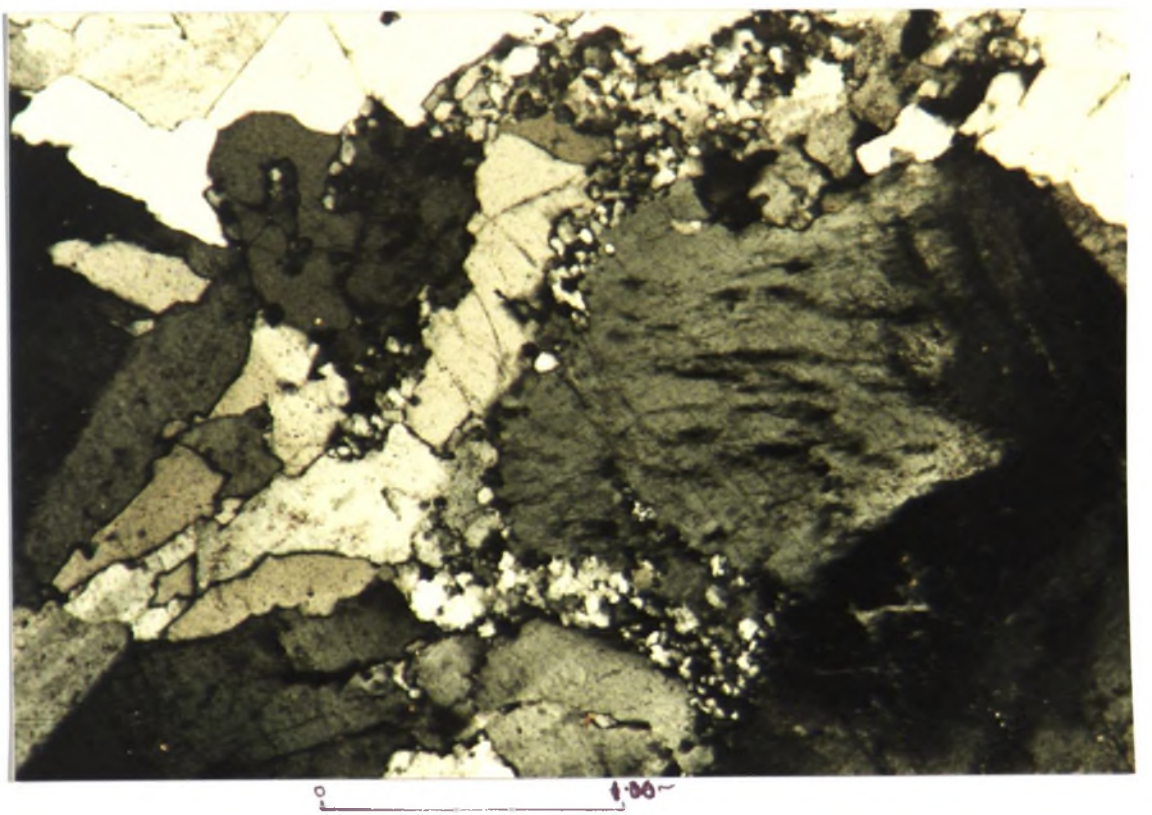

PLATE 4.2.5 : MISORIENTATED AND ROTATED PLAGIOCLASE GRAINS
( MU46119 )

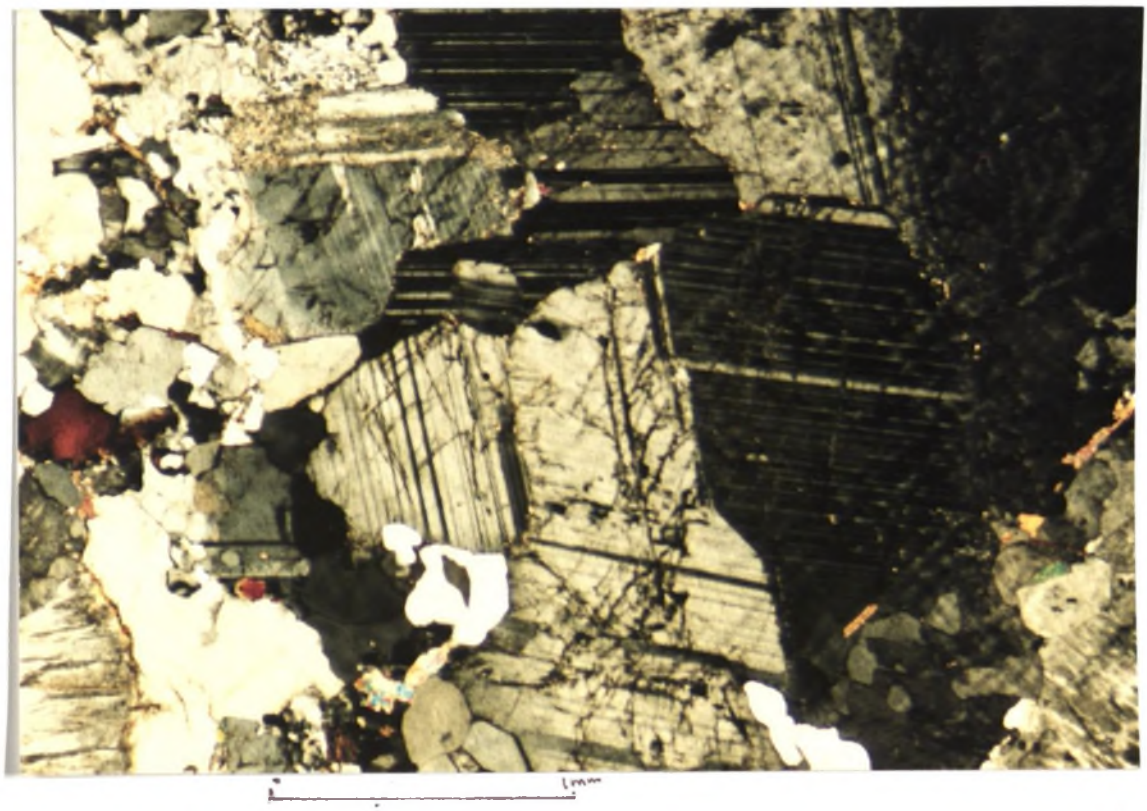


PLATE 4.2.6 : DEFORMATION TWINS IN PLAGIOCLASE ( MU46119 )

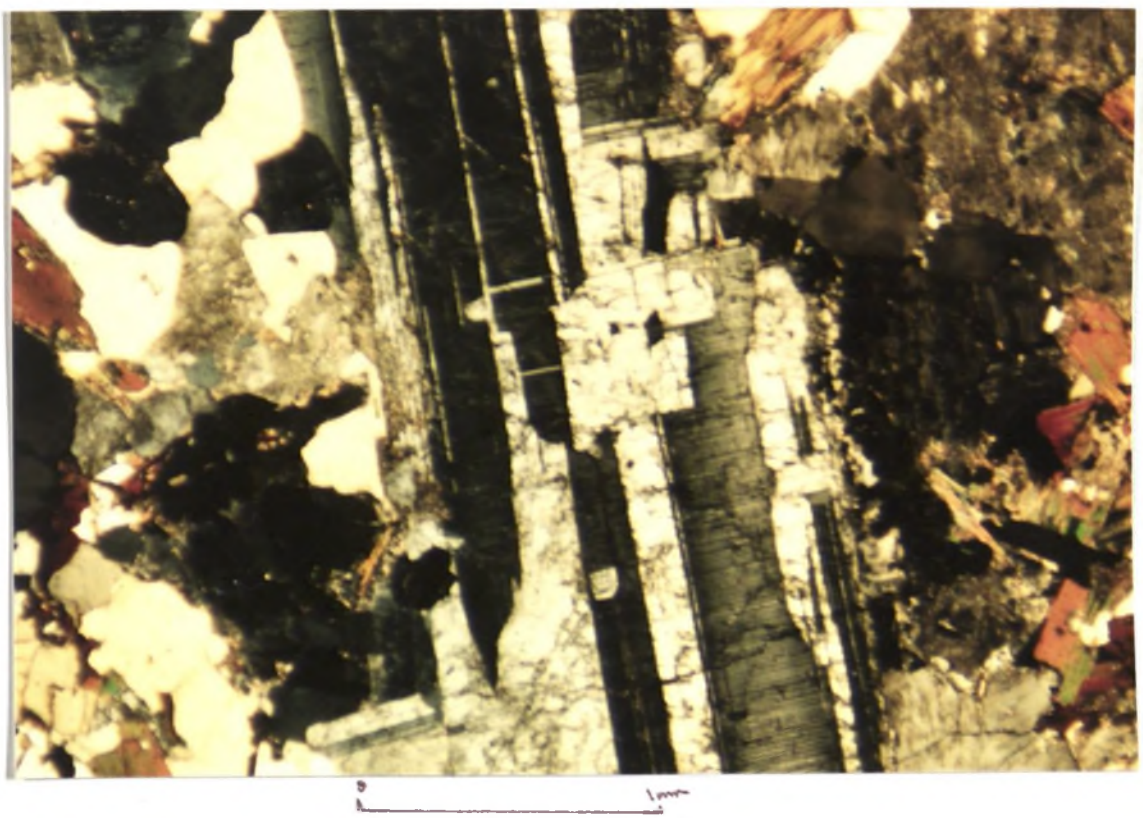

PLATE 4.2.7 : SHARP TAPERING DEFORMATION TWINS IN PLAGIOCLASE FELDSPAR ( MU46123 )

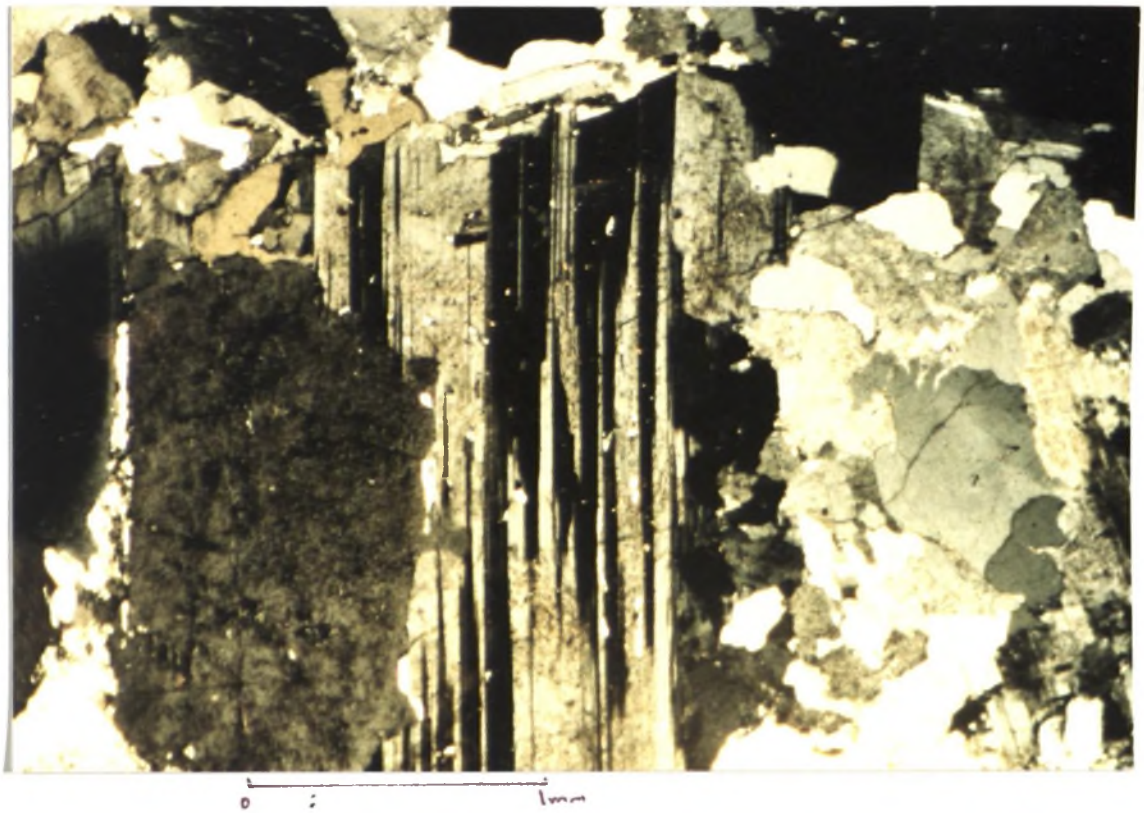


PLATE 4.2.8 : LARGE QUARTZ AGGREGATE CONTAINING GRAINS WITH WELL DEVELOPED MIGRATIONAL BOUNDARIES ( MU46104 )

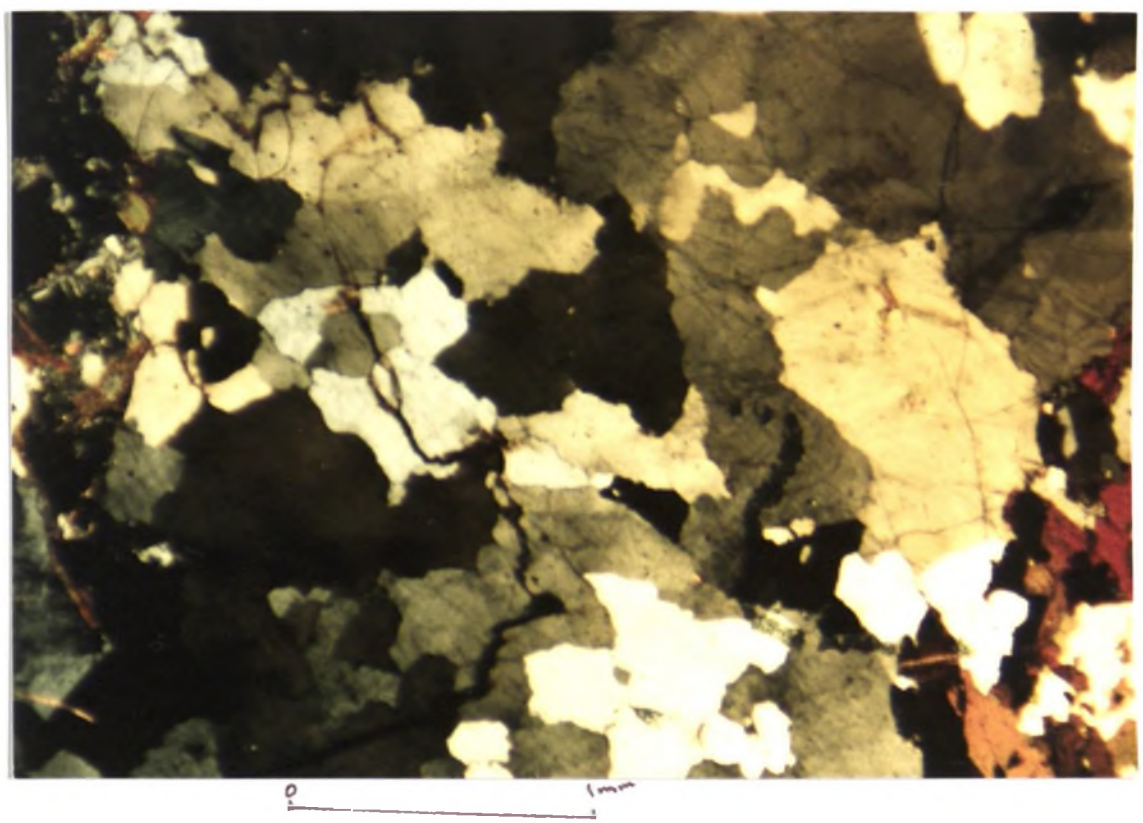

PLATE 4.2.9 : INDIVIDUAL QUARTZ GRAIN SHOWING BANDED EXTINCTION AND WELL DEVELOPED BULGE NUCLEATION ( MU46123 )

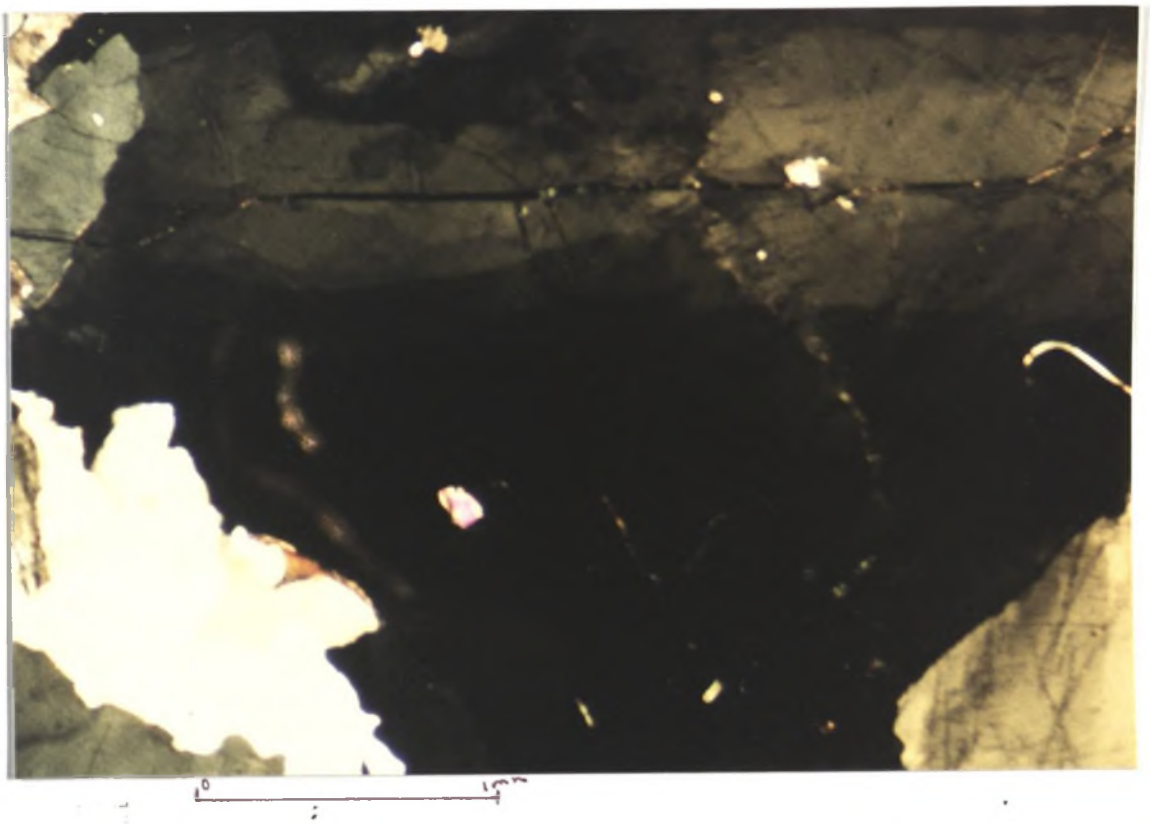


PLATE 4.2.10 : BANDED EXTINCTION IN QUARTZ AND BULGE NUCLEATION NEAR COMPLETION ( BOTTOM RIGHT OF CENTRE ) AND AT COMPLETION IN THE BOTTOM CENTRE ( MU46145 )

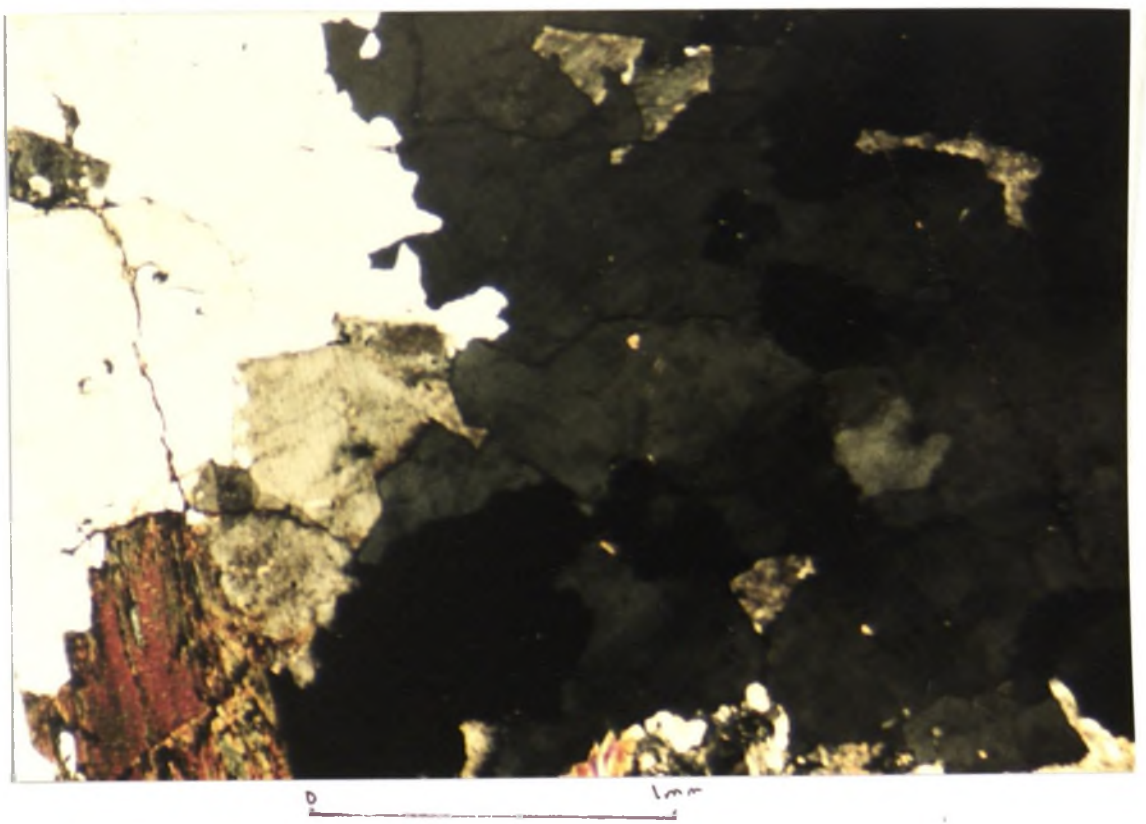

PLATE 4.2.11 : INTERGRANULAR QUARTZ RECRYSTALLISATION WELL DEVELOPED AT ONCE SUTURED GRAIN BOUNDARIES ( MU46125 )

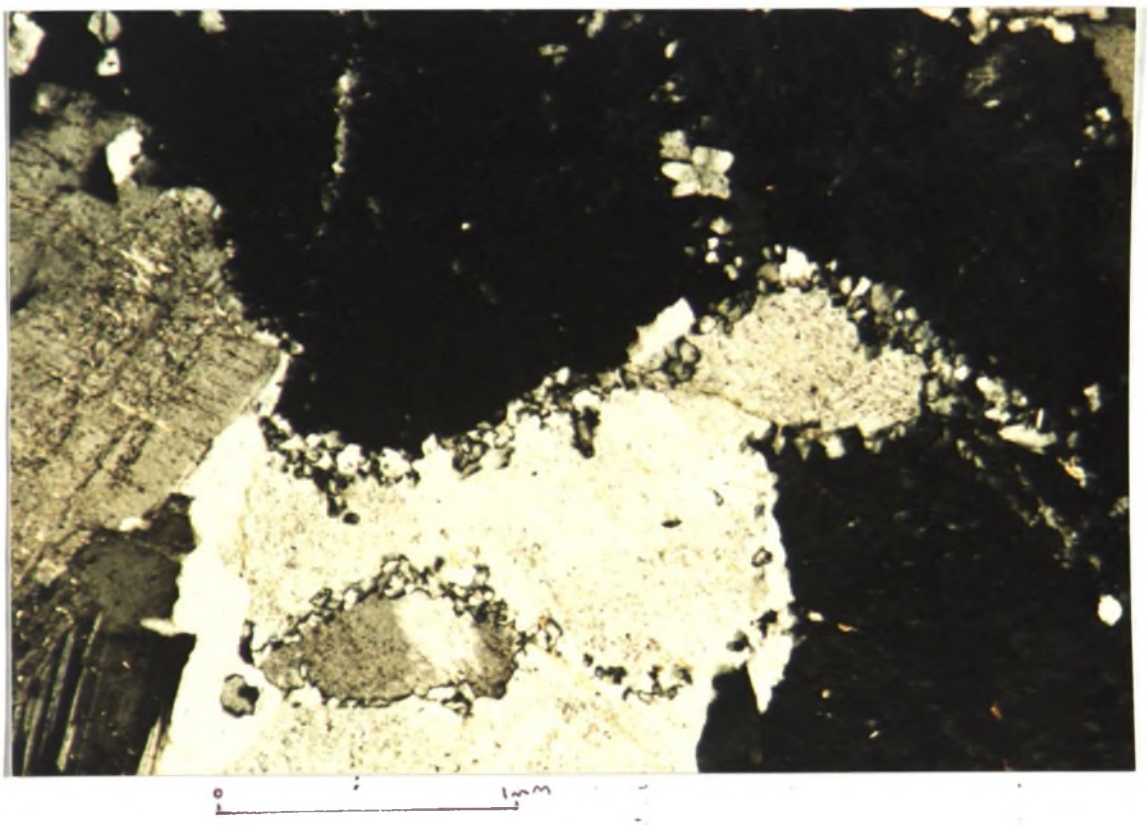


PLATE 4.2.12 : CLUSTERING OF RECRYSTALLISED GRAINS AT A QUARTZ - K-FELDSPAR GRAIN BOUNDARY NEW GRAINS SHOW COMPLETE EXTINCTION AND NO STRAIN ( MU46102 )

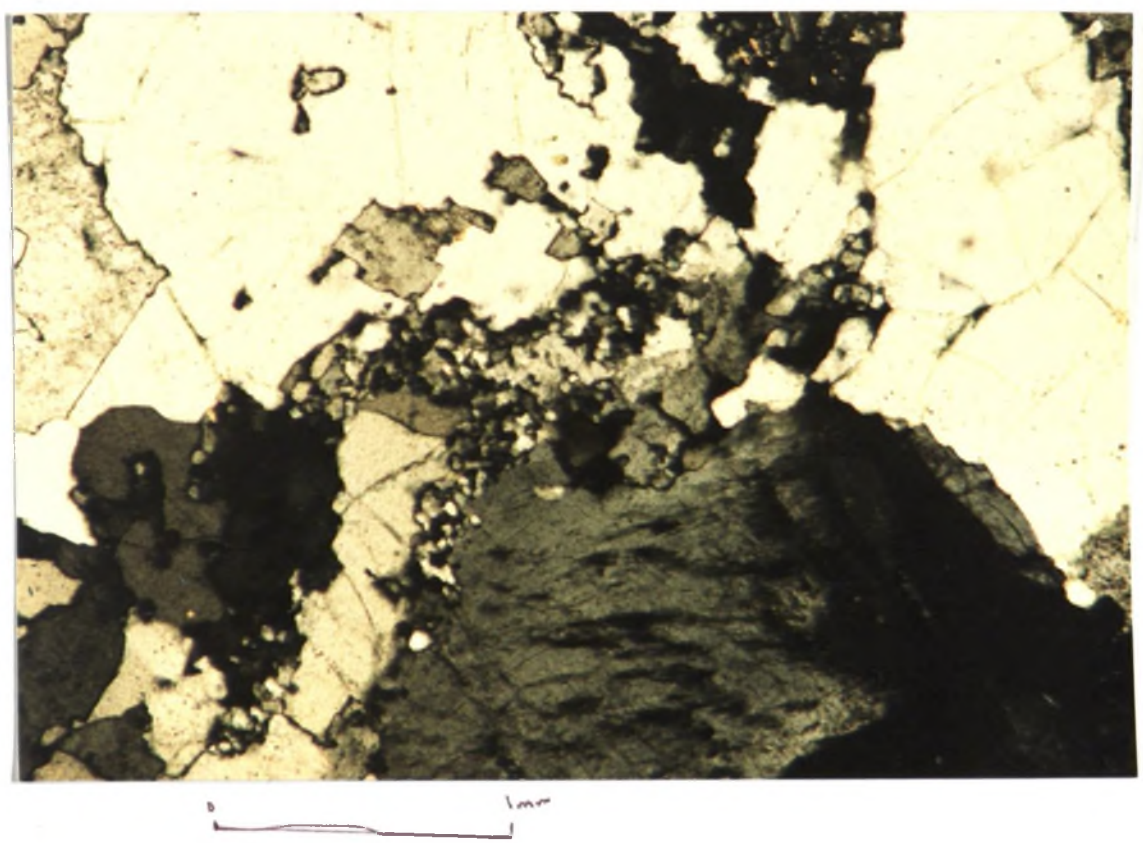

to recovery and recrystallisation microstructures might imply that the strain that occured in the low grade zone, although present in the high grade zone, is annealled by higher temperatures nearer the intruding pluton.

### 4 . 2 . 4 : QUARTZ

Quartz in the regional zone shows weakly developed undulose extinction, interstitial grain boundaries and no evidence of any high strain related microstructures. The low grade zone shows extremely high abundances of sutured grain boundaries and subgrain boundaries in both quartz aggregates (plate 4.2.8) and individual grains (plates 4.2.9 and 10). No evidence has been observed for any pressure shadow surfaces or creep deformation and thus sutured grain boundaries are likely to be a result of grain boundary migration and bulge nucleation (Vernon, 1976). Plate 4.2.8 shows a large quartz aggregate where grain boundary migration is evident. Plates 4.2.9 and 10 show individual quartz grains where bulge nucleation is evident at the lower bottom left of plate 4.2.9 and at completion with a separated, still optically continuous new grain in the bottom central right of plate 4.2.10.

In the high grade zone recrystallised quartz grains are more common. Plates 4.2.11,12 and 4 all demonstrate that once sutured intergranular grain boundaries have become zones of recrystallised quartz. The majority of these recrystallised quartz grains have uniform extinction and are granoblastic. Plate 4.2.11 shows that recrystallised grains have also developed along original subgrain boundaries.

### 4 . 2 . 5 : BIOTITE

Biotite in the regional zone shows no evidence of bending, kinking or recrystallisation and again shows intergranular reltionships typical of a granitic micrstructure. In the low grade zone, many biotite grains show low angle ( 15 degrees) warps and bends evident in the bent 001 cleavage and patchy extinction (plate 4.2.13). This would imply strains were insufficient to produce significant bending or to initiate kinking and that although a deformation was present it was of low magnitude.

In the immediate contact zone the biotites maintain the low angle bends and warps but are less common. No biotite recrystallisation has been observed, however some quartz grain boundaries do noticeably abutt biotite at high angles (70 - 80 degrees on average) suggesting re- equilibration to attain lower surface energy interfaces.

### 4 . 2 . 6 : MYRMEKITE

Myrmekite in the regional zone occurs as bleby - vermicular intergrowths in thin rims and only traces of lobes extending into K-feldspar grains. Phillips (1974) divided myrmekite into continuous rim styles for undeformed hosts and discontinuous lobate - bulbous styles for deformed host rocks. The fact that rim styles predominate in this regional zone might suggest the pluton microstructurally may be classed as undeformed.

PLATE 4.2.13 : LOW ANGLE BENDS AND WARPS IN BIOTITE GRAINS ( MU46104 )

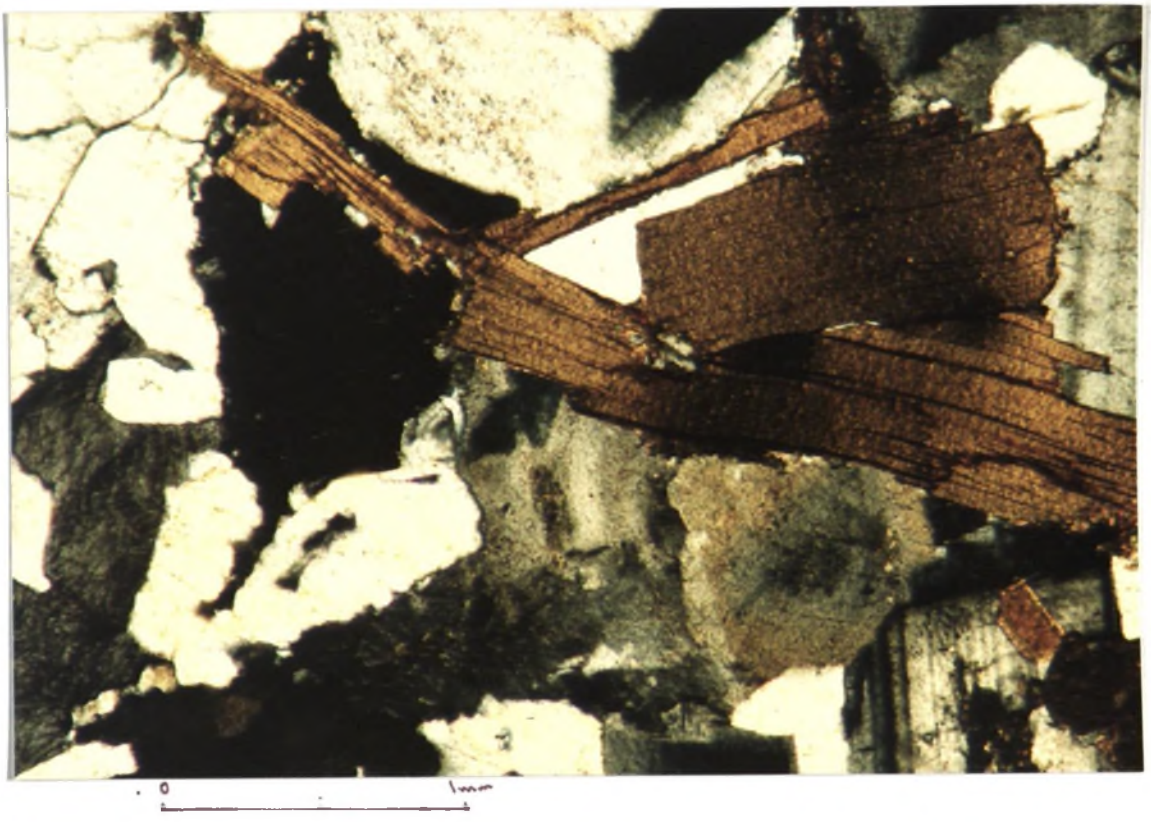

PLATE 4.2.14 : THICK RIM OF MYRMEKITE ASSOCIATED WITH A SINGLE GRAIN ( MU46104 )

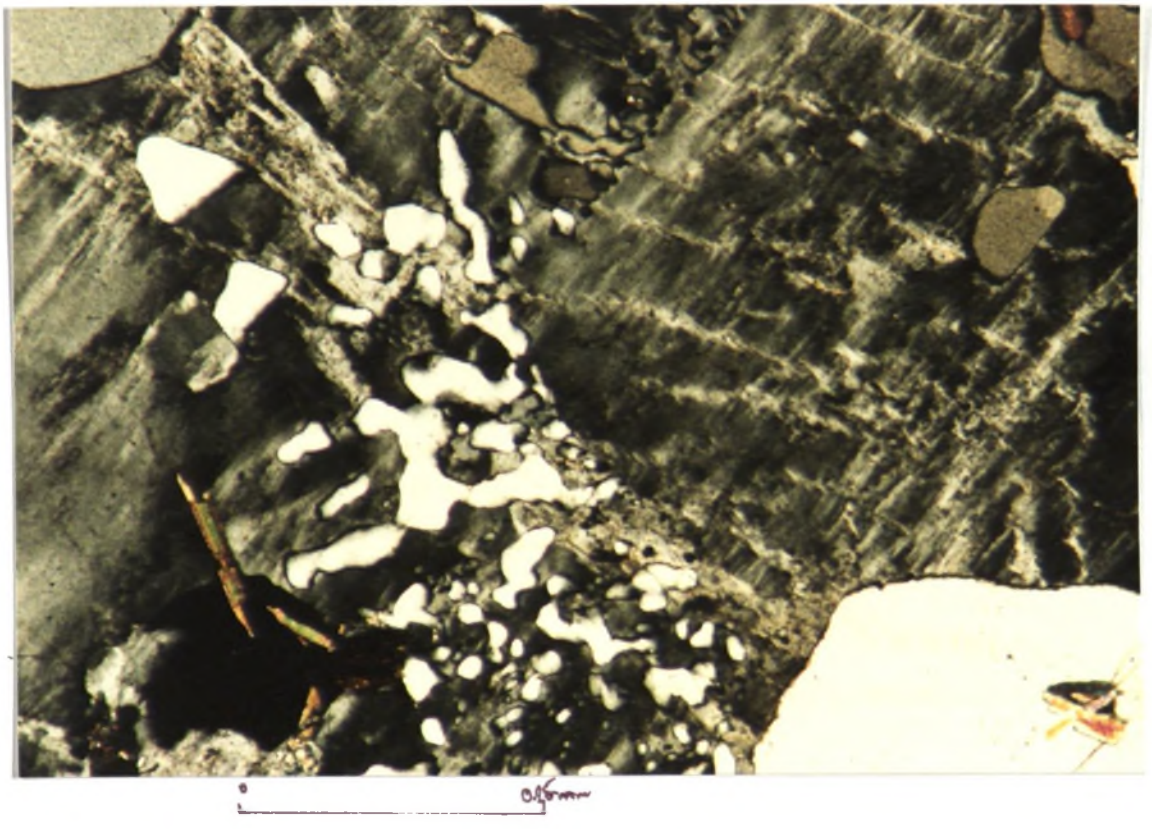

PLATE 4.2.15 : K-FELDSPAR GRAIN SHOWING RIM MYRMEKITE AND A 'REPLACEMENT' STYLE MYRMEKITE PENETRATING THE GRAIN ITSELF ( MU46119 )

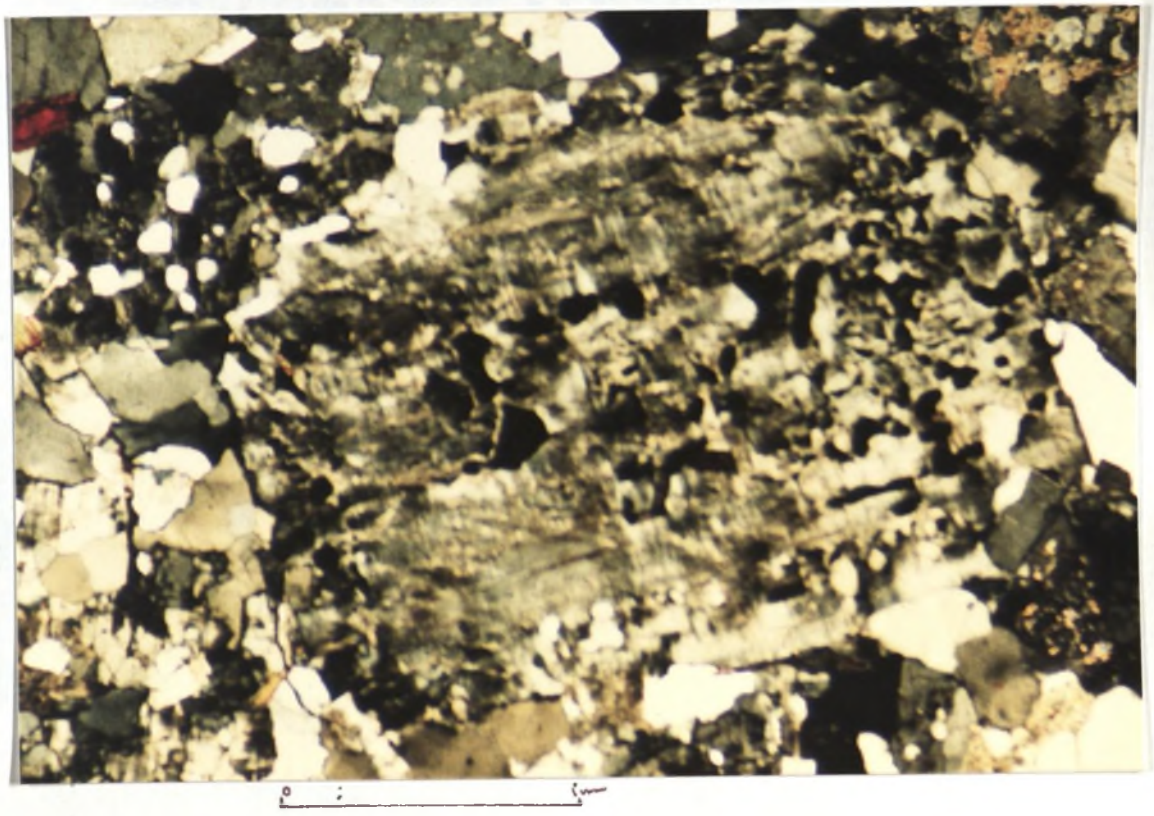


PLATE 4.2.16 : PENETRATIVE 'REPLACEMENT' STYLE MYRMEKITE AND REVEALLING AN ORIGINALLY SECTOR ZONED K-FELDSPAR ( CENTRE LEFT ) NOW PSEUDOMORPHED ( MU46119 )

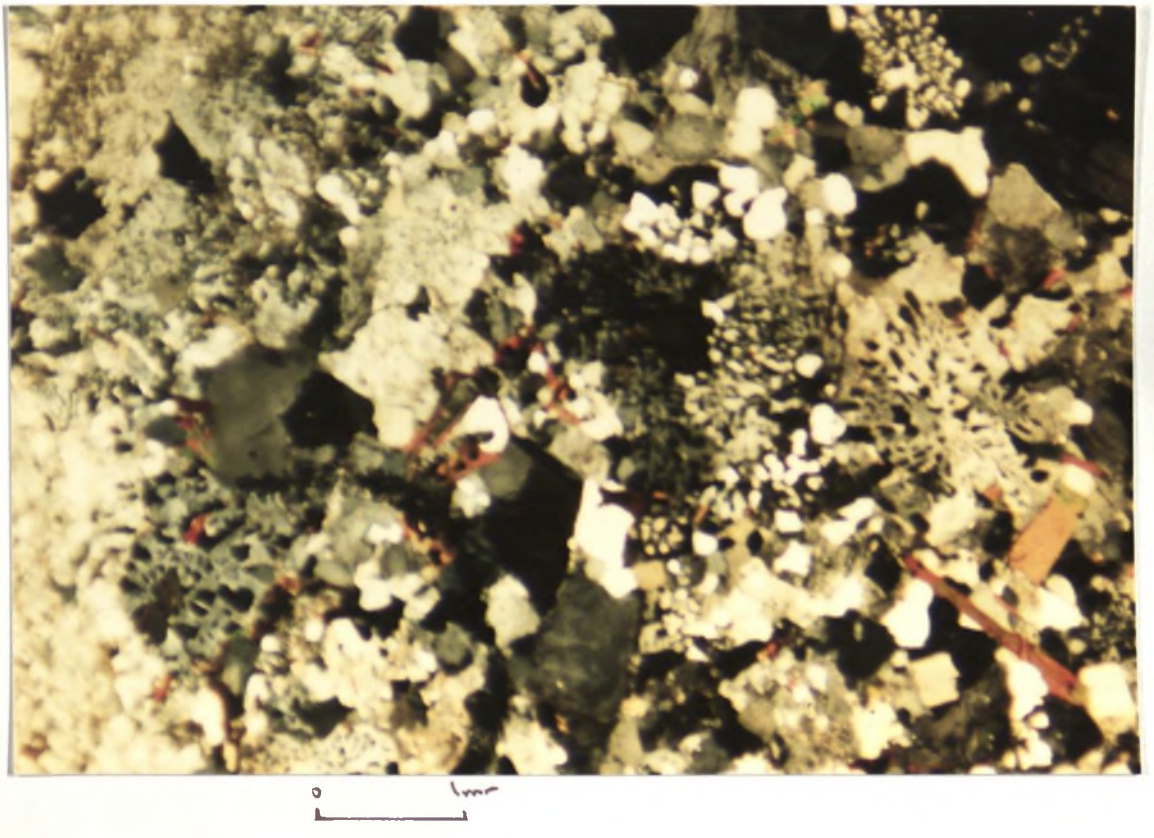

PLATE 4.2.17 : PENETRATIVE 'REPLACEMENT' STYLE MYRMEKITE
( MU46123 )

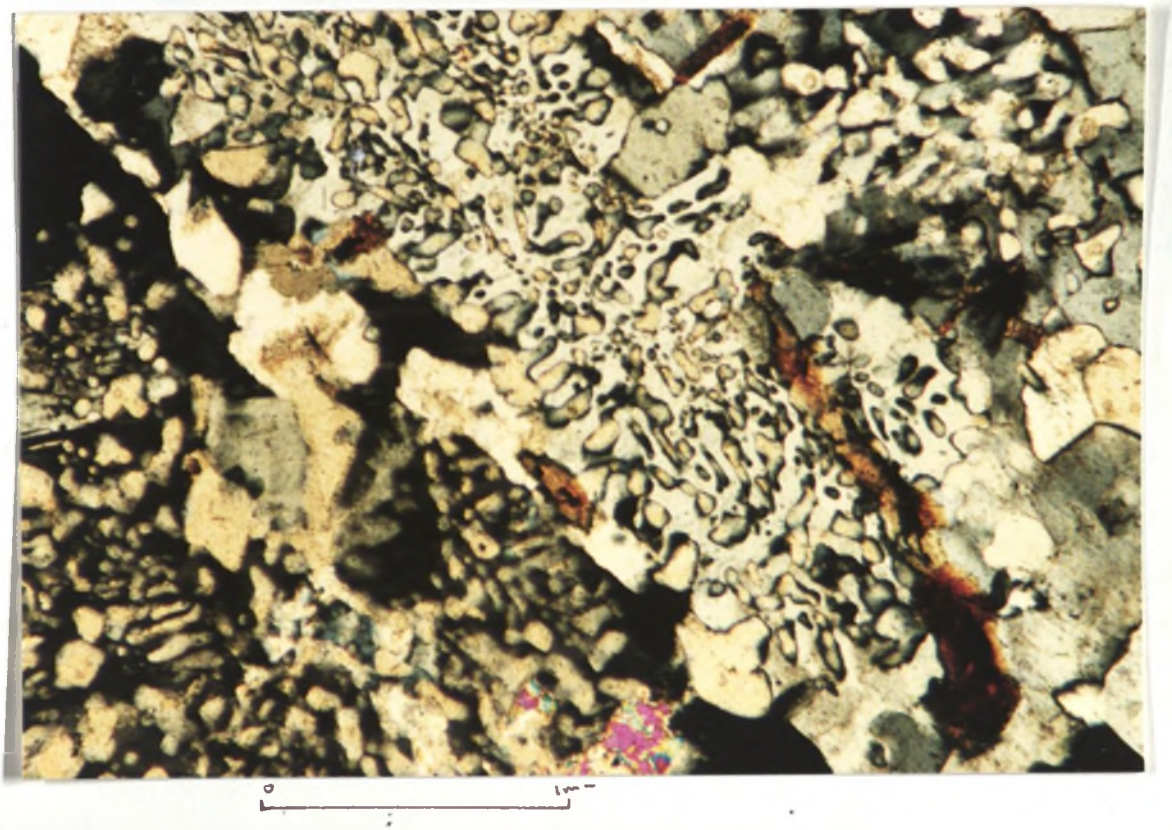

The most obvious differences between the regional zone and the low grade zone is the considerably higher abundance and different morphology of the myrmekite. Not only are rim myrmekites noticeably thicker in this zone, plate 4.2.14, but lobate and 'replacement' style myrmekite (Binns, 1966) is also common. Plate 4.2.15, although slightly out of focus, shows myrmekite on the rims of a grid-twinned microcline and penetrative to the core of the grain. This 'invasive' nature is seen in plates 4.2.16 and 17 where myrmekite occurs pervasively without any apparent relationship to particular K-feldspar grains. These extensive myrmekites (especially in plate 4.2.17) may suggest a pseudomorphing relationship to the original (now engulfed) K-feldspar grain. All the myrmekitic features in this zone would imply a localised deformational strain has been active parallel to the Gwydir River's contact.

Myrmekite at the highest grade is typified by moderately thick rims and only very minor abundances of lobate and bulbous myrmekite. Rims and lobes are noticealby thicker and more abundant than in the regional grade zone, but less than in the low grade zone and no 'invasive' myrmekite is observed. The myrmekite style and abundance in this zone suggests that, although deformational strain is present, its effect has been diminished and may be explained by higher contact temperatures near the Gwydir River Adamellite.

## 4.2.7 : PERTHITE

The potassium feldspars in the Yarrowyck Granodiorite are all microperthitic, albeit in low abundance. They show only limited variation in style and abundance with grade but do follow similar trends to those observed in part A.

In the regional zone perthite is only weakly developed and occurs as only fine grained blebs and stringlets in the K-feldspar host and is in low abundances. Perthite in the low grade zone is noticeably higher in abundance but still only represents a small area of host grains (up to 5 %), The style is similar but the lamellae are wider and longer. No kinking, bending or deflection of perthite was observable, but the higher abundance and wider lamellae imply increased perthitic exsolution in this zone.

Perthite in the high grade zone is not dissimilar to the regional grade zone. However, lower abundances and finer stringlet lamellae suggest perthitic exsolution has been restricted in this zone and may be due to higher contact temperatures and the subsequent disordering and re-equilibrising of K-feldspars. This is confirmed by higher unexsolved Ab contents in the K-feldspars outlined in the previous chapter.

## 4.2.8 : SUMMARY

Figure 4.2.1 summarises the main microstructural trends observed in the Yarrowyck Granodiorite. The most significant implication of these results is that it is not adequate to observe country rocks (in particular a metagranite)

FIGURE B.4.9 : SUMMARY DIAGRAM OF THE MAIN MICROSTRUCTURAL CHANGES OBSERVED IN THE YARROWYCK GRANODIORITE.

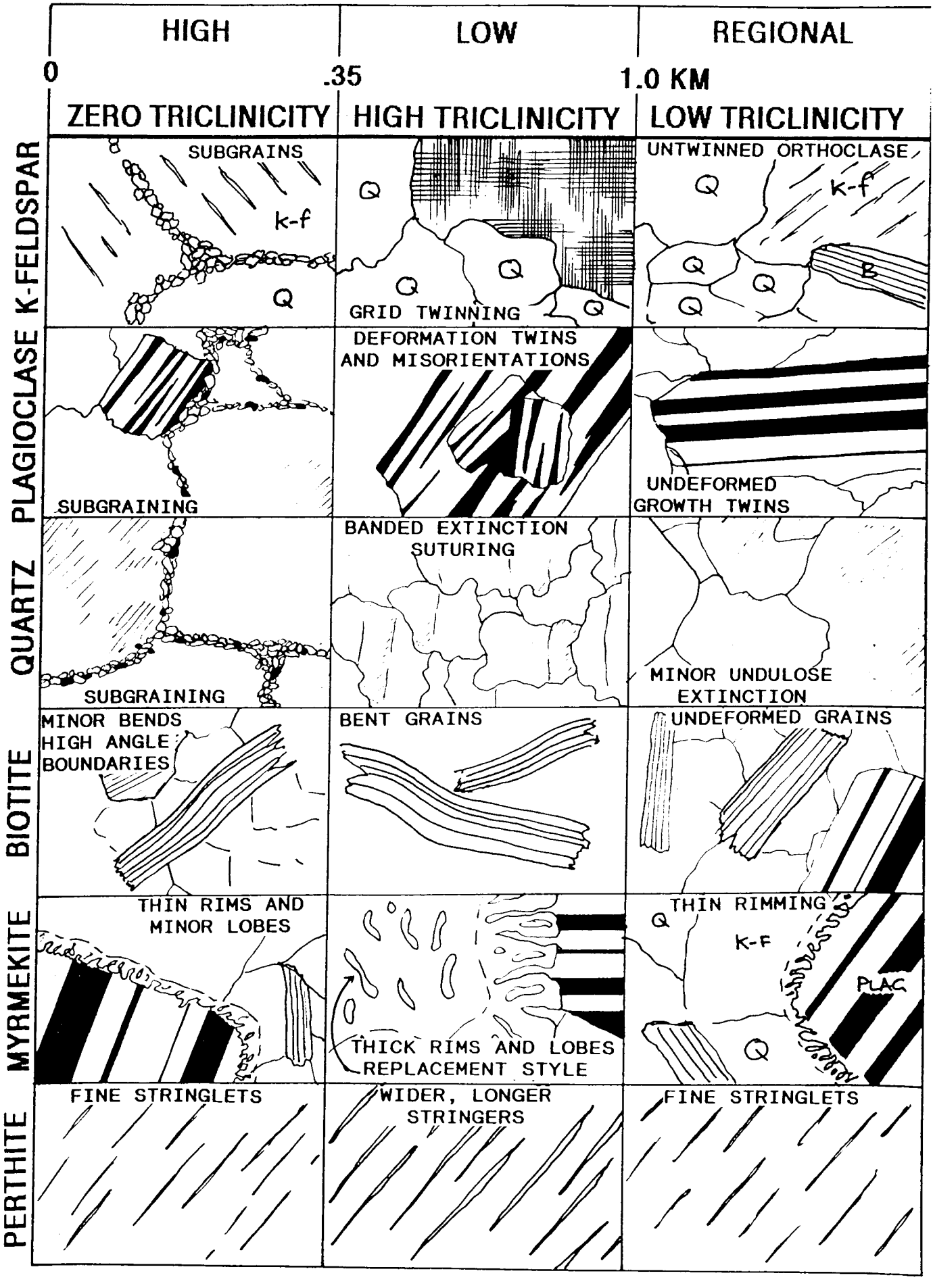

in a later intrusive aureole solely in terms of thermal effects but that strain effects (albethey weak) must be analysed. Also of importance is that there appears to be a strong relationship between K-feldspar ordering and composition (as outlined in the previous section), the abundance and style of both myrmekitic and perthitic intergrowths and the active processes of their formation. Highly exsolved and ordered K-feldspars occur with high abundances of wide perthitic lamellae (as is expected) and with high abundances of thick variable morphology myrmekite under high strain conditions. This would imply that conditions of higher deformational strain favouring more ordered K-feldspar, also favours extensive exsolution induced intergrowths of both perthite and myrmekite and therefore that stability fields for the order-disorder endmembers in the K-feldspar system have distinct microstructural morphologies. This relationship is not well understood and requires further work (outside the scope of this thesis) in order to understand it more fully.

# B . CHAPTER 5 : SUMMARY

The contact metamorphism induced by the Gwydir River Adamellite on the surrounding 'country rocks' has been tabulated in figure B.5.1 and enables a delineation of a metamorphic zonation for the aureole of the Gwydir River Adamellite.

## B . 5 . 1 : METAMORPHIC ZONATION

### 5 . 1 . 1 : REGIONAL ZONE ( 1 - 1.5 km from contact):

This zone is unaffected by contact metamorphism induced by the Gwydir River Pluton. Further than 1.5 km no hornfelsic type rocks are seen and only low regional grade metamorphism can be observed. The metagranite shows typical igneous microstructures, only thin rim myrmekite (suggesting an undeformed host, Phillips, 1974) and K-feldspar is orthoclase and minor low triclinicity microcline, suggesting only a very localised insipient deformation of these rocks has occurred regionally.

### 5 . 1 . 2 : LOW GRADE ZONE (0.35 - 1 km from contact)

The only evidence of contact metamorphism in the hornfelsic rocks in this zone are the pelitic biotite and metabasaltic actinolitic hornblende metamorphic isograds (suggesting albite - epidote hornfels facies). The metagranite, however, records many features suggestive of deformation. The K-feldspar is microcline with high triclinicity (0.82 maximum, due to ordering under strain) and low albite compositional contents (Or90-100) and associated higher abundances of perthitic exsolution; plagioclase exhibits misorientated subgrains and deformation twins; quartz has abundant sutured subgrain boundaries; and biotite exhibits warping and bending of grains. In addition, perthite is in marginally higher abundance than in the regional zone and myrmekite is not only in higher abundance but occurs as thick rims, lobes and in a replacement style (Binns, 1966) implying deformed host rock (Phillips, 1974).

### 5 . 1 . 3 : HIGH GRADE ZONE ( 350 m from contact)

This zone is recorded in all aureole rocks. The siliceous metasediments show a marked grainsize increase and their pelitic counterparts record increased thermal grade with the incoming of the cordierite, almandine and cordierite - K-feldspar isograds. The metabasalts record a progression from olive - green to green ragged magnesio-hornblende and to brown granoblastic tschermakitic hornblende. Although the metagranite doesn't record the same detail of prograde metamorphism in the last 350 m it does record the boundary between the high and intermediate grades sharply. There is an abrupt change from near maximum microcline to orthoclase as thermal disordering of the K-feldspars occurs. Associated with this, the amount of unexsolved albite in these feldspars increases (Or70). Microstructurally, this can be observed by a discernible decrease in perthite lamellae abundance

FIGURE B.5.1 : SUMMARY DIAGRAM FOR THE CORRELATED METAGRANITE AND HORNFELS CONTACT METAMORPHIC EFFECTS OBSERVED WITHIN THE AUREOLE OF THE GWYDIR RIVER ADAMELLITE

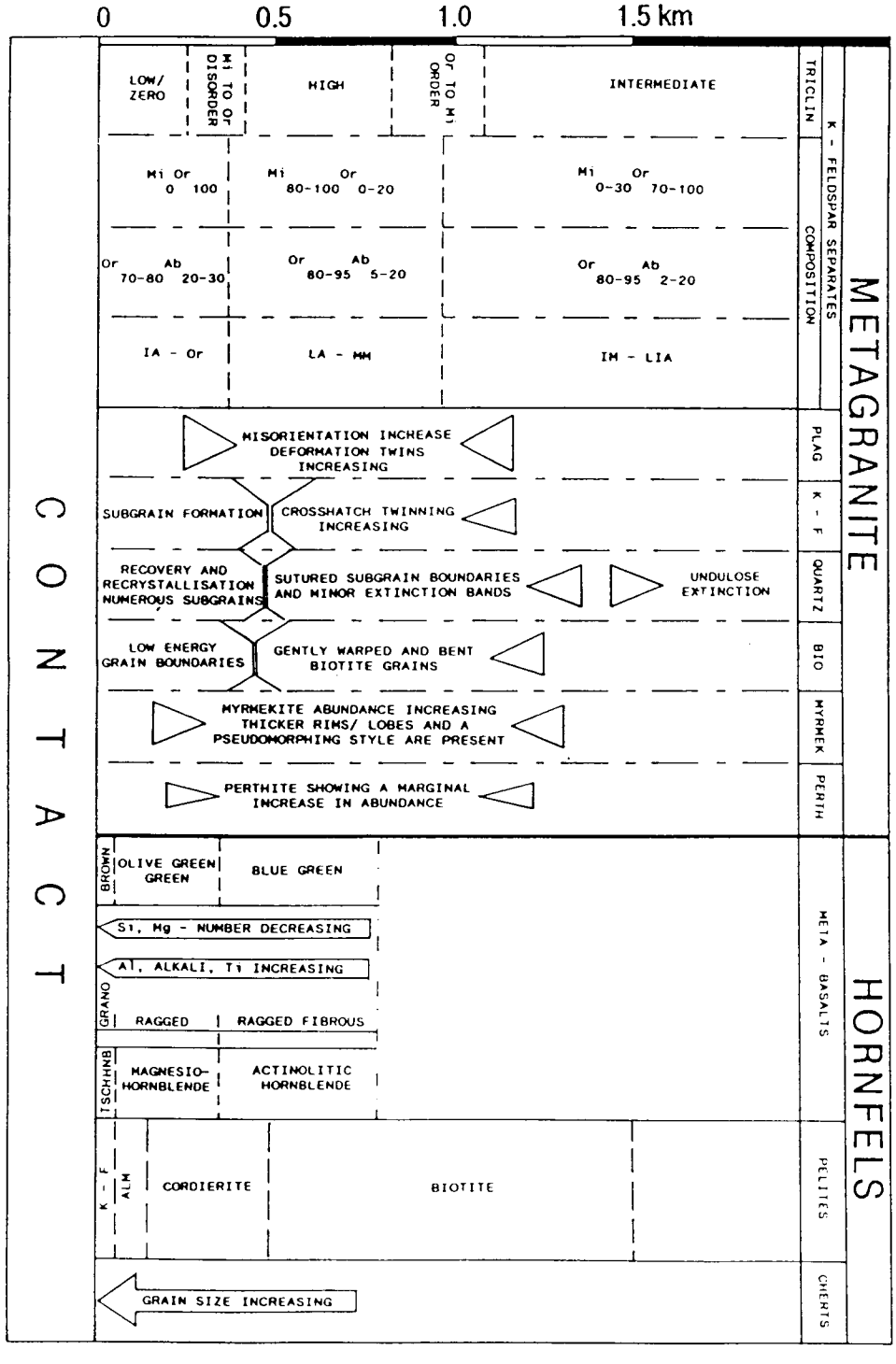

and width. All the framework silicates in the metagranite record abundant recovery and recrystallisation microstructures with the greatest concentration of recrystallised subgrains occurring at grain boundaries. The abundance of myrmekite in this zone is noticeably lower than in the intermediate grade zone and occurs predominantly as thin rims, suggestive of an essentially unstrained host rock. If it is fair to assume that this zone undergoes similar straining to the low grade zone but records no strained microstructural features due to continuous thermal annealing associated with higher contact temperatures then it would strongly suggest that in the high grade zone conditions were unfavourable for myrmekite formation. The implications are important for myrmekite formation and its relationship to temperature and strain and requires a more detailed study to be performed at a later date. This metamorphic zonation, its comparison with the Bendemeer Adamellite's aureole, and their joint implications for emplacement mechanisms, will be addressed in Part C.

# C : DISCUSSION: A CORRELATED CONTACT METAMORPHIC ZONATION AND ITS IMPLICATIONS UPON EMPLACEMENT MECHANISMS

## C . 1 : REVIEW OF FINDINGS

The studies of the contact aureoles of the Bendemeer and Gwydir River Adamellites reveals that two emplacement induced metamorphic zones (or envelopes) can be identified in the intruded plutons.

### C . 1 . 1 : Outer envelope (low grade zone)

This envelope has been observed in the metagranites and is characterised by K-feldspar with high triclinicity values, high proportions of exsolved perthite and an absence of orthoclase. The ordering of the K-feldspar and high perthite abundances are characteristics that have been attributed elsewhere in regional metamorphic terrains to increased deformational strain (Gorbatschev, 1972; Nilssen and Smithson, 1969). Microstructural evidence within this outer envelope confirms such a straining, recording bent biotites, bent and deformation twins and misorientations in plagioclase, bent and misorientated perthite lamellae and banded extinction and suturing in quartz. In addition, the abundance of myrmekitic intergrowths can be correlated with increases in perthite abundance and triclinicity values. In addition, the myrmekite rims become thicker and lobes and 'replacement' styles (Binns, 1966) also occur. These latter styles have been attributed by Phillips (1974) to be characteristic of a deformed host rock. These features combine to suggest a cold outer envelope which records minor ductile deformation produced by the younger pluton.

### C . 1 . 2 : Inner envelope (high grade zone)

The inner envelope, recorded in both the hornfelses and metagranites, reveals increased temperature from the outer margin (400 degrees celcius) to the immediate contact (approximately 600 - 650 degrees celcius). This envelope is characterised in the metagranite's K-feldspars by low to zero triclinicity values (disordering occurring above 400 degrees celcius (Wright, 1968)), and by the andalusite and cordierite metamorphic isograds in the S-type Banalasta Adamellite. The metapelites record the more conventional biotite, cordierite, cordierite-almandine and cordierite-K-feldspar isograds with increasing proximity to the contacts in both areas. The metabasalts likewise record a zonation in colour, texture and composition from pale blue-green fibrous-ragged actinolitic hornblende to brown granoblastic tschermakitic hornblende and confirm the temperature gradient up to 600 - 650 degrees celcius. These features combine to suggest that although equivelant strains occur in this zone, temperatures were sufficently high enough to continually anneal out the strain effects and therefore not record any singifiant strain features.

## C . 1 . 3 : Strain estimates :

Calculations of the strain difference to determine shortening for the Banalasta Adamellite was performed on 5 quartz aggregates in both the horizontal and the vertical plane parallel to the Bendemeer Adamellite's contact and is given in appendix 2. It reveals a maximum emplacement induced shortening in the aureole of 17.9% (at 300 m from the contact). However, this estimate of shortening rides on the assumption that the metagranite was originally isotropic. This is clearly not the case as shown by measurements of a contact parallel flow foliation recorded in the Banalasta Adamellite (section 4.2). Thus, although a straining (and expected shortening) is evident microstructurally in the metagranite, the greatest shortening occuring is expected to be considerably less than the apparent 17.9% recorded within the anisotropic rim of the Banalasta Adamellite.

## C . 1 . 4 : Aureole width differences

The essential difference between the two metagranite areas is the width of their aureoles. In the aureole of the Bendemeer Adamellite the distances from the contact of the outer and inner envelopes is 4 km and 1.5 km respectively. The Gwydir River Adamellite's inner and outer envelopes, however, are at distances of 1.2 km and 0.35 km respectively. It is known that the two areas differ in character in that the Gwydir River pluton is larger ( up to 17 km diameter ) than the Bendemeer pluton ( 10 km ), intrudes an I-type instead of an S-type metagranite and is of similar age to the pluton it is intruding ( both Permian ) unlike the Permian - Carboniferous age difference in the Bendemeer area. One would expect the larger pluton size to produce wider enveloping surfaces, however this is clearly not the case. Although it has not been determined it is believed that both I and S-type granitoids would deform to a similar degree. The proposed narrow time range between the two Uralla Suite plutons in the Yarrowyck area may be the answer to this difference as the Yarrowyck granodiorite ( although crystallised ) might still be at temperatures above 500 degrees celcius in from the contact at the time of the Gwydir River Adamellite's emplacement. This might restrict the width in which K-feldspar ordering and deformation microstructures could develop to the outer cooled rim of the Yarrowyck pluton. This is only conjecture and would be worthy of further examination at a later date.

## C . 1 . 5 : Emplacement criteria

Based on the findings of this study the following characteristics are required to be produced by the high-level emplacement mechanism that emplaced the Bendemeer and Gwydir River Adamellites.

i. Undisturbed bedding and structures within metres of the intrusive contact.

ii. Sharp intrusive contacts

iii. Low abundances of marginal stoped blocks.

iv. Evidence of only minor aureole foliations (Vernon, 1987. in press).

v. developement of a dual zoned contact aureole around the pluton.

vi. aureole strains producing a shortening of 17.9 % perpendicular to the intrusive contact.

vii. no recorded geochemical contamination of intruding pluton

# C . 2 : EMPLACEMENT MECHANISMS AND A MODEL FOR THE STUDY AREAS

## C . 2 . 1 : Review of current emplacement models.

Current emplacement mechanisms are summarised by Castro (1987) and Marsh (1982) and can be categorised under seven broad models: doming; melt zoning; ballooning diapirism; stoping; dyke propagation; diapirism; and roof-lifting. Factors controlling the mechanisms are: the active tectonic regime (Neugebauer, 1987); buoyancy forces (Pitcher, 1978); viscosity differences (Marsh, 1982); temperature differences and heat transfer (Hodge, 1974); structural controls in the crust (Pitcher, 1978) and ascent velocities (Marsh and Kantha, 1978).

### 2 . 1 . 1 : Mechanisms

The seven mechanisms will be critically reviewed with reference to the relevant evidence in the study areas.

'DOMING': This mechanism is commonly typically argued for concordant gneissic domes, that have risen on account of buoyancy and the mechanism therefore has a gravitational origin. The fact that the domes are concordant and commonly deformed, would suggest that they are more likely highly deformed older granites partially remobilised equivalents or form in the lower more plastic part of the crust (Pitcher, 1978; Castro, 1987). The two study areas show high-level, unremobilised, post-tectonic plutons and on this basis a doming mechanism can be rejected.

MELT ZONING: A mechanism whereby an intrusive body melts its way up through the crust. The driving force for this is based on high temperature differences between the floor and roof of the magma chamber resulting in convective cells that may produce country rock roof melting (Ahern,1981). It is most effective when magma temperatures are high, magma - country rock temperature differences low and magma viscosities low. A critical feature of the mechanism is a zone of country rock 'melt' around the pluton. The two study areas show sharp contacts, no evidence of contact melt zones and low intrusive temperatures (700-800 degrees celcius) and hence do not warrant a zone melting mechanism.

BALLOONING DIAPIRISM : This diapiric inflation mechanism works by shortening, compression and 'shouldering aside' of country rocks as proposed by Brindley (1973) and more recently Bateman (1985) and results in a concordant relationship between the country rocks and an internally deformed pluton. Brindley applies this inflation mechanism to the Ardara Pluton, Ireland, although a previous study by Pitcher and Berger (1972) suggested the concordant deformational effects were equally recorded in the pluton itself and implied post-emplacement deformation.

Bateman (1985) who proposed this model for the Cannibal Creek Granite, North Queensland, argued for aureole shortening of 65 % due to inflational emplacement. Paterson (1988,in press) however, states that the concordant regional structures are more likely due to a known post-emplacement deformation phase and that no microstructural evidence exists within the pluton to suggest a 65 % shortening. On this basis Paterson argued that all the deformation within the pluton is post-emplacement. In the two study areas, no such concordant contact zones or deformation is observed within the intruding pluton and only a weak regional deformation is evident. Thus a ballooning diapir mechanism cannot be applied to the study areas.

STOPING: Pitcher et al ( 1985 ) in an examination of the Peru batholith proposed a method of emplacement by stoping whereby a single large central block is dislodged from above the magma chamber and sinks while magma rises to fill the space left by the removed block. Such a method could be applied as a feasible mechanism for the two study areas, but would require : a means by which contamination of the pluton did not occur; rapid block sinking to permit high enough ascent velocities to entrain mafic enclaves as suggested by White et al (1974); and limited disruption of surrounding wallrocks (to account for the low abundances of marginal stoped blocks). Such a mechanism would explain the room problem but could not account for the presence of a deformation envelope for both aureoles and a suggested wallrock shortening (although weak) in the Banalasta Adamellite.

DYKE PROPAGATION: This emplacement mechanism has been suggested by Castro (1987) as the principle magma transport mechanism from depth. It relies upon fracture development at depth due to anisotropic stress fields, high fluid pressures and a magma source. The meridonal nature of the plutonic suites in the New England Batholith may suggest such a mechanism might apply regionally at depth. However, the plutons studied have elliptical shapes and long axes directions inconsistent with the regional fault trends (E-W for the Bendemeer Adamellite with faults trending approxiamately N-S). On this basis a dyke propagation mechanism is unlikely for these high-level plutons.

DIAPIRISM: Diapirism, a mechanism resulting in a typical rim synclinal structure to the surrounding country rocks, involves the rising of a magma by buoyancy forces and in addition requires: the existance of a zone of partial melt

around the ascending body (Marsh,1982); circular to ovoid pluton shapes; contact parallel aureole foliations; an approach to concordancy for adjacent regional structures; contact metamorphic pophyroblasts showing synkinematic growth; and strains that record bulk shortening (Bateman, 1984).

Both study areas record ovoid pluton shapes and minor suggested shortening. However, no rim synclines is observed, no strong contact parallel aureole foliations are seen, regional structures are disconcordant and no synkinematic porphyroblast growth was observed (although a weak contact parallel matrix foliation drapes around cordierite porphyroblasts in the Walcha Road Adamellite's aureole, Teale, 1974; Vernon, 1987, in press). If a diapiric mechanism is applicable to the two areas studied then it is not completely consistant with the stated requirements for diapirism. However it is possible that components of diapirism are seen in the study areas.

ROOF-LIFTING: This has been proposed by Pitcher et al (1985) for the Peru Batholith. He suggested a combined emplacement mechanism of stoping, cauldron subsidence and an associated final lifting of roof rocks due to the buoyancy forces of the rising pluton. The implication of his findings is that roof-lifting is a final emplacement feature and is not a primary means of emplacement.

### 2 . 1 . 2 : A high-level stoping emplacement mechanism with associated final - emplacement diapiric processes for two I-type granitoids in the Southern New England Batholith.

The criteria outlined in section C.1.3 rule out the first three mechanisms of doming, zone melting and ballooning diapirism as no melting or concordancy is observable. In the author's view not one of the remaining four models singularly explains the plutons emplacement at high levels in the study areas.

Although dyke propagation would account for an initial emplacement to high levels from deep in the crust it is not consistant with the elliptical pluton shapes observed. Unroofing would seem to be a secondary process of emplacement rather than a primary mechanism. Both stoping and diapirism contain components in agreement with criteria in section C.1.3 but both contain critical features conflicting with the findings for parts A & B. Stoping would account for the room problem but cannot explain a suggested small magnitude wallrock shortening and observed microstructural deformation evident out as far as 4 km from the pluton's contact. Diapirism, although capable of explaining such deformation, cannot account for discordant, sharp contacts and only minor shortening and does not effectively explain the room problem for these plutons.

Thus an emplacement mechanism of primarily stoping and minor final emplacement diapiric processes is proposed for the two areas, whereby a magma rises by dyke propagation ( Castro, 1987) and diapiric means in the plastic to semi - brittle lower crust and then stopes its way to higher levels by a series of single block stoping events ( Pitcher et

al, 1985 ). Once removal of the final block (possibly with a chilled granitic carapace) has occurred the magma continues its last stages of discordant emplacement. Localised stoping of weakened marginal rocks may occur and internal pressures of the still emplacing pluton, although insufficient to cause little if any further rise, may act diapirically causing straining of the country rocks resulting in minor shortening and the formation of a deformation envelope. Contemporaneous with this, wallrock heating results in a thermal envelope where high contact strains are not recorded due to continual annealling, recovery and recrystallisation.

Such a mechanism would explain : discordant, sharp, undisturbed wallrocks; low abundances of marginal stoped blocks; minor aureole foliation evidence (Vernon, 1987, in press), the occurrence of the aureole's two envelopes; aureole strains resulting in minor shortening nearest the contact and no geochemical contamination of the intruding pluton.

Thus the author believes that an emplacement mechanism of stoping and associated late stage diapiric processes would account for the features observed in the aureoles of two I-type plutons in the New England Batholith.

## C . 3 : CONCLUSIONS

The aim of this study has been to present a petrological and structural study of both contact metamorphosed plutons and hornfelses in the aureoles of two plutons from the Southern New England Batholith. The purpose being to record both mineralogical and microstructural effects within the metagranite, correlate them with the more conventional hornfelsic isograds and use the results to erect criteria for evaluating emplacement mechanisms for the Southern New England Batholith.

Both areas have produced very similar results and the following conclusions have been drawn :

### 1. THE METAGRANITES :

The results of both the contact metamorphosed S-type microcline bearing Banalasta Adamellite and the I-type, predominantly orthoclase bearing Yarrowyck Granodiorite when combined enable the following points to be concluded :

(i) That this study not only confirms the existance of a low triclinicity zone (due to thermal disordering) in the contact aureole of the later intrusives, but goes further to suggest that contemporaneous with this, an outer high triclinicity zone exists where ordering has occured due to emplacement induced strains from the later intrusive.

(ii) Associated with the structural state change in K-feldspar is a compositional change. The strained high triclinicty zone contains low albite - maximum microcline microperthitic k-feldspar with high proportions of exsolved

albite. The thermally disordered low triclinicity zone contains orthoclase - intermediate albite microperthitic K-feldspar with low proportions of unexsolved albite.

(iii) In addition to this, a microstructural analysis of the metagranites within the aureoles of the later intrusives reveals two zones :

a) an outer low grade zone showing microstructures suggestive of ductile deformation (e.g plagioclase with misoriented subgrains, deformation and kinked twins; K-feldspar with coarse perthite lamellae; quartz showing sutured subgrains and banded extinction; kinked and bent biotites; and thick rim and lobate myrmekite indicating a deformed host rock).

b) an inner high grade zone showing microstructures in keeping with recovery and recrystallisation due to a thermal effect (e.g. intergranular recrystallised unstrained new grains, finer perthite lamellae, less abundant deformational microstructures and thin rim myrmekite indicative of an undeformed host rock).

(v) An additional observation in the Banalasta Adamellite is the incoming of metamorphic andalusite and cordierite within the inner high grade zone. These isograds are an important finding in the metagranite and correlate well with the similarly placed andalusite and cordierite isograds in the metapelites.

(vi) The above observations imply the following relationships :

(a) Associated with the K-feldspar high triclinicities in the contact aureoles is more abundant perthitic exsolution, ductily deformed, unrecovered microstructures and higher abundances of myrmekite.

(b) Associated with the low triclinicity zone is low abundances of exsolved perthite, thermally annealled recovery and recrystallisation microstructures and low myrmekite abundances.

The fact that myrmekite does not uniformly increase right up to the later intrusive contact might suggest that its formation is isochemical and may be linked to the stability conditions under which the K-feldspar structural state endmembers form.

(iv) Correlation of points (i) to (iii) has enabled two emplacement induced metamorphic envelopes to be proposed. An outer low grade envelope recording essentially 'cold' ductile deformation without recovery and an inner high grade envelope that, although it contains the same emplacement induced strains, is affected by temperatures

sufficently high enough to result in disordering of K-feldspar (400 degrees celcius), continuous annealling out of strains by recovery and recrystallisation and conditions unfavourable for perthite and myrmekite development.

## 2. HORNFELS :

A contact metamorphic zonation of the more conventional isograds for both metapelitic and metabasaltic rocks has been established : (i) examination of the metapelitic rocks revealed a progression from the albite-epidote hornfels facies up to the cordierite-K-feldspar hornfels facies by delineation of the biotite, andalusite, cordierite, cordierite-almandine and cordierite-K-feldspar isograds. These rocks record only thermal effects although in the immediate contact a matrix is observed. (ii) The metabasalts show a similar progression recording a colour, microstructural and compositional progression in metabasaltic amphiboles from pale blue-green, fibrous-ragged actinolitic hornblende to olive green - brown, ragged-granoblastic tschermakitic hornblende. (iii) Correlation of both these hornfelsic contact metamorphic zonations with the grade zones in the metagranite shows a correlation only with the metagranite's high grade zone and therefore they provide a finer subdivision of the inner thermal envelope of the contact aureole.

3. Correlation of these contact metamorphic zonations reveals a critical finding that the contact aureoles of the two intrusives studied not only show the typical thermal envelope associated with an emplaced pluton, but also a more extensive outer deformational strained envelope as part of the aureole.

4. These major findings coupled with other examinations in this thesis, require an emplacement mechanism for the high-level Bendemeer and Gwydir River Adamellites to : not disturb wallrock bedding and structures; produce sharp intrusive contacts; have only minor marginal stoping; produce only a minor aureole foliation; results in sufficent strain and heat on the surrounding rocks to produce a broad weak ductile deformaion envelope and a narrower thermal continuous recovery envelope; record only minor shortening; and no contamination of the intruding pluton.

5. A review of current emplacement mechanisms, in the light of these criteria, suggests a mechanism of stoping and associated late stage diapiric processes for the two I-type plutons in the southern New England Batholith.

# BIBLIOGRAPHY

Ahern, J.L. et al,1981, On the upward migration of an intrusion, J. of Geol. vol. 89, pp 421-432.

Baker, G., 1940, Cordierite granite from Terip Terip, Victoria, Am. Mineral. vol.25, pp 543-548.

Bateman, R.J.,1983, Structure, petrology, and emplacement processes of the Cannibal Creek Granite, Queensland. Unpub. Ph.D. thesis, James Cook Univ., Queensland.

Bateman, R.J.,1985, Aureole deformation by flattening around a diapir during in situ ballooning: TheCannibal Creek Granite, J. of Geology,vol.93, pp 293-310.

Bateman, R.J.,1984, On the role of diapirism in the segre- gation, ascent and final emplacement of granitoid magmas, Tectonophysics, vol. 110, pp 211-231.

Best, M.G.,1982, Igneous and Metamorphic Petrology, W.H. Freeman & Co., San Francisco.

Binns, R.A., 1965, The mineralogy of metamorphosed basicrocks from the Willyama Complex, Broken Hill district, New South Wales. Part I. Hornblende. Mineralog. Mag. London. 35, 306-326

Binns, R.A., 1966, Granitic intrusions and regional meta- morphic rocks of Permian age from the Wongwi-binda District, North-eastern New South Wales, Journal and Proceedings, Roy. Soc. of New SouthWales

Binns, R.A., 1966, Hornblendes from some basic hornfelses in the New England region, New South Wales, Min.Mag., vol. 34, pp 52-65.

Birch, W.D., and Gleadow, A.J.W.,1974, The genesis of garnet and cordierite in acid volcanic rocks: evidence from the Cerberean Cauldron, Central Victoria, Australia, Contr. Mineral. and Petrol.,vol.45, pp

Brindley, J.C., 1973, Some aspects of batholithic intrusion, Geol. Soc. S. Africa, vol.3, pp 35 - 44

Brown, R.E., 1986, Geological notes based on observations recorded during field checking the manilla 1:250,000 sheet, Geological Survey of New SouthWales, Department of Mineral Resources.

Brown, R.E., 1986, Preliminary geological notes for the manilla 1:250,000 sheet, Geological Survey ofNew South Wales, Department of Mineral Resources.

Bryan ,W.B. & Moore, J.G., 1977, Compositional variations ofyoung basalts in the Mid-Atlantic Ridge rift valley near lat 36 49'N. Geol.Soc.Amer.Bull. vol.88,pp361-378

Castro, A.,1987, On granitoid emplacement and related structures. A review, Geologische Rundschau,vol. 76/1, pp 101-124.

Chappell, B.W. & White, A.J.R., 1974, Two contrasting granite types. Pac. Geol., vol.8, pp173-174

Chappell, B.W., 1978, Granitoids from the Moonbi District, New England Batholith, Eastern Australia, J. of Geol. Soc. of Aust. vol.25, pt 5, pp 267-283.

Clemens, J. & Wall, V., 1981, Origin and crystallization of some peraluminous (S-type) granitic magmas, Can. Min. vol.19, pp 111-131.

Corbett, G.J.,1976, A new fold structure in the Woolomin Beds suggesting a sinistral movement on the peel fault, J. of Geol. Soc. of Aust., vol.23, pt 4, pp 401-406.

Coward, M.P., 1981, Diapirism and gravity tectonics: report of a Tectonic Studies Group conference held at Leeds University, 25-26 March 198O, J. ofStructural Geol., vol.3, no.l,pp 89-95.

Cuddy, R.G., 1978, Internal structures and tectonic setting of part of the New England Batholith andassociated volcanic rocks, Northern New South Wales. PhD thesis, University of New England. Armidale (ur

Deer, W., et al, 1966, An Introduction to the Rock-forming Minerals, Longmans, London.

Dixon, J.M., 1975, Finite strain and progressive deformation in models of diapiric structures, Tectono-physics, vol.28, pp 89-124.

Durney, D.W., 1988, Strain analysis procedures, pers. comm.

Eggleton, R.A., and Buseck, P.R., 1980, The orthoclase- microcline inversion: A high-resolution transmission electron microscope study and strain analysis, Contrib. Mineral. Petrol. vol. 74, pp 123-133.

Eskola, P.,1951, Around Pitkaranta, Ann. Acad. Scien.Fennica ser.A.III, 90pp

Flood, R. H., 1971, A study of part of the New England Batholith, New South Wales, Ph.D. thesis,Univ. of New England, Armidale, NSW, Australia

Flood, R.H. and Shaw, S.E., 1975, A cordierite-bearing granite suite from the New England Batholith, NSW, Australia, Contrib. Mineral. Petrol. vol.52, pp 157-164.

Flood, R.H., and Shaw, S.E., 1977, Two "S-Type" granite suites with low initial 87Sr/86Sr ratios from the New England Batholith, Australia, Contrib.Mineral. Petrol., vol.6l, pp 163-173.

Flood, R.H., and Shaw, S.E., 1988, Norm and modal analyses for the Yarrowyck Gwydir River plutons. Pers. comm.

Flood, R.H., and Vernon, R.H., 1988, Microstructural evidence of orders of crystallization in granitoid rocks, Lithos, vol.2l, pp 237-245.

Gorbatschev, R., 1972, The X-ray obliquity of potassic feldspar in the granites of Jamtland, Northern central Sweden, Geologiska Foreningen i StockholmForhandlingar, vol.94, pt. 2, pp 213-228.

Green, T.H., and Vernon, R.H., 1974, Cordierite breakdown under high pressure, hydrous conditions, Contrib.Mineral. and Petrol., vol.46, pp 215-226.

Greenwood, H.J., 1976, Metamorphism at moderate temperatures and pressures. In Bailey, D.K. & McDonald, R. (eds) The evolution of crystalline rocks. New York: Academic press, pp 187-259.

Griggs, D.T. & Blacic, J.D., 1965, Quartz: anomalous weakness of synthetic crystals. Science, vol.147, pp292-295

Gulson, B.L., and Lovering, J.F., 1968, Rock analysis using the electron probe, Geoschimica et Cosmochimica Acta, vol.32, pp 119-122.

Hallimond, A.F., 1943, On the graphical representation of the calciferous amphiboles, The Amer. Mineral.vol.28, no.2, pp 65-89.

Harrington, H.J., and Korsch, R.J., 1985. Tectonic model for the Devonian to middle Permian of the New England Orogen, Aust. J. of Earth Sciences,vol.32, pp 163-179.

Hanmer, S.K., et al, 1982, The role of Hercynian granites in the deformation and metamorphism of Brioverian and Palaeozoic rocks of Central Brittany,J. Geol. Soc., vol. 139, pp 85-93.

Hensel, H.D. et al, 1985, The New England Batholith: constraints on its derivation from Nd and Sr isotopic studies of granitoids and country rocks, Geochemica et Cosmochimica Acta, vol. 49,pp 369-384.

Hensen, B.J., and Green, D.H., 1972, Experimental study of the stability of cordierite and garnet in pelitic compositions at high pressures and temperatures Contri. Mineral. and Petrol. vol.35, pp 331-354

Hodge, D.S., 1974, Thermal model for origin of granitic batholiths, Nature, vol. 251, pp 297-299

Holder, M.T., 1981, An emplacement mechanism for post- tectonic granites and its implications for their geochemical features, Origin of GraniteBatholiths - Geochemical evidence, Shiva Publishing Ltd,

Howarth, F., 1973, Some contact metamorphic and mangani- ferous rocks from southern New England, thesissubmitted for B.A. (Hons), Macquarie Univ. NSW

Hsu, L.C. & Burnham, C.W., 1969, Phase relationships in thesystem Fe3Al2Si3O12 - Mg3Al2Si3O12 - H2O at 2.0 Kilobars. Geol.Soc.Am.Bull., vol.80,pp2393-2408

Irvine, T.N., and Baragar, W.R.A., 1971, A guide to the chemical classification of the common volcanic rocks, Can. J. of Earth Sciences, vol.8, pp 523-548

Ishiga, E.C. et al, 1988, Radiolarian and conodont biostrati -graphy of siliceous rocks from the New England Fold Belt, Aust. J. Ea. Sci., vol.35, no.1, pp 73-80

Joyce, A.S., 1964, Geology of the Yarrowyck area, Unpub.thesis submitted for B.Sc. (Hons), Univ. of New England (Armidale), NSW.

Karamata, S., 1961, Einfluss der geologischen Alters und des tektonischen Drucks auf die Art derAlkalifeldspate. Instituto Lucas Mallada,Cursillos y Conferencias, vol.8, p127-130. ( extract )

Kuehn, P.E., 1985, The geology of Giants Den - HanningCentral Moonbi Ranges, NSW, unpub. thesis submitted for B.Sc (Hons), Univ. of Newcastle.

Leake, B.E., 1960, Compilation of chemical analyses and physical constants of natural cordierites, Amer. Mineralogist, vol. 45, pp 282-298

Leake, B.E., 1965, The relationship between composition of calciferous amphibole and grade of metamorphism in Controls of Metamorphism, Ed. W.S. Pitcher & G.W.Flinn: Oliver and Boyd, Edinburgh,pp299

Leake, B.E., 1968, A catalog of analyzed calciferous and subcalciferous amphiboles together with their nomenclature and associated minerals, The Geol.Soc. of America Inc., Boulder, Colorado.

Leitch, E.C., et al, 1971, Dorrigo-Coffs Harbour 1:250000geological series sheet SH56-10211.Geol.Surv, N.S.W.

Leitch, E.C., 1974, The geological development of thesouthern part of the New England fold belt, J. of Geol. Soc. of Aust., vol. 2l, pt 2, pp 133-156

Leitch, E.C., 1975, Plate tectonic interpretation of the paleozoic history of the New England fold belt, Geol. Soc. of Amer. Bulletin, vol.86,pp 141-144

Lewington, G.L.D., 1973, The geology of an area east and south- east of Limbri, NSW, Unpub. thesis submitted for B.A. (Hons), Macquarie Univ.

Liou, J.G., et al, 1974, Experimental studies of the phase relations between greenschist and amphibolite in a basaltic system, Amer. J. of Sci., vol.274 pp 613-632

Liou, J.G., and Apted, M.J.,1983, Phase relations among greenschist, epidote-amphibolite, andamphibolite in a basaltic system, Amer. J. of Sci. vol. 283-A, pp 328-354.

Lister, L.A., 1973, Symposium on granites, gneisses and related rocks, Geol. Soc. of S. Africa, No.3

Loomis, A.A., 1966, Contact metamorphic reactions andprocesses in the Mt.Tallac roof remnant, Sierra Nevada, California: J.Petrol., vol.7, p221-245

Marsh, B.D., and Kantha, L.H., 1978, On the heat and mass transfer from an ascending magma, Earth and Planetary Science Letters, vol. 39, pp 435-443

Marsh, B.D., 1982, On the mechanics of igneous diapirism, stoping, and zone melting, Amer. J. of Sci.,vol. 282, pp 808-855

Murray, C.G., et al, 1987, Plate tectonic model for the carboni- ferous evolution of the New England fold belt, Aust. J. Earth Sci., vol.34, pp 213-236

Naggar & Atherton, 1970, J. Petrol, vol.11, p582

Neugebauer, H.J., and Reuther, C., 1987, Intrusion of igneous rocks - physical aspects, Geologische Rundschauvol. 76, pt. l, pp 89-99

Nicholls, I.A., 1974, A direct fusion method of preparing silicate rock glasses for energy-dispersive electron microprobe analysis, Chem. Geol. vol.l4,pp 151-157

Nilssen, B. and Smithson, S.B., 1965, Studies of the Precambrian Herefoss Granite, Norsk Geol. Tidsskr.,vol.45 pp 367-398

Nilssen, B., 1967, Separation of perthitic microcline by heavy liquid fractionation - a too sensitive method? Norsk Geolo. Tidsskr., vol.47, pt.2, pp 149-157

Olatunji, J.A., 1976, Petrogenetic significance of the state of k-feldspars from spatially related granitic intrusives in West Herberton, North Queensland, J. Geol. Soc. Aust., vol.24, pt. 1, pp 15-18

O'Neil, J.R., 1977, Oxygen and hydrogen isotope compositions as indicators of granite genesis in the NewEngland Batholith, Australia, Contrib. Mineral.Petrol., vol. 62, pp 313-328

Orville, P.M.,1960, Powder X-ray mehtod for determination of (Ab + An) content of microcline (abs). Geol.Soc.Am.Bull., vol.71, pp1939-1940

Orville, P.M.,1963, Alkali ion exchange between vapour andfeldspar phases. Amer.J.Sci., vol.261,pp201-237

Paterson, S.R., 1988, Cannibal Creek Granite: Post-tectonic 'ballooning' intrusive or pre-tectonic piercement diapir?, (in press)

Phillips, G.N., and Wall, V.J., 1981, Geology and metamorphism of the Bonnie Doon Area, Victoria, Geol. Soc. Aust., pp 33 - 42

Phillips, E.R., and Ransom, D.M., 1970, Myrmekitic and non-myrmekitic plagioclase compositions in gneisses from Broken Hill, NSW, Mineral. Mag. vol.37, pp 729 - 732

Phillips, E.R., and Stone, I.J.,1974, Reverse zoning between myrmekite and albite in a quartzofeldspathic gneiss from Broken Hill, NSW, Mineral. Mag., vol. 39, pp 654-657

Phillips, E.R., 1974, Myrmekite - one hundred years later,Lithos, vol. 7, pp 181-194

Phillips, E.R., and Carr, G.R., 1973, Myrmekite associated with alkali feldspar megacrysts in felsic rocks from New South Wales, Lithos, vol.6, pp 245-260

Pitcher, W.S. & Berger, A.R., 1972, The geology of Donegal: astudy of granite emplacement and unroofing. In. L.U. de Sitter (Ed), Regional Geology series. Wilcy-Interscience, New York, 435pp

Pitcher, W.S., 1978, The nature, ascent and emplacement of granitic magmas, J. Geol. Soc. London, vol.136, pp 627 - 662

Pitcher, W.S., et al, 1985, Magmatism at a plate edge, Blackie & Son Ltd., Glasgow.

Ransley, J.E., 1970, The petrology of the New England Batholith in the Yarrowyck - Balala - Uralla area, north-eastern New South Wales, Unpub. thesis for M.Sc, Univ. of New England (Armidale).

Reed, S.J.B., 1970, The analysis of rocks in the electron probe Geochimica et Cosmochimica Acta, vol.34, pp 416 - 421

Ribbe, P.H.,1975, The chemistry, structure, and nomenclature of feldspars; Feldspar Mineralogy, Short Course notes, vol.2, Min. Soc. of Amer., pp R-1 - R-52

Roberts, J., and Engel, B.A., 1980, Carboniferous palaeography of the Yarrol and New England Orogens, eastern Australia, Geol. Soc. of Aust., pp 167 - 183

Roberts, J., and Engel, B.A., 1987, Depositional and tectonic history of the southern New England Orogen, Aust. J. of Earth Sciences, vol. 34, pp 1 - 20

Shaw, S.E., and Flood, R.H., 198l, The New England Batholith, eastern Australia. Geochemical variations intime and space, J. of Geophysical Research,vol. 86, no B11, pp 10530 - 10544

Shido, F., and Miyashiro, A., 1959, Hornblendes of basic meta- morphic rocks, Univ. Tokyo, Fac. Sci. J., sec.II, vol.12, pp 85 - 102

Smith, K.L., et al, 1986, Optical and electron microscope investigation of temperature-dependent micro-structures in anorthoclase, Can. J. Earth Sci.vol. 24, pp 528 - 543

Smithson, S.B. 1963, Granite studies: II. The Precambrian Fla granite, a geological and geophysicalinvetsigation. Norges geol. undersok. 219, 212pp

Sobolev, V.L., 1970, The Facies of Metamorphism., Translated by Brown, D.A., ANU, Dept of Geology Publ.,1972

Speer, J.A.,1981, The nature and magnetic expression of isograds in the contact aureole of the Liberty Hill pluton, South Carolina, Geol. Soc. of Amer. Bulletin, Pt 11, vol.92, pp 1262 - 1358

Speer, J. A., 1981, Petrology of cordierite- and almandine- bearing granitoid plutons of the southernAppalachian Piedmont, USA, Can. Mineralogist,vol. 19, pp 35 - 46

Steiger, R.H., and Hart, S.R., 1967, The microcline-orthoclase transition within a contact aureole, Amer.Mineralogist, vol. 52, pp 87 - 116

Stewart, D.B., and von Limbach, D., 1967, Thermal expansion of low and high albite, Amer. Mineralogist, vol.52 pp 389 - 413

Stewart, D.B. 1975, Lattice parameters, composition, and Al/ Si order in alkali feldspars, Feldspar Mineralogy Short Course Notes, vol. 2, Min. Soc. of Amer., pp St-1 - St-30

Stormer, J.C., Jr. 1975, A practical two-feldspar geothermometer Amer. Minealogist, vol.60, pp 667 - 674

Swanson, S.E., et al, 1988, Petrogenesis of the Ear Mountain Tin Granite, Seward Peninsula, Alaska, EconomicGeol., vol.83, pp 46 - 61

Suppe, J., 1985, Principles of structural geology, Prentice- Hall Inc., Englewood Cliffs, New Jersey.

Teale, G.S.,1974, Thermal metamorphic schists adjacent to the Walcha Road Adamellite, New England, New South Wales, Unpub. thesis for B.A. (Hons), Macquarie Univ.

Tilling, R.I., 1968, Zonal distribution of variations instructural state of alkali feldspar within the Rader Creek Pluton, Boulder Batholith, Montana, J. of Petrology, vol. 9, pt 3, pp 331-357

Turner, F.J., 1968, Metamorphic petrology: New York, McGrawHill, 403pp

Turner, F., 1981, Metamorphic Petrology, Hemisphere Publi- cations, San Francisco.

Vaniman, D.,1978, Crystallization history of sector-zoned microcline megacrysts from the Godani Valley pluton, Nigeria, Mineralogical Mag., vol.42, pp 443 - 451

Vernon, R.H., 1976, Metamorphic Processes, George Allen & Unwin London.

Vernon, R.H., 1977, Microfabric of mica aggregates in partly recrystallized biotite, Contrib. Mineral. Petrol. vol. 61, pp 175 - 185

Vernon, R.H., 1987, Evidence of syndeformational contact meta- morphism from porphyroblast-matrix micro-structural relationships, Tectonophysics,in press

White, A.J.R., et al, 1974, Geologic setting and emplacement of some Australian paleozoic batholiths and implications for intrusive mechanisms, Pacific Geol., vol.8, pp 159 - 171

Whitney, J.A., and Stormer, J.C., Jr.,1977, Two-feldspar geothermometry, geobarometry in mesozonal granitic intrusions: three examples from the Piedmont of Georgia, Contrib. Mineral. Petrol. vol. 63, pp 51

Winchell, A.N., 1943, Variations in composition and properties of the calciferous amphiboles, Amer. Mineral.vol.28, pp 27 - 50

Winkler, H.G.F., 1967, Petrogenesis of metamorphic rocks, 2nd ed Springer Verlag, New York.

Wiseman, J.D.H. 1934, The central and southwest Highlandepidiorites : a study in progressive metamorphism Quart.J.geol.Soc.London., vol90, pp354-417

Wright, T.L., 1967, The microcline-orthoclase transformation in the contact aureole of the Eldora Stock, Colorado Amer. Mineralogist, vol.52, pp 117 - 136

Wright, T.L., 1968, X-ray and optical Study of alkali feldspar: An x-ray method for determining the composition and structural state from measurement of 20 values for three reflections, Amer. Mineralogist, vol.

## D . 2 . A P P E N D I X  1 : M E T H O D S

A . K-FELDSPAR SEPARATES

B . METABASALTIC BULK ROCK ANALYSIS

C . STRAIN ANALYSIS

## APPENDIX 1 : ANALYTICAL METHODS

### A. K-FELDSPAR SEPARATES :

Potassium feldspar samples were prepared for x-ray diffraction analysis by crushing and sifting (250-mesh) the granite samples, washing repeatedly to remove the fine dust and then using either a tetrabromoethane - acetone mix or a sodium metatungstate - water mix (the sodium metatungstate method proved the more effective, as it produced the same quality of separation in half the time and has a considerably higher recovery rate). The density range was determined by using albite and orthoclase density chips. The resultin K-feldspar separate was further crushed and adhered to glass slides for x-ray analysis.

The x-ray diffraction runs were performed at 0.5 degrees per minute, 1cm per minute and on settings of Imp/s = 2 X 10^3 and T(s) = 2 for the diffractometer. The following angular ranges were run for the peaks given :

| | ANGULAR RANGE | | PEAKS | |
|---|---|---|---|---|
| (i) | 27 - 32 degrees | = | 131 and 131 | (STRUCTURAL STATE) |
| (ii) | 20 - 22 degrees | = | 201 | |
| (iii) | 41 - 42 degrees | = | 060 | (COMPOSITION) |
| (iv) | 50 - 51 degrees | = | 204 | |

**B. METBASALTIC BULK ROCK ANALYSIS :**

The metabasaltic samples were prepared for bulk rock analysis on the electron microprobe, using hte method of making glass buttons outlined by Gulson (1968), Reed (1970) and Nicholls ( 1974).

The metabasaltic samples were crushed to a fine pwder after removal of oxidised rims and veining from the field samples. A small amount of this powder for each sample was placed on a molybdenum strip and subjected to high votlages for one minute in an evacuated chamber to avoid oxidation and to homogeneously melt the sample. The voltage was then rapidly reduced and the chamber filled with argon gas to quench the sample and leave a glass button of the original metabasaltic sample. These glass buttons were then mounted on a microprobe slide and probed using a computed area analysis to obtain an average bulk rock composition for each sample.

Because the method uses the microprobe, the Fe2O3 and FeO propotions were recalculated afterwards using a standard proportion for basaltic samples.

**C. STRAIN ANALYSIS :**

Two oriented and htree randomly oriented samples were collected from the field and cut with 3 perpendicular faces ( for the oriented samples these were a known horizonal plane and two vertical planes).

Quartz aggregates on all 3 faces were then measured for there long and short axes and their ratio (long/short) calculated along with the aggreagtes orientation with respect to a fixed reference point for each sample ( the same apex for the two oriented samples).

Using a strain ratio analysis program (EIGENR.EXE) supplied by Dr. D.W. Durney, the following data was obtained and a resulting estimate of shortening calculated :

(following page)

## EIGEN VALUES AND VECTORS FOR THE QUARTZ STRAN ANALYSES

| SAMPLE | PLUNGE / DIRECTION | | | PRINCIPLE RATIO | | |
|---|---|---|---|---|---|---|
| | X | Y | Z | X | Y | Z |
| **ORIENTED :** | | | | | | |
| MU45842 | 46.21/052.24 | 17.77/161.87 | -38.40/086.58 | 3.25 | 1.26 | 1 |
| ( 300 m ) | | | | | | |
| MU45808 | 36.48/046.74 | 19.30/153.50 | -44.23/083.43 | 1.83 | 1.14 | 1 |
| ( 6 km ) | | | | | | |
| **UNORIENTED :** | | | | | | |
| MU45858 | 28.78/027.30 | 08.75/122.15 | -59.67/047.41 | 1.33 | 1.17 | 1 |
| MU45853 | 47.69/037.84 | 23.28/156.06 | -33.01/082.30 | 1.77 | 1.31 | 1 |
| MU45868 | 36.31/043.50 | 50.82/205.60 | -13.67/057.45 | 2.57 | 1.12 | 1 |
| | | **UNORIENTED AVERAGE ( Rav ) =** | | 1.89 | 1.20 | 1 |
| **ESTIMATED ORIENTED STRAIN DIFFERENCES :** | | | | | | |
| | R | R(MU45808)/Rav | = | 0.97 | 0.95 | 1 |
| | R | R(MU45842)/Rav | = | 1.72 | 1.05 | 1 |

now, $V = X \cdot Y \cdot Z$ therefore V(MU45808) = 0.92

V(MU45843) = 1.81

now shortening, $e_3 = 1 - \frac{1}{3V}$ therefore,

**$e_3$ (MU45808) = 2.82 %**

expressed as a percentage

**$e_3$ (MU45843) = -17.90 %**

## D . 3 . A P P E N D I X 2 : D A T A

- BENDEMEER GRID REFERENCES
  ( BENDEMEER AND HANING 1:25000 SHEETS )
- YARROWYCK GRID REFERENCES
  ( YARROWYCK AND BALALA 1:25000 SHEETS )
- BENDEMEER TRICLINICITY VALUES
- YARROWYCK TRICLINICITY VALUES
- AMPHIBOLE MICROPROBE ANALYSES FOR THE BENDEMEER METABASALTIC SAMPLES

## BENDEMEER GRID REFERENCES

| MU NUMBER | GRID REF. | MU NUMBER | GRID REF. | MU NUMBER | GRID REF. |
|---|---|---|---|---|---|
| 45801 | - | 45831 | 315854 | 45861 | 288864 |
| 45802 | - | 45832 | 319856 | 45862 | 288870 |
| 45803 | - | 45833 | 324853 | 45863 | 285870 |
| 45804 | - | 45834 | 324852 | 45864 | 282874 |
| 45805 | - | 45835 | 295836 | 45865 | 277876 |
| 45806 | - | 45836 | 296837 | 45866 | 279883 |
| 45807 | 248922 | 45837 | 296838 | 45867 | 275871 |
| 45808 | 252907 | 45838 | 297841 | 45868 | 271867 |
| 45809 | 255895 | 45839 | 237845 | 45869 | 277850 |
| 45810 | 255884 | 45840 | 235844 | 45870 | 213883 |
| 45811 | 256876 | 45841 | 242845 | 45871 | 216880 |
| 45812 | 257873 | 45842 | 242846 | 45872 | 217876 |
| 45813 | 259863 | 45843 | 242848 | 45873 | 219874 |
| 45814 | 258857 | 45844 | 247852 | 45874 | 223871 |
| 45815 | 257854 | 45845 | 245854 | 45874a | 225872 |
| 45816 | 256850 | 45846 | 243858 | 45875 | 218886 |
| 45817 | 257849 | 45847 | 242861 | 45876 | 230863 |
| 45818 | 295877 | 45848 | 239864 | 45877 | 231849 |
| 45819 | 226867 | 45849 | 237867 | 45878 | 285893 |
| 45820 | 228859 | 45850 | 236872 | 45879 | 290890 |
| 45821 | 229860 | 45851 | 235875 | 45880 | 297886 |
| 45822 | 301843 | 45852 | 234878 | 45881 | 297892 |
| 45823 | 302844 | 45853 | 231883 | 45882 | 301878 |
| 45824 | 303846 | 45854 | 233849 | 45883 | 306914 |
| 45825 | 304847 | 45855 | 305852 | 45884 | 312902 |
| 45826 | 305849 | 45856 | 302852 | 45885 | 318902 |
| 45827 | 307850 | 45857 | 301853 | 45886 | 319901 |
| 45828 | 308852 | 45858 | 299854 | 45887 | 324867 |
| 45829 | 311853 | 45859 | 296856 | 45888 | 353914 |
| 45830 | 314853 | 45860 | 293858 | | |

| MU NUMBER | GRID REF. | MU NUMBER | GRID REF. | MU NUMBER | GRID REF. |
|---|---|---|---|---|---|
| | | | | 45992 | 208877 |
| 45901 | 232848 | 45947 | 241845 | 45992a | 205883 |
| 45902 | 229844 | 45948 | 234844 | 45993 | 203885 |
| 45903 | 228844 | 45949 | 184830 | 45994 | 199881 |
| 45904 | 224843 | 45950 | 186826 | 45995 | 200879 |
| 45905 | 217844 | 45951 | 187825 | 45996 | 195877 |
| 45906 | 215845 | 45952 | 190824 | 45997 | 194876 |
| 45907 | 213845 | 45953 | 193825 | 45998 | 194871 |
| 45908 | 212847 | 45954 | 195823 | 45999 | 189859 |
| 45909 | 208847 | 45955 | 198822 | 46000 | 187856 |
| 45910 | 207847 | 45956 | 200820 | 46001 | 180854 |
| 45911 | 206847 | 45957 | 299854 | 46002 | 178857 |
| 45912 | 206849 | 45958 | 222840 | 46003 | 178864 |
| 45913 | 205852 | 45959 | 222840 | 46004 | 179869 |
| 45914 | 207853 | 45960 | 221843 | 46005 | 180871 |
| 45915 | 211860 | 45961 | 219841 | 46006 | 180873 |
| 45916 | 212861 | 45962 | 216840 | 46007 | 182874 |
| 45917 | 214862 | 45963 | 215838 | 46008 | 183877 |
| 45918 | 218864 | 45964 | 205837 | 46009 | 189870 |
| 45919 | 219864 | 45965 | 207835 | 46010 | 192867 |
| 45920 | 220865 | 45966 | 209835 | 46011 | 297805 |
| 45921 | 223865 | 45967 | 207835 | 46012 | 296805 |
| 45922 | 224865 | 45968 | 210833 | 46013 | 295805 |
| 45923 | 225867 | 45969 | 209831 | 46014 | 294804 |
| 45924 | 226867 | 45970 | 208828 | 46015 | 294803 |
| 45925 | 223858 | 45971 | 207825 | 46016 | 293802 |
| 45926 | 224858 | 45972 | 205823 | 46017 | 292802 |
| 45927 | 325851 | 45972a | 263779 | 46018 | 292800 |
| 45928 | 326849 | 45973 | 277785 | 46019 | 289799 |
| 45929 | 326848 | 45974 | 273782 | 46020 | 288798 |
| 45930 | 328847 | 45975 | 269779 | 46021 | 290796 |
| 45931 | 329844 | 45976 | 264777 | 46022 | 291795 |
| 45932 | 329844 | 45977 | 266774 | 46023 | 291793 |
| 45933 | 328844 | 45978 | 266779 | 46024 | 296795 |
| 45934 | 327843 | 45979 | 264779 | 46025 | 301799 |
| 45935 | 326843 | 45980 | 222841 | 46026 | 301802 |
| 45936 | 325844 | 45981 | 223841 | 46027 | 300803 |
| 45937 | 324843 | 45982 | 225841 | 46028 | 299807 |
| 45938 | 322842 | 45983 | 226840 | 46029 | 304807 |
| 45939 | 321838 | 45984 | 208863 | 46030 | 305807 |
| 45940 | 317833 | 45985 | 211864 | 46031 | 306810 |
| 45941 | 316831 | 45986 | 212864 | 46032 | 309819 |
| 45942 | 314830 | 45987 | 213867 | 46033 | 311818 |
| 45943 | 312829 | 45988 | 214870 | 46034 | 307815 |
| 45944 | 311827 | 45989 | 213874 | 46035 | 296809 |
| 45945 | 307827 | 45990 | 211876 | 46036 | 222870 |
| 45946 | 235844 | 45991 | 209876 | | |

| MU NUMBER | GRID REF. | MU NUMBER | GRID REF. | MU NUMBER | GRID REF. |
|---|---|---|---|---|---|
| 46051 | 235837 | 46056 | 238843 | 46061 | 245795 |
| 46052 | 234838 | 46057 | 241844 | 46062 | 258787 |
| 46053 | 233840 | 46058 | 282838 | 46063 | 262781 |
| 46054 | 232842 | 46059 | 283841 | 46063a | 299817 |
| 46055 | 236844 | 46060 | 205817 | 46064 | 225836 |
| 46071 | 320900 | 46074 | 330884 | 46077 | 338911 |
| 46072 | 328902 | 46075 | 335891 | 46078 | 347912 |
| 46073 | 323875 | 46076 | 336900 | | |

# YARROWYCK GRID REFERENCES

| MU NUMBER | GRID REF. | MU NUMBER | GRID REF. | MU NUMBER | GRID REF |
|---|---|---|---|---|---|
| 46101 | 461267 | 46124 | 406248 | 46147 | 438257 |
| 46102 | 446289 | 46125 | 404146 | 46148 | 453233 |
| 46103 | 447288 | 46126 | 407246 | 46149 | 463224 |
| 46104 | 448286 | 46127 | 428256 | 46150 | 397237 |
| 46105 | 451284 | 46128 | 465293 | 46151 | 405202 |
| 46106 | 453277 | 46129 | 464294 | 46152 | 403207 |
| 46107 | 449271 | 46130 | 464297 | 46153 | 402212 |
| 46108 | 444269 | 46131 | 458298 | 46154 | 402215 |
| 46109 | 441273 | 46132 | 457301 | 46155 | 400219 |
| 46110 | 439273 | 46133 | 456302 | 46156 | 399224 |
| 46111 | 438275 | 46134 | 453303 | 46157 | 488292 |
| 46112 | 437276 | 46135 | 452302 | 46158 | 485292 |
| 46113 | 439242 | 46136 | 452303 | 46159 | 482292 |
| 46114 | 435244 | 46137 | 396226 | 46160 | 477292 |
| 46115 | 434247 | 46138 | 390261 | 46161 | 473292 |
| 46116 | 429256 | 46139 | 469235 | 46162 | 479283 |
| 46117 | 396247 | 46140 | 452234 | 46163 | 485269 |
| 46118 | 396244 | 46141 | 451247 | 46164 | 477266 |
| 46119 | 399240 | 46142 | 452248 | 46165 | 471266 |
| 46120 | 402237 | 46143 | 450251 | 46166 | 476268 |
| 46121 | 404232 | 46144 | 447250 | 46167 | 457228 |
| 46122 | 383238 | 46145 | 438277 | 46168 | photo sample near bridge |
| 46123 | 406246 | 46146 | 438277 | | |

| MU NUMBER | GRID REF. | MU NUMBER | GRID REF. | MU NUMBER | GRID REF. |
|---|---|---|---|---|---|
| 46201 | 456302 | 46236 | 346260 | 46271 | 458346 |
| 46202 | 453303 | 46237 | 347257 | 46272 | 457344 |
| 46203 | 459315 | 46238 | 348255 | 46273 | 456344 |
| 46204 | 455311 | 46239 | 355253 | 46274 | 455344 |
| 46205 | 470326 | 46240 | 356252 | 46275 | 454342 |
| 46206 | 471326 | 46241 | 357351 | 46276 | 453341 |
| 46207 | 477326 | 46242 | 358249 | 46277 | 452341 |
| 46208 | 478327 | 46243 | 359249 | 46278 | 438252 |
| 46209 | 481332 | 46244 | 470297 | 46279 | 436254 |
| 46210 | 482334 | 46245 | 467301 | 46280 | 434256 |
| 46211 | 484337 | 46246 | 466305 | 46281 | 432258 |
| 46212 | 484340 | 46247 | 466308 | 4282 | 337274 |
| 46213 | 480350 | 46248 | 466312 | 46283 | 348255 |
| 46214 | 476356 | 46249 | 471314 | 46284 | 349253 |
| 46215 | 473357 | 46250 | 473319 | 46285 | 348250 |
| 46216 | 462343 | 46251 | 478318 | 46286 | 349247 |
| 46217 | 461340 | 46252 | 481318 | 46287 | 351245 |
| 46218 | 460336 | 46253 | 491314 | 46288 | 354243 |
| 46219 | 460335 | 46254 | 490312 | 46289 | 355241 |
| 46220 | 381247 | 46255 | 489304 | 46290 | 355240 |
| 46221 | 382246 | 46256 | 488302 | 46291 | 355239 |
| 46222 | 382245 | 46257 | 488301 | 46292 | 355235 |
| 46223 | 381244 | 46258 | 488299 | 46293 | 357232 |
| 46224 | 382244 | 46259 | 487298 | 46294 | 362228 |
| 46225 | 383244 | 46260 | 485294 | 46295 | 365226 |
| 46226 | 384243 | 46261 | 452234 | 46296 | 367224 |
| 46227 | 383240 | 46262 | 457235 | 46297 | 372223 |
| 46228 | 383239 | 46263 | 461233 | 46298 | 372225 |
| 46229 | 383229 | 46264 | - | 46299 | 370233 |
| 46230 | 383226 | 46265 | 469238 | 46300 | 372235 |
| 46231 | 397229 | 46266 | 462242 | 46301 | 374242 |
| 46232 | 397231 | 46267 | 460242 | 46302 | 377245 |
| 46233 | 389243 | 46268 | 442250 | 46303 | 381246 |
| 46234 | 353260 | 46269 | 446247 | | |
| 46235 | 350261 | 46270 | - | | |

| MU NUMBER | GRID REF. | MU NUMBER | GRID REF. | MU NUMBER | GRID REF. |
|---|---|---|---|---|---|
| 46351 | 414305 | 46367 | 464331 | 46383 | 355258 |
| 46352 | 437276 | 46368 | 462328 | 46384 | 353262 |
| 46353 | 419296 | 46369 | 385251 | 46385 | 374252 |
| 46354 | 407284 | 46370 | 384250 | 46386 | 369254 |
| 46355 | 479256 | 46371 | 383250 | 46387 | 469337 |
| 46356 | 434267 | 46372 | 383247 | 46388 | 465344 |
| 46357 | 397246 | 46373 | 386248 | 46389 | 453339 |
| 46358 | 404247 | 46374 | 381247 | 46390 | 343278 |
| 46359 | 417254 | 46375 | 383244 | 46391 | 382246 |
| 46360 | 427255 | 46376 | 384243 | 46392 | 437276 |
| 46361 | 442292 | 46377 | 383246 | | |
| 46362 | 462326 | 46378 | 363256 | | |
| 46363 | 463325 | 46379 | 362255 | | |
| 46364 | 468326 | 46380 | 359256 | | |
| 46365 | 462334 | 46381 | 357256 | | |
| 46366 | 463333 | 46382 | 356257 | | |
| 46401 | 359256 | 46405 | 356252 | 46409 | 364250 |
| 46402 | 357256 | 46406 | 374252 | 46410 | 364252 |
| 46403 | 355257 | 46407 | 369254 | 46411 | 364254 |
| 46404 | 355253 | 46408 | 364248 | 46412 | 364255 |

## BENDEMEER CONTOURS MAP 2

| MU NUMBER | TRICLINICITY VALUE | MU NUMBER | TRICLINICITY VALUE |
|---|---|---|---|
| 45801 | 0 | 45846 | .1268 |
| 45802 | 0 | 45847 | .7017 |
| 45803 | 0 | 45848 | .6423 |
| 45804 | 0 | 45849 | .6597 |
| 45805 | 0 | 45850 | .5726 |
| 45806 | 0 | 45851 | .4333 |
| 45807 | .3618 | 45852 | .4810 |
| 45808 | .6067 | 45853 | .3314 |
| 45809 | .5122 | 45854 | .1371 |
| 45810 | .6841 | 45855 | .1512 |
| 45811 | .7524 | 45856 | .1417 |
| 45812 | .7212 | 45857 | .3586 |
| 45813 | .7853 | 45858 | .3860 |
| 45814 | .1574 | 45859 | .3784 |
| 45815 | 0 | 45860 | .7067 |
| 45816 | 0 | 45861 | .8331 |
| 45817 | 0 | 45862 | .7788 |
| 45818 | .1214 | 45863 | .6150 |
| 45819 | .1470 | 45864 | .7400 |
| 45820 | .7125 | 45865 | .6892 |
| 45821 | .1600 | 45866 | .6816 |
| 45822 | 0 | 45867 | .7548 |
| 45823 | 0 | 45868 | .6548 |
| 45824 | 0 | 45869 | .1290 |
| 45825 | .1061 | 45870 | .5405 |
| 45826 | 0 | 45871 | .5294 |
| 45827 | 0 | 45872 | .5767 |
| 45828 | .1106 | 45873 | .4632 |
| 45829 | 0 | 45874 | .3971 |
| 45830 | 0 | 45875 | .6169 |
| 45831 | 0 | 45876 | .4820 |
| 45832 | 0 | 45877 | .5721 |
| 45833 | 0 | 45878 | .7862 |
| 45834 | 0 | 45879 | .6735 |
| 45835 | 0 | 45880 | .7993 |
| 45836 | 0 | 45881 | .7380 |
| 45837 | 0 | 45882 | .7353 |
| 45838 | 0 | 45883 | .6816 |
| 45839 | .0300 | 45884 | .6171 |
| 45840 | 0 | 45885 | .1602 |
| 45841 | 0 | 45886 | 0 |
| 45842 | 0 | 45887 | .1107 |
| 45843 | 0 | 45888 | 0 |
| 45844 | 0 | | |
| 45845 | 0 | | |

## YARROWYCK CONTOURS MAP 5

| MU NUMBER | TRICLINICITY VALUE | MU NUMBER | TRICLINICITY VALUE |
|---|---|---|---|
| 46101 | .180 | 46141 | 0 |
| 46102 | .300 | 46142 | .150 |
| 46103 | .700 | 46143 | .160 |
| 46104 | .010 | 46144 | .180 |
| 46105 | 0 | 46145 | .010 |
| 46106 | .130 | 46146 | .460 |
| 46107 | 0 | 46147 | .010 |
| 46108 | .110 | 46148 | .720 |
| 46109 | .070 | 46149 | .290 |
| 46110 | .010 | 46150 | .120 |
| 46111 | .460 | 46151 | .160 |
| 46112 | 0 | 46152 | .350 |
| 46113 | .230 | 46153 | .100 |
| 46114 | .010 | 46154 | .550 |
| 46115 | .010 | 46155 | .470 |
| 46116 | 0 | 46156 | .420 |
| 46117 | 0 | 46157 | .250 |
| 46118 | 0 | 46158 | .170 |
| 46119 | .820 | 46159 | .160 |
| 46120 | .010 | 46160 | .170 |
| 46121 | .010 | 46161 | .390 |
| 46122 | .732 | 46162 | .370 |
| 46123 | .720 | 46163 | .250 |
| 46124 | 0 | 46164 | .160 |
| 46125 | 0 | 46165 | .150 |
| 46126 | 0 | 46166 | .140 |
| 46127 | .010 | 46167 | .250 |
| 46128 | .130 | 46168 | 0 |
| 46129 | .010 | 46169 | 0 |
| 46130 | 0 | 46170 | 0 |
| 46131 | .010 | 46171 | 0 |
| 46132 | .700 | 46172 | 0 |
| 46133 | .300 | 46173 | 0 |
| 46134 | 0 | 46200 | .201 |
| 46135 | 0 | 46201 | .721 |
| 46136 | 0 | 46202 | .513 |
| 46137 | .210 | 46203 | .342 |
| 46138 | .730 | | |
| 46139 | .150 | | |
| 46140 | .340 | | |

| | | | | | | | | | | | | | | | | | |
|---|---|---|---|---|---|---|---|---|---|---|---|---|---|---|---|---|---|
| SiO2 | 46.32 | 6.7660 | 47.99 | 7.0702 | 46.79 | 6.8634 | 48.73 | 7.0805 | 47.38 | 6.9165 | 50.75 | 7.2371 | 49.87 | 7.1212 | 46.27 | 6.8334 | 47.96 | 6.9368 |
| TiO2 | 0.50 | 0.0548 | 0.34 | 0.0381 | 0.34 | 0.0372 | 0.26 | 0.0286 | 0.51 | 0.0558 | 0.36 | 0.0381 | 0.45 | 0.0484 | 0.29 | 0.0321 | 0.70 | 0.0759 |
| Al2O3 | 10.76 | 1.8502 | 7.45 | 1.2919 | 9.26 | 1.5993 | 7.56 | 1.2938 | 8.80 | 1.5126 | 6.02 | 1.0106 | 6.97 | 1.1715 | 9.31 | 1.6189 | 8.44 | 1.4375 |
| FeO | 17.02 | 2.0787 | 16.63 | 2.0485 | 16.95 | 2.0797 | 16.85 | 2.0473 | 17.09 | 2.0870 | 16.36 | 1.9510 | 16.36 | 1.9532 | 17.15 | 2.1180 | 17.30 | 2.0923 |
| MnO | 0.26 | 0.0318 | 0.28 | 0.0344 | 0.27 | 0.0339 | 0.26 | 0.0314 | 0.21 | 0.0262 | 0.29 | 0.0352 | 0.23 | 0.0278 | 0.28 | 0.0349 | 0.26 | 0.0314 |
| MgO | 10.74 | 2.3380 | 12.41 | 2.7252 | 11.97 | 2.6173 | 12.60 | 2.7302 | 12.05 | 2.6223 | 13.69 | 2.9093 | 13.35 | 2.8412 | 11.67 | 2.5697 | 12.11 | 2.6106 |
| CaO | 11.81 | 1.8489 | 11.40 | 1.7998 | 11.38 | 1.7880 | 11.65 | 1.8141 | 11.38 | 1.7799 | 12.21 | 1.8663 | 12.34 | 1.8881 | 11.60 | 1.8358 | 11.89 | 1.8422 |
| Na2O | 1.84 | 0.5221 | 1.57 | 0.4474 | 1.85 | 0.5275 | 1.43 | 0.4038 | 1.79 | 0.5053 | 1.15 | 0.3192 | 1.29 | 0.3562 | 1.82 | 0.5218 | 1.58 | 0.4441 |
| K2O | 0.23 | 0.0434 | 0.13 | 0.0243 | 0.16 | 0.0296 | 0.15 | 0.0281 | 0.17 | 0.0321 | 0.12 | 0.0216 | 0.15 | 0.0266 | 0.20 | 0.0380 | 0.19 | 0.0348 |
| | 99.48 | 15.5340 | 98.19 | 15.4797 | 98.98 | 15.5759 | 99.51 | 15.4579 | 99.38 | 15.5378 | 100.95 | 15.3884 | 101.00 | 15.4343 | 98.60 | 15.6025 | 100.41 | 15.5058 |
| Mg# | | 52.9 | | 57.1 | | 55.7 | | 57.1 | | 55,7 | | 59.9 | | 59.3 | | 54.8 | | 55.5 |
| SiO2 | 47.55 | 6.8458 | 48.94 | 7.0877 | 44.79 | 6.6021 | 50.72 | 7.2715 | 50.23 | 7.1939 | 47.47 | 6.8357 | 46.67 | 6.8662 | 48.97 | 7.0369 | 48.59 | 7.0085 |
| TiO2 | 0.34 | 0.0371 | 0.37 | 0.0407 | 0.51 | 0.0564 | 0.23 | 0.0247 | 0.17 | 0.0187 | 0.80 | 0.0869 | 0.70 | 0.0776 | 0.54 | 0.0586 | 0.58 | 0.0628 |
| Al2O3 | 9.63 | 1.6325 | 6.68 | 1.1395 | 11.52 | 1.9986 | 5.80 | 0.9790 | 6.61 | 1.1148 | 9.14 | 1.5494 | 8.95 | 1.5502 | 7.70 | 1.3027 | 7.77 | 1.3192 |
| FeO | 16.47 | 1.9824 | 16.83 | 2.0386 | 17.57 | 2.1666 | 16.24 | 1.9466 | 15.74 | 1.8848 | 17.96 | 2.1635 | 17.78 | 2.1881 | 17.02 | 2.0455 | 17.20 | 2.0748 |
| MnO | 0.26 | 0.0318 | 0.29 | 0.0353 | 0.29 | 0.0366 | 0.25 | 0.0299 | 0.25 | 0.0304 | 0.32 | 0.0384 | 0.29 | 0.0362 | 0.27 | 0.0323 | 0.23 | 0.0286 |
| MgO | 12.37 | 2.6539 | 13.22 | 2.8536 | 10.87 | 2.3880 | 13.66 | 2.9186 | 13.75 | 2.9364 | 11.68 | 2.5075 | 11.48 | 2.5174 | 12.76 | 2.7340 | 12.45 | 2.6774 |
| CaO | 11.96 | 1.8445 | 12.42 | 1.9273 | 11.07 | 1.7483 | 12.30 | 1.8889 | 12.09 | 1.8560 | 12.05 | 1.8590 | 11.28 | 1.7778 | 11.82 | 1.8196 | 12.16 | 1.8796 |
| Na2O | 1.82 | 0.5069 | 1.17 | 0.3291 | 2.28 | 0.6521 | 1.04 | 0.2892 | 1.31 | 0.3626 | 1.75 | 0.4880 | 1.75 | 0.4996 | 1.49 | 0.4159 | 1.45 | 0.4051 |
| K2O | 0.18 | 0.0338 | 0.14 | 0.0257 | 0.18 | 0.0332 | 0.10 | 0.0182 | 0.13 | 0.0240 | 0.17 | 0.0318 | 0.17 | 0.0310 | 0.15 | 0.0271 | 0.15 | 0.0274 |
| | 100.58 | 15.5687 | 100.07 | 15.4775 | 99.07 | 15.6819 | 100.33 | 15.3665 | 100.28 | 15.4216 | 101.33 | 15.5602 | 99.07 | 15.5441 | 100.72 | 15.4727 | 100.58 | 15.4834 |
| Mg# | | 57.2 | | 58.3 | | 52.4 | | 60.0 | | 60.9 | | 53.7 | | 53.5 | | 57.? | | 56.3 |
| SiO2 | 46.15 | 6.7197 | 47.98 | 6.9913 | 48.28 | 7.0424 | 47.60 | 7.0584 | 49.76 | 7.1993 | 46.05 | 6.7990 | 49.85 | 7.1258 | 48.52 | 7.0434 | 48.78 | 7.1732 |
| TiO2 | 0.83 | 0.0907 | 0.36 | 0.0394 | 0.33 | 0.0367 | 0.40 | 0.0446 | 0.59 | 0.0640 | 0.46 | 0.0515 | 0.23 | 0.0244 | 0.23 | 0.0252 | 0.13 | 0.0142 |
| Al2O3 | 10.13 | 1.7370 | 8.26 | 1.4168 | 8.92 | 1.5326 | 7.06 | 1.2327 | 6.11 | 1.0409 | 9.87 | 1.7154 | 7.31 | 1.2304 | 7.87 | 1.3451 | 6.79 | 1.1754 |
| FeO | 18.05 | 2.1973 | 16.57 | 2.0193 | 15.89 | 1.9383 | 16.69 | 2.0699 | 16.03 | 1.9401 | 16.64 | 2.0549 | 15.92 | 1.9037 | 16.22 | 1.9691 | 15.97 | 1.9638 |
| MnO | 0.25 | 0.0309 | 0.27 | 0.0334 | 0.24 | 0.0297 | 0.18 | 0.0231 | 0.28 | 0.0342 | 0.24 | 0.0305 | 0.30 | 0.0369 | 0.23 | 0.0286 | 0.22 | 0.0268 |
| MgO | 11.02 | 2.3923 | 12.57 | 2.7307 | 11.62 | 2.5269 | 12.59 | 2.7828 | 13.65 | 2.9451 | 11.65 | 2.5641 | 13.49 | 2.8740 | 13.05 | 2.8242 | 12.85 | 2.8181 |
| CaO | 11.91 | 1.8585 | 11.46 | 1.7893 | 11.13 | 1.7401 | 11.65 | 1.8505 | 11.61 | 1.7996 | 11.26 | 1.7817 | 11.94 | 1.8288 | 11.40 | 1.7730 | 11.65 | 1.8351 |
| Na2O | 1.95 | 0.5498 | 1.58 | 0.4457 | 2.06 | 0.5821 | 1.41 | 0.4055 | 1.28 | 0.3586 | 1.91 | 0.5479 | 1.41 | 0.3897 | 1.67 | 0.4702 | 1.43 | 0.4071 |
| K2O | 0.18 | 0.0343 | 0.17 | 0.0316 | 0.16 | 0.0291 | 0.15 | 0.0280 | 0.13 | 0.0245 | 0.19 | 0.0365 | 0.15 | 0.0277 | 0.14 | 0.0260 | 0.14 | 0.0257 |
| | 100.47 | 15.6105 | 99.22 | 15.4974 | 98.63 | 15.4579 | 97.74 | 15.4956 | 99.44 | 15.4062 | 98.29 | 15.5814 | 100.60 | 15.4414 | 99.34 | 15.5049 | 97.95 | 15.4394 |
| Mg# | | 52.1 | | 57.5 | | 56.6 | | 57.3 | | 60.3 | | 55.5 | | 60.2 | | 58.9 | | 58.9 |
| SiO2 | 49.03 | 7.2430 | 51.14 | 7.3456 | 46.72 | 6.8897 | 48.51 | 7.0920 | | | | | | | | | | |
| TiO2 | 0.21 | 0.0235 | 0.12 | 0.0133 | 0.61 | 0.0676 | 0.50 | 0.0549 | | | | | | | | | | |
| Al2O3 | 6.13 | 1.0661 | 5.26 | 0.8901 | 9.84 | 1.7080 | 8.38 | 1.4421 | | | | | | | | | | |
| FeO | 15.65 | 1.9336 | 16.50 | 1.9820 | 16.49 | 2.0337 | 15.68 | 1.9165 | | | | | | | | | | |
| MnO | 0.25 | 0.0319 | 0.27 | 0.0323 | 0.23 | 0.0289 | 0.28 | 0.0343 | | | | | | | | | | |
| MgO | 13.23 | 2.9145 | 13.68 | 2.9289 | 10.99 | 2.4149 | 11.58 | 2.5247 | | | | | | | | | | |
| CaO | 11.27 | 1.7834 | 12.09 | 1.8610 | 10.97 | 1.7340 | 11.38 | 1.7828 | | | | | | | | | | |
| Na2O | 1.32 | 0.3782 | 0.95 | 0.2636 | 2.06 | 0.5895 | 1.90 | 0.5385 | | | | | | | | | | |
| K2O | 0.15 | 0.0274 | 0.11 | 0.0195 | 0.15 | 0.0290 | 0.14 | 0.0268 | | | | | | | | | | |
| | 97.25 | 15.4016 | 100.11 | 15.3362 | 98.07 | 15.4953 | 98.35 | 15.4126 | | | | | | | | | | |
| Mg# | | 60.1 | | 59.6 | | 54.3 | | 56.8 | | | | | | | | | | |

| | | | | | | | | | | | | | | | | | |
|---|---|---|---|---|---|---|---|---|---|---|---|---|---|---|---|---|---|
| SiO2 | 49.02 | 7.0782 | 47.59 | 6.9787 | 52.62 | 7.5191 | 48.24 | 7.0582 | 50.84 | 7.3319 | 49.57 | 6.9081 | 49.93 | 7.1959 | 56.53 | 7.2462 | 51.61 | 7.3942 |
| TiO2 | 0.36 | 0.0391 | 0.42 | 0.0468 | 0.24 | 0.0261 | 0.54 | 0.0594 | 0.22 | 0.0242 | 0.36 | 0.0379 | 0.33 | 0.0362 | 0.18 | 0.0176 | 0.26 | 0.0276 |
| Al203 | 8.09 | 1.3753 | 9.02 | 1.5569 | 4.70 | 0.7910 | 7.88 | 1.3574 | 6.73 | 1.1426 | 22.61 | 3.7093 | 7.33 | 1.2444 | 22.69 | 3.4242 | 5.51 | 0.9287 |
| FeO | 14.85 | 1.7928 | 14.96 | 1.8349 | 14.67 | 1.7535 | 14.90 | 1.8236 | 13.69 | 1.6506 | 6.84 | 0.7973 | 14.69 | 1.7704 | 5.85 | 0.6270 | 13.96 | 1.6726 |
| MnO | 0.48 | 0.0586 | 0.34 | 0.0421 | 0.42 | 0.0505 | 0.38 | 0.0468 | 0.40 | 0.0484 | 0.00 | 0.0000 | 0.47 | 0.0569 | 0.00 | 0.0000 | 0.43 | 0.0523 |
| MgO | 12.75 | 2.7441 | 11.80 | 2.5800 | 13.67 | 2.9128 | 12.41 | 2.7060 | 13.19 | 2.8367 | 5.19 | 1.0777 | 13.13 | 2.8200 | 3.53 | 0.6751 | 13.92 | 2.9724 |
| CaO | 12.56 | 1.9429 | 12.03 | 1.8898 | 12.62 | 1.9317 | 12.74 | 1.9974 | 12.20 | 1.8858 | 5.47 | 0.8169 | 12.21 | 1.8852 | 9.05 | 1.2427 | 12.60 | 1.9338 |
| Na20 | 0.85 | 0.2367 | 1.17 | 0.3334 | 0.44 | 0.1224 | 1.01 | 0.2868 | 0.81 | 0.2276 | 4.48 | 1.2114 | 0.87 | 0.2418 | 5.41 | 1.3433 | 0.62 | 0.1727 |
| K20 | 0.29 | 0.2327 | 0.15 | 0.0273 | 0.13 | 0.0242 | 0.10 | 0.0186 | 0.11 | 0.0211 | 2.57 | 0.4563 | 0.15 | 0.0278 | 1.40 | 0.2291 | 0.15 | 0.0278 |
| | 99.23 | 15.3206 | 97.49 | 15.2960 | 99.53 | 15.1314 | 98.20 | 15.3543 | 98.20 | 15.1686 | 97.09 | 15.0149 | 99.10 | 15.2786 | 104.64 | 14.8051 | 99.05 | 15.1821 |
| Mg# | | 60.5 | | 58.4 | | 62.4 | | 59.7 | | 63.2 | | 57.5 | | 61.4 | | 51.8 | | 64.0 |
| SiO2 | 46.03 | 6.9130 | 50.41 | 7.0543 | 50.87 | 7.3317 | 50.43 | 7.2351 | 45.48 | 6.7132 | 47.07 | 6.8899 | 47.51 | 6.9405 | | | | |
| TiO2 | 0.38 | 0.0425 | 1.07 | 0.1125 | 0.31 | 0.0337 | 0.35 | 0.0383 | 0.52 | 0.0580 | 0.36 | 0.0400 | 0.56 | 0.0610 | | | | |
| Al203 | 9.69 | 1.7140 | 20.21 | 3.3301 | 6.17 | 1.0468 | 6.93 | 1.1706 | 10.74 | 1.8659 | 9.61 | 1.6563 | 9.16 | 1.5759 | | | | |
| FeO | 14.44 | 1.8136 | 8.22 | 0.9622 | 13.55 | 1.6325 | 14.81 | 1.7765 | 14.95 | 1.8456 | 14.89 | 1.8227 | 14.55 | 1.7775 | | | | |
| MnO | 0.36 | 0.0461 | 0.12 | 0.0144 | 0.47 | 0.0569 | 0.45 | 0.0548 | 0.38 | 0.0478 | 0.41 | 0.0511 | 0.34 | 0.0424 | | | | |
| MgO | 11.39 | 2.5496 | 6.11 | 1.2750 | 13.69 | 2.9403 | 13.09 | 2.7990 | 11.48 | 2.5252 | 11.73 | 2.5601 | 12.29 | 2.6757 | | | | |
| CaO | 11.72 | 1.8849 | 3.62 | 0.5435 | 12.57 | 1.9411 | 12.35 | 1.8992 | 12.44 | 1.9677 | 12.87 | 2.0186 | 12.39 | 1.9400 | | | | |
| Na20 | 1.02 | 0.2962 | 3.77 | 1.0233 | 0.81 | 0.2269 | 0.82 | 0.2271 | 1.46 | 0.4191 | 1.23 | 0.3497 | 1.16 | 0.3277 | | | | |
| K20 | 0.40 | 0.0767 | 4.03 | 0.7191 | 0.14 | 0.0262 | 0.09 | 0.0162 | 0.51 | 0.0955 | 0.28 | 0.0521 | 0.25 | 0.0458 | | | | |
| | 95.43 | 15.3367 | 97.56 | 15.0344 | 98.58 | 15.2361 | 99.31 | 15.2161 | 97.97 | 15.5379 | 98.45 | 15.4404 | 98.18 | 15.3864 | | | | |
| Mg# | | 58.4 | | 57.0 | | 64.3 | | 61.2 | | 57.8 | | 58.4 | | 60.1 | | | | |

MU45962B

202

| | MU45964 | | MU45968 | | | | MU45961 | | | | MU45982 | | | |
|---|---|---|---|---|---|---|---|---|---|---|---|---|---|---|
| SiO2 | 51.44 | 7.6402 | 47.13 | 6.8319 | 48.18 | 7.0217 | 47.75 | 6.9885 | 50.88 | 7.3090 | 51.87 | 7.5033 | 44.40 | 6.5238 | 40.29 | 6.2356 |
| TiO2 | 0.18 | 0.0202 | 0.72 | 0.0788 | 0.62 | 0.0695 | 0.61 | 0.0675 | 0.28 | 0.0307 | 0.12 | 0.0136 | 1.15 | 0.1274 | 1.43 | 0.1659 |
| Al2O3 | 3.29 | 0.5751 | 10.30 | 1.7585 | 8.04 | 1.3797 | 8.64 | 1.4883 | 6.52 | 1.1021 | 4.97 | 0.8465 | 11.67 | 2.0189 | 12.98 | 2.3643 |
| FeO | 20.16 | 2.5039 | 14.52 | 1.7598 | 14.60 | 1.7797 | 14.22 | 1.7402 | 13.44 | 1.6150 | 14.04 | 1.6992 | 14.75 | 1.8128 | 15.53 | 2.0099 |
| MnO | 1.61 | 0.2021 | 0.23 | 0.0279 | 0.22 | 0.0276 | 0.18 | 0.0222 | 0.27 | 0.0326 | 0.27 | 0.0330 | 0.26 | 0.0327 | 0.28 | 0.0364 |
| MgO | 9.94 | 2.2018 | 12.03 | 2.5988 | 13.23 | 2.8742 | 12.91 | 2.8170 | 14.01 | 3.0010 | 13.81 | 2.9774 | 11.13 | 2.4375 | 9.27 | 2.1377 |
| CaO | 11.70 | 1.8625 | 12.01 | 1.8653 | 11.80 | 1.8422 | 11.68 | 1.8316 | 11.97 | 1.8431 | 12.08 | 1.8726 | 12.59 | 1.9815 | 12.14 | 2.0122 |
| Na2O | 0.28 | 0.0813 | 1.90 | 0.5350 | 1.47 | 0.4141 | 1.56 | 0.4428 | 0.73 | 0.2032 | 0.56 | 0.1562 | 2.20 | 0.6279 | 2.23 | 0.6693 |
| K2O | 0.05 | 0.0095 | 0.20 | 0.0377 | 0.17 | 0.0308 | 0.22 | 0.0418 | 0.13 | 0.0241 | 0.14 | 0.0262 | 0.94 | 0.1756 | 1.18 | 0.2321 |
| | 98.66 | 15.0966 | 99.04 | 15.4938 | 98.35 | 15.4394 | 97.77 | 15.4400 | 98.24 | 15.1601 | 97.85 | 15.1280 | 99.09 | 15.7381 | 95.31 | 15.8635 |
| Mg# | | 46.8 | | 59.6 | | 61.8 | | 61.8 | | 65.0 | | 63.7 | | 57.3 | | 51.5 |
| SiO2 | 51.59 | 7.6061 | 47.91 | 6.9858 | 47.51 | 6.8687 | 46.25 | 6.7579 | 52.13 | 7.4943 | 51.24 | 7.4096 | 35.01 | 4.9917 | 38.70 | 5.9929 |
| TiO2 | 0.13 | 0.0143 | 0.58 | 0.0636 | 0.64 | 0.0696 | 0.81 | 0.0890 | 0.21 | 0.0229 | 0.25 | 0.0276 | 0.69 | 0.0743 | 1.60 | 0.1864 |
| Al2O3 | 3.87 | 0.6715 | 8.72 | 1.4976 | 9.81 | 1.6698 | 11.91 | 2.0492 | 5.08 | 0.8598 | 6.50 | 1.1061 | 21.80 | 3.6606 | 14.34 | 2.6140 |
| FeO | 18.44 | 2.2741 | 14.32 | 1.7464 | 14.71 | 1.7782 | 14.12 | 1.7258 | 14.90 | 1.7914 | 15.06 | 1.8209 | 9.22 | 1.0990 | 17.43 | 2.2574 |
| MnO | 1.31 | 0.1638 | 0.16 | 0.0196 | 0.23 | 0.0276 | 0.18 | 0.0222 | 0.30 | 0.0359 | 0.25 | 0.0304 | 0.08 | 0.0101 | 0.28 | 0.0361 |
| MgO | 10.79 | 2.3714 | 12.80 | 2.7815 | 12.27 | 2.6452 | 10.75 | 2.3408 | 13.41 | 2.8734 | 12.27 | 2.6439 | 16.60 | 3.5286 | 8.24 | 1.9020 |
| CaO | 12.01 | 1.8971 | 11.98 | 1.8720 | 12.19 | 1.8876 | 11.45 | 1.7927 | 12.31 | 1.8955 | 12.10 | 1.8751 | 10.83 | 1.6540 | 12.20 | 2.0245 |
| Na2O | 0.28 | 0.0797 | 1.54 | 0.4345 | 1.84 | 0.5160 | 2.32 | 0.6567 | 0.51 | 0.1408 | 0.58 | 0.1639 | 7.35 | 2.0308 | 2.28 | 0.6857 |
| K2O | 0.05 | 0.0092 | 0.17 | 0.0313 | 0.21 | 0.0391 | 0.21 | 0.0388 | 0.09 | 0.0159 | 0.14 | 0.0252 | 0.71 | 0.1291 | 1.56 | 0.3075 |
| | 98.47 | 15.0873 | 98.17 | 15.4323 | 99.41 | 15.5019 | 97.99 | 15.4732 | 98.92 | 15.1300 | 98.39 | 15.1027 | 102.28 | 17.1782 | 96.64 | 16.0064 |
| Mg# | | 51.0 | | 61.4 | | 59.8 | | 57.6 | | 61.6 | | 59.2 | | 76.3 | | 45.7 |
| SiO2 | 48.49 | 7.1916 | 42.96 | 6.3983 | 47.05 | 6.8434 | 45.69 | 6.7709 | 51.42 | 7.4887 | 52.05 | 7.3467 | 40.22 | 6.0688 | 41.41 | 6.6226 |
| TiO2 | 0.30 | 0.0332 | 0.30 | 0.0333 | 0.75 | 0.0821 | 0.70 | 0.0785 | 0.14 | 0.0151 | 0.23 | 0.0248 | 1.47 | 0.1663 | 1.20 | 0.1445 |
| Al2O3 | 7.22 | 1.2605 | 13.27 | 2.3262 | 10.73 | 1.8379 | 9.63 | 1.6809 | 4.57 | 0.7830 | 6.22 | 1.0329 | 14.57 | 2.5896 | 8.06 | 1.5178 |
| FeO | 19.72 | 2.4453 | 15.98 | 1.9910 | 14.19 | 1.7257 | 14.12 | 1.7496 | 14.38 | 1.7510 | 13.73 | 1.6208 | 16.42 | 2.0726 | 16.44 | 2.1993 |
| MnO | 1.24 | 0.1561 | 0.24 | 0.0299 | 0.22 | 0.0267 | 0.20 | 0.0247 | 0.24 | 0.0302 | 0.29 | 0.0349 | 0.23 | 0.0293 | 0.25 | 0.0344 |
| MgO | 9.45 | 2.0901 | 10.81 | 2.3992 | 11.52 | 2.4977 | 12.68 | 2.8006 | 13.86 | 3.0087 | 14.56 | 3.0638 | 9.23 | 2.0766 | 9.86 | 2.3519 |
| CaO | 11.67 | 1.8538 | 11.64 | 1.8574 | 11.86 | 1.8483 | 12.16 | 1.9312 | 12.47 | 1.9460 | 12.00 | 1.8143 | 12.41 | 2.0069 | 12.63 | 2.1641 |
| Na2O | 0.69 | 0.1990 | 2.37 | 0.6848 | 1.92 | 0.5426 | 1.75 | 0.5029 | 0.36 | 0.1021 | 0.74 | 0.2023 | 2.29 | 0.6692 | 2.08 | 0.6440 |
| K2O | 0.14 | 0.0258 | 0.25 | 0.0483 | 0.21 | 0.0395 | 0.21 | 0.0395 | 0.13 | 0.0241 | 0.14 | 0.0253 | 1.26 | 0.2428 | 1.13 | 0.2299 |
| | 98.92 | 15.2555 | 97.81 | 15.7684 | 98.45 | 15.4438 | 97.13 | 15.5788 | 97.56 | 15.1490 | 99.97 | 15.1656 | 98.10 | 15.9222 | 93.06 | 15.9086 |
| Mg# | | 46.1 | | 54.6 | | 59.1 | | 61.5 | | 63.2 | | 65.4 | | 50.0 | | 51.7 |
| SiO2 | 51.47 | 7.7074 | 46.87 | 6.8192 | 46.79 | 6.8653 | | | 50.31 | 7.3067 | | | 39.10 | 6.0201 | 47.16 | 6.9644 |
| TiO2 | 0.29 | 0.0328 | 0.49 | 0.0541 | 0.65 | 0.0714 | | | 0.39 | 0.0422 | | | 1.31 | 0.1520 | 0.38 | 0.0426 |
| Al2O3 | 2.46 | 0.4335 | 10.03 | 1.7183 | 9.91 | 1.7125 | | | 6.23 | 1.0651 | | | 14.61 | 2.6477 | 8.63 | 1.5001 |
| FeO | 22.18 | 2.7781 | 13.74 | 1.6721 | 14.69 | 1.8032 | | | 16.21 | 1.9685 | | | 16.34 | 2.1042 | 13.50 | 1.6676 |
| MnO | 1.85 | 0.2349 | 0.24 | 0.0294 | 0.21 | 0.0256 | | | 0.29 | 0.0360 | | | 0.30 | 0.0388 | 0.29 | 0.0368 |
| MgO | 8.97 | 2.0015 | 12.82 | 2.7797 | 11.80 | 2.5809 | | | 12.50 | 2.7076 | | | 8.92 | 2.0472 | 12.26 | 2.6984 |
| CaO | 11.33 | 1.8173 | 12.24 | 1.9078 | 11.94 | 1.8776 | | | 12.11 | 1.8839 | | | 12.20 | 2.0119 | 13.24 | 2.0954 |
| Na2O | 0.19 | 0.0553 | 1.90 | 0.5347 | 1.75 | 0.4972 | | | 0.68 | 0.1906 | | | 2.34 | 0.6995 | 1.30 | 0.3724 |
| K2O | 0.10 | 0.0186 | 0.18 | 0.0339 | 0.21 | 0.0390 | | | 0.13 | 0.0234 | | | 1.31 | 0.2565 | 0.52 | 0.0984 |
| | 98.84 | 15.0793 | 98.52 | 15.5493 | 97.95 | 15.4726 | | | 98.83 | 15.2240 | | | 96.42 | 15.9780 | 97.30 | 15.4761 |
| Mg# | | 41.9 | | 62.4 | | 58.9 | | | | 57.9 | | | | 49.3 | | 61.8 |
| SiO2 | 51.99 | 7.4446 | 46.06 | 6.7798 | 47.84 | 6.9492 | | | 52.11 | 7.5321 | | | | | 43.18 | 6.5428 |
| TiO2 | 0.17 | 0.0181 | 0.56 | 0.0623 | 0.65 | 0.0707 | | | 0.22 | 0.0235 | | | | | 1.23 | 0.1406 |
| Al2O3 | 5.78 | 0.9742 | 10.07 | 1.7453 | 8.73 | 1.4939 | | | 4.58 | 0.7787 | | | | | 10.30 | 1.8377 |
| FeO | 19.05 | 2.2817 | 14.08 | 1.7336 | 14.31 | 1.7387 | | | 15.30 | 1.8499 | | | | | 14.68 | 1.8595 |
| MnO | 1.32 | 0.1596 | 0.19 | 0.0237 | 0.21 | 0.0264 | | | 0.26 | 0.0316 | | | | | 0.28 | 0.0357 |
| MgO | 10.78 | 2.3013 | 12.83 | 2.8156 | 13.08 | 2.8325 | | | 13.23 | 2.8515 | | | | | 10.78 | 2.4344 |
| CaO | 11.80 | 1.8106 | 11.65 | 1.8366 | 12.03 | 1.8719 | | | 12.35 | 1.9122 | | | | | 13.40 | 2.1756 |
| Na2O | 0.36 | 0.1013 | 1.88 | 0.5370 | 1.64 | 0.4626 | | | 0.45 | 0.1266 | | | | | 1.98 | 0.5830 |
| K2O | 0.09 | 0.0156 | 0.18 | 0.0344 | 0.18 | 0.0326 | | | 0.12 | 0.0225 | | | | | 0.80 | 0.1546 |
| | 101.33 | 15.1071 | 97.51 | 15.5683 | 98.67 | 15.4785 | | | 98.62 | 15.1284 | | | | | 96.63 | 15.7638 |
| Mg# | | 50.2 | | 61.9 | | 62.0 | | | | 60.7 | | | | | | 56.7 |

| | | | | | | | | | | | | | | | | | | |
|---|---|---|---|---|---|---|---|---|---|---|---|---|---|---|---|---|---|---|
| SiO2 | 46.03 | 7.0379 | 46.27 | 7.0368 | 46.82 | 7.0337 | 46.97 | 7.0134 | 47.44 | 7.1696 | 47.69 | 7.0938 | 48.19 | 7.0943 | 47.98 | 7.1326 | 47.70 | 7.1410 |
| TiO2 | 1.09 | 0.1258 | 1.02 | 0.1167 | 0.98 | 0.1105 | 1.00 | 0.1125 | 0.91 | 0.1031 | 0.94 | 0.1046 | 1.01 | 0.1119 | 0.95 | 0.1067 | 1.01 | 0.1140 |
| Al2O3 | 7.15 | 1.2867 | 6.97 | 1.2480 | 6.93 | 1.2261 | 7.37 | 1.2959 | 6.32 | 1.1243 | 7.01 | 1.2276 | 7.03 | 1.2188 | 6.74 | 1.1792 | 7.54 | 1.3283 |
| FeO | 13.02 | 1.6648 | 13.25 | 1.6846 | 13.21 | 1.6598 | 14.08 | 1.7579 | 12.74 | 1.6107 | 13.36 | 1.6623 | 13.02 | 1.6032 | 13.65 | 1.6964 | 12.81 | 1.6035 |
| MnO | 0.24 | 0.0317 | 0.25 | 0.0318 | 0.25 | 0.0324 | 0.24 | 0.0305 | 0.17 | 0.0215 | 0.25 | 0.0315 | 0.25 | 0.0315 | 0.23 | 0.0292 | 0.16 | 0.0200 |
| MgO | 12.42 | 2.8304 | 12.85 | 2.9130 | 12.91 | 2.8901 | 12.70 | 2.8272 | 13.36 | 3.0101 | 12.98 | 2.8788 | 13.64 | 2.9938 | 13.03 | 2.8881 | 12.29 | 2.7417 |
| CaO | 12.13 | 1.9875 | 12.07 | 1.9666 | 12.81 | 2.0615 | 12.20 | 1.9523 | 11.83 | 1.9149 | 12.29 | 1.9583 | 11.95 | 1.8854 | 12.01 | 1.9120 | 11.61 | 1.8624 |
| Na2O | 1.37 | 0.4047 | 1.35 | 0.3971 | 1.41 | 0.4092 | 1.44 | 0.4169 | 1.27 | 0.3708 | 1.40 | 0.4042 | 1.53 | 0.4374 | 1.39 | 0.3997 | 1.69 | 0.4897 |
| K2O | 0.25 | 0.0478 | 0.25 | 0.0492 | 0.23 | 0.0443 | 0.27 | 0.0523 | 0.25 | 0.0479 | 0.28 | 0.0538 | 0.26 | 0.0498 | 0.27 | 0.0505 | 0.24 | 0.0463 |
| | 93.71 | 15.4173 | 94.27 | 15.4437 | 95.55 | 15.4676 | 96.27 | 15.4588 | 94.28 | 15.3728 | 96.20 | 15.4149 | 96.90 | 15.4261 | 96.25 | 15.3944 | 95.04 | 15.3468 |
| Mg# | | 63.0 | | 63.4 | | 63.5 | | 61.7 | | 65.1 | | 63.4 | | 65.1 | | 63.0 | | 63.1 |
| SiO2 | 50.70 | 7.2328 | 50.51 | 7.1392 | 47.62 | 6.5698 | 46.52 | 6.9640 | 46.40 | 7.1024 | 48.22 | 7.0460 | 47.12 | 7.1454 | 48.14 | 7.1713 | 50.60 | 7.4844 |
| TiO2 | 0.84 | 0.0905 | 1.42 | 0.1509 | 1.16 | 0.1205 | 1.17 | 0.1316 | 1.03 | 0.1184 | 1.22 | 0.1336 | 0.79 | 0.0900 | 0.56 | 0.0629 | 0.51 | 0.0568 |
| Al2O3 | 11.72 | 1.9690 | 8.51 | 1.4156 | 14.10 | 2.2904 | 7.79 | 1.3730 | 6.42 | 1.1566 | 7.17 | 1.2340 | 6.44 | 1.1497 | 6.60 | 1.1580 | 4.55 | 0.7922 |
| FeO | 10.28 | 1.2262 | 14.48 | 1.7122 | 13.07 | 1.5084 | 13.88 | 1.7372 | 12.94 | 1.6560 | 13.90 | 1.6988 | 13.13 | 1.6649 | 13.00 | 1.6201 | 11.97 | 1.4814 |
| MnO | 0.17 | 0.0208 | 0.17 | 0.0200 | 0.20 | 0.0232 | 0.24 | 0.0302 | 0.24 | 0.0305 | 0.23 | 0.0281 | 0.22 | 0.0278 | 0.21 | 0.0268 | 0.22 | 0.0270 |
| MgO | 9.63 | 2.0472 | 11.74 | 2.4730 | 12.72 | 2.6160 | 12.53 | 2.7950 | 12.91 | 2.9453 | 13.31 | 2.8992 | 13.10 | 2.9611 | 13.56 | 3.0117 | 14.30 | 3.1530 |
| CaO | 10.85 | 1.6584 | 12.11 | 1.8344 | 12.24 | 1.8088 | 12.12 | 1.9431 | 12.00 | 1.9680 | 12.35 | 1.9335 | 11.88 | 1.9294 | 12.04 | 1.9222 | 12.17 | 1.9292 |
| Na2O | 2.97 | 0.8206 | 1.65 | 0.4518 | 1.48 | 0.3946 | 1.45 | 0.4208 | 1.34 | 0.3983 | 1.44 | 0.4067 | 1.32 | 0.3878 | 1.33 | 0.3831 | 0.87 | 0.2494 |
| K2O | 0.37 | 0.0678 | 0.32 | 0.0579 | 0.30 | 0.0529 | 0.33 | 0.0628 | 0.24 | 0.0460 | 0.27 | 0.0498 | 0.27 | 0.0520 | 0.22 | 0.0411 | 0.14 | 0.0257 |
| | 97.53 | 15.1335 | 100.90 | 15.2549 | 102.89 | 15.3848 | 96.02 | 15.4577 | 93.51 | 15.4214 | 98.09 | 15.4297 | 94.26 | 15.4080 | 95.67 | 15.3971 | 95.32 | 15.1991 |
| Mg# | | 62.5 | | 59.1 | | 63.4 | | 61.7 | | 64.0 | | 63.1 | | 64.0 | | 65.0 | | 68.0 |
| SiO2 | 46.73 | 7.0200 | 47.49 | 7.0734 | 49.58 | 7.3042 | 45.09 | 6.9111 | 43.30 | 6.5855 | 42.56 | 6.4466 | 48.60 | 7.1133 | 48.86 | 7.2993 | 50.64 | 7.3098 |
| TiO2 | 1.15 | 0.1302 | 1.26 | 0.1415 | 0.65 | 0.0723 | 1.18 | 0.1363 | 0.94 | 0.1070 | 0.25 | 0.0284 | 0.93 | 0.1022 | 0.50 | 0.0558 | 0.71 | 0.0766 |
| Al2O3 | 7.25 | 1.2822 | 6.84 | 1.1996 | 5.51 | 0.9565 | 8.00 | 1.4430 | 11.16 | 1.9980 | 12.41 | 2.2137 | 12.17 | 2.0970 | 5.28 | 0.9287 | 4.72 | 0.8029 |
| FeO | 13.65 | 1.7145 | 13.46 | 1.6766 | 12.26 | 1.5106 | 13.69 | 1.7540 | 14.29 | 1.8179 | 14.50 | 1.8363 | 9.72 | 1.1894 | 12.34 | 1.5413 | 12.67 | 1.5298 |
| MnO | 0.18 | 0.0231 | 0.20 | 0.0254 | 0.21 | 0.0268 | 0.24 | 0.0309 | 0.26 | 0.0330 | 0.18 | 0.0229 | 0.14 | 0.0169 | 0.27 | 0.0340 | 0.23 | 0.0282 |
| MgO | 12.74 | 2.8527 | 13.05 | 2.8981 | 14.57 | 3.2020 | 12.02 | 2.7468 | 11.20 | 2.5391 | 11.41 | 2.5762 | 8.84 | 1.9282 | 14.00 | 3.1188 | 13.71 | 2.9507 |
| CaO | 12.12 | 1.9511 | 12.26 | 1.9562 | 11.94 | 1.8854 | 11.78 | 1.9342 | 11.29 | 1.8394 | 11.71 | 1.9001 | 11.67 | 1.8307 | 12.63 | 2.0216 | 15.31 | 2.3673 |
| Na2O | 1.41 | 0.4097 | 1.32 | 0.3807 | 1.17 | 0.3333 | 1.59 | 0.4713 | 2.34 | 0.6914 | 2.48 | 0.7280 | 3.04 | 0.8625 | 1.11 | 0.3216 | 0.93 | 0.2591 |
| K2O | 0.29 | 0.0564 | 0.24 | 0.0451 | 0.21 | 0.0391 | 0.38 | 0.0742 | 0.41 | 0.0798 | 0.27 | 0.0529 | 0.26 | 0.0478 | 0.20 | 0.0377 | 0.18 | 0.0325 |
| | 95.52 | 15.4398 | 96.13 | 15.3965 | 96.08 | 15.3301 | 93.96 | 15.5017 | 95.18 | 15.6911 | 95.77 | 15.8052 | 95.35 | 15.1879 | 95.19 | 15.3588 | 99.10 | 15.3568 |
| Mg# | | 62.5 | | 63.4 | | 67.9 | | 61.0 | | 58.3 | | 58.4 | | 61.8 | | 66.9 | | 65.9 |
| SiO2 | 49.89 | 7.2677 | 48.80 | 7.2076 | | | | | | | | | | | | | | |
| TiO2 | 0.67 | 0.0736 | 0.81 | 0.0900 | | | | | | | | | | | | | | |
| Al2O3 | 5.63 | 0.9651 | 6.06 | 1.0537 | | | | | | | | | | | | | | |
| FeO | 13.30 | 1.6203 | 12.57 | 1.5530 | | | | | | | | | | | | | | |
| MnO | 0.28 | 0.0345 | 0.28 | 0.0352 | | | | | | | | | | | | | | |
| MgO | 14.17 | 3.0773 | 14.18 | 3.1230 | | | | | | | | | | | | | | |
| CaO | 12.56 | 1.9603 | 12.04 | 1.9045 | | | | | | | | | | | | | | |
| Na2O | 1.14 | 0.3209 | 1.30 | 0.3729 | | | | | | | | | | | | | | |
| K2O | 0.17 | 0.0309 | 0.22 | 0.0412 | | | | | | | | | | | | | | |
| | 97.80 | 15.3506 | 96.27 | 15.3810 | | | | | | | | | | | | | | |
| Mg# | | 65.5 | | 66.8 | | | | | | | | | | | | | | |

MU45983

# D.3 : MAPS

N

GLENCLAIR ADAMELLITE

PRINGLES ADAMELLITE

BANALASTA ADAMELLITE

LOOANGA ADAMELLITE

BENDEMEER ADAMELLITE

HORNFELS

HORNFELS

MOONBI ADAMELLITE

WATSON'S CREEK

MCDONALD RIVER

RETREAT

ARMIDALE

ARMIDALE

NEW ENGLAND HWY

ARLEMORT

"VERMONT"

"SUTTON PARK"

"NANLINDY"

"BENDEMEER STATION"

BENDEMEER TOWNSHIP

GUNNALONG

WALCHA

TAMWORTH

KEY

- GEOLOGICAL BOUNDARIES
- MAJOR ROADS
- MINOR ROADS
- RIVER
- DYKES
- SHEAR
- FOLIATION - LINEATION
- DIP AND STRIKE
- MINE
- DATA POINTS
- STRUCTURAL TRENDS

0 1 2 3 4 KM

SCALE 1:25000

1

# BENDEMEER - HANNING GEOLOGICAL MAP

N

GLENCLAIR ADAMELLITE

PRINGLES ADAMELLITE

BANALASTA ADAMELLITE

LOOANGA ADAMELLITE

HORNFELS

HORNFELS

BENDEMEER ADAMELLITE

MCDONALD RIVER

NEW ENGLAND HWY

KEY

GEOLOGICAL BOUNDARIES

MAJOR ROADS

RIVER

DATA POINTS

CONTOURS

CONTOURS ARE IN ISOCLINES
= LINES OF EQUAL TRICLINICITY
WHERE 0 = ORTHOCLASE
AND 1 = MAXIMUM MICROCLINE

0 1 2 3 4 KM

SCALE 1:25000

# 2

# ISOCLINAL MAP FOR THE BANALASTA ADAMELLITE

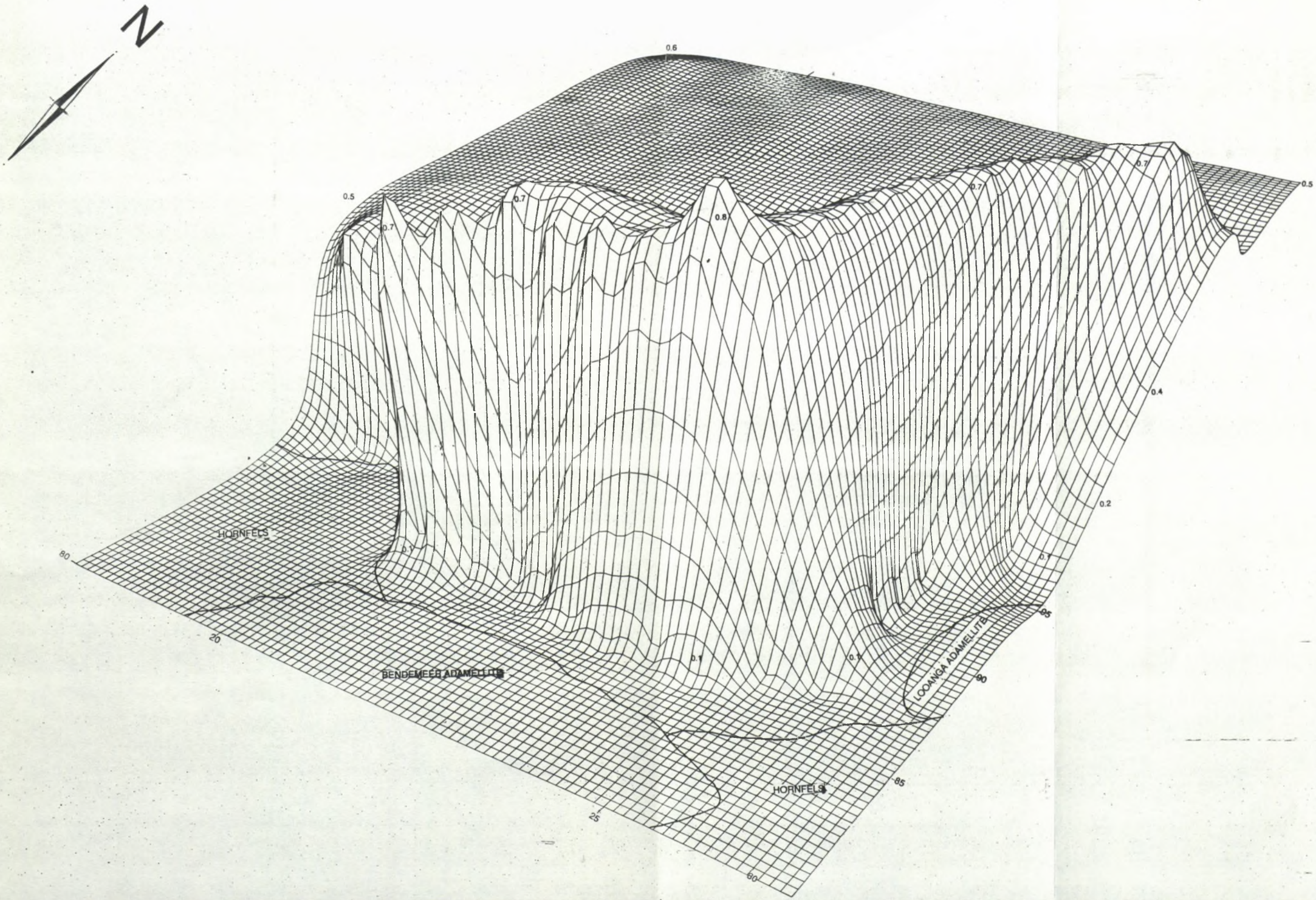


3

# COMPUTED THREE DIMENSIONAL TRICLINICITY SURFACE OF THE SOUTHERN BUNDARRA SUITE PLUTONS

# YARROWYCK-BALALA GEOLOGICAL MAP

4

N

BUNDARRA

KINGSTOWN

"EUREKA"

"HARWOOD"

"MYANBAH"

"RIVERVIEW"

"KOORINGLE"

"YARROWYCK STATION"

GWYDIR RIVER

SPRING CREEK

BOOROLONG CREEK

URALLA

(FS 237)

GWYDIR RIVER ADAMELLITE

MYANBAH LEUCOADAMELLITE

HORNFELS

HORNFELS

YARROWYCK GRANODIORITE

KEY

- GEOLOGICAL BOUNDARIES
- MAJOR ROADS
- MINOR
- RIVER
- DYKES
- SHEAR
- FOLIATION-LINEATION
- DIP AND STRIKE
- MINE
- DATA POINTS
- STRUCTURAL TREND

SCALE 1:25000

0 1 2 3 4 KM

35 40 45 50

34 38 42 46 50

N

GWYDIR RIVER ADAMELLITE

HORNFLES

GWYDIR RIVER

MYANBAH LEUCOADAMELLITE

HORNFELS

YARROWYCK GRANODIORITE

KEY

GEOLOGICAL BOUNDARIES

MAJOR ROADS

RIVER

DATA POINTS

CONTOURS

CONTOURS ARE IN ISOCLINES
= LINES OF EQUAL TRICLINICITY,
WHERE 0 = ORTHOCLASE
AND 1 = MAXIMUM MICROCLINE

0 1 2 3 4 KM

SCALE 1:25000

5

# ISOCLINAL MAP FOR THE I-TYPE YARROWYCK GRANODIORITE

34 30 26 22

36 40 44 48 52

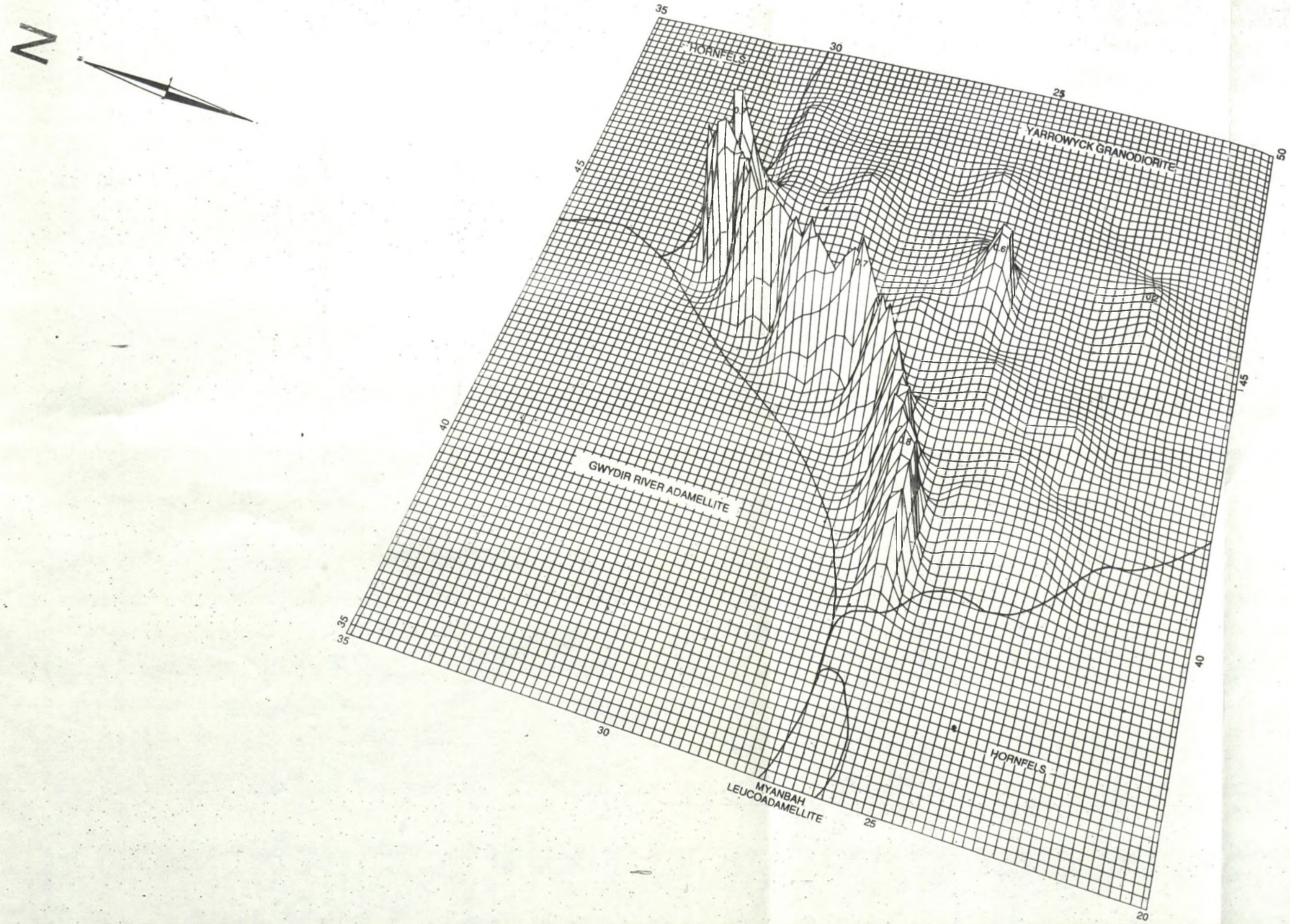


6

# COMPUTED THREE DIMENSIONAL TRICLINICITY SURFACE OF THE YARROWYCK GRANODIORITE